

# Creating Novel Antimicrobial Peptides: From Gramicidin A to Screening a Cyclic Peptide Library

Author: Breanna L. Zerfas

Persistent link: <http://hdl.handle.net/2345/bc-ir:107444>

This work is posted on [eScholarship@BC](#),  
Boston College University Libraries.

---

Boston College Electronic Thesis or Dissertation, 2017

Copyright is held by the author, with all rights reserved, unless otherwise noted.

# Creating Novel Antimicrobial Peptides: From Gramicidin A to Screening a Cyclic Peptide Library

Breanna L. Zerfas

A dissertation

submitted to the Faculty of

the department of Chemistry

in partial fulfillment

of the requirements for the degree of

Doctor of Philosophy

Boston College  
Morrissey College of Arts and Sciences  
Graduate School

May 2017



# Creating Novel Antimicrobial Peptides: From Gramicidin A to Screening a Cyclic Peptide Library

Breanna L. Zerfas

Advisor: Prof. Jianmin Gao, PhD.

As the threat of microbial resistance to antibiotics grows, we must turn in new directions to find new drugs effective against resistant infections. Antimicrobial peptides (AMPs) and host-defense peptides (HDPs) are a class of natural products that have been well-studied towards this goal, though very few have found success clinically. However, as there is much known about the behavior of these peptides, work has been done to manipulate their sequences and structures in the search for more drug-like properties. Additionally, novel sequences and structures mimicking those seen in nature have been discovered and characterized.

Herein, we demonstrate our ability to finely tune the antimicrobial activity of various peptides, such that they can be provided with more clinically desirable characteristics. Our results show that gramicidin A (gA) can be made to be less toxic via incorporation of unnatural cationic amino acids. This is achieved by synthesizing lysine analogues with diverse hydrophobic groups alkylated to the side-chain amine. Through exploring different groups, we achieved peptide structures with improved selectivity for bacterial over mammalian membranes. Additionally, we were able to achieve novel broad-spectrum gram-negative

activity for gA peptides.

In efforts to combat bacterial resistance to cationic antimicrobial peptides (CAMPs), we have directed our reported amine-targeting iminoboronate chemistry towards neutralizing Lys-PG in bacterial membranes. Originally incorporating 2-APBA into gA, we found this to hinder the peptide's activity. However, we were successful in increasing the potency of gA3R, a cationic mutant of gA, towards *S. aureus* by using a co-treatment of this peptide with a Lys-PG binding structure. Currently, we are exploring this strategy further.

Finally, we describe our work towards establishing a novel cyclic peptide library incorporating a 2-APBA warhead for iminoboronate formation with a given target. In this, we have achieved intermolecular reduction of iminoboronates, strengthening the stringency of library screening. Although we were unsuccessful in finding a potent hit for binding of the lipid II stem peptide, screening against human transferrin yielded selective hits. Currently we are investigating these hits to understand their activity and therapeutic potential.

## TABLE OF CONTENTS

<b>List of tables</b> .....	<b>viii</b>
<b>List of figures</b> .....	<b>ix</b>
<b>List of schemes</b> .....	<b>xii</b>
<b>List of abbreviations</b> .....	<b>xiii</b>
<b>Acknowledgements</b> .....	<b>xix</b>
<b>1.0 Chapter 1: Introduction</b> .....	<b>1</b>
<b>1.1 Antibiotic Resistance</b> .....	<b>2</b>
<b>1.2 From the End of the Golden Era to Now: The State of Antibiotic Discovery</b> ...	<b>5</b>
<b>1.3 Host-Defense Peptides (HDPs)</b> .....	<b>8</b>
<b>1.4 Commercial Use of Peptides as Antibiotics</b> .....	<b>9</b>
1.4.1 Nisin .....	10
1.4.2 Polymyxins .....	11
1.4.3 Daptomycin .....	12
<b>1.5 Conclusions</b> .....	<b>13</b>
<b>1.6 References</b> .....	<b>13</b>
<b>2.0 Chapter 2: Creating Selectivity with Cationic Mutants of Gramicidin A</b>	<b>18</b>
<b>2.1 Introduction</b> .....	<b>19</b>
2.1.1 Gramicidin A .....	19
<b>2.2 Synthesis of gA Mutants Containing Alkylated Lysines</b> .....	<b>23</b>
2.2.1 Synthesis of Alkylated Lysines .....	23
2.2.2 Synthesis and Structural Characterization of Cationic gA Peptides .....	28
<b>2.3 Studies of gA3K Peptides' Activities in Cell-Based Assays</b> .....	<b>30</b>
2.3.1 Antimicrobial Activity Towards Gram-Positive Bacteria .....	30
2.3.2 Antimicrobial Activity Towards Gram-Negative Bacteria .....	36
2.3.3 Toxicity of gA Mutants Towards Human Red Blood Cells .....	39
<b>2.4 Mechanistic Studies of gA3K Mutants</b> .....	<b>41</b>
2.4.1 Membrane Binding vs. Cell Killing .....	42
2.4.2 Measuring Membrane Permeability .....	45
<b>2.5 Conclusions</b> .....	<b>49</b>
<b>2.6 Experimental Procedures</b> .....	<b>50</b>
2.6.1 General Methods .....	50

2.6.2	Synthesis of Unnatural Amino Acids.....	51
2.6.3	Peptides Synthesis and Characterization.....	61
2.6.4	Circular Dichroism Spectroscopy with Model Membranes.....	63
2.6.5	Minimal Inhibitory Concentration Measurements.....	64
2.6.6	Cell Killing Assay with <i>S. aureus</i> .....	65
2.6.7	Cell Killing Assay with <i>E. coli</i> .....	66
2.6.8	Hemoglobin Release from Human Red Blood Cells.....	67
2.6.9	Binding of gA Mutants to Live Cells.....	67
2.6.10	Assessing Cell Permeability Using Flow Cytometry.....	68
<b>2.7</b>	<b>References.....</b>	<b>70</b>
<b>3.0</b>	<b>Targeting Lys-PG Based Antibiotic Resistance with 2-Acetylphenyl Boronic Acid Presenting Peptides.....</b>	<b>71</b>
<b>3.1</b>	<b>Introduction.....</b>	<b>72</b>
3.1.1	Bacterial Resistance to Cationic Antimicrobials.....	72
3.1.2	Multiple Peptide Resistance Factor (MprF)-Mediated Resistance and the Significance of Lys-PG.....	75
3.1.3	Use of Reversible Covalent Interactions for Drug Target Affinity.....	77
3.1.4	Designing Peptides Incorporating 2-APBA for Potent Antibacterial Activity Towards Lys-PG Presenting <i>S. aureus</i> .....	80
<b>3.2</b>	<b>Use of AB3-containing gA3R Mutants for Treatment of Lys-PG Presenting Bacteria.....</b>	<b>83</b>
3.2.1	Synthesis of Fmoc-AB3(pin)-OH.....	83
3.2.2	Synthesis of gA3R(AB3-15).....	84
3.2.3	Characterizing the Antimicrobial Activity of gA3R(AB3-15)-NH <sub>2</sub> .....	89
<b>3.3</b>	<b>Resensitizing <i>S. aureus</i> to gA3R Using a Lys-PG Binding Peptide.....</b>	<b>92</b>
<b>3.4</b>	<b>Conclusions and Future Work.....</b>	<b>95</b>
<b>3.5</b>	<b>Experimental Procedures.....</b>	<b>96</b>
3.5.1	General Methods.....	96
3.5.2	Synthesis of Fmoc-AB3(pin)-OH.....	97
3.5.3	Conjugation of AB3 to Wang Resin.....	102
3.5.4	Synthesis of 2-(Fmoc-amino)ethanol.....	103
3.5.5	Preparation of 2-(Fmoc-amino)ethanol Wang Resin.....	104
3.5.6	Synthesis of gA3R Peptides.....	105
3.5.7	Minimum Inhibitory Concentration Measurements.....	106
3.5.8	Cell Killing Assay with <i>S. aureus</i> .....	107
<b>3.6</b>	<b>References.....</b>	<b>108</b>
<b>4.0</b>	<b>Design and Screen of a Cyclic Peptide Library Containing a 2-APBA Warhead for the Discovery of Novel Binders to Lipid II Stem Peptide. 111</b>	
<b>4.1</b>	<b>Introduction.....</b>	<b>112</b>
4.1.1	Use of Libraries for Novel Peptide Discovery.....	112
4.1.2	Peptidoglycan and Vancomycin.....	116
4.1.3	Design and Evolution of Library Scaffold.....	119

4.1.4	Design of a Stringent Screening Procedure .....	121
<b>4.2</b>	<b>Exploration of a DNA-Encoded Peptide Library .....</b>	<b>123</b>
4.2.1	Preparation of Tentagel Resin .....	123
4.2.2	Optimization of DNA Tag Synthesis and Sequencing .....	124
4.2.3	Simultaneous Peptide Synthesis and DNA Ligation Conditions.....	129
<b>4.3</b>	<b>One-Bead Two-Compound Library of Monocyclic Peptides .....</b>	<b>132</b>
4.3.1	Library Structure Design.....	132
4.3.2	Utilization of a Core-and-Shell Strategy .....	133
4.3.3	Cysteine Disulfide Formation for Reversible Cyclization.....	136
4.3.4	Total Synthesis of the Library.....	138
4.3.5	Quality Control Analysis of the Library .....	139
<b>4.4</b>	<b>Design and Validation of a Screening Scheme for Lipid II Stem Peptide Binders .....</b>	<b>139</b>
4.4.1	Developing Intermolecular Imine Reduction Conditions for 2-APBA and Lysine .....	139
4.4.2	Hit Selection via Affinity-mediated Pull-down.....	143
4.4.3	Selection of Hits Using Fluorescence Microscopy .....	145
4.4.4	Final Screening Scheme and Known Sequence Validation .....	149
4.4.5	Screening and Sequencing of the Library .....	151
<b>4.5</b>	<b>Hit Validation.....</b>	<b>152</b>
4.5.1	Synthesis of Selected Hits .....	152
4.5.2	Validating Hits Using MIC .....	152
4.5.3	Validating Hits Using a UV-Vis Titration with the Target Peptide.....	153
4.5.4	Validating Hits Using Iminoboronate Reduction.....	158
4.5.5	Hit Validation - What May Have Gone Wrong? .....	158
<b>4.6</b>	<b>Targeting Transferrin: Selective Binding to a Single Protein in a Complex Mixture.....</b>	<b>160</b>
4.6.1	Designing a Screen for Transferrin .....	161
4.6.2	Screen and Hit Selection for Transferrin Binding Cyclic Peptides.....	162
4.6.3	Sequencing and Analysis of Hits from Screening Transferrin .....	163
4.6.4	Hit Validation for Transferrin .....	165
<b>4.7</b>	<b>Conclusions and Future Work.....</b>	<b>168</b>
<b>4.8</b>	<b>Experimental Procedures.....</b>	<b>170</b>
4.8.1	General Materials and Methods.....	170
4.8.2	Preparation of Tentagel Resin for Library Synthesis (Tentagel-Gly Resin).....	171
4.8.3	Preparation of Peptide for On-Resin DNA Ligation.....	171
4.8.4	Click Reaction for the Attachment of DNA Headpiece.....	172
4.8.5	DNA Ligation to Resin.....	173
4.8.6	Simultaneous Peptide Synthesis and DNA Ligation .....	175
4.8.7	PCR Analysis of DNA Tag.....	176
4.8.8	DNA Extraction from Gel .....	177
4.8.9	UV Cleavage of Peptides from Tentagel Resin.....	178
4.8.10	Peptide Library Preparation .....	178
4.8.11	Synthesis of Dual-labelled Target Peptide .....	179
4.8.12	Preparation of Quality Control Single-Bead Samples.....	180
4.8.13	LC-MS/MS Sequencing of Single Bead Samples.....	180
4.8.14	Sodium Borohydride Reduction of Intermolecular Iminoboronates.....	181



4.8.15	Screening of Library Against Lipid II Stem Peptide .....	182
4.8.16	Preparation of Hit Samples for Sequencing .....	183
4.8.17	Synthesis of Hit Peptides for Validation.....	183
4.8.18	Minimum Inhibitory Concentration Assay .....	184
4.8.19	UV-Vis Titration of Hit Peptides with Biotin-Lipid II Stem Peptide.....	184
4.8.20	Sodium Borohydride Reduction of Hit Peptides and Biotin-Lipid II Stem Peptide .....	185
4.8.21	Screening of Library against Rhodamine-Transferrin .....	185
4.8.22	Synthesis of Hit Peptides for Validation.....	186
4.8.23	Fluorescence Anisotropy for Hit Validation with Transferrin .....	186
<b>4.9</b>	<b>References .....</b>	<b>187</b>
<b>5.0</b>	<b>Conclusions .....</b>	<b>191</b>

## LIST OF TABLES

<b>1</b>	<b>Introduction</b>	
<b>2</b>	<b>Creating Selectivity with Cationic Mutants of Gramicidin A</b>	
2-1	Optimization of Acid Conditions for Benzylation of Lysine .....	26
2-2	Dependence of Equilibration Time on Alkylation with 2-pyridine carboxaldehyde .....	27
2-3	List of Alkylated Lysines and their Corresponding Peptides.....	28
2-4	Measured MIC ( $\mu\text{M}$ ) of gA Mutants Against Various Gram-Positive Bacteria .....	32
2-5	Measured MIC ( $\mu\text{M}$ ) of gA Mutants Against Various Gram-Negative Bacteria .....	37
2-6	Measured Binding of gA Mutants .....	45
2-7	Naming Scheme and Mass-spectrometry Characterization of gA Mutants .....	62
<b>3</b>	<b>Targeting Lys-PG Based Antibiotic Resistance with 2-Acetylphenyl Boronic Acid Presenting Peptides</b>	
3-1	Bacterial resistance mechanisms to CAMPs involving covalent modifications to cell surface molecules.....	73
3-2	MICs of common CAMPs towards wild-type and <i>mprF</i> knockout <i>S. aureus</i> .....	76
<b>4</b>	<b>Design and Screen of a Cyclic Peptide Library Containing a 2-APBA Warhead for the Discovery of Novel Binders to Lipid II Stem Peptide</b>	
4-1	Quality Control Analysis of Library Sequencing .....	139
4-2	Optimization of Iminoboronate Reduction .....	141
4-3	Hits from Library Screening of Lipid II Stem Peptide .....	151
4-4	Hits from Library Screening of Transferrin.....	164
4-5	Sequences of Oligomers for DNA-Encoded Library .....	174

4-6 - Sequences of PCR Primers .....	177
4-7 - Thermocycling Conditions for PCR.....	177

## LIST OF FIGURES

### 1 Introduction

1-1 – Curves showing the crude mortality rates .....	2
1-2 – Antibiotic timeline.....	3
1-3 – Chemical structures of penicillin and clavulanic acid .....	5
1-4 – Chemical structures of ciprofloxacin and linezolid.....	6
1-5 – Notable examples of HDPs and their origins.....	10

### 2 Creating Selectivity with Cationic Mutants of Gramicidin A

2-1 – Primary sequence and secondary structure of gramicidin A .....	19
2-2 – Hypothesis of cationic gA mutants for selectivity.....	22
2-3 – Structures of synthesized lysine derivatives .....	27
2-4 – Circular dichroism spectra of gA mutants .....	29
2-5 – Bactericidal activity of gA3K(CyMe) with <i>S. aureus</i> .....	33
2-6 – Cell killing activity of select peptides towards <i>S. aureus</i> .....	35
2-7 – Cell killing activity of select peptides towards <i>S. aureus</i> in the presence of human serum .....	36
2-8 – Bactericidal activity of gA3K(4AMBn) with <i>E. coli</i> .....	38
2-9 – Cell killing of select gA mutants towards <i>E. coli</i> .....	39
2-10 – Hemolytic activity of gA mutants.....	41
2-11 – Depiction of the mechanism of action of gA .....	42
2-12 – Comparing cell binding with cell killing activities of select gA mutants .....	46
2-13 – Flow cytometry analysis of cell permeability of select gA mutants .....	48

### 3 Targeting Lys-PG Based Antibiotic Resistance with 2-Acetylphenyl Boronic Acid Presenting Peptides

3-1 – Lipid A and its modified structures that can elicit CAMP resistance .....	74
3-2 – Phosphatidylglycerol and its modified structures that can elicit CAMP resistance .....	74

3-3 - Depiction of MprF in a bacterial membrane .....	75
3-4 - Examples of small molecule drugs that bind using reversible covalent interactions .....	78
3-5 - Depiction of Schiff base and iminoboronate formation under physiological conditions.....	79
3-6 - Study of Hlys-AB1 with Jurkat and <i>S. aureus</i> cells .....	79
3-7 - Structures of gA3R mutants.....	82
3-8 - Preparation of resin for gA3R(AB3-15) synthesis.....	86
3-9 - Solid state FT-IR spectra for the conversion of Wang to TCA resin .....	87
3-10 - Solid state FT-IR spectra for the coupling of 2-(Fmoc-amino)ethanol to TCA resin .....	88
3-11 - Structure of final gA3R(AB3-15)-NH <sub>2</sub> from Rink amide resin.....	89
3-12 - MIC assay of gA3R mutants with <i>S. aureus</i> .....	90
3-13 - MIC assay of gA3R(AB3-15)-NH <sub>2</sub> with <i>S. aureus</i> .....	91
3-14 - Cell killing assay of gA3R mutants with <i>S. aureus</i> .....	91
3-15 - Structure and characterization of KAM-CT .....	94
3-16 - MIC assay with various concentrations of KAM-CT with <i>S. aureus</i> .....	94
3-17 - MIC assay of gA3R with and without KAM-CT with <i>S. aureus</i> .....	95

#### **4 Targeting Lys-PG Based Antibiotic Resistance with 2-Acetylphenyl Boronic Acid Presenting Peptides**

4-1 - Depiction of two major classes of peptide library scaffolds.....	113
4-2 - Literature reported examples of modifications that can be made on phage display libraries.....	114
4-3 - Cartoon of a one-bead two-compound library .....	115
4-4 - Depiction of DNA-encoded library .....	116
4-5 - Cartoon depiction of the exterior of a gram-positive cell.....	117
4-6 - Structure of vancomycin binding to the lipid II stem peptide.....	119
4-7 - Depiction of iminoboronate formation between lysine of the lipid II stem peptide and AB3 in a designed peptide.....	120
4-8 - Proposed strategy for the covalent capture of hits via iminoboronate reduction .	122
4-9 - Structure of the photolabile linker used for the library and resulting products after UV cleavage.....	124
4-10 - LC/MS data for CuAAC test reaction with azido-lysine .....	127
4-11 - Sequence of DNA used for testing of library ligation conditions .....	128
4-12 - Denaturing PAGE of PCR reactions for single beads .....	128
4-13 - Structure of bicyclic peptide used to test conditions for simultaneous DNA ligation and peptide synthesis .....	129
4-14 - Results of library test ligation.....	130

4-15 - LC/MS analysis of peptide from test DNA encoded library synthesis .....	131
4-16 - LC/MS analysis of peptide from test DNA encoded library synthesis after azido acetic acid capping.....	132
4-17 - Structures of seven amino acids chosen for library.....	133
4-18 - Structure of core/shell arrangement for our one-bead two-compound library ..	134
4-19 - LC/MS analysis of a model core/shell peptide.....	136
4-20 - Structure of final library design .....	137
4-21 - Test reaction used for optimizing conditions of intermolecular iminoboronate reduction.....	141
4-22 - NMR spectrum of 2-APBA and lysine reduction with NaBH <sub>4</sub> .....	142
4-23 - Test reaction between 2-APBA and Fmoc-lysine.....	142
4-24 - Structure of positive control on Tentagel resin.....	144
4-25 - Microscopy images from Dynabead magnetic pull-down optimization .....	146
4-26 - Structure of P13 peptide on Tentagel resin.....	147
4-27 - Fluorescence microscopy images of various sets of prepared Tentagel resin.....	148
4-28 - Depiction of final optimized screening scheme for our cyclic library against lipid II stem peptide.....	149
4-29 - MIC plots for first four hits with <i>S. aureus</i> .....	153
4-30 - Titration of AB3 with lysine monitored by UV-vis spectroscopy .....	154
4-31 - Example titrations of hit peptides with 2-MEA .....	156
4-32 - Titrations of hit peptides with biotin-lipid II stem peptide .....	156
4-33 - Titrations of AB3 with biotin-lipid II stem peptide.....	157
4-34 - Microscopy of blank Tentagel resin under the rhodamine-Tf screening conditions .....	163
4-35 - Microscopy images of library resin under the rhodamine-Tf screening conditions after reduction.....	164
4-36 - Hit 1 validation by fluorescence anisotropy with Tf and HSA .....	166
4-37 - Hit 2 validation by fluorescence anisotropy with Tf and HSA .....	167
4-38 - Hit 10 validation by fluorescence anisotropy with Tf and HSA .....	167
4-39 - Fluorescein control for validation by fluorescence anisotropy with Tf and HSA .....	168

## LIST OF SCHEMES

<b>1</b>	<b>Introduction</b>	
<b>2</b>	<b>Creating Selectivity with Cationic Mutants of Gramicidin A</b>	
2-1	The general synthetic route for monoalkylated lysine derivatives in preparation for solid-phase peptide synthesis .....	24
<b>3</b>	<b>Targeting Lys-PG Based Antibiotic Resistance with 2-Acetylphenyl Boronic Acid Presenting Peptides</b>	
3-1	Synthetic route to Fmoc-AB3(pin)-OH.....	83
<b>4</b>	<b>Targeting Lys-PG Based Antibiotic Resistance with 2-Acetylphenyl Boronic Acid Presenting Peptides</b>	
4-1	CuAAC Reaction for the Covalent Attachment of DNA to Tentagel Resin .....	125
4-2	Test CuAAC Reaction for Conjugation to Tentagel Resin .....	126

## LIST OF ABBREVIATIONS

<b>(Boc)<sub>2</sub>O</b>	Boc-anhydride
<b>(CF<sub>3</sub>SO<sub>2</sub>)<sub>2</sub>O</b>	Trifluormethanesulfonic anhydride
<b>2-APBA</b>	2-acetylphenyl boronic acid
<b>2-FPBA</b>	2-formylphenyl boronic acid
<b>2-MEA</b>	2-methoxyethylamine
<b>2-pyr</b>	2-pyridinyl
<b>3-pyr</b>	3-pyridinyl
<b>4AMBn</b>	4-aminomethyl benzyl
<b>4-pyr</b>	4-pyridinyl
<b>A, Ala</b>	Alanine
<b>AADase</b>	Acetoacetate decarboxylase
<b>AMP</b>	Anti-microbial peptide
<b>Aq</b>	Aqueous
<b>ATCC</b>	American Type Culture Collection
<b>B<sub>2</sub>pin<sub>2</sub></b>	Bis(pinacolato)diboron
<b>Bn</b>	Benzyl
<b>Boc</b>	<i>Tert</i> -butoxycarbonyl
<b>BSA</b>	Bovine serum albumin
<b>BTPBB</b>	Bis-tris propane breaking buffer
<b>BTPLB</b>	Bis-tris propane ligation buffer
<b>BTPWB</b>	Bis-tris propane washing buffer
<b>C, Cys</b>	Cysteine
<b>CAMP</b>	Cationic antimicrobial peptide
<b>CD</b>	Circular dichroism



<b>CED</b>	Convection-enhanced delivery
<b>cfu/mL</b>	Colony forming units per milliliter
<b>CRB</b>	Click reaction buffer
<b>CuAAC</b>	Cu(I) catalyzed azide alkyne cycloaddition
<b>Cy</b>	Cyclohexyl
<b>CyMe</b>	Cyclohexylmethyl
<b>D, Asp</b>	Aspartic acid
<b>D<sub>2</sub>O</b>	Deuterium oxide
<b>Dap</b>	Diaminopropionic acid
<b>DBU</b>	1,8-diazabicyclo[5.4.0]undec-7-ene
<b>DCM</b>	Dichloromethane
<b>DI</b>	Deionized
<b>DIC</b>	<i>N,N'</i> -diisopropylcarbodiimide
<b>DIPEA</b>	Diisopropylethylamine
<b>DMAP</b>	4-dimethylaminopyridine
<b>DMF</b>	<i>N,N</i> -dimethylformamide
<b>DMSO</b>	Dimethylsulfoxide
<b>DNA</b>	Deoxyribose nucleic acid
<b>DPC</b>	Fos-phosphatidylcholine-C <sub>12</sub>
<b>Dppf</b>	Bis(diphenylphosphino)ferrocene ligand
<b>E, Glu</b>	Glutamic acid
<b>EDTA</b>	Ethylenediaminetetraacetic acid
<b>ESI</b>	Eletrospray ionization
<b>ESKAPE</b>	<i>Enterococcus faecium</i> , <i>Staphylococcus aureus</i> , <i>Klebsiella pneumoniae</i> , <i>Acinetobacter baumannii</i> , <i>Pseudomonas aeruginosa</i> , and <i>Enterobacter</i> species
<b>Et<sub>2</sub>O</b>	Diethyl ether
<b>Et<sub>3</sub>N</b>	Triethylamine
<b>EtOAc</b>	Ethyl acetate
<b>F, Phe</b>	Phenylalanine
<b>FBS</b>	Fetal bovine serum

<b>FDA</b>	US Food and Drug Administration
<b>FITC</b>	Fluorescein isothiocyanate
<b>FITC</b>	Fluorescein isothiocyanate
<b>Fmoc</b>	Fluorenylmethyloxycarbonyl
<b>Fmoc-OSu</b>	N-(9-fluorenylmethoxycarbonyloxy) succinimide
<b>FT-IR</b>	Fourier transform infrared spectroscopy
<b>G, Gly</b>	Glycine
<b>gA</b>	Gramicidin A
<b>gB</b>	Gramicidin B
<b>gC</b>	Gramicidin C
<b>gD</b>	Gramicidin D
<b>GSK</b>	GlaxoSmithKline
<b>H, His</b>	Histidine
<b>HATU</b>	<i>O</i> -(7-azabenzotriazol-1-yl)- <i>N,N,N',N'</i> -tetramethyluronium hexafluorophosphate
<b>HBTU</b>	<i>O</i> -benzotriazole- <i>N,N,N',N'</i> -tetramethyluronium hexafluorophosphate
<b>HC<sub>50</sub></b>	Concentration of 50% hemoglobin release from red blood cells
<b>HCl</b>	Hydrochloride
<b>HCOOH</b>	Formate
<b>HDP</b>	Host-defense peptide
<b>HOBt</b>	Hydroxybenzotriazole
<b>HPLC</b>	High-performance liquid chromatography
<b>hRBC</b>	Human red blood cell
<b>HSA</b>	Human serum albumin
<b>HTS</b>	High-throughput screening
<b>I, Ile</b>	Isoleucine
<b>iPr</b>	Isopropyl
<b>IR</b>	Infrared spectroscopy
<b>K, Lys</b>	Lysine
<b>K<sub>d</sub></b>	Equilibrium dissociate constant

<b>L, Leu</b>	Leucine
<b>Lac</b>	Lactate
<b>L-Ara4N</b>	4-amino-4-deoxy- L-arabinose
<b>LB</b>	Luria-Bertani
<b>LC/MS</b>	High performance liquid chromatograph/mass-spectrometry
<b>LPS</b>	Lipopolysaccharide
<b>Lys-PG</b>	Lysyl-phosphatidylglycerol
<b>M, Met</b>	Methionine
<b>MH</b>	Mueller-Hinton
<b>MIC</b>	Minimum inhibitory concentration
<b>MprF</b>	Multi-peptide resistance factor
<b>MRSA</b>	Methicillin-resistant <i>S. aureus</i>
<b>N, Asn</b>	Asparagine
<b>Na<sub>2</sub>SO<sub>4</sub></b>	Sodium sulfate
<b>NaBH<sub>4</sub></b>	Sodium borohydride
<b>NaCNBH<sub>3</sub></b>	Sodium cyanoborohydride
<b>NAG</b>	<i>N</i> -acetylglucosamine
<b>NAM</b>	<i>N</i> -acetylmuramic acid
<b>NaOH</b>	Sodium hydroxide
<b>NMM</b>	<i>N</i> -methylmorpholine
<b>NMR</b>	Nuclear magnetic resonance spectroscopy
<b>OBOC</b>	One-bead one-compound
<b>OBTC</b>	One-bead two-compound
<b>OD600</b>	Optical density at 600 nm
<b>P, Pro</b>	Proline
<b>PAGE</b>	Polyacrylamide gel electrophoresis
<b>Pbf</b>	2,2,4,6,7-Pentamethyldihydrobenzofuran-5-sulfonyl chloride
<b>PBP</b>	Penicillin binding protein
<b>PBS</b>	Phosphate-buffered saline
<b>PC</b>	Phosphatidylcholine
<b>PCR</b>	Polymerase chain reaction

<b>Pd(dppf)Cl<sub>2</sub></b>	1,1'-Bis(diphenylphosphino)ferrocene]dichloropalladium(II)
<b>PDB</b>	Protein Data Bank
<b>PE</b>	Phosphatidylethanolamine
<b>PEG</b>	Poly(ethylene glycol)
<b>PEtN</b>	Phosphoethanolamine
<b>PG</b>	Phosphatidylglycerol
<b>PI</b>	Propidium iodide
<b>Pin</b>	Pinacol
<b>PLL</b>	Photolabile linker
<b>Pra</b>	Propargylglycine
<b>PTFE</b>	Polytetrafluoroethylene
<b>Q, Gln</b>	Glutamine
<b>QC</b>	Quality control
<b>R, Arg</b>	Arginine
<b>RP-HPLC</b>	Reverse-phase high performance liquid chromatography
<b>rpm</b>	Revolutions per minute
<b>RT</b>	Room temperature
<b>RV</b>	Reaction vessel
<b>S, Ser</b>	Serine
<b>SDS</b>	Sodium dodecyl sulfate
<b>SM</b>	Sphingomyelin
<b>SPPS</b>	Solid-phase peptide synthesis
<b>T, Thr</b>	Threonine
<b>Tbp</b>	Transferrin binding proteins
<b>TBTA</b>	Tris[(1-benzyl-1 <i>H</i> -1,2,3-triazol-4-yl)methyl]amine
<b>tBu</b>	<i>Tert</i> -butyl
<b>TCA</b>	Trichloroacetimidate
<b>TCEP</b>	Tris-(2-carboxyethyl)phosphine
<b>TEAA</b>	Triethylammonium acetate
<b>Tf</b>	Transferrin
<b>TFA</b>	Trifluoroacetic acid

<b>TFE</b>	Trifluoroethanol
<b>THF</b>	Tetrahydrofuran
<b>TIS</b>	Triisopropylsilane
<b>TOF</b>	Time of flight
<b>Tris</b>	Tris(hydroxymethyl)aminomethane
<b>Trt</b>	Trityl
<b>UV</b>	Ultraviolet
<b>UV-vis</b>	Ultraviolet-visible spectroscopy
<b>V, Val</b>	Valine
<b>VRE</b>	Vancomycin-resistant <i>Enterococci</i>
<b>W, Trp</b>	Tryptophan
<b>WHO</b>	World Health Organization
<b>WT</b>	Wild-type
<b>Y, Tyr</b>	Tyrosine
<b>ε</b>	Molar absorptivity constant

## ACKNOWLEDGEMENTS

I would first like to thank my advisor, Professor Jianmin Gao. The amount of enthusiasm he has for science and the research we have done in this lab has kept me optimistic and working hard towards my goals. I have always appreciated the attention he gave to making sure that I was interested in what I was working on and that it was something helping me towards my long term goals.

I would also like to thank my committee, Professor Eranthie Weerapana and Abhishek Chatterjee, for their thoughtful feedback and for taking the time to read and review my dissertation.

Coming into graduate school, I expected for it to be some of the worst and most stressful years of my life. Although they have certainly been stressful, the people I have met at BC have kept me laughing and enjoying the time I have spent here even when everything was going wrong. One of the things I loved and appreciated the most was the close knit department we have, especially between our group and the Weerapana and Chatterjee labs. Knowing that there was always someone who I could ask for help when I was learning something new or having a problem I couldn't work out got me through a lot of rough

patches in my projects. I would especially like to thank those I have directly collaborated with, including Aaron Mauris.

I would like to thank all of my co-workers. Our lab has been a lively place to come to work and I would like to say we were more than just co-workers but also friends. I worked side-by-side with Kaicheng Li on my last project for the past year. With his “culture differences” and hilarious anecdotes, we have become good friends and have pushed each other to get our best work done. Kelly McCarthy and Sam Cambray have been some of my best friends here at BC. I’m really going to miss our countless coffee walks to Dunkin’ and lunches outside.

There are two people I met at BC who have really changed my life and made the biggest difference on it. First, Elsie Yu, my roommate and best friend for the past five years. I would not have made it to this point without you. You have been there every step of the way since open house when we first met to know as I’m about to move away. I could always count on you for a shoulder to cry on or to order food with when we were both too lazy to cook. You will forever be one of my best friends.

To Jacob, for all of the love you have brought into my life over the past two years. You have supported me through some of my most difficult times, sometimes being the only thing that could make me smile. You have helped me grow as a scientist and as a person. You are one of the best things I have in my life and I cannot wait to see what life brings us together. I love you.

To my biggest support group, my family. To my brothers and sisters, Kristina & Jamie, Jason & Jenn, Keith & Sam, Laura & Scott, Sheena and Tara: I cannot imagine life without any of you. For the original six, you will always be my best friends and my greatest comfort. Being your sister and having you all as wonderful role models has gotten me where I am today. To my grandparents, aunts, uncles and cousins, thank you for all the support, love and encouragement you have given me through the years.

Finally, to Mom and Dad, who have given me unwavering love and support throughout my life, all while showing me the best example of what love is. I will never be able to thank you enough for everything you have done for me and for making me the strong, independent woman I am today. This thesis reflects your hard work as much as it does mine.



**Chapter 1**  
**Introduction**

## 1.1 Antibiotic Resistance

Before the discovery of penicillin by Alexander Fleming<sup>1</sup>, infectious diseases were a life-threatening condition. But as this and other antibiotics began to see civilian use nearly 80 years ago, health care was revolutionized. Mortality rates from infections have steadily decreased in this time compared to unrelated causes of death (Figure 1-1).<sup>2</sup> Additionally, it opened the door for other lifesaving practices, such as surgery for repair to internal organs or organ transplants, by making them less risky post-op. However, these amazing benefits have not come without their troubles. Perhaps due to the rapid increase in their use, the misuse or the over prescribing of different antibiotics, we are currently facing a refreshed epidemic caused by bacterial resistance to antibiotics.

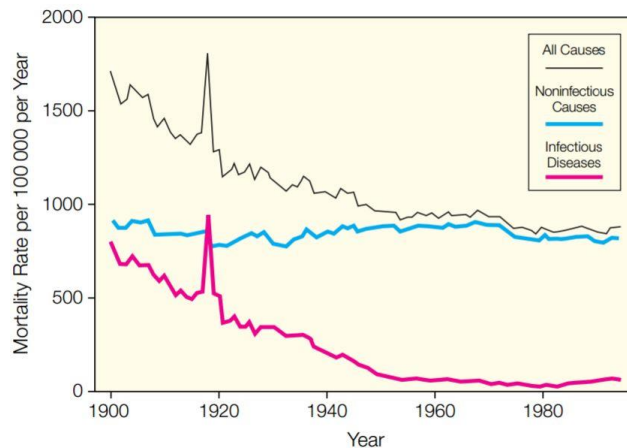


**Figure 1-1:** Curves showing the crude mortality rate for all causes (black), non-infectious diseases (blue) and infectious diseases (pink). A clear decrease in the blue line compared to the pink line can be observed in the late 1930's, around the time of deployment of penicillin and other early antibiotics. Taken from ref. 2.

The increased use of antibiotics put pressure on the bacteria to come up with designed mechanisms against them for their own survival, and this is a challenge they met at full force. On average, antibiotics survive on the market for

about a decade before resistance can be observed (Figure 1-2).<sup>3,4</sup> As the golden era of antibiotics came to an end in the 1960s, it became clear that the practice of mining soil for natural products with antibiotic properties was no longer going to be sufficient to keep up with the new demand.<sup>5</sup> The lag that followed in novel antibiotic discovery gave bacteria ample time to develop greater resistances, and this was notably observed in the clinic. Taking penicillin as an example, practically all clinical gram-positive infections were susceptible to this treatment in the late 1940's but by the late 1990's, a high majority of these were now resistant to not only penicillin but also other important drugs from the same class.<sup>6</sup> With the number of available drugs to treat such infections dwindling, there has been a near desperate initiative towards the discovery of novel antibiotics.

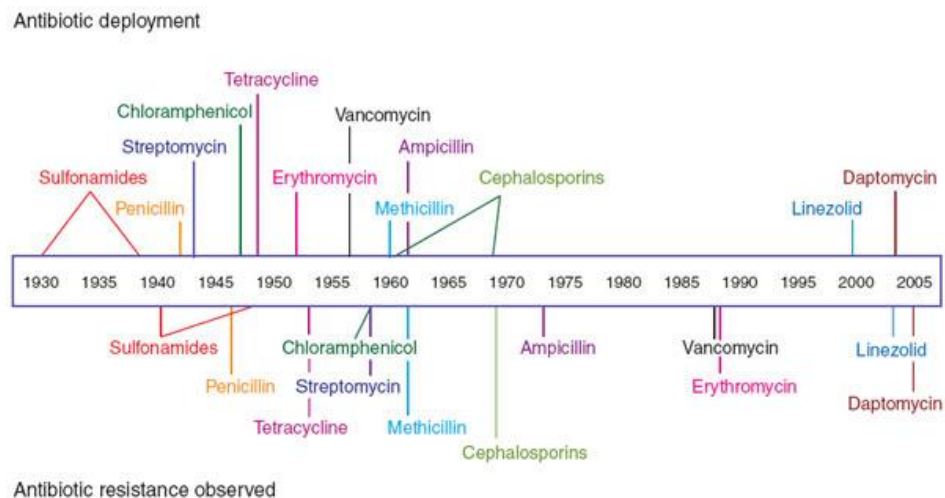


**Figure 1-2:** Timeline demonstrating the year of antibiotic deployment (top) and when the first resistance was observed in the clinic (bottom). Taken from ref. 4.

Antibiotic resistance has grown to such a dangerous level for several reasons. First of all, several antibiotics use the same mechanism of action to target bacteria. This creates strains resistant to one or more classes of antibiotics instead

of just a single drug.<sup>5</sup> Also, there are several non-specific resistance mechanisms that can be effective towards multiple classes of antibiotics; this includes decreased cell penetration and the expression of transmembrane proteins that act as efflux pumps for varied hydrophobic molecules.<sup>7,8</sup> Resistance mechanism of these types require especially creative strategies to circumvent them. Finally, there is the risk of horizontal gene transfer across species. Commonly, several different species of bacteria can be found in close proximity. With this probability of contact, resistance genes are being found in some species with no prior deliberate exposure to a specific antibiotic. It is also not unlikely that this occurred before commercial use of these drugs, as they are natural products and many come from different bacterial species. This exchange of genes should be considered more threatening, as it can lead to “superbugs” with resistance to several different antibiotics.<sup>9</sup>

In the late 1950's, scientists began to seek a way to fight against resistant infections in the clinic. An early example of this was the development of  $\beta$ -lactamase inhibitors. Responsible for resistance to penicillin and other  $\beta$ -lactam-containing antibiotics (Figure 1-3A), the first  $\beta$ -lactamase was discovered in *E. coli* in 1940, before penicillin was even on the market as an antibiotic.<sup>10</sup>  $\beta$ -lactamases are enzymes which catalyze the opening up of the  $\beta$ -lactam ring in these antibiotics, rendering them inactive. Early  $\beta$ -lactamase inhibitors, such as clavulanic acid (Figure 1-3B), behaved as “suicide inhibitors;”<sup>11</sup> designed to favor binding to enzyme with a structure mimicking the drug, they formed covalent

adducts with the enzyme, inactivating it. When the two molecules are co-administered, this allows the  $\beta$ -lactam antibiotic to survive and act as was intended. The first example of a drug combination like this on the market was amoxicillin-clavulanate, approved in the United States in 1984.<sup>12</sup> Unfortunately, within several years of clinical use, species were isolated with resistance to these types of combinations.

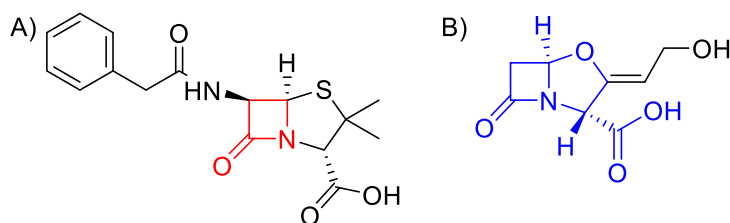


**Figure 1-3:** Chemical structures of (A) antibiotic penicillin with the common  $\beta$ -lactam structure in red and (B)  $\beta$ -lactamase inhibitor, clavulanic acid. The  $\beta$ -lactamase inhibitors form a more stable covalent intermediate with the enzymes responsible for  $\beta$ -lactam resistance, preventing them from deactivating the more potent drug.

Perhaps the greatest lesson that has been learned from this history of antibiotic resistance is that new discovery methods are necessary to combat it. Additionally, the focus should be put on novel mechanisms of action, such that new drugs can have a chance for a longer lifetime on the market before resistance is overwhelming.

### ***1.2 From the End of the Golden Era to Now: The State of Antibiotic Discovery***

The approach popularized by Selman Waksman and Fleming of mining soil for novel antibiotics was quickly adopted by many pharmaceutical companies after seeing the success of penicillin.<sup>13</sup> This strategy was initially extremely successful; nearly two-thirds of all known antibiotic drugs were discovered from

species of *Streptomyces* using this method. However, primarily due to the rediscovery of known compounds,<sup>5,14</sup> this type of discovery venture has seen little success in producing anything novel since the mid-1980s. With the rate of bacterial resistance quickly catching up to that of drug discovery, it was clear that an alternative was vehemently needed.

Near the end of the golden era of antibiotic discovery, two different classes of synthetic antibiotics were developed: fluoroquinolones and oxazolidinones (Figure 1-4). Fluoroquinolones were a crucial discovery, as they were observed to have broad-spectrum activity; at the time, ciprofloxacin was reported as effective in 98.2% of more than 20,000 tested bacterial strains.<sup>15</sup> Fluoroquinolones were especially important because they acted through a novel mechanism and therefore were not susceptible to the resistances mechanisms known at the time. Additionally, they were relatively slower to develop resistance than earlier antibiotics, as they target two separate proteins.<sup>16</sup> To date, more than 10,000 quinolones have been synthesized.

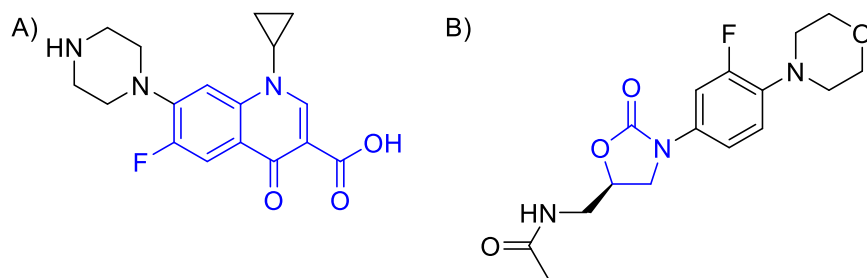


**Figure 1-4:** Structures of example A) fluoroquinolone (ciprofloxacin) and B) oxazolidinone (linezolid) synthetic antibiotics. The core structures for each family of antibiotics is shown in blue.

When first discovered, oxazolidinones were considered relatively less ground breaking. Although the first patent for this class of antibiotics was obtained by Dupont in 1978, it took nine years before any derivative was tested clinically in humans and another 13 years before the first drug (linezolid) was put on the market.<sup>17</sup> Currently considered a “reserve antibiotic,” linezolid is active against all gram-positive species, importantly including MRSA and vancomycin resistant *Enterococci* (VRE). So far, only few cases of resistance have been reported.<sup>18</sup>

The success of fluoroquinolones and oxazolidinones, partnered with the decline in natural product discovery, led to a drive towards synthetic antibiotic discovery in the late 1980's to early 1990's. These efforts were notably increased in the mid-90's as a result of the determination of a complete bacterial genome.<sup>19</sup> With this on hand, the discovery and validation of new possible targets for antibiotics grew. Furthermore, by studying the similarities across species, the focus was put on targets with the best chance at broad-spectrum applicability.<sup>20</sup>

At this time, many pharmaceutical companies began to invest in high-throughput screening (HTS) programs. In 2007, GlaxoSmithKline published a review of their findings over the seven years of HTS campaigns.<sup>21</sup> Although they were successful in identifying several potential targets for antibiotic treatments, through 70 campaigns they were only able to obtain five leads; none of these progressed to clinical trials. The efforts of GSK are mirrored in many of its

competitors that took similar approaches to antibiotic discovery.<sup>19</sup> There are many reasons why so many failed. Unfortunately, what appeared to be emphasized by these efforts is that the previous natural products appeared to have privileged structures to allow them to penetrate bacterial cells, and designing novel structures towards this goal appeared to be more nontrivial than anticipated. This observation and the minimal return on expensive investments led many pharmaceutical companies to back out of antibiotic discovery all together.

Due to the mass abandonment of this direction of research, there have been few new clinically useful classes of antibiotics discovered since daptomycin in 1985.<sup>5</sup> Currently, many discovery efforts have shifted back to natural product mining, looking at previously untapped sources in the hope of avoiding rediscovery of known compounds.<sup>22,23</sup>

### ***1.3 Host-Defense Peptides (HDPs)***

Host-defense peptides (HDPs), as part of nature's front line of defense against infection,<sup>24,25</sup> have been a severely neglected class of antibiotics. Being found in nearly every life form, HDPs are vastly abundant. Most commonly, these peptides are short, cationic and amphiphilic in structure.<sup>26</sup> These features allow many of them to fold well into and disrupt cellular membranes of bacteria, a non-specific target that gives them broad-spectrum activity.<sup>27-29</sup> Initially given the name of antimicrobial peptides (AMPs), it was later observed that peptides in this



class can also behave as innate immunity modulators, changing their moniker to HDPs to demonstrate this broader role.<sup>30</sup>

As mentioned above, many HDPs have been observed to have membrane-targeting antimicrobial activity. They are believed to be effective by folding into the membrane and disrupting its integrity, typically creating pores or causing full lysis of the cell. Several general models have been proposed for how the peptides are able to do this,<sup>27</sup> but usually this is best described in a case-by-case basis. With further studies of their behavior, several more specific mechanisms for how HDPs kill bacteria have been discovered.<sup>24,31</sup> For example, nisin, produced by *Lactococci* and commonly used as a food preservative, was found to act by binding lipid II with high affinity to disrupt the cell wall.<sup>32</sup>

#### ***1.4 Commercial Use of Peptides as Antibiotics***

Over the years, some HDPs have found commercial approval and success, such as nisin,<sup>33</sup> polymyxin B,<sup>34</sup> and daptomycin,<sup>35</sup> but most have not. Hurdles met with the development of HDPs include those met by peptide drugs in general, such as expensive costs of large scale synthesis and short serum half-lives due to proteolytic degradation. Additionally, many have been limited in clinical use due to toxicity caused by a lack of membrane selectivity.<sup>26</sup> Nonetheless, as solutions to many of these issues are being investigated, HDPs still remain a promising prospect in antibiotic research.

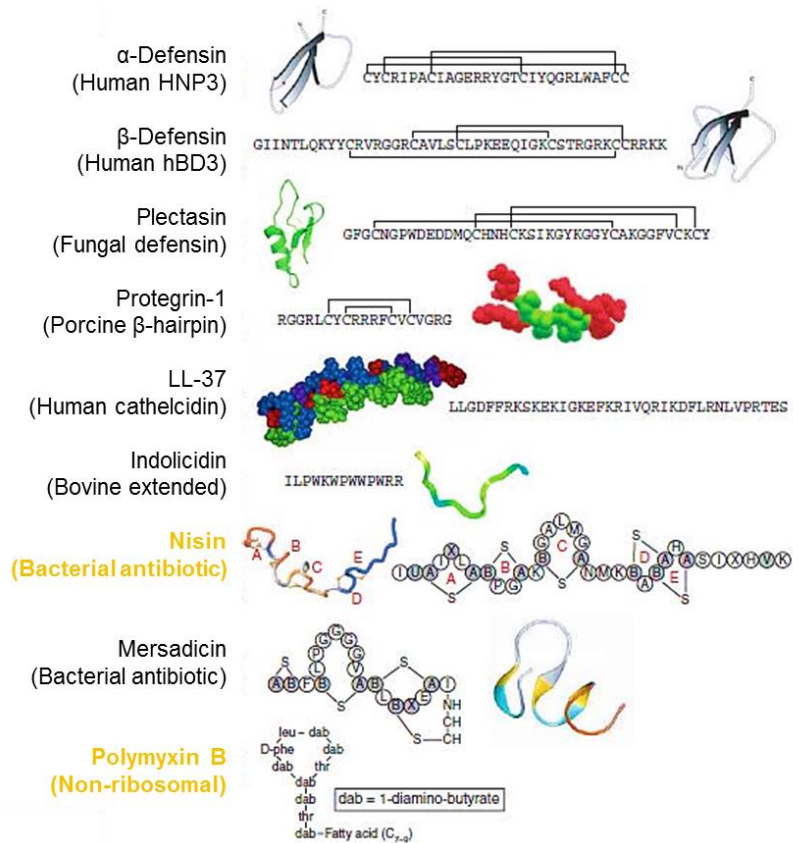


**Figure 1-5:** Notable examples of HDPs and their sources. Highlighted in yellow are nisin, which is currently used as a food preservative, and Polymixin B, which is approved for use with drug-resistant gram-negative infections. Modified from ref. 26.

### 1.4.1 Nisin

Lantibiotics have been a prominent class of HDPs studied for their antimicrobial properties.<sup>36</sup> They contain multicyclic structures, characterized by their thioether linkages. Along with their observed activities towards gram-positive bacteria, they are also attractive due to their low cytotoxicity and low tendency to produce antimicrobial resistance. A prominent example from this class is nisin.<sup>33</sup>

Nisin has been used since the mid-1980s in the United States as a broad-range food preservative, preventing spoiling caused by bacteria growth. Considering its usage, nisin's mechanism of action has been well studied.<sup>32,37,38</sup> By binding to lipid II, it can both inhibit peptidoglycan synthesis and use lipid II as an anchor for membrane pore formation. This type of dual functionality is typically suggested to be partially responsible for the lower occurrence of antimicrobial resistance. However, nisin and other lantibiotics involve a more complicated synthetic route; this may be one of the primary reasons they have not been utilized clinically as of yet.

#### 1.4.2 Polymyxins

Polymyxin B is a mixture of lipopeptides with a bactericidal mechanism via permeabilization of the outer-membrane of gram-negative species.<sup>39</sup> This detergent-like mechanism allows for polymyxins to behave as a broad-spectrum drug. Produced by *Bacillus polymyxa* and related species, the peptide mixture is collected and purified after the fermentation of the bacteria in an optimized growth media.<sup>40</sup> Although five different polymyxin mixtures have been reported, only two have been used clinically: polymyxin B and E (colistin).

When they were first introduced in the 1950s, polymyxins were not studied well enough to reveal their nephrotoxic side effects.<sup>41</sup> As these became more apparent, the use of polymyxin B and colistin became much less frequent and now both are reserved for use in gram-negative infections with resistance to other

antibiotics.<sup>42</sup> With interest in these drugs revived, further studies into their pharmacokinetics and pharmacodynamics have allowed for optimized dosing protocols, reducing this side effect.

### 1.4.3 Daptomycin

The most recent novel class of antibiotic to be approved, daptomycin, is also a lipopeptide, with a similar structure to polymyxins. However, it is specific towards gram-positive bacteria, with a mechanism of action involving pore formation mediated by the binding of the phosphatidylglycerol head group.<sup>43</sup> Originally discovered in the late 1980s by researchers at Eli Lilly,<sup>44</sup> daptomycin originally failed in phase I/II clinical trials due to side effects towards skeletal muscle.<sup>45</sup> Only after its rights were acquired by Cubist Pharmaceuticals in 1997 was daptomycin successful in FDA-approval for gram-positive infections. In a dog study performed by Cubist, it was found that the negative side effects towards the skeletal muscle could be abated through a careful dosing regimen.<sup>46</sup>

Originally expected to be resistant to resistance, daptomycin resistance was reported in the United States.<sup>47</sup> Most frequently, resistance is reported *in vivo* during patient treatment, making mechanisms difficult to reproduce *in vitro*. Although the antimicrobial mechanism of resistance has not yet been confirmed, it is speculated to be caused by target modification. Specifically, resistance is believed to result from the acylation of the PG head group, preventing the binding of daptomycin.<sup>48</sup>

## 1.5 Conclusion

The need for new and novel antibiotics is becoming overwhelming. It has become apparent that the traditional discovery platform of panning for small molecule natural products will not be sustainable, as the occurrences of infections resistant to these classes of drugs is growing. A somewhat neglected class of natural product antibiotics is host defense peptides (HDPs).

Recently, with the approval of lipopeptide daptomycin and advances in the synthesis and formulation of these peptides, HDPs have a revived potential for the goals against antibiotic resistance. Herein, we describe the work that we have been doing towards discovering a novel peptide antibiotic. Specifically, we have addressed this goal through three different avenues:

- 1) The use of unnatural cationic amino acids to gain selectivity for natural antimicrobial peptide, gramicidin A (**Chapter 2**)
- 2) Overcoming resistance towards cationic antimicrobial peptides (CAMPs) through the use of amine-specific 2-acetylphenyl boronic acid (2-APBA) warheads (**Chapter 3**)
- 3) Library discovery of novel peptide structures containing 2-APBA warheads by screening against a validated bacterial target (**Chapter 4**).

## 1.6 References

- (1) Fleming, A. *Br. J. Exp. Pathol.* **1929**, *10*, 226–236.

- (2) Armstrong, G. L.; Conn, L. A.; Pinner, R. W. *JAMA* **1999**, 281 (1), 61.
- (3) Palumbi, S. R. *Science* **2001**, 293 (5536), 1786–1790.
- (4) Clatworthy, A. E.; Pierson, E.; Hung, D. T. *Nat. Chem. Biol.* **2007**, 3 (9), 541–548.
- (5) Lewis, K. *Nat. Rev. Drug Discov.* **2013**, 12 (5), 371–387.
- (6) Abramson, M. A.; Sexton, D. J. *J. Infect. Dis.* **1999**, 20 (6), 408–411.
- (7) Wright, G. D. *Chem. Commun.* **2011**, 47 (14), 4055.
- (8) Li, X.-Z.; Nikaido, H. *Drugs* **2004**, 64 (2), 159–204.
- (9) Levy, S. B.; Marshall, B. *Nat. Med.* **2004**, 10 (12s), S122–S129.
- (10) Abraham, E. P.; Chain, E. *Nature* **1940**, 146, 837.
- (11) Bush, K. *Clin. Microbiol. Rev.* **1988**, 1 (1), 109–123.
- (12) Drawz, S. M.; Bonomo, R. A. *Clin. Microbiol. Rev.* **2010**, 23 (1), 160–201.
- (13) Drews, J. *Science* **2000**, 287 (5460), 1960–1964.
- (14) Baltz, R. H. *J. Ind. Microbiol. Biotechnol.* **2006**, 33 (7), 507–513.
- (15) Mohr, K. I. In *How to Overcome the Antibiotic Crisis*; Springer International Publishing, 2016; pp 237–272.
- (16) Hooper, D. C. *Clin. Infect. Dis.* **2000**, 31 (Supplement 2), S24–S28.
- (17) Batts, D. H. *Oncology* **2000**, 14 (Supplement 6), 23–29.
- (18) Pandit, N.; Singla, R. K.; Shrivastava, B. *Int. J. Med. Chem.* **2012**, 2012, 159285.
- (19) Chan, P. F.; Holmes, D. J.; Payne, D. J. *Drug Discov. Today Ther. Strateg.* **2004**, 1 (4), 519–527.

- (20) Brown, J. R.; Warren, P. V. *Drug Discov. Today* **1998**, 3 (12), 564–566.
- (21) Payne, D. J.; Gwynn, M. N.; Holmes, D. J.; Pompliano, D. L. *Nat. Rev. Drug Discov.* **2007**, 6 (1), 29–40.
- (22) Fischbach, M. A.; Walsh, C. T. *Science* **2009**, 325 (5944), 1089–1093.
- (23) Clardy, J.; Fischbach, M. A.; Walsh, C. T. *Nat. Biotechnol.* **2006**, 24 (12), 1541–1550.
- (24) Zasloff, M. *Nature* **2002**, 415 (6870), 389–395.
- (25) Shai, Y. *Curr. Pharm. Des.* **2002**, 8 (9), 715–725.
- (26) Hancock, R. E. W.; Sahl, H.-G. *Nat. Biotechnol.* **2006**, 24 (12), 1551–1557.
- (27) Brogden, K. A. *Nat. Rev. Microbiol.* **2005**, 3 (3), 238–250.
- (28) Shai, Y. *Biochim. Biophys. Acta* **1999**, 1462 (1–2), 55–70.
- (29) Huang, H. W. *Biochemistry* **2000**, 39 (29), 8347–8352.
- (30) Hilchie, A. L.; Wuerth, K.; Hancock, R. E. W. *Nat. Chem. Biol.* **2013**, 9 (12), 761–768.
- (31) Hancock, R. E. W.; Sahl, H.-G. *Nat. Biotechnol.* **2006**, 24 (12), 1551–1557.
- (32) Brötz, H.; Josten, M.; Wiedemann, I.; Schneider, U.; Götz, F.; Bierbaum, G.; Sahl, H.-G. *Mol. Microbiol.* **1998**, 30 (2), 317–327.
- (33) Kindrachuk, J.; Jenssen, H.; Elliott, M.; Nijnik, A.; Magrangeas-Janot, L.; Pasupuleti, M.; Thorson, L.; Ma, S.; Easton, D. M.; Bains, M.; Finlay, B.; Breukink, E. J.; Sahl, H.-G.; Hancock, R. E. *Innate Immun.* **2012**, 19 (3), 315–327.
- (34) Kvitko, C. H.; Rigatto, M. H.; Moro, A. L.; Zavascki, A. P. *J. Antimicrob.*

- Chemother.* **2011**, 66 (1), 175–179.
- (35) Baltz, R. H.; Miao, V.; Wrigley, S. K. *Nat. Prod. Rep.* **2005**, 22 (6), 717.
- (36) Smith, L.; Hillman, J. D. *Curr. Opin. Microbiol.* **2008**, 11 (5), 401–408.
- (37) Wiedemann, I.; Breukink, E.; van Kraaij, C.; Kuipers, O. P.; Bierbaum, G.; de Kruijff, B.; Sahl, H. G. *J. Biol. Chem.* **2001**, 276 (3), 1772–1779.
- (38) Hsu, S.-T. D.; Breukink, E.; Tischenko, E.; Lutters, M. a G.; de Kruijff, B.; Kaptein, R.; Bonvin, A. M. J. J.; van Nuland, N. a J. *Nat. Struct. Mol. Biol.* **2004**, 11 (10), 963–967.
- (39) Vaara, M. *Microbiol. Rev.* **1992**, 56 (3), 395–411.
- (40) Bushby, S. R. M. Manufacture of polymyxins b and e. US 2,759,868, 1956.
- (41) Cunha, B. A. *Med. Clin. North Am.* **2006**, 90 (6), 1089–1107.
- (42) Vaara, M. *Curr. Opin. Microbiol.* **2010**, 13 (5), 574–581.
- (43) Pogliano, J.; Pogliano, N.; Silverman, J. A. *J. Bacteriol.* **2012**, 194 (17), 4494–4504.
- (44) Debono, M.; Barnhart, M.; Carrell, C. B.; Hoffmann, J. A.; Occolowitz, J. L.; Abbott, B. J.; Fukuda, D. S.; Hamill, R. L.; Biemann, K.; Herlihy, W. C. *J. Antibiot. (Tokyo)*. **1987**, 40 (6), 761–777.
- (45) Eisenstein, B. I.; Oleson, Jr., F. B.; Baltz, R. H. *Clin. Infect. Dis.* **2010**, 50 (s1), S10–S15.
- (46) Oleson, F. B.; Berman, C. L.; Kirkpatrick, J. B.; Regan, K. S.; Lai, J. J.; Tally, F. P.; Tally, F. P. *Antimicrob. Agents Chemother.* **2000**, 44 (11), 2948–2953.
- (47) Sharma, M.; Riederer, K.; Chase, P.; Khatib, R. *Eur. J. Clin. Microbiol. Infect.*



*Dis.* **2008**, 27 (6), 433–437.

- (48) Bayer, A. S.; Schneider, T.; Sahl, H.-G. *Ann. N. Y. Acad. Sci.* **2013**, 1277 (1), 139–158.

**Chapter 2**  
**Creating Selectivity with Cationic Mutants of Gramicidin A**

## 2.1 Introduction

### 2.1.1 Gramicidin A

Gramicidin A (gA) is a HDP produced by *Bacillus brevis* first discovered in the 1930s.<sup>1</sup> As part of the bacteria's external self-defense mechanism, gA is released from the cells with a mixture of related peptides into their surroundings. With a unique structure of alternating L- and D-amino acids, the active form of gA folds into lipid bilayers as a  $\beta$ -helix.<sup>2,3</sup> This secondary structure displays all of the side chains on the outside of the helix, where they can interact with the tails of membrane phospholipids. With 6.3 residues per turn, the folded helix has an inner diameter of about 4 Å. A monomer of the peptide, being about 10 Å long, spans half of the typical membrane lipid bilayer. Peptides in opposite faces of the membrane can dimerize in a head-to-head fashion via six hydrogen bonds.<sup>4,5</sup> When this occurs, a channel is produced that is large enough to accommodate monovalent cations and water molecules.<sup>6,7</sup>

Primary sequence: formyl-V-G-A-dL-A-dV-V-dV-W-dL-W-dL-W-dL-W-NHCH<sub>2</sub>CH<sub>2</sub>OH

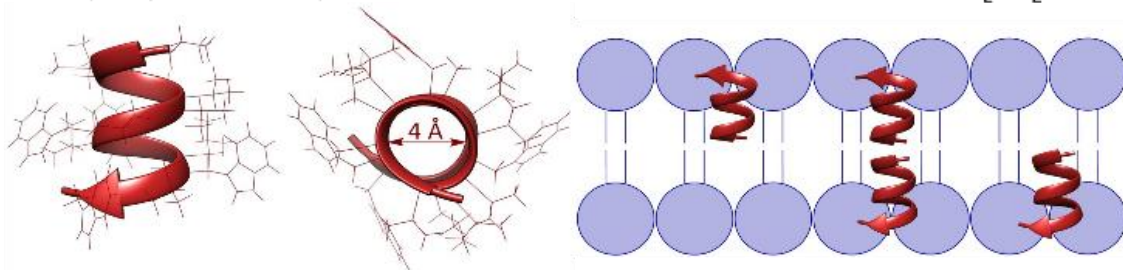


**Figure 2-1:** Primary sequence and secondary structure of gramicidin A. Its  $\beta$ -helical structure, showing all of the side chains being projected on the outside, produces a 4 Å wide pore. Also shown is the folding of gA in a lipid bilayer, with gating of the channel occurring due to the formation and dissociation of the dimer. PBD file 1JNO, solved by solution phase NMR in micelles.

The antimicrobial activity of gA lies in its channel forming ability. As it allows for the passive movement of small cations across the membrane, the critical ion gradient between the cytoplasm and the extracellular environment is disrupted upon treatment with the peptide, leading to cell death. As part of the mixture tyrothricin, gA and its related structures gB and gC were one of the first commercially available antibiotics.<sup>8,9</sup> However, the high hydrophobic content of gA makes it non-selective, with potent activity towards eukaryotic cells also observed. As such, gramicidin A's clinical use has since been limited to part of a topical mixture of antibiotics, called Polysporin, in Canada.<sup>10</sup>

Gramicidin A has many attractive features for development as a systemic antibiotic.<sup>10,11</sup> This includes its alternating sequence of natural and unnatural amino acids as well as its modified N- and C-termini. Both of these features are beneficial for stability from proteolytic degradation. The lack of the difficult linkages prevalent in other HDPs, such as the thioether bonds found in lantibiotics, makes it relatively more simple to scale up its chemical synthesis. Finally, its broad spectrum activity towards gram-positive bacteria and general mechanism of action increases its possibilities for clinical use. The greatest drawbacks preventing gA from widespread use is its aforementioned high toxicity towards human cells along with its miniscule water solubility.

The common cationic charge of HDPs is believed to contribute to their selectivity for microbial membranes.<sup>12</sup> An inherent difference between microbial and eukaryotic membranes is their lipid composition, especially on the outer leaflet. Microbial membranes are predominantly made up of negatively charged phospholipids, such as phosphatidylglycerol and cardiolipin. In contrast, mammalian cell membranes are composed of higher amounts of zwitterionic lipids, including phosphatidylcholine and sphingomyelin. HDPs including cationic residues gain selectivity by taking advantage of favorable electrostatic interactions for membrane association.

Previously, our group had worked on mimicking this characteristic for selectivity by mutating different residues on gA to cationic lysines or arginines.<sup>10,11</sup> Briefly, peptides with specific combinations of cationic residues in place of D-leucines at positions 10, 12 and 14 were synthesized and studied for their ability to tune the activities from those of wild type gA. These positions were chosen as they lie near the membrane-water interface and thus would best tolerate mutations that result in a decrease in hydrophobicity.<sup>13,14</sup> From this, we learned that increasing cationic charge leads to decreased toxicity to human red blood cells, as measured by the leakage of hemoglobin. The red blood cells showed the greatest resistance to hemolysis with gA-5, which is the triple lysine mutant of gA. However, a trend in decreasing potency towards the gram-positive bacteria *Staphylococcus aureus* was also observed for the peptides with multiple cationic

charges. This was most likely a result of the difference in hydrophobicity between leucine and lysine, decreasing the general ability of the peptide to favorably interact with lipid tails.<sup>10</sup> Attempts to tune this potency back with di- and trimethylated versions of lysine were not as successful as hoped for; it would appear that the hydrogen bonding capability of the lysine plays an important role in the peptide's interactions with the lipid's phosphate group.<sup>11</sup> These results do suggest, however, that attempts to tune the net hydrophobicity of the peptide via monoalkylation of the lysine side chain may be more fruitful.

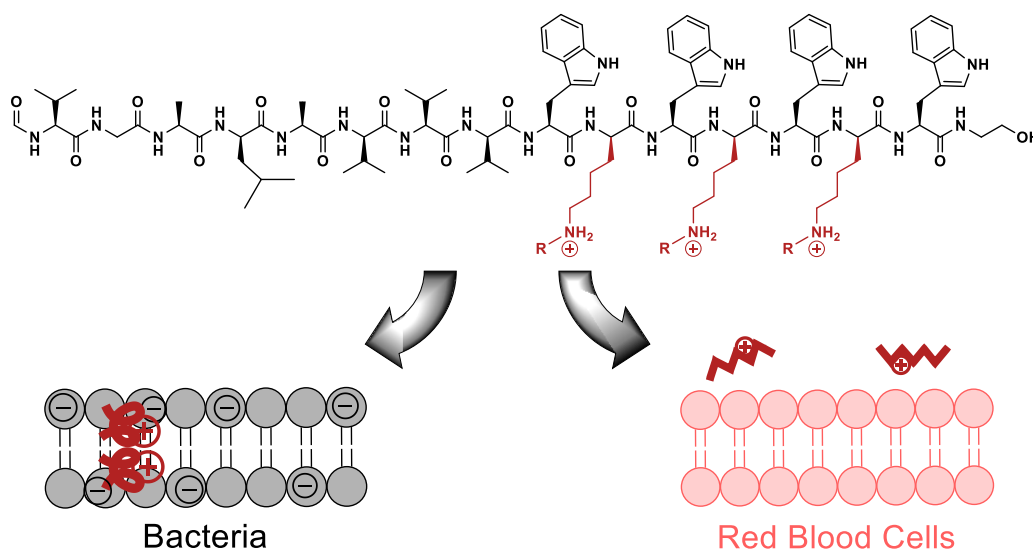


**Figure 2-2:** Hypothesis of cationic gA mutants for selectivity. The incorporation of monoalkylated lysines should maintain cationic charge for selectivity towards bacterial membranes over red blood cells. By tuning the alkyl group on lysine, we expect to be able to tune the antimicrobial potency.

We hypothesized that a systematic tuning of the hydrophobicity, and therefore the membrane association, could be achieved by incorporating

monoalkylated D-lysine analogues into the gA sequence at positions 10, 12 and 14 (Figure 2-2). By synthesizing D-lysine with various substitutions, we sought to determine a structure activity relationship between the different analogues. Various potencies of these cationic gA mutants were observed towards gram-positive bacteria, including a strain of methicillin-resistant *S. aureus* (MRSA). Additionally, two of the mutants, the benzyl-lysine (Figure 2-3D, gA3K(Bn)) and 4-(aminomethyl)benzyl-lysine (Figure 2-3H, gA3K(4AMBn)) peptides, showed potent activity against important gram-negative bacteria, which is an unprecedented observation for gA peptides. Furthermore, gA3K(4AMBn) showed little hemolytic activity at its minimum inhibitory concentration (MIC) for the tested bacteria, indicating a high degree of selectivity was maintained. Overall, the presented results suggest monoalkylation and subsequent incorporation of lysine analogues into gramicidin A is a viable strategy to achieve both high potency and selectivity.

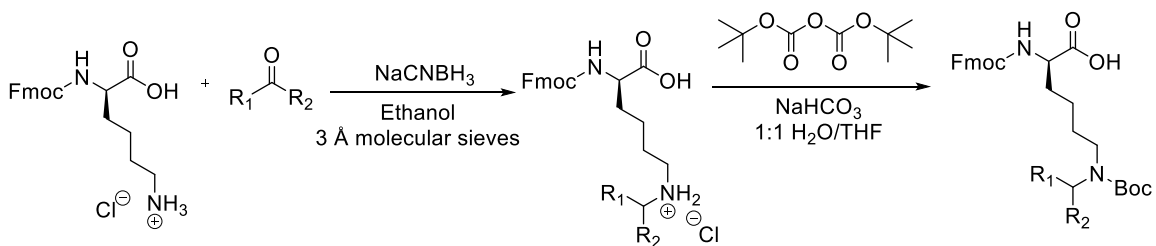
## ***2.2 Synthesis of gA Mutants Containing Alkylated Lysines***

### ***2.2.1 Synthesis of Alkylated Lysines***

In our initial work with di- and trimethylated lysine, Fmoc-D-Lys(Me)<sub>2</sub>-OH was synthesized via reductive amination with formaldehyde as the alkylating agent and sodium cyanoborohydride as the hydride donor; to ensure full conversion to the dimethyl species, the reaction was performed using 5 eq of

formaldehyde.<sup>11</sup> We envisioned that monoalkylated analogues of lysine could be obtained by carefully controlling the stoichiometry of lysine to alkylating agent and the time of the reaction.

*Scheme 2-1: The General Synthetic Route for Monoalkylated Lysine Derivatives in Preparation for Solid-Phase Peptide Synthesis*



In reductive amination, the alkylating agent used is the aldehyde or ketone derivative of the group you wish to install on the amine (see Scheme 2-1), making this strategy very attractive for us, as it would allow for very broad substrate options that were relatively inexpensive. Initially, we set out with the goal of synthesizing Fmoc-D-Lys(Me)-OH, such that we could use it for comparison to the di- and trimethylated versions of gA-5. Unfortunately, this product was not easily obtained from our proposed route. We turned instead to a protocol which first added a benzyl protecting group to the amine before methylation; the desired product could be obtained by removing the benzyl group with palladium on carbon under a H<sub>2</sub> atmosphere.<sup>15</sup> Although the desired intermediate of Fmoc-D-Lys(Bn,Me)-OH was obtained as the major product after subsequent reductive amination steps, debenzylation was never achieved.



In these initial attempts, we learned several things about the nature of this reaction. First of all, we observed a high percentage of Fmoc-deprotection during work-up of the reaction. It was found that, upon concentration of the product by rotary evaporation, the remaining sodium cyanoborohydride was cleaving the Fmoc group. This was easily remedied by first quenching the borohydride with 0.5 N HCl before extraction.

As was used for the synthesis of Fmoc-D-Lys(Me)<sub>2</sub>-OH, the initial starting material used was the formate salt of Fmoc-D-Lys-OH. However, this resulted in only about 50% conversion of the initial starting material during benzylation with a 1.3:1 ratio of Fmoc-D-Lys(Bn)-OH to Fmoc-D-Lys(Bn)<sub>2</sub>-OH. Upon switching to the HCl salt as a starting material, we were able to obtain up to 85% conversion of starting material with the product mixture being a 7:1 ratio of Fmoc-D-Lys(Bn)-OH to Fmoc-D-Lys(Bn)<sub>2</sub>-OH. This drastic difference led us to investigate the role of acid in the conversion of the free amine and the ratio of alkylated products. In order to do this, we used the free base Fmoc-Lysine-OH with varying amounts of trifluoroacetic acid (TFA) and monitored the reaction by analytical HPLC. Results can be seen in Table 2-1. After considering these results, we chose to use the conditions in the final entry of Table 2-1; this was due to HCl salt being three times less expensive than the free base. This general protocol was followed for all other lysine derivatives.

*Table 2-1: Optimization of Acidic Conditions for Benzylation of Lysine*

Starting Material	Equivalents TFA	Conversion	Ratio Mono:Di
Fmoc-Lysine-OH	0.3	57%	1.7:1
Fmoc-Lysine-OH	0.75	80.5%	4:1
Fmoc-Lysine-OH	1.0	82.5%	14:1
Fmoc-Lysine-OH	1.1	89%	10:1
Fmoc-Lysine-OH	1.5	42%	No dialkyl
Fmoc-Lysine-OH HCOOH Salt	0	52.5%	1.3:1
Fmoc-Lysine-OH HCl Salt	0	85%	7:1

The other condition optimized for this series of substrates was the reaction time for each aldehyde before the addition of sodium cyanoborohydride. Best displayed with the 2-pyridine carboxaldehyde substrate (Table 2-2), conversion of the starting material was dependent on allowing the association of the aldehyde and lysine to reach equilibrium before reduction. Without this step, we observed a quicker conversion of the monoalkylated product to the dialkylated, decreasing the overall conversion of the starting material as the aldehyde is consumed. As such, sodium cyanoborohydride was added to the reaction after one hour, balancing optimal conversion with reaction time efficiency. The two exceptions to this were the Fmoc-D-Lys(iPr)-OH and Fmoc-D-Lys(Cy)-OH. For both of these derivatives, ketones served as alkylating agents and no dialkylated product was observed. This is most likely due to steric hindrance of a second attack by the amine. Therefore, much higher concentrations of the ketone could be used and no pre-equilibration time was necessary. For the iPr substrate, the reaction was performed with its alkylating agent (acetone) as the solvent and still no dialkylation was observed.

**Table 2-2: Dependence of Equilibration Time on Alkylation with 2-Pyridine Carboxaldehyde**

Time Before Addition of NaCNBH <sub>3</sub>	Conversion of Lysine
0 min	24%
30 min	63%
1 hour	74%
12-14 hours	73%

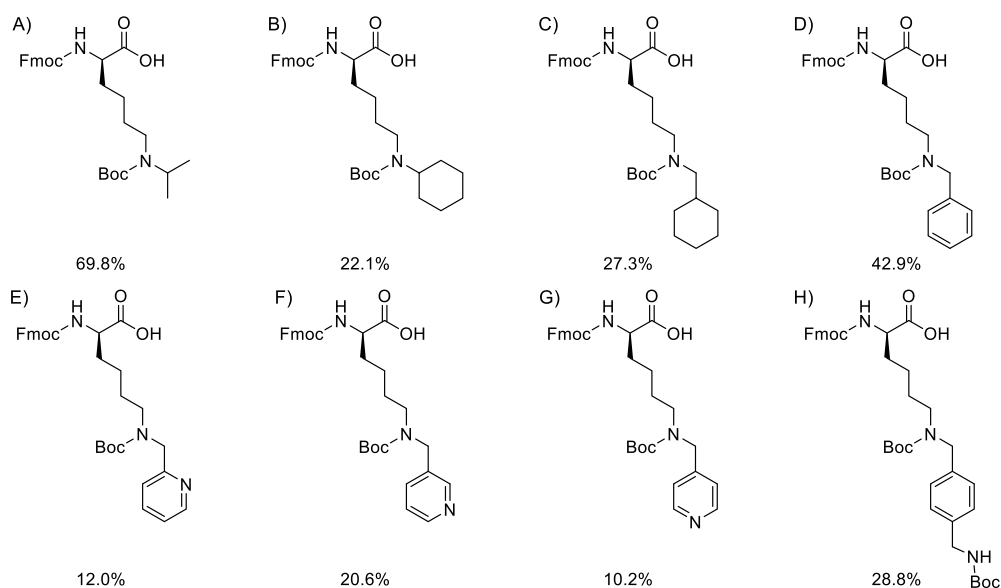


**Figure 2-3:** Structures of synthesized lysine derivatives. Under each structure is the overall yield of the two steps. A) Fmoc-D-Lys(iPr)(Boc)-OH; B) Fmoc-D-Lys(Cy)(Boc)-OH; C) Fmoc-D-Lys(CyMe)(Boc)-OH; D) Fmoc-D-Lys(Bn)(Boc)-OH; E) Fmoc-D-Lys(2-pyr)(Boc)-OH; F) Fmoc-D-Lys(3-pyr)(Boc)-OH; G) Fmoc-D-Lys(4-pyr)(Boc)-OH; H) Fmoc-D-Lys(4AMBn)(Boc)-OH.

After alkylation, the crude material was taken forward for Boc-protection of the side chain to prepare the amino acids for Fmoc-based solid-phase peptide synthesis (SPPS). Final products were purified using silica gel column chromatography. In total, eight derivatives were synthesized in sufficient yields

for peptide synthesis (Figure 2-3). The naming scheme for amino acids and their corresponding peptides are included in Table 2-3.

**Table 2-3:** List of Alkylated Lysines and their Corresponding Peptides

Amino Acid	Alkylating Substrate	Peptide Name
Fmoc-D-Lys(iPr)(Boc)-OH	Acetone	gA3K(iPr)
Fmoc-D-Lys(Cy)(Boc)-OH	Cyclohexanone	gA3K(Cy)
Fmoc-D-Lys(CyMe)(Boc)-OH	Cyclohexane carboxaldehyde	gA3K(CyMe)
Fmoc-D-Lys(Bn)(Boc)-OH	Benzaldehyde	gA3K(Bn)
Fmoc-D-Lys(2-pyr)(Boc)-OH	2-pyridine carboxaldehyde	gA3K(2pyr)
Fmoc-D-Lys(3-pyr)(Boc)-OH	3-pyridine carboxaldehyde	gA3K(3pyr)
Fmoc-D-Lys(4-pyr)(Boc)-OH	4-pyridine carboxaldehyde	gA3K(4pyr)
Fmoc-D-Lys(4AMBn)(Boc)-OH	<i>Tert</i> -butyl-4-formyl benzyl carbamate	gA3K(4AMBn)

### 2.2.2 Synthesis and Structural Characterization of Cationic gA Peptides

All peptides were synthesized using Fmoc/HBTU based SPPS, as previously reported by our group.<sup>10</sup> Briefly, the peptide is elongated on a Fmoc-Trp(Boc) functionalized Wang resin. The Formyl-Val-OH was installed as a peptide building block, instead of Fmoc-Val-OH, to incorporate the N-terminal modification. After this, the peptides were cleaved from resin using 40% ethanolamine in DMF then precipitated with water. TFA treatment afforded the crude side-chain deprotected peptide after ether precipitation. Finally, peptides were purified using preparative scale RP-HPLC and the pure products were characterized for purity (>95%) by LC/MS.

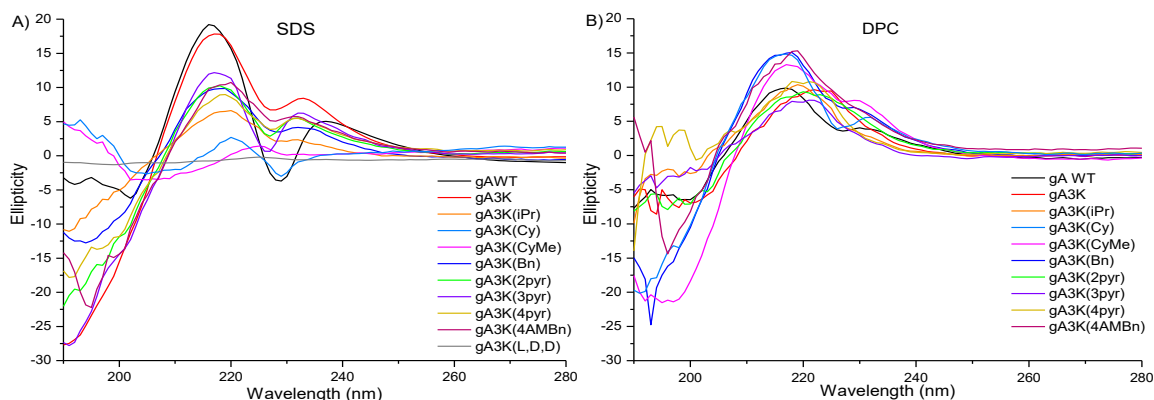


**Figure 2-4:** Circular dichroism signatures of gA mutants. Samples are prepared in A) SDS and B) DPC micelles. The designed negative control, gA3K(L,D,D), is unable to fold into a  $\beta$ -helix due to its clashing stereochemistry at residue 10. Both gA3K(Cy) and gA3K(CyMe) suffered from low solubility in the SDS micelle solution, which led to their poorly defined signature. Since both peptides had better solubility and a better signature in DPC, their structure was believed to be intact.

The mechanism of action of gA and related mutants are dependent on their ability to fold into a  $\beta$ -helix. As such, we sought to confirm that the mutations we had made to the peptide's sequence did not negatively affect its secondary structure. To do this, we analyzed the circular dichroism (CD) signature of each peptide in model membrane systems (Figure 2-4). The channel-forming conformation of gA is characterized by positive maxima at wavelengths of 218 and 235 nm.<sup>16,17</sup> Of these two points, the maxima at 218 nm corresponds to the backbone amides, being slightly red-shifted from a typical CD signature for  $\alpha$ -helices, distinguishing the two. The other maximum at 235 nm falls in the wavelength region where UV absorbent side chains tryptophan, tyrosine and phenylalanine are observed. This region is known to be altered based on the local environment of these side chains.

Given this information, we confirmed from studying our peptides in both SDS and DPC micelles that the  $\beta$ -helical backbone structure was intact. Unsurprisingly, the second maxima of the peptides did not overlap well with that of the wild type structure, as the mutations occurring at the residues surrounding the tryptophans are expected to have an effect on their local environment. Included as a negative control is peptide gA3K(L,D,D), in which the stereochemistry of residue 10 is reversed. As can be observed from its flat CD signature in SDS micelles, this peptide is unable to fold into a  $\beta$ -helix due to this side chain mismatch.

Two peptides, namely gA3K(Cy) and gA3K(CyMe), suffered from poor solubility with SDS micelle solutions, leading to a dampened signal. However, their improved signatures with DPC micelles allowed us to conclude that this was indeed due to lower solubility compared to the other peptides and not a loss of structure.

### ***2.3 Studies of gA3K Peptides' Activities in Cell-Based Assays***

#### *2.3.1 Antimicrobial Activity Towards Gram-Positive Bacteria*

Gramicidin A in its wild-type form, similar to many membrane-targeting peptides, only has antimicrobial activity towards gram-positive species of bacteria. Especially relevant is its activity against *S. aureus*, whose methicillin resistant strains are one of the most prevalent threats to public health.<sup>18,19</sup> All peptides were initially tested against *Bacillus subtilis* and *S. aureus* using a standard

microdilution assay.<sup>20</sup> The most potent peptides were then studied with a strain of MRSA to evaluate if they could maintain activity against resistant bacteria. The concentration of a stock solution of each peptide in DMSO was determined by UV-vis spectroscopy, measuring the absorbance of the tryptophan residues at 280 nm. An aliquot from this stock was then diluted to a final concentration of 1.0 mM, serving as the highest concentration used for each minimum inhibition concentration (MIC) assay. Under the assay conditions, this yielded a final concentration of 10  $\mu$ M. The remaining peptide solutions were obtained through a two-fold serial dilution starting at 1.0 mM. The MIC is determined to be the lowest concentration that prevents growth of the bacteria cultures. The results for each peptide are listed in Table 2-4.

Several of the peptides in this series achieved wild type-like activity against *B. subtilis*, including gA3K(Bn), gA3K(Cy), gA3K(CyMe) and gA3K(4AMBn). Peptides which were observed to be more potent to *B. subtilis* in comparison to gA3K were also observed to have relatively improved activity toward *S. aureus*. Those peptides with the most potent activity towards *S. aureus* were observed to maintain similar activities with MRSA. Unsurprisingly, gA3K(L,D,D), which was shown to be unable to form channel-active  $\beta$ -helical conformation, was not active towards any of the tested species. For this reason, we retained this peptide as a negative control for further studies.

**Table 2-4:** Measured MIC ( $\mu\text{M}$ ) of gA Mutants Against Various Gram-Positive Bacteria

	<i>B. subtilis</i>	<i>S. aureus</i>	MRSA
gA-WT	2.5	2.5	2.5
gA3K <sup>[a]</sup>	5	>10 (80%)	Not tested
gA3K(iPr)	>10 <sup>[b]</sup> (40%)	>10 (0%) <sup>[c]</sup>	Not tested
gA3K(Cy)	1.2	5	5
gA3K(CyMe)	1.2	2.5	1.2
gA3K(Bn)	1.2	5	2.5
gA3K(2pyr)	10	>10 (45 $\pm$ 1%)	Not tested
gA3K(3pyr)	>10 (33 $\pm$ 16%)	>10 (19 $\pm$ 7%)	Not tested
gA3K(4pyr)	>10 (37 $\pm$ 26%)	>10 (0%) <sup>[c]</sup>	Not tested
gA3K(4AMBn)	1.2	>10 (93 $\pm$ 1%)	Not tested
gA3K(L,D,D)	>10 (0%) <sup>[c]</sup>	>10 (0%) <sup>[c]</sup>	Not tested

MIC values are determined as the lowest concentration where no bacteria growth is observed when bacteria have grown past logarithmic phase. Peptides which had potent activity (MIC <10  $\mu\text{M}$ ) were run twice with triplicate samples in each to confirm activity. [a] Data for gA3K previously reported. [b] For those peptides which did not achieve full killing at the maximum concentration, percent inhibition is given in parentheses with error given as the standard deviation between triplicate samples. [c] No error given because all samples observed to have no inhibition or slightly improved growth compared to the untreated samples.

At this point, we were interested in determining a rational structure activity relationship for these peptides. However, based on the MIC data with *S. aureus*, several of the peptides were indistinguishable and only broad correlations could be drawn. We began to consider an alternative way to compare the antimicrobial activity of these peptide to one another. As their mechanism is bactericidal, we chose to study each peptide's ability to kill *S. aureus* in a minimal growth



environment. This cell killing assay was first optimized using one of the most potent peptides, gA3K(CyMe).

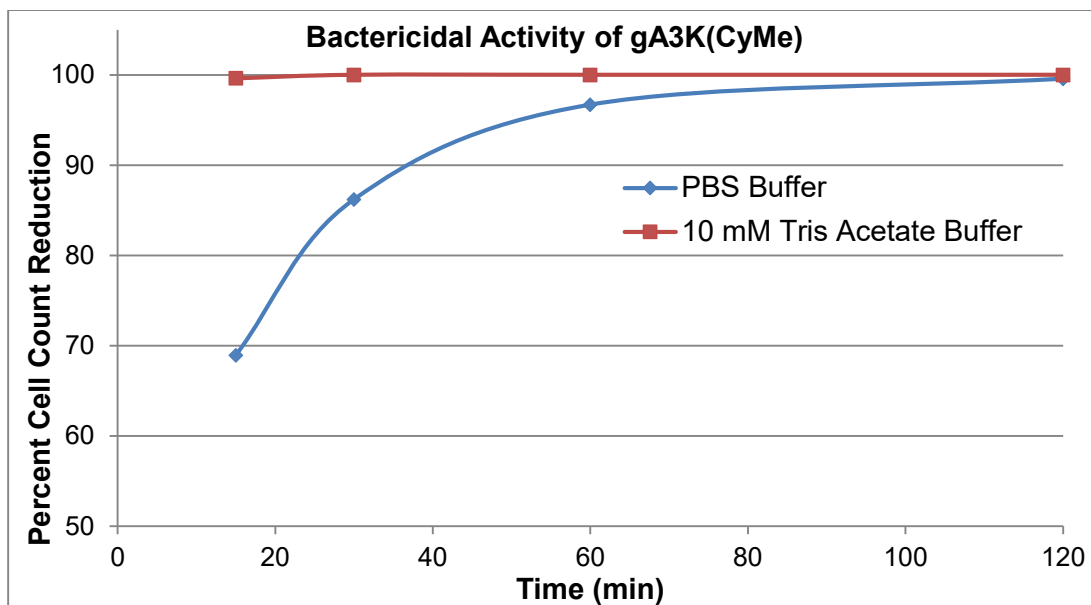


**Figure 2-5:** Bactericidal activity of gA3K(CyMe) with *S. aureus*. Time dependent activity was measured at 2.5  $\mu$ M with *S. aureus* in two different buffer conditions, 1xPBS (blue) and 10 mM tris acetate (red). Both buffers show nearly complete killing of *S. aureus* after one hour.

We chose two relevant buffers, a standard 1xPBS buffer (pH 7.4) and a 10 mM tris acetate buffer (pH 7.4) that was used in mechanistic studies (see Section 2.4). *S. aureus* cell cultures were grown to an OD600 = 0.6, then exchanged to the respective buffer before dilution to  $5 \times 10^5$  cfu/mL in the same way as the MIC assay. gA3K(CyMe) was added to a final concentration of its MIC (2.5  $\mu$ M) and its activity was monitored at several time intervals (Figure 2-5). At each time point, an aliquot was removed from the sample and diluted 100 times before being spread on a LB agar plate. The plates were then incubated at 37°C overnight and

the colonies on each plate were counted. The percent cell reduction was determined by comparing each point with a corresponding sample with no peptide treatment.

These results show that gA3K(CyMe) displayed rapid killing kinetics in minimal media. We chose to study the remaining peptides in the tris acetate buffer with a 10-minute incubation time, in order to make results as closely comparable to the mechanistic studies presented in the next section of this chapter. Each peptide was studied at a final concentration of 1.25  $\mu\text{M}$  in an attempt to distinguish the most potent mutants from each other (Figure 2-6). As none of the pyridinyl series behaved well in the MIC assay, they were not included in this study. Instead, gA3K(iPr) was used as a representative inactive compound.

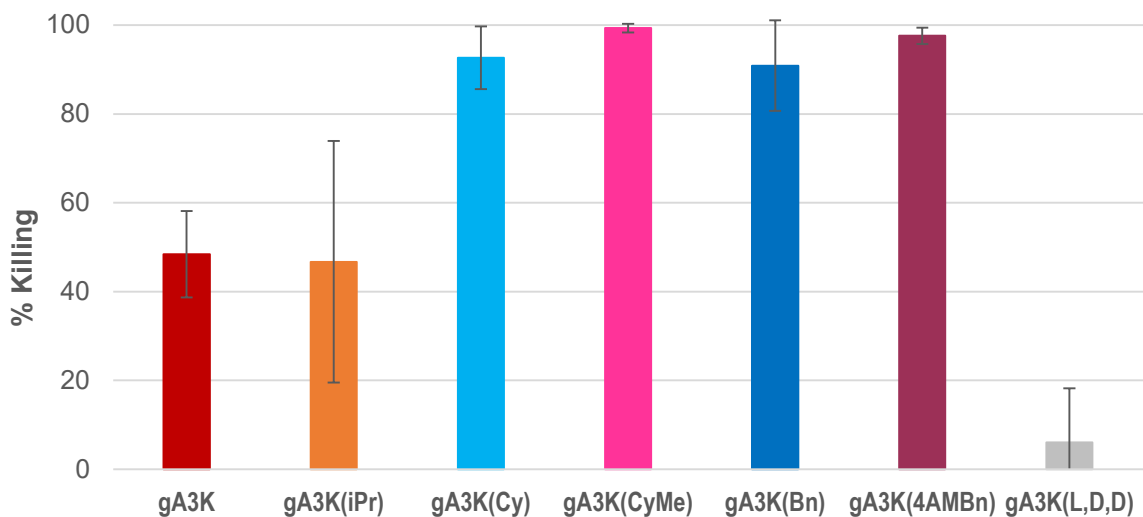


**Figure 2-6:** Cell killing activity of select peptides towards *S. aureus*. Peptides were added at a final concentration of 1.25  $\mu$ M to *S. aureus* cells in 10 mM tris acetate buffer (pH 7.4) at a density of  $5 \times 10^5$  cfu/mL. Triplicate samples were incubated for 10 minutes then diluted 100 times before spreading on a LB agar plate. After overnight incubation, the number of colonies formed on each plate were counted and compared to that of an untreated sample to determine percent killing.

From this cell killing assay, we observed an unexpected result with regards to gA3K(4AMBn). Although this peptide did not perform well in the MIC assay, it was one of the best peptides in this assay. Most likely, there is something in the LB media used in the MIC assay trapping this peptide due to its higher cationic charge. We also used this assay to evaluate whether these peptides can overcome serum inhibition, which is much more representative of the *in vivo* environment, compared to gA WT. To do this, we repeated the assay with the most potent peptides using buffer that contained 10% v/v human serum in 10 mM tris acetate buffer (Figure 2-7). With the exception of gA3K(4AMBn), the activities of these peptides were severely inhibited by the presence of human serum. This is, again,

most likely due to the higher cationic charge of this peptide, resulting in fewer non-specific hydrophobic interactions between the peptides and serum proteins.

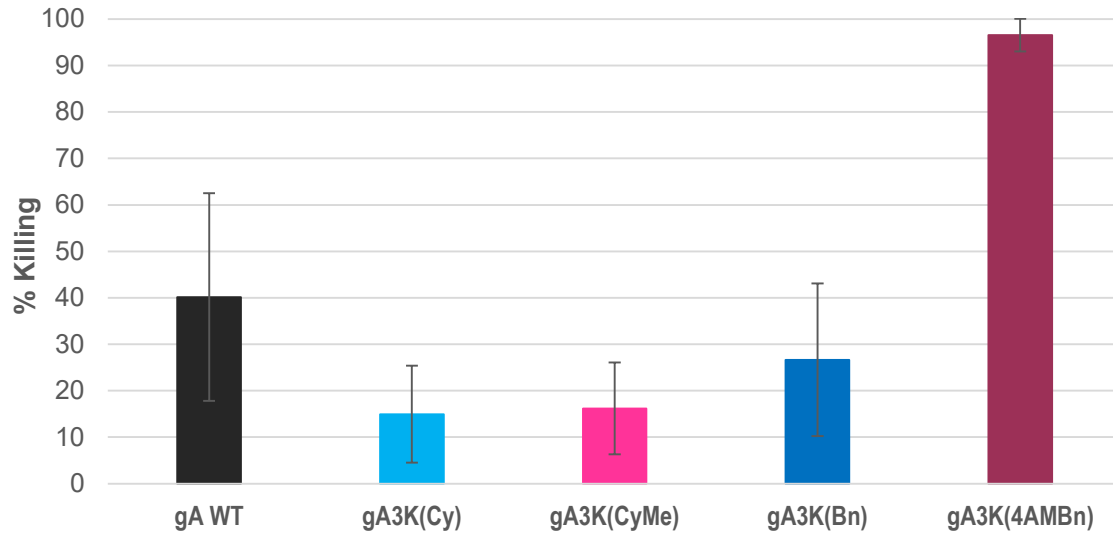


**Figure 2-7:** Cell killing activity of select peptides towards *S. aureus* in the presence of human serum. Peptides were added at a final concentration of 1.25  $\mu\text{M}$  to *S. aureus* cells in 10 mM tris acetate buffer (pH 7.4) with 10% v/v human serum at a density of  $5 \times 10^5$  cfu/mL. Triplicate samples were incubated for 10 minutes then diluted 100 times before spreading on a LB agar plate. After overnight incubation, the number of colonies formed on each plate were counted and compared to that of an untreated sample to determine percent killing.

### 2.3.2 Antimicrobial Activity Towards Gram-Negative Bacteria

It is generally known that gA and closely related peptides will not be active towards gram-negative species of bacteria. This is thought to be because of the additional challenge presented by the outer membrane. However, after observing the interesting activity of gA3K(4AMBn), we hypothesized that this type of structure might allow for gram-negative activity. As such, we chose to study the activity of this peptide towards gram-negative relevant species. In order to directly

analyze the role of the extra charge, we also studied the activity of gA3K(Bn) (Table 2-5).

**Table 2-5:** Measured MICs ( $\mu\text{M}$ ) gA Mutants towards Various Gram-negative Bacteria

	<i>E. coli</i>	<i>K. pneumoniae</i>	<i>P. aeruginosa</i>
gA3K(Bn)	10	>25 <sup>[a]</sup> (72 $\pm$ 11%)	>12.5 (28 $\pm$ 15%)
gA3K(4AMBn)	10	10	12.5
MIC values are determined as the lowest concentration where no bacteria growth is observed. Peptides which had potent activity (MIC <10 $\mu\text{M}$ ) were run twice with triplicate samples in each to confirm activity. [a] For those peptides which did not achieve full killing at the maximum concentration, percent inhibition is given in parentheses with error given as the standard deviation between triplicate samples.			

We first tested the peptides' activities towards *Escherichia coli*, as it was readily available in the lab and traditionally serves as a good model system. We found that both peptides had relatively potent activity with MICs of 10  $\mu\text{M}$ . With these preliminary results, we chose to examine other gram-negative species and purchased strains of *Klebsiella pneumoniae* and *Pseudomonas aeruginosa*. These two species were selected as both of them are part of the ESKAPE pathogens, which are the bacteria with resistant strains considered to be the most threatening by WHO. We were happy to see that gA3K(4AMBn) was able to maintain similar potency with both of these important pathogens, even though gA3K(Bn) did not.

Similar to the work done with *S. aureus*, we wanted to establish a way to differentiate the activities of similar peptides towards *E. coli*. Considering our hypothesized mechanism of action, we expected that the peptides would require

a longer incubation time in the cell killing assay. Consequently, we chose to switch to using a M9 minimal media supplemented with 0.20% sodium succinate as the carbon source, which has been reported to maintain cell viability with limited growth for as long as 24 hours.<sup>21</sup> We monitored the cell killing ability of gA3K(4AMBn) at 10  $\mu$ M for *E. coli* in this M9 media (Figure 2-8). We observed nearly complete killing after 2 hours with the cell density of the untreated sample maintaining good viability up to 3 hours. As such, we chose to use an incubation of 2 hours for further studies.

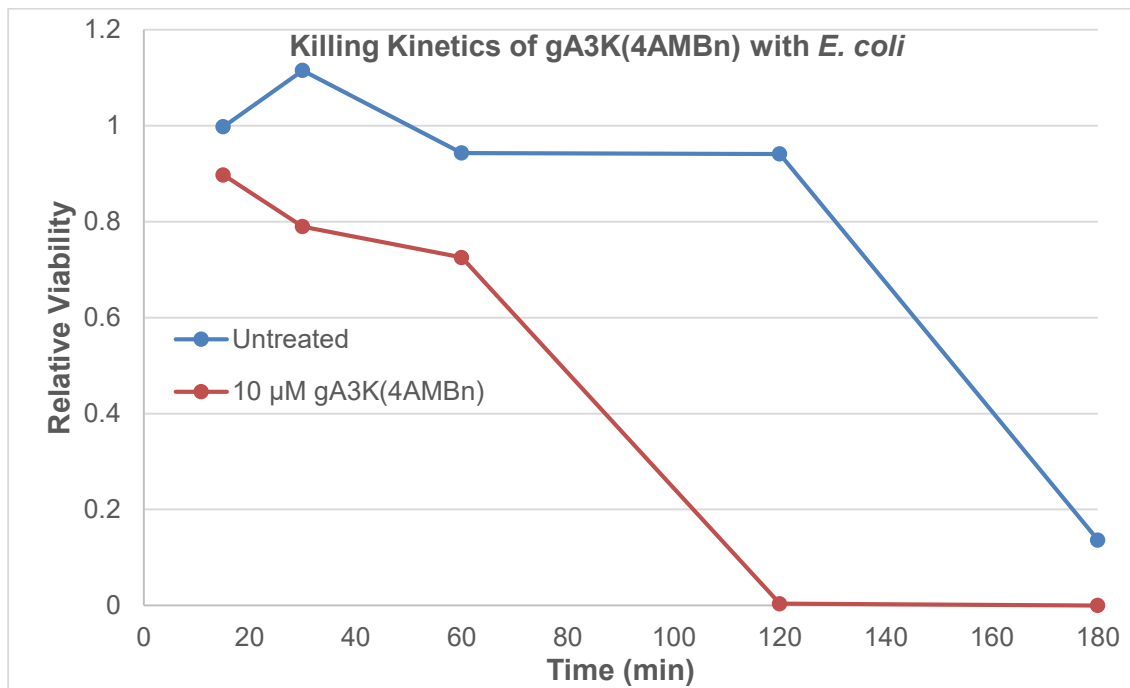


**Figure 2-8:** Bactericidal activity of gA3K(4AMBn) with *E. coli*. Time dependent activity with gA3K(4AMBn) at 10  $\mu$ M towards *E. coli* in M9 minimal media with 0.20% sodium succinate. The untreated sample (blue) maintains similar cell counts after two hours while the gA3K(4AMBn) treated sample (red) shows nearly complete killing after 2 hours.

Using these conditions, we studied other peptides from this gA series (Figure 2-9). In this assay, both gA3K(Cy) and gA3K(CyMe) performed with potency close to that of gA3K(Bn). Interestingly, even though they had the same MIC for *E. coli*, gA3K(4AMBn) was much more potent than gA3K(Bn) in this experiment. The results of this assay suggest that the alkylated lysines are crucial for this observed activity towards gram-negative bacteria, as gA3K performed near the same potency as our negative control.

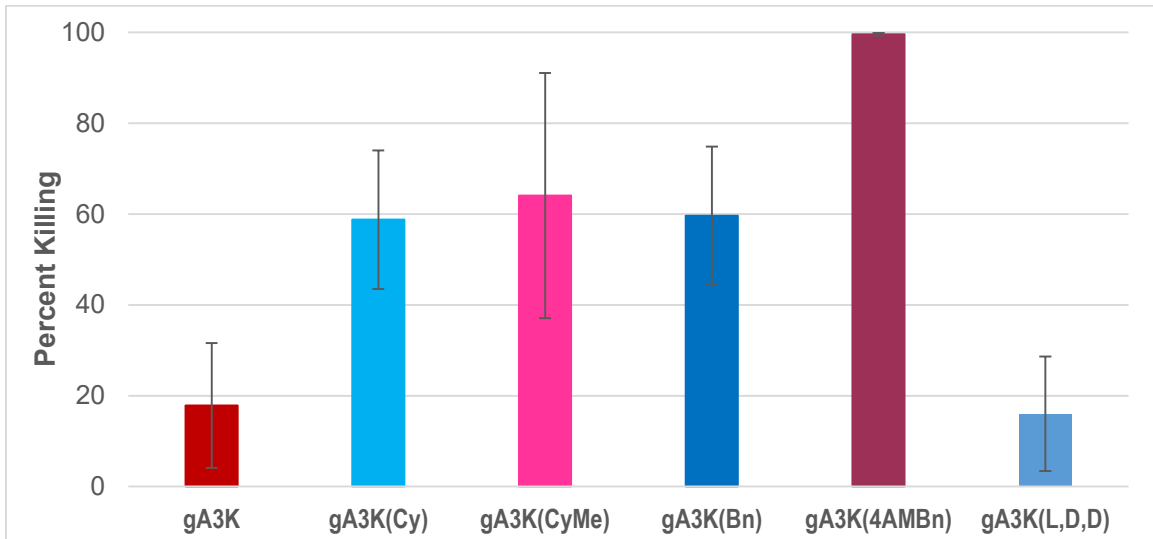


**Figure 2-9:** Cell killing of select gA mutants towards *E. coli*. Peptides were added at a final concentration of 10  $\mu$ M to *E. coli* cells in M9 minimal media with 0.20% sodium succinate (pH 7.4) at a density of  $5 \times 10^5$  cfu/mL. Triplicate samples were incubated for 2 hours then diluted 100 times before spreading on a LB agar plate. After overnight incubation, the number of colonies formed on each plate were counted and compared to that of an untreated sample to determine percent killing.

### 2.3.3 Toxicity of gA Mutants Towards Human Red Blood Cells

Keeping in mind that our goal in designing this series of peptides was to enhance potency while maintaining selectivity, we needed to evaluate any change

in toxicity that we had caused with these mutations. One of the quickest and most straightforward ways to do this is by measuring a peptide's activity with human red blood cells (hRBCs). Not having a nucleus or other organelles, hRBCs can be thought of as a complex model membrane system that has an accurate composition for mammalian plasma membranes. Additionally, being rich in UV-active hemoglobin, hRBCs have an inherent reporter for membrane permeabilization.

To measure the hemolytic activity of the peptides,<sup>22</sup> hRBCs are suspended in PBS buffer (pH 7.4) and treated with the same final concentration of peptides as in the bacterial MIC assay. After one hour of incubation at 37°C, the samples are centrifuged and an aliquot of the supernatant is added to a 96-well plate; final samples are diluted two-fold with DI water to prevent signal saturation. To determine the percent hemolysis that has occurred, a separate sample is prepared with the addition of 1% Triton-X100 to fully lyse the cells. This sample is then set as 100% hemolysis and the peptide treated samples are scaled accordingly (Figure 2-10). HC<sub>50</sub>s are reported as the concentration of peptide that results in the leakage of 50% of the total hemoglobin.

This data shows that some of the more potent peptides, namely gA3K(Bn) and gA3K(CyMe), displayed similar toxicity profiles to gA WT (HC<sub>50</sub> = 2.5 μM). However, gA3K(Cy) was found to be about five-fold less toxic than gA WT; having similar bacterial potencies, this would allow gA3K(Cy) to be a more selective



peptide compared to gA WT. Additionally, gA3K(4AMBn) showed improved toxicity compared to gA3K. These two examples demonstrate our ability to tune potency of gA3K mutants without significantly increasing human toxicity.

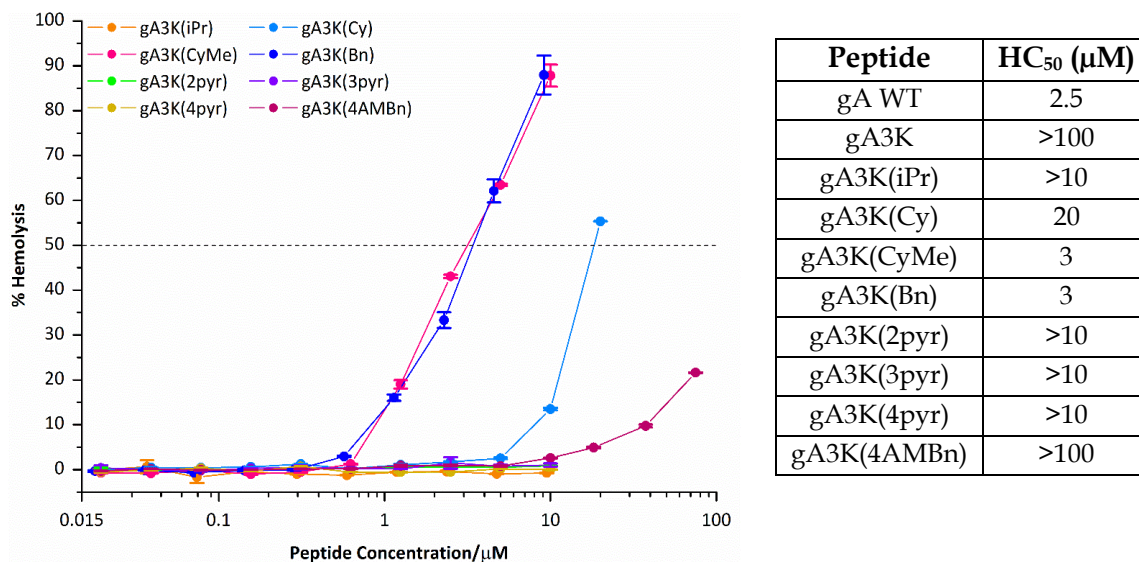


**Figure 2-10:** Hemolytic activity of gA mutants. Percent hemolysis is calculated compared to a fully lysed sample treated with 1% Triton-X100. Error bars represent the standard deviation of triplicate samples. HC<sub>50</sub> values are provided in the given table.

#### 2.4 Mechanistic Studies of gA3K Mutants

Interested in gaining some insight into how and why these peptides possess the activities discussed above, we began to perform studies to gain a structure activity relationship. With the mechanism of action for gA WT having been well studied and widely accepted to be a result of its membrane pore formation, we focused on studies that would examine different aspects of this. A cartoon demonstrating the critical steps in this mechanism is provided in Figure 2-11.

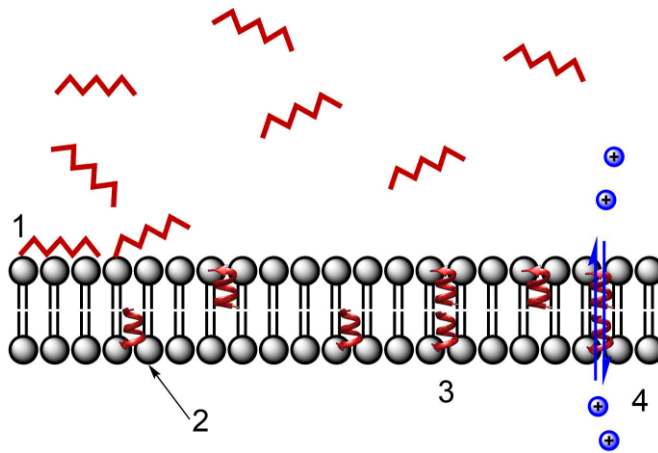


**Figure 2-11:** Depiction of the mechanism of action of gA. 1) Membrane association; 2) Membrane insertion as the channel-forming  $\beta$ -helix; 3) Translocation within the membrane to form dimer; 4) Disruption of cation gradient across the membrane.

#### 2.4.1 Membrane Binding vs. Cell Killing

With the first step of the gA mechanism being association with the membrane, we sought to design an assay that would allow for the measurement of binding to live bacteria cells. A common way of doing this is simply attaching a fluorophore to the peptide of interest and measure cell labeling using flow cytometry or fluorescence. In our case, there were a few different characteristics that kept us from using this strategy. Specifically, there was a lack in understanding of the consequences to the peptide's structure that could come from attaching a bulky, hydrophobic structure in the sequence. Overall, this would likely lead to inaccurate data on how the peptide is able to insert into the membrane.

Instead, we turned to the intrinsic absorbance and fluorescence of the four tryptophans within the gA sequence. With measuring absorbance, we predicted

to see an increase in tryptophan absorbance with increasing concentrations of peptide, as more of it binds to the cell. In the case of fluorescence, the properties of tryptophan are known to change based on its local environment, such that the fluorescence should increase upon insertion into a hydrophobic membrane. Considering these two characteristics, we first attempted to determine the degree of binding by measuring the change in either absorbance or fluorescence with the addition of peptides to bacteria cultures. Unfortunately, both techniques gave us several problems with sensitivity and reproducibility. The cause of most of these issues was suspected to come from the presence of other sources of tryptophan along with other structures that absorb at 280 nm in our samples. For these reasons, we chose to develop a HPLC-based method, such that we could be confident the absorbance we focused on was from the gA peptide alone.

In order to measure the initial binding of each peptide, cells were grown to an OD<sub>600</sub>=0.6, then pelleted and exchanged into a tris-buffered saline solution (10 mM tris acetate, 150 mM sodium chloride, pH 7.4). This buffer was chosen as it contained fewer components than either LB media or other common buffers, which would decrease the complication of the sample components when analyzing by LC/MS. After diluting to a final density of  $5 \times 10^5$  cfu/mL, triplicate samples were treated with each peptide at a final concentration of 1.25  $\mu$ M and incubated for 10 minutes. We chose to use this concentration as it was below the MIC for all studied peptides and therefore cell death was expected to cause little

interference. After this incubation period, cells were spun down at max speed and an aliquot of the supernatant was removed to be run on LC/MS. As a standard, samples were prepared under the same conditions without any cells.

Initial optimization of conditions showed that gA WT was too hydrophobic to be analyzed in this way; it was thus eliminated from this study. Optimization also showed that the LC/MS system was not sensitive enough to distinguish the small changes in concentration we were expecting. To solve this problem, we chose to lyophilize the supernatant samples, allowing us to concentrate them by 10-fold before analysis. As we were increasing the final concentration of the peptide, we redissolved each sample in a 1:1 ratio of water to acetonitrile, to ensure differences in solubility would not skew our analysis. Finally, in order to get full recovery of the peptides from the lyophilized sample, we eliminated the sodium chloride from our assay buffer. This was due to the observation that peptides from standard samples were not being fully recovered after lyophilization due to poor solubility of sodium chloride.

Having observed a linear relationship between peak area and peptide concentration with our standards, we compared the peak area of each sample to that of the standard for a given peptide. As this would give us the concentration of the peptide that had been in the supernatant, the concentration of peptide bound to the cells was then considered to be the difference between the total concentration of peptide and the concentration found in the supernatant. By

comparing this to the total amount of peptide, a percent binding can be reported (Table 2-6).

**Table 2-6:** Measured of Binding for gA Mutants

Peptide	% Bound – <i>S. aureus</i>	% Bound – <i>E. coli</i>
gA3K	49 ± 4.2	88 ± 7.7
gA3K(iPr)	41 ± 0.63	N/A
gA3K(Cy)	44 ± 3.3	58 ± 5.1
gA3K(CyMe)	54 ± 5.1	49 ± 0.8
gA3K(Bn)	65 ± 3.6	61 ± 9.2
gA3K(2pyr)	43 ± 2.9	N/A
gA3K(3pyr)	50 ± 1.3	N/A
gA3K(4pyr)	52 ± 3.4	N/A
gA3K(4AMBn)	61 ± 8.7	68 ± 6.7
gA3K(L,D,D)	17 ± 30.	None*

\* Negative value obtained for this peptide

This data shows that all of the peptides have relatively similar binding for both species tested, such that no trend can be observed between the MIC and binding. This is demonstrated further when comparing the degree of cell killing to that of binding (Figure 2-12). Without being able to confirm any correlation between cell binding and antimicrobial activity, we moved on to consider what occurs after membrane association that could be leading to this differentiation in activity.

#### 2.4.2 Measuring Membrane Permeability

Considering the steps following binding in the mechanism of action of gA (Figure 2-11), we imagined that membrane permeability (step 4) would be the most straightforward to measure directly in live cells. Additionally, given that the

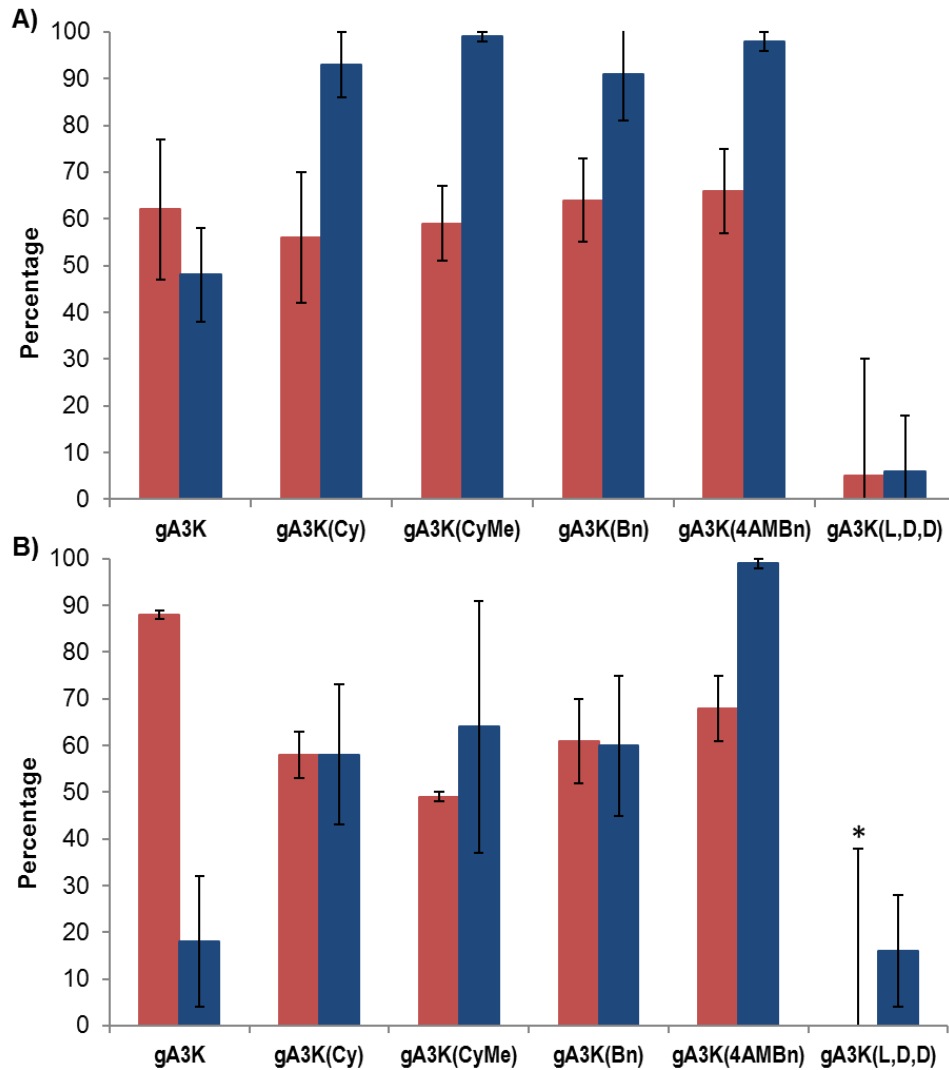


**Figure 2-12:** Comparing cell binding with cell killing activities of select gA mutants. Cell binding (red) and cell killing (blue) activities of gA mutants against A) *S. aureus* and B) *E. coli*. \* Some negative values were found for this peptide and were considered to represent no binding.

membrane association of the peptides are relatively the same, measuring the degree of permeabilization can provide information on the net difference of the later steps. As of now, techniques have been developed that can look at the gA conformations and dimerization in model systems; in fact, a few of the mutants described here were studied using such a technique in collaboration with Prof.

David Russell's lab at Texas A&M University.<sup>23</sup> However, these have yet to be applied to *in vitro* systems.

Several options were considered and studied, including monitoring the  $\beta$ -galactosidase activity on cell impermeable galactosides, but in the end, we found flow cytometry to provide the most reliable data. For this, we examined cell staining with propidium iodide (PI). PI is a fluorescent dye which intercalates with nucleic acids. As it is not membrane permeable, it is only able to stain cells which have compromised membranes. By treating our samples with PI followed by flow cytometry analysis, we were able to distinguish cells with and without membrane permeability. Comparing the number of cells in both of these populations, we were able to determine the degree to which treatment with different peptides created membrane disruption.

Samples of *S. aureus* and *E. coli* were prepared using the same conditions as their respective cell killing assays. After incubation was complete, PI was added to a final concentration of 0.2  $\mu\text{g}/\text{mL}$ . The samples were then analyzed by flow cytometry, gating for forward and side scattering based on an untreated cell sample. Fluorescence was recorded for the cells within this gate and plotted as histograms (Figure 2-13). A clear division into two populations was observed, defined by the negative and positive controls. Those cells within the non-fluorescent population were considered to have maintained membrane integrity

while those observed to be fluorescent were considered to have compromised membranes.

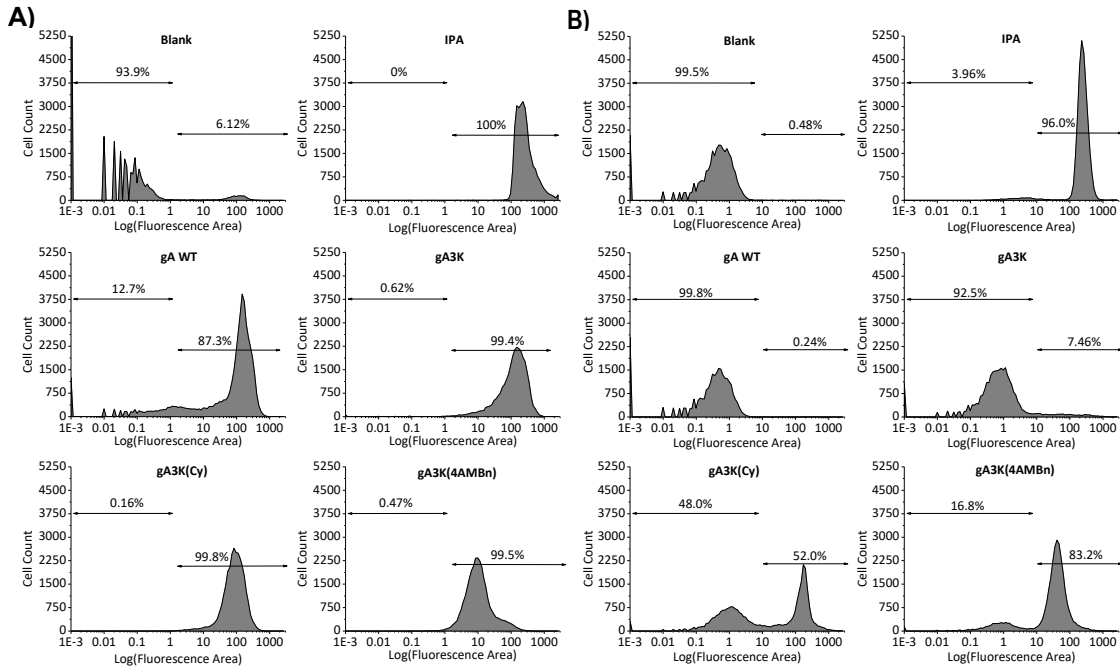


**Figure 2-13:** Flow cytometry analysis of cell permeability of select gA mutants. Histogram of PI fluorescence for A) *S. aureus* and B) *E. coli* cells treated with various peptides. Cells suspended in 70% isopropanol (IPA) in water were used as a positive control. The two populations are shown with double-headed arrows with the percentage of cells listed above. Histograms display averages of three samples for each peptide.

The flow cytometry data for *S. aureus* demonstrates that all peptide treated samples have nearly identical degrees of membrane permeabilization. This would suggest that membrane integrity cannot be used as a measure for a defined structure activity relationship. On the other hand, a clear trend can be seen for the *E. coli* samples that agrees with that which was observed from the cell killing assay. This agrees with the suggestion that peptides must reach the inner membrane of the gram-negative bacteria to achieve cell killing, as the samples with the highest



cell staining also have the best cell killing activity. It can then be suggested from this data that peptides with better membrane permeabilization in gram-negative cells will be more potent against these bacteria.

## 2.5 Conclusions

In summary, we have demonstrated that the use of alkylated lysines in the gramicidin A structure is an effective strategy to improve upon potency and selectivity of this family of peptides. This work led to the first observation of a gA peptide, namely gA3K(4AMBn), with potent activities against several important gram-positive and gram-negative bacteria. Our efforts towards a mechanistic understanding of these peptides demonstrated that potency cannot be estimated by membrane association, but rather there is a clear correlation between peptide-induced membrane permeability and cell killing in *E. coli*. Considering both of these observations, it would appear that less potent peptides most likely fail to either fold into the proper structure after membrane association or cannot efficiently travel through the lipid bilayer for dimerization.

Taking into consideration all of the results presented above, several peptides have displayed appealing characteristics for their development as antibiotics. Specifically, gA3K(Cy) and gA3K(4AMBn) both exhibit preferred selectivity for bacteria with much less toxicity towards hRBCs. Finally, while still more toxic than desired, gA3K(Bn) has an attractive broad-spectrum activity, which may allow it to be a more effective topical agent.

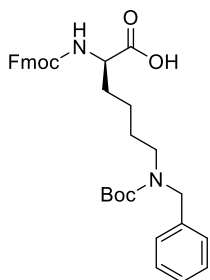
## 2.6 Experimental Procedures

### 2.6.1 General Methods

Fmoc-Trp-Wang resin and all Fmoc-protected amino acids were purchased from either Advanced Chemtech (Louisville, KY) or Chem Impex Int. Inc. (Wood Dale, IL). Unprotected valine and other chemicals were obtained from Sigma-Aldrich or Fisher unless otherwise indicated. *Tert*-butyl 4-formylbenzyl carbamate was purchased from Astatech Inc. (Bristol, PA). Peptide synthesis was carried out on a Tribute peptide synthesizer (Protein Technologies, Tucson, AZ). <sup>1</sup>HNMR data were collected on a VNMRS 500 MHz or 600MHz NMR spectrometer, as indicated. Mass spectrometry data were generated by using an Agilent 6230 LC TOF mass spectrometer or obtained from the Boston College Mass-Spectrometry facility. The peptide concentration of all samples used in this study was determined by measuring their absorbance at 280 nm ( $\epsilon = 22760 \text{ M}^{-1}\text{cm}^{-1}$  total of four tryptophan residues) on a Nanodrop 2000c UV/Vis spectrometer by cuvette. Gram-positive *Bacillus subtilis* (ATCC 663) and *Staphylococcus aureus* (ATCC 6538) were purchased as lyophilized cell pellets from Microbiologics (Cloud, MN). Gram-positive methicillin-resistant *S. aureus* (MRSA, ATCC 43300), *Klebsiella pneumoniae* (ATCC 4352) and *Pseudomonas aeruginosa* (ATCC 27853) were purchased from ATCC (Manassas, VA). Gram-negative *E. coli* (BL21) was a gift from the lab of Prof. Mary F. Roberts at Boston College.

## 2.6.2 Synthesis of Unnatural Amino Acids

**Fmoc-D-Lysine(Bn)(Boc)-OH:** Fmoc-D-lysine hydrochloride (1 eq, 4.94 mmol,

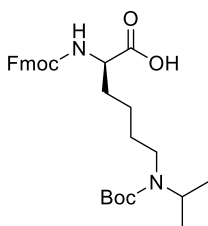


2.0g) was dissolved in 200 proof ethanol (40 mL) and stirred with 3Å molecular sieves. To this, freshly distilled benzaldehyde (1.2 eq, 5.93 mmol, 0.629 g) was added. This mixture was allowed to stir for 1 hour before sodium cyanoborohydride (1.2 eq, 5.93

mmol, 0.3725 g) was added. This was allowed to stir overnight. The mixture was acidified by adding 0.5 N aqueous hydrochloric acid dropwise to reduce any excess sodium cyanoborohydride. The mixture was decanted from the molecular sieves and the solvent was removed by rotary evaporation. The dried mixture was resuspended in acetone and centrifuged to remove borohydride salts. The supernatant was decanted from the pellet and the acetone was removed by rotary evaporation to give a white solid. The solid was dissolved in a 1:1 v/v water/tetrahydrofuran solution (30 mL) and put in an ice bath. This was allowed to stir as enough sodium bicarbonate was added to bring the pH of the solution to ~8-9 (3.0 eq, 15 mmol, 1.26 g). To this mixture, di-*tert*-butyl dicarbonate (1.2 eq, 6.00 mmol, 1.31 g) was added. The reaction was stirred in the ice bath for 30 min then allowed to stir overnight at room temperature. After 20 hours, the reaction showed to be incomplete, at which point an additional equivalent of di-*tert*-butyl dicarbonate (1.0 eq, 4.94 mmol, 1.078 g) and additional sodium bicarbonate to return the pH to ~8-9 (2.5 eq, 12.35 mmol, 1.04 g) were added with 20 mL of the

reaction solvent. This was stirred for an additional 15 hours. When the reaction was done, the mixture was first extracted with diethyl ether (2 x 75 mL). After the extraction, the aqueous layer was acidified with 2N hydrochloric acid to a pH of ~6. This was then extracted with dichloromethane (3 x 75 mL). All organic layers were collected and washed with brine (1 x 350 mL) and dried over sodium sulfate. The product was purified by silica gel chromatography (1:1 ethyl acetate/hexanes with 1% by volume acetic acid) and the desired product was obtained as a white solid. Yield: 1.1827 g (42.9% yield). NMR:  $\delta$  H (500 MHz, Methanol-d<sub>4</sub>) 7.77 (2 H, d, J 7.6), 7.66 (2 H, dd, J 10.3, 7.5), 7.36 (2 H, td, J 7.5, 2.8), 7.32 – 7.26 (4 H, m), 7.25 – 7.17 (3 H, m), 4.41 (2 H, s), 4.34 (2 H, dd, J 7.1, 2.6), 4.20 (1 H, t, J 7.0), 4.12 (1 H, dd, J 9.4, 4.7), 3.27 – 3.10 (2 H, m), 1.88 – 1.75 (1 H, broad m), 1.72 – 1.59 (1 H, broad m), 1.57 – 1.29 (13 H, m);  $\delta$  C (126 MHz, cd<sub>3</sub>od) 174.45, 157.23, 143.92, 141.16, 128.13, 127.35, 126.74, 126.72, 124.82, 119.49, 79.83, 66.51, 53.72, 46.14, 30.94, 27.31, 22.78. Calculated Mass: 558.27; ESI+ Mass Found: 559.28 [M+H]<sup>+</sup>.

**Fmoc-D-Lysine(iPr)(Boc)-OH:** Fmoc-D-lysine hydrochloride (1 eq, 4.94 mmol,

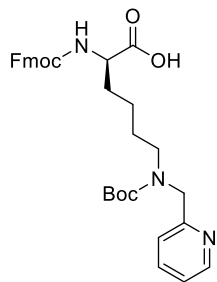


2.0g) was suspended in acetone (250 mL), which had been dried over sodium sulfate for 90 min, and stirred with 3Å molecular sieves for one hour. To this, sodium cyanoborohydride (1.1 eq,

5.48 mmol, 0.3443 g) was added. This was allowed to stir for another hour. Methanol was added to dissolve any product that had crashed out of solution before the mixture was filtered to remove the molecular sieves. The solvent was

removed by rotary evaporation to produce a cream-colored solid. The solid was dissolved in a 1:1 mixture by volume water/tetrahydrofuran (50 mL) and stirred in an ice bath. To this, sodium bicarbonate was added to bring the pH to ~8-9 (3.0 eq, 14.82 mmol, 1.24 g) followed by the di-*tert*-butyl dicarbonate (1.2 eq, 5.93 mmol, 1.29 g). This was allowed to stir in the ice bath for 30 min then stirred at room temperature for two days. This was first concentrated by rotary evaporation to remove the THF. To the aqueous mixture, DCM (50 mL) was added. While stirring, 2N HCl was added dropwise until the pH was ~3. The mixture was extracted once, then again with DCM (50 mL) and the organic layers were combined. The organic layer was washed with brine (1x100 mL) and dried over sodium sulfate. The final mixture was dried by rotary evaporation. The final product was obtained as a white solid after silica gel column purification (5% methanol, 1% acetic acid in DCM). Yield: 1.7629 g (69.8%). NMR:  $\delta$  H (500 MHz, Methanol-d<sub>4</sub>) 7.79 (2 H, d, J 7.5), 7.72 - 7.64 (2 H, m), 7.38 (2 H, t, J 7.5), 7.30 (2 H, td, J 7.5, 1.1), 4.34 (2 H, qd, J 10.6, 7.1), 4.22 (1 H, t, J 7.1), 4.14 (1 H, dd, J 9.3, 4.7), 4.06 - 3.92 (1 H, broad m), 3.16 - 3.01 (2 H, broad m), 1.94 - 1.80 (1 H, broad m), 1.76 - 1.65 (1 H, broad m), 1.64 - 1.49 (2 H, broad m), 1.44 (9 H, s), 1.41 - 1.33 (2 H, m, broad), 1.13 (6 H, d, J 6.8);  $\delta$  C (126 MHz, cd<sub>3</sub>od) 174.59, 157.27, 155.76, 143.74, 141.17, 127.63, 127.07, 126.43, 124.40, 119.47, 79.35, 66.54, 53.92, 46.88, 31.02, 27.50, 27.14, 23.07, 19.49. Calculated Mass: 510.27 ESI+ Mass Found: 511.28 [M+H]<sup>+</sup>.

**Synthesis of Fmoc-D-Lysine(2-pyr)(Boc)-OH:** Fmoc-D-lysine hydrochloride (1 eq,

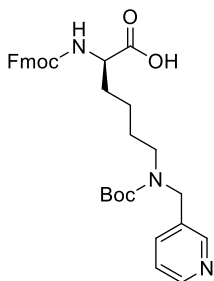


4.94 mmol, 2.0g) was dissolved in 200 proof ethanol (15 mL) and stirred with 3Å molecular sieves. To this, 2-pyridine carboxaldehyde (1.5 eq, 7.41 mmol, 0.794 g) was added. This mixture was allowed to stir for 1 hour before sodium

cyanoborohydride (1.5 eq, 7.41 mmol, 0.466 g) was added. This was allowed to stir overnight. The solution was acidified to pH ~3-4 using 2N HCl and decanted from the molecular sieves. The solvent was removed by rotary evaporation and a solid was obtained. The crude solid was dissolved in 30% THF in saturated sodium bicarbonate (150 mL) and stirred as di-*tert*-butyl dicarbonate (dissolved in 1 mL of THF) was added. This was allowed to stir for two hours and confirmed to be complete by TLC. The THF was removed by rotary evaporation. To the aqueous mixture, ethyl acetate (100 mL) was added. This was stirred as the mixture was acidified to pH ~3-4 using 2N HCl. The organic layer was removed and the aqueous layer was extracted with ethyl acetate (100 mL). The organic layers were combined and washed with brine (100 mL) then dried over sodium sulfate. The white solid obtained was purified by silica gel column purification (4:3:1 hexanes/ethyl acetate/ethanol with 1% by volume acetic acid). Yield: 0.3317 g (12% yield). NMR:  $\delta$  H (500 MHz, Acetone- $d_6$ ) 8.50 (1 H, d, J 4.9), 7.85 (2 H, d, J 7.5), 7.80 - 7.65 (3 H, m), 7.40 (2 H, t, J 7.5), 7.36 - 7.19 (4 H, m), 4.52 (2 H, s), 4.33 (2 H, d, J 7.2), 4.24 (2 H, t, J 7.1), 3.33 (2 H, d, J 29.2), 1.91 (1 H, d, J 12.8), 1.84 - 1.71 (1

H, m), 1.67 – 1.54 (2 H, m), 1.52 – 1.26 (11 H, m);  $\delta$  C (126 MHz, cd3od) 174.46, 157.23, 148.26, 143.93, 143.75, 141.16, 137.43, 127.34, 126.74, 126.72, 126.30, 124.86, 124.82, 119.48, 66.51, 53.81, 52.06, 51.99, 51.26, 48.09, 47.00, 30.97, 27.47, 27.39, 27.26, 27.24, 27.15, 22.80. Calculated Mass: 559.27; ESI+ Mass Found – 560.28 [M+H]<sup>+</sup>.

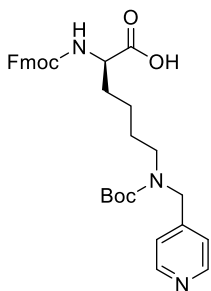
**Fmoc-D-Lysine(3-pyr)(Boc)-OH:** Fmoc-D-lysine hydrochloride (1 eq, 4.94 mmol,



2.0g) was dissolved in 200 proof ethanol (15 mL) and stirred with 3Å molecular sieves. To this, 3-pyridine carboxaldehyde (1.2 eq, 5.93 mmol, 0.6349 g) was added. This mixture was allowed to stir for 1 hour before sodium cyanoborohydride (1.2 eq, 5.93 mmol, 0.3725 g) was added. This was allowed to stir overnight. The solution was acidified to pH ~3-4 using 5% aqueous HCl and decanted from the molecular sieves. The solvent was removed by rotary evaporation and a solid was obtained. The mixture was dissolved in saturated sodium bicarbonate (100 mL). While stirring, di-*tert*-butyl dicarbonate was added (1.1 eq, 5.36 mmol, 1.171 g, dissolved in 2 mL THF). This was allowed to stir for six hours. The mixture was then acidified using 1N HCl to a pH of ~2. This was then extracted with DCM (3x150 mL). The organic layers were combined and washed with brine (1x300 mL) and dried over sodium sulfate. The solvent was removed by rotary evaporation to provide a white solid. The final product was obtained as a white solid after silica gel column purification (5% methanol and 1% acetic acid by volume in DCM). Yield: 0.5687 g (20.6% yield). NMRs:  $\delta$  H (600 MHz, Acetone-d<sub>6</sub>) 8.51 (2 H, d, J 34.6), 7.92 – 7.61 (5 H, m), 7.46 –

7.21 (5 H, m), 4.48 (2 H, s), 4.38 - 4.28 (m, 1H), 4.27 - 4.19 (2 H, m), 3.27 (2 H, d, J 40.8), 1.95 - 1.84 (1 H, m), 1.81 - 1.69 (1 H, m), 1.63 - 1.26 (13 H, m);  $\delta$  C (126 MHz, cd3od) 174.49, 157.24, 147.48, 147.25, 143.92, 143.77, 143.73, 141.17, 141.14, 127.63, 127.08, 127.04, 127.03, 126.44, 126.42, 124.15, 123.63, 123.61, 119.48, 80.21, 66.52, 53.80, 30.98, 27.50, 27.14, 26.97, 22.74. Calculated Mass: 559.27; ESI+ Mass Found - 560.28 [M+H]<sup>+</sup>.

**Fmoc-D-Lysine(4-pyr)(Boc)-OH:** Fmoc-D-lysine hydrochloride (1 eq, 6.175 mmol,

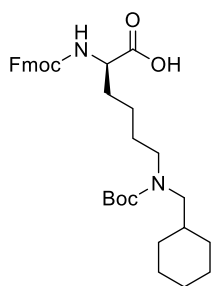


2.5 g) was dissolved in 200 proof ethanol (200 mL) and stirred with 3Å molecular sieves as diisopropyl ethylamine (1.0 eq, 6.175 mmol, 1.10 mL) was added. This caused a chloride salt to crash out of solution. To this, 4-pyridine carboxaldehyde (1.5 eq, 9.263 mmol, 1.137 g) was added. This mixture was allowed to stir for 1 hour before sodium cyanoborohydride (1.2 eq, 5.93 mmol, 0.3725 g) was added. This was allowed to stir overnight. The mixture was acidified using 1N HCl to a pH of ~2-3. This was then decanted from the sieves and concentrated by rotary evaporation to obtain a yellow solid. The crude solid was dissolved in a 1:1 mixture of water and THF (100 mL). To this, sodium bicarbonate (12.0 eq, 74.1 mmol, 6.225 g) was added to reach a pH of ~9-10. While stirring, di-*tert*-butyl dicarbonate (2.0 eq, 12.35 mmol, 2.695 g) was added. This was stirred overnight. To the mixture, ethyl acetate (100 mL) was added and the solution was then acidified using 5% aqueous HCl until a pH of ~2 was reached. The organic layer was removed and the aqueous



layer was extracted with ethyl acetate (2x100 mL). The organic layers were combined and washed with brine (1x200 mL). The final organic solution was dried over sodium sulfate and then concentrated to provide a yellow solid. Silica gel column purification was run twice. First using 4:3:1 hexane/ethyl acetate/ethanol with 1% by volume acetic acid. The product, collected with about 15% impurity, was further purified using 25% toluene, 25% of 3:1 ethyl acetate/ethanol, 49% hexane and 1% acetic acid by volume. The final product was obtained as a yellow solid. Yield: 0.3519 g (10.2% yield). NMRs:  $\delta$  H (500 MHz, Methanol-d<sub>4</sub>) 8.52 – 8.38 (2 H, m), 7.77 (2 H, d, J 7.5), 7.70 – 7.55 (2 H, m), 7.37 (2 H, t, J 7.5), 7.32 – 7.22 (4 H, m), 4.46 (2 H, s), 4.33 (2 H, dd, J 7.0, 3.8), 4.20 (1 H, t, J 7.0), 4.14 (1 H, dd, J 9.4, 4.6), 3.28 – 3.18 (2 H, m), 1.89 – 1.79 (1 H, m), 1.73 – 1.63 (1 H, m), 1.60 – 1.52 (2 H, m), 1.51 – 1.30 (11 H, m);  $\delta$  C (126 MHz, cd<sub>3</sub>od) 174.77, 157.19, 148.61, 143.92, 141.16, 128.91, 126.72, 124.85, 122.47, 119.49, 80.26, 66.51, 53.91, 31.08, 27.22, 27.16, 23.48, 22.73. Calculated Mass: 559.27; ESI+ Mass Found – 560.28 [M+H]<sup>+</sup>.

**Fmoc-D-Lysine(CyMe)(Boc)-OH:** Fmoc-D-lysine hydrochloride (1 eq, 3.70 mmol,

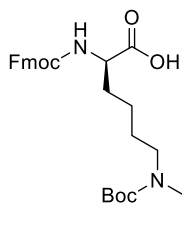


1.5 g) was dissolved in dry methanol (15 mL) and stirred with 3Å molecular sieves. To this, cyclohexane carboxaldehyde (1.2 eq, 4.45 mmol, 0.4987 g) was added. This mixture was allowed to stir for 1 hour before sodium cyanoborohydride (1.2 eq, 4.45 mmol,

0.2800 g) was dissolved in dry methanol (8 mL) and added to the mixture. This was allowed to stir overnight. The mixture was acidified with 1N HCl to pH ~2-3

and decanted from the sieves. The solvent was removed by rotary evaporation to obtain a solid. The crude solid was dissolved in a 1:1 mixture of water and THF (100 mL). To this, sodium bicarbonate (3 eq, 11.1 mmol, 0.9324 g) was added to bring the pH to ~8-9. While stirring, di-*tert*-butyl dicarbonate (1.2 eq, 4.45 mmol, 0.9712 g) was added. This was allowed to stir overnight. The THF was removed by rotary evaporation. To the aqueous mixture, ethyl acetate (50 mL) was added. While stirring, the mixture was acidified using 2N HCl to pH ~2-3. The organic layer was separated and the aqueous mixture was extracted with ethyl acetate (2x50 mL). The organic layers were combined and washed with brine (1x200 mL). The organic layer was then dried over sodium sulfate. The crude solid was obtained as a white solid after removing the solvent by rotary evaporation. Pure product was obtained as a white solid after silica gel column purification (4:3:1 hexane/ethyl acetate/ethanol with 1% acetic acid by volume). Yield: 0.5713 g (27.3% yield).  $\delta$  H (500 MHz, Methanol-d<sub>4</sub>) 7.79 (2 H, d, J 7.5), 7.67 (2 H, t, J 8.2), 7.38 (2 H, t, J 7.5), 7.30 (2 H, td, J 7.5, 1.1), 4.34 (2 H, d, J 7.8), 4.22 (1 H, t, J 7.1), 4.15 (1 H, dd, J 9.2,4.3), 3.24 – 3.09 (2 H, m), 3.01 (2 H, d, J 7.1), 1.93 – 1.81 (1 H, m), 1.74 – 1.51 (9 H, m), 1.43 (9 H, s), 1.40 – 1.34 (2 H, m), 1.31 – 1.10 (4 H, m), 0.95 – 0.82 (2 H, m);  $\delta$  C (126 MHz, cd<sub>3</sub>od) 174.49, 157.26, 156.26, 143.90, 141.16, 127.35, 126.74, 124.84, 119.49, 79.31, 66.57, 53.72, 52.98, 52.61, 47.07, 36.64, 30.99, 30.63, 30.50, 27.34, 26.19, 25.62, 22.81. Calculated Mass: 564.32; ESI+ Mass Found – 565.33 [M+H]<sup>+</sup>.

**Fmoc-D-Lysine(Cy)(Boc)-OH:** Fmoc-D-lysine hydrochloride (1 eq, 3.71 mmol, 1.51



g) was dissolved in 200 proof ethanol (15 mL) and stirred with

3Å molecular sieves. To this, cyclohexanone (2.0 eq, 7.42 mmol,

0.7291 g) was added. This mixture was allowed to stir for 1 hour

before sodium cyanoborohydride (1.2 eq, 4.46 mmol, 0.2800 g) was added to the

mixture. This was allowed to stir overnight. The mixture was acidified with 5%

aqueous HCl to pH ~3-4 and decanted from the sieves. The solvent was removed

by rotary evaporation to obtain a solid. The crude solid was dissolved in a 1:1

mixture of water and THF (20 mL). To this, sodium bicarbonate (3.1 eq, 11.4 mmol,

0.9610 g) was added to bring the pH to ~8-9. To this, di-*tert*-butyl dicarbonate (3.1

eq, 11.5 mmol, 2.5074 g) was added. This was allowed to stir overnight. To the

mixture, DCM (25 mL) was added. The mixture was acidified using 5% aqueous

HCl to pH ~3. The DCM was removed and the aqueous layer was extracted with

DCM (25 mL). The combined organic layers were washed with brine (1x50 mL)

and then dried over sodium sulfate. The solvent was removed by rotary

evaporation to provide a solid. The crude solid was purified by silica gel column

chromatography (25% toluene, 25% of 3:1 ethyl acetate/ethanol, 49% hexane, 1%

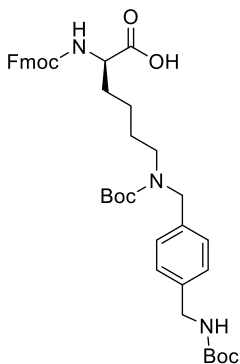
acetic acid) to yield the final product as a white solid. Yield: 0.4516 g (22.1% yield).

NMR:  $\delta$  C (126 MHz,  $cd_3od$ ) 174.52, 157.26, 155.83, 143.76, 141.16, 127.35, 126.72,

124.82, 119.49, 79.36, 66.58, 53.68, 48.08, 46.99, 31.00, 27.39, 25.77, 25.15, 23.04.

Calculated Mass: 550.30; ESI+ Mass Found - 551.33 [M+H]<sup>+</sup>.

**Fmoc-D-Lysine(4AMBn)(Boc)-OH:** Fmoc-D-lysine hydrochloride (1 eq, 2.47

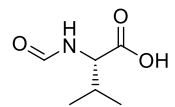


mmol, 1.0g) was dissolved in 200 proof ethanol (25 mL) and stirred with 3Å molecular sieves. To this, *tert*-butyl 4-formylbenzyl carbamate (1.2 eq, 2.96 mmol, 0.6973 g) was added. This mixture was allowed to stir for 1 hour before sodium cyanoborohydride (1.2 eq, 2.96 mmol, 0.1862 g) was

added. This was allowed to stir overnight. After decanting from the molecular sieves, the mixture was acidified by adding 5% aqueous hydrochloric acid dropwise to reduce any excess sodium cyanoborohydride. Removing the solid by rotary evaporation provided an off-white solid. The crude solid was dissolved in a 1:1 mixture of water and THF (130 mL) and stirred as sodium bicarbonate (6 eq, 14.82 mmol, 1.250 g) was added to bring the pH to ~8-9. To this, di-*tert*-butyl dicarbonate was added and the mixture was allowed to stir for 6 hours. The THF was removed by rotary evaporation. To the aqueous solution, ethyl acetate (200 mL) was added. This was then acidified using 1N HCl to a pH of ~2-3. The ethyl acetate was removed and the aqueous solution was extracted with ethyl acetate (2x200mL). The combined organic layers were washed with brine (1x500mL) and dried over sodium sulfate. The solvent was removed by rotary evaporation to provide a white solid. The final product was obtained after purification by preparative HPLC. Yield: 0.4885 g (28.8% yield). NMRs:  $\delta$  H (500 MHz, Methanol-d<sub>4</sub>) 7.78 (2 H, d, J 7.4), 7.66 (2 H, dd, J 10.6, 7.5), 7.37 (2 H, tt, J 7.4, 3.9), 7.32 - 7.26

(2 H, m), 7.25 – 7.14 (4 H, m), 4.43 – 4.32 (4 H, m), 4.24 – 4.16 (3 H, m), 4.10 (1 H, dd, J 9.3, 4.6), 3.23 – 3.10 (2 H, m), 1.84 – 1.75 (1 H, broad m), 1.70 – 1.60 (1 H, broad m), 1.53 – 1.32 (22 H, m);  $\delta$  C (126 MHz, cd3od) 174.49, 157.23, 143.92, 141.16, 138.59, 134.88, 128.91, 127.35, 126.94, 126.74, 124.82, 123.58, 119.49, 119.41, 79.84, 78.77, 66.51, 53.71, 47.01, 46.17, 43.33, 30.93, 29.71, 27.35, 27.32, 27.23, 26.91, 22.77. Calculated Mass: 687.35; ESI+ Mass Found – 688.36 [M+H]<sup>+</sup>.

**Formyl-L-valine:** Synthesis was performed as previously reported by our group.<sup>10</sup>

 L-Valine (8.35 mmol, 1.0g) was dissolved in formic acid (0.32 mmol, 12.0 mL) and allowed to stir in an ice bath for 15 minutes. To this, acetic anhydride (0.04 mmol, 4.0 mL) was added dropwise. When the addition was complete, the ice bath was removed and the reaction was allowed to stir at room temperature for 24 hours. The product was recrystallized using ethyl acetate and the product was collected as a white solid by vacuum filtration. NMR:  $\delta$  H (600 MHz, Acetone-d<sub>6</sub>) 8.22 (s, 1H), 7.41 (broad m, 1H), 4.50 (m, 1H), 2.22 (m, 1H), 0.98 (m, 6H).

### 2.6.3 Peptide Synthesis and Characterization

Synthesis was performed as previously reported by our group<sup>10</sup>. All peptides were synthesized on Fmoc-Trp-Wang resin (100 mg, 0.500 mmol/g, 0.05 mmol) using standard Fmoc/tBu chemistry. Five equivalents of each amino acid were used for the coupling reaction with 4.5 equivalents of HBTU. For Fmoc-D-Lys(3pyr)(Boc)-OH, Fmoc-D-Lys(4pyr)(Boc)-OH and Fmoc-D-Lys(4AMBn)(Boc)-OH, three equivalents were used instead of five with 2.25 equivalents of HBTU and the

coupling time was extended to 1.5 hours. The peptides were cleaved off the resin by treatment with ethanolamine (40% v/v in DMF, 55°C, 5 hours). Then the resin was filtered through a medium fritted plastic funnel and rinsed three times with DCM and methanol. To precipitate the peptide, six to seven times in volume DI water was added. The peptide was collected by centrifugation (14,000 rpm, 1.5 hr) and the pellet was dried by lyophilizer to receive the side-chain protected peptide. The boc protecting group on D-lysine and L-tryptophan was removed by treating the pellet with a mixture of 95% TFA, 2.5% TIS and 2.5% H<sub>2</sub>O at room temperature for two hours. Once the reaction was finished, cold diethyl ether was added to precipitate the crude peptide which was again centrifuged (14,000 rpm, 1.5 hours) and lyophilized. The crude material was purified by RP-HPLC (Waters Prep LC, Jupiter 10 μm C4 300A Column). The identity and purity of each peptide was confirmed by LC/MS (Agilent 2630 LC TOF, Phenomenex, Jupiter 5 μm C4 300R column) (Table 2-7). All peptides were confirmed to have purity of 95% or higher.

**Table 2-7.** Naming Scheme and Mass-spectrometry Characterization of gA Mutants. Each amino acid is named according to the functional group added, with the truncated structure shown along with the name of each corresponding peptide.

Peptide	<i>m/z</i> Calculated	<i>m/z</i> Found
gA3K(Bn)	2196.24 [M] <sup>+</sup>	733.43 [M+4H] <sup>3+</sup> , 1099.63 [M+3H] <sup>2+</sup> , 2198.26 [M+2H] <sup>+</sup>
gA3K(iPr)	2052.24 [M] <sup>+</sup>	685.42 [M+3H] <sup>3+</sup> , 1027.63 [M+3H] <sup>2+</sup> , 2054.25 [M+2H] <sup>+</sup>
gA3K(CyMe)	2214.38 [M] <sup>+</sup>	739.48 [M+4H] <sup>3+</sup> , 1108.71 [M+3H] <sup>2+</sup> , 2216.42 [M+2H] <sup>+</sup>
gA3K(Cy)	2172.34 [M] <sup>+</sup>	725.48 [M+4H] <sup>3+</sup> , 1087.72 [M+3H] <sup>2+</sup> , 2174.44 [M+2H] <sup>+</sup>

gA3K(2pyr)	2199.23 [M] <sup>+</sup>	734.43 [M+4H] <sup>3+</sup> , 1101.12 [M+3H] <sup>2+</sup> , 2201.24 [M+2H] <sup>+</sup>
gA3K(3pyr)	2199.23 [M] <sup>+</sup>	551.07 [M+5H] <sup>4+</sup> , 734.42 [M+4H] <sup>3+</sup> , 1101.13 [M+3H] <sup>2+</sup>
gA3K(4pyr)	2199.23[M] <sup>+</sup>	734.42 [M+4H] <sup>3+</sup> , 1101.12 [M+3H] <sup>2+</sup> , 2201.24 [M+2H] <sup>+</sup>
gA3K(4AMBn)	2283.32[M] <sup>+</sup>	572.07 [M+5H] <sup>4+</sup> , 762.43 [M+4H] <sup>3+</sup> , 1143.14 [M+3H] <sup>2+</sup> , 2285.27 [M+2H] <sup>+</sup>
gA3K(L,D,D)	1926.10[M] <sup>+</sup>	643.38 [M+4H] <sup>3+</sup> , 964.56 [M+3H] <sup>2+</sup> , 1928.11 [M+2H] <sup>+</sup>

#### 2.6.4 Circular Dichroism Spectroscopy with Model Membranes

Each peptide (0.1  $\mu\text{mol}$ ) dissolved in 2,2,2-trifluoroethanol (TFE, 20  $\mu\text{L}$ ) was mixed with sodium dodecyl sulfate (SDS, 5  $\mu\text{mol}$ ) or Fos-phosphatidylcholine-C12 (DPC, 4  $\mu\text{mol}$ ) in water (20  $\mu\text{L}$ ). The final samples were diluted to 1 mL with water. The samples were transferred into a quartz cuvette and CD spectrum were recorded (25°C, 1 cm path length, scan 190-280 nm with 1 nm step, 10 sec averaging time, 0.33 sec settling time) on the AVIV model 420 Circular Dichroism Spectrometer (Biomedical Inc., Lakewood, NJ). Spectrum of micelles alone were recorded under the same conditions and a blank subtraction was done for each peptide. CD spectra were replicated and the traces provided were the average of these two trials. The wild type peptide has a distinctive positive extreme near 218 nm, corresponding to the  $\beta$ -helical conformation of the amide backbone. In SDS samples, the negative control, gA3K(L, D, D), only appeared as a straight line, suggesting no secondary structure, and gA3K(CyMe) showed poor structure similarity to gA, with its positive extreme being slightly shifted. In the case of gA3K(CyMe), lack of the

defined signature was found to be a result of poor solubility in the SDS solution, as the sample became cloudy after addition of the peptide but remained clear for the other peptides. With its better signature in the sample with DPC micelles, the structure was confirmed to not be significantly different from the natural peptide. The second positive extreme observed in the wild type sequence appears near 235 nm and corresponds to the absorbance of the four tryptophans at the C-terminus of the peptide. In the studied peptides, this extreme shifted slightly in both samples. This reflects the disruption in the local environment of the tryptophans caused by the change of neighbouring leucines to the lysine analogues.

#### 2.6.5 Minimal Inhibitory Concentration Measurements<sup>20</sup>

Minimal inhibitory concentrations (MICs) were measured against gram-positive *Bacillus subtilis* (ATCC 663), *Staphylococcus aureus* (ATCC 6538) and methicillin-resistant *S. aureus* (MRSA, ATCC 43300) and gram-negative *E. coli* (BL21, gift from Prof. Mary Roberts), *Klebsiella pneumoniae* (ATCC 4352) and *Pseudomonas aeruginosa* (ATCC 27853) using the broth microdilution method. Gram-positive bacteria were tested in LB media and gram-negative in MH media. Specifically, a single colony selected from a LB agar plate was grown overnight in broth at 37°C with agitation and diluted 100 times into fresh broth the next morning. OD600 was monitored until a value between 0.5 and 0.6 was reached. The cells were diluted by a factor previously determined to a concentration of  $\sim 5 \times 10^5$  colony forming units per mL (cfu/mL). In a sterile 96-well plate, the cell suspension (200  $\mu$ L) was added to each



well. To each well, serial diluted (2-fold) peptides in DMSO (2  $\mu$ L) were added in triplicates. Using a microtiter plate reader (SpectraMax M5, Molecular Devices, Sunnyvale, CA), the OD600 was monitored overnight while incubating at 37°C, with readings taken every 10 minutes after the plate was shook for 15 seconds. Using the time point where OD600 of the blank (untreated) sample began to level off, MICs were determined to be the lowest concentration for which cell growth was not observed. To confirm this concentration in cases of high background, an aliquot was taken from each well and diluted  $10^4$  times in fresh broth before being spread on LB agar plates (100  $\mu$ L). This was also done for each blank. After overnight incubation of the plates, the MIC was confirmed if no colony growth was observed.

#### 2.6.6 Cell Killing Assay with *S. aureus*

A single colony of *S. aureus* was selected from a LB agar plate and grown overnight in LB broth, incubating at 37°C with agitation. In the morning, an aliquot was taken and diluted 100 times in fresh broth. The OD600 was monitored until it reached  $\sim 0.6$ . This culture was centrifuged (4000 rpm, 5 min) and washed with 10 mM tris acetate buffer (pH 7.4) two times. The final cell solution was diluted to  $\sim 5 \times 10^5$  cfu/mL in fresh buffer. In a sterile 96-well plate, 200  $\mu$ L was added to each well. To each well, 2  $\mu$ L of 125 $\mu$ M peptide in DMSO were added in triplicate. The plate was incubated for 10 min at 37°C. Aliquots of each sample (10  $\mu$ L) was diluted into fresh buffer (990  $\mu$ L) and mixed before being spread on LB agar plates. The plates

were allowed to incubate at 37°C overnight. Individual colonies were counted on each plate and triplicates were averaged for each peptide. To calculate a percent viability, the average number of colonies for each peptide was divided by the average number of colonies for blank samples and multiplying by 100. Percent killing was then considered to be the percent viability subtracted from 100. Experiments were replicated and error was calculated to be the standard deviation between percent killing for the six samples.

#### 2.6.7 Cell Killing Assay with *E. coli*

A single colony of *E. coli* was selected from a LB agar plate and grown overnight in LB broth, incubating at 37°C with agitation. In the morning, an aliquot was taken and diluted 100 times in fresh broth. The OD600 was monitored until it reached ~0.6. This culture was centrifuged (4000 rpm, 5 min) and washed with M9 media with 0.20% sodium succinate (pH 7.4) two times. The final cell solution was diluted to  $\sim 5 \times 10^5$  cfu/mL in fresh media. In a sterile 96-well plate, 200  $\mu$ L of cell suspension was added to each well. To each well, 125 $\mu$ M peptide in DMSO (2  $\mu$ L) were added in triplicate. The plate was incubated for two hours at 37°C. Aliquots of each sample (10  $\mu$ L) were diluted into fresh buffer (990  $\mu$ L) and mixed before being spread on LB agar plates. The plates were allowed to incubate at 37°C overnight. Individual colonies were counted on each plate and triplicates were averaged for each peptide. To calculate a percent viability, the average number of colonies for each peptide was divided by the average number of colonies for blank

samples and multiplying by 100. Percent killing was then considered to be the percent viability subtracted from 100. Experiments were replicated and error was calculated to be the standard deviation between percent killing for the six samples.

#### *2.6.8 Hemoglobin Release from Human Red Blood Cells<sup>22</sup>*

Fresh human red blood cells (hRBCs) were centrifuged (3500 rpm, 10 min) and washed with sterile PBS buffer until the supernatant was clear. The hRBCs were then resuspended and diluted in PBS buffer to a final concentration of 1% v/v and used immediately. To sterile Eppendorf tubes, hRBC solution (1.5 mL) was added and mixed with serial dilutions (2-fold) of peptides in DMSO or DMSO alone (1.5  $\mu$ L). As a positive control, a sample was treated with 1% TritonX-10. The samples were incubated at 37°C for 1 hour and then centrifuged (3500 rpm, 10 min). In a sterile 96-well plate, sample supernatant (50  $\mu$ L) was mixed with fresh Nanopure water (50  $\mu$ L) in triplicate. The absorbance of each sample at 415 nm was recorded. The triplicates were averaged and calculated using percentage hemolysis =  $100 \times (A_{415, \text{peptide}} - A_{415, \text{DMSO}}) / (A_{415, \text{TritonX-100}} - A_{415, \text{DMSO}})$ .

#### *2.6.9 Binding of gA Mutants to Live Cells*

A single colony of *S. aureus* or *E. coli* was grown overnight in LB media while incubating at 37°C with agitation. Cell suspensions were diluted 100 times in fresh media the next morning and the OD<sub>600</sub> was monitored until a value of ~0.6 was obtained. The cell suspension was centrifuged (4000 rpm, 5 min) and washed with a 10 mM tris acetate buffer (pH 7.4) two times. After washing, cells were diluted

to  $\sim 5 \times 10^5$  cfu/mL in fresh buffer. The cell suspension was aliquoted (1 mL) into sterile Eppendorf tubes to which each peptide at a concentration of 1.25 mM in DMSO (1  $\mu$ L) was added in triplicates, giving the final concentration of 1.25  $\mu$ M. Samples were incubated at room temperature for 10 min then centrifuged (14,000 rpm, 1 min). 0.5 mL of the supernatant was removed and lyophilized. Once dry, 50% nanopure water/50% HPLC-grade acetonitrile solution (50  $\mu$ L) was added to each tube. The tubes were sonicated for 10 minutes to ensure full recovery of peptide and then centrifuged (14,000 rpm, 10 min) to remove any insoluble salts. Samples were analyzed by LC/MS. To determine percent binding, the peak area of the triplicate samples was averaged and compared to a corresponding standard. Peptide standards were prepared using the same conditions stated above, but using buffer that did not contain any cells and also performed in triplicates and averaged. By taking the ratio of the averaged sample peak area to the average standard peak area  $\times 100$ , the percent of the peptide remaining in each sample is calculated; percent binding is calculated by subtracting this value from 100. Experiments were replicated and error is calculated as the standard deviation between percent binding of the six individual samples.

#### *2.6.10 Assessing Cell Permeability Using Flow Cytometry*

Samples of *S. aureus* and *E. coli* were subjected to the same conditions as in the respective cell killing assays using 1 mL of cell suspension with 1  $\mu$ L of 1.25 mM (for *S. aureus*) or 10 mM (for *E. coli*) of peptides dissolved in DMSO. For each

sample, a stock solution of PI (0.5 mg/mL in sterile PBS buffer, 0.4  $\mu$ L) was added before the peptide. As a negative control, a blank sample was measured without adding any PI. As a positive control, cells were suspended in 70% isopropanol in DI water after washing and incubated for 10 minutes at room temperature before being diluted to  $5 \times 10^5$  cfu/mL. Samples were measured on a Bio-Rad S3 Cell Sorter (Hercules, CA) and analyzed using FlowJo (Tree Star, Inc.) Samples measured of peptides alone showed no significant background except for gA WT. To compensate for this, the gA WT samples were gated based on forward and side scattering to eliminate the region that the peptide appeared.

## 2.7 References

- (1) Dubos, R. J. *J. Exp. Med.* **1939**, 70 (1).
- (2) Townsley, L. E.; Tucker, W. A.; Sham, S.; Hinton, J. F. *Biochemistry* **2001**, 40 (39), 11676–11686.
- (3) Ketchum, R. R.; Lee, K.-C.; Huo, S.; Cross, T. A. *J. Biomol. NMR* **1996**, 8 (1).
- (4) Kelkar, D. A.; Chattopadhyay, A. *Biochim. Biophys. Acta* **2007**, 1768 (9), 2011–2025.
- (5) Urry, D. W. *Proc. Natl. Acad. Sci. U. S. A.* **1971**, 68 (3), 672–676.
- (6) Wesolowski, R.; Sommer, A.; Arndt, H.-D.; Koert, U.; Reiss, P.; Wimmers, S.; Strauss, O. *Chembiochem* **2007**, 8 (5), 513–520.
- (7) Reiss, P.; Al-Momani, L.; Koert, U. *Chembiochem* **2008**, 9 (3), 377–379.
- (8) Dubos, R. J.; Hotchkiss, R. D. *Trans. Stud. Coll. Physicians Philadelphia* **1942**, 10 (1), 11–19.
- (9) Dubos, R. J.; Hotchkiss, R. D.; Coburn, A. F. *J. Biol. Chem.* **1942**, 146, 421–426.
- (10) Wang, F.; Qin, L.; Pace, C. J.; Wong, P.; Malonis, R.; Gao, J. *ChemBioChem*

- 2012**, 13 (1), 51–55.
- (11) Wang, F.; Qin, L.; Wong, P.; Gao, J. *Biopolymers* **2013**, 100 (6), 656–661.
- (12) Zasloff, M. *Nature* **2002**, 415 (6870), 389–395.
- (13) Hessa, T.; Meindl-Beinker, N. M.; Bernsel, A.; Kim, H.; Sato, Y.; Lerch-Bader, M.; Nilsson, I.; White, S. H.; von Heijne, G. *Nature* **2007**, 450 (7172), 1026–1030.
- (14) Killian, J. A.; von Heijne, G. *Trends Biochem. Sci.* **2000**, 25 (9), 429–434.
- (15) Huang, Z. P.; Du, J. T.; Su, X. Y.; Chen, Y. X.; Zhao, Y. F.; Li, Y. M. *Amino Acids* **2007**, 33 (1), 85–89.
- (16) Koeppe, R. E.; Anderson, O. S. *Annu. Rev. Biophys. Biomol. Struct.* **1996**, 25, 231–258.
- (17) Wallace, B. A.; Veatch, W. R.; Blout, E. R. *Biochemistry* **1981**, 20 (20), 5754–5760.
- (18) Rice, L. B. *J. Infect. Dis.* **2008**, 197 (8), 1079–1081.
- (19) Boucher, H. W.; Talbot, G. H.; Bradley, J. S.; Edwards, J. E.; Gilbert, D.; Rice, L. B.; Scheld, M.; Spellberg, B.; Bartlett, J. *Clin. Infect. Dis.* **2009**, 48 (1), 1–12.
- (20) Wiegand, I.; Hilpert, K.; Hancock, R. E. W. *Nat. Protoc.* **2008**, 3 (2), 163–175.
- (21) Paliy, O.; Gunasekera, T. S. *Appl. Microbiol. Biotechnol.* **2006**, 73 (5), 1169–1172.
- (22) Meng, H.; Kumar, K. *J. Am. Chem. Soc.* **2007**, 129 (50), 15615–15622.
- (23) Patrick, J. W.; Zervas, B.; Gao, J.; Russell, D. H. *Analyst* **2017**, 142 (2), 310–315.

## **Chapter 3**

# **Targeting Lys-PG Based Antibiotic Resistance with 2-Acetylphenyl Boronic Acid Presenting Peptides**

### **3.1 Introduction**

#### *3.1.1 Bacterial Resistance to Cationic Antimicrobials*

Similar to small molecule natural products, cationic antimicrobial peptides (CAMPs) have suffered from the threats of bacterial resistance. As this class of antibiotics typically takes advantage of charge-charge interactions with the negatively-charged cell surface of bacteria, resistance mechanisms observed include covalent modification of targeted cell surface molecules.<sup>1</sup> Through these modifications, bacteria decrease their negative charge, thus decreasing the energetic favorability of the binding of CAMPs. This has led to several different resistance mechanisms in many species (Table 3-1).<sup>1-3</sup>

One relevant example of this is observed in gram-negative bacterial resistance towards polymyxin B. Polymyxins initially bind the highly anionic lipopolysaccharide (LPS), subsequently using the association to cause permeabilization of the membrane. To fight against this, bacteria have developed different covalent modifications of the lipid A moiety.<sup>3</sup> Modifications include the addition of phosphoethanolamine (PEtN) and 4-amino-4-deoxy-L-arabinose (L-Ara4N) to the phosphate groups of Lipid A through an elegant cascade of genes being turned on after polymyxin exposure (Figure 3-1). Of these two, the L-Ara4N modification is not only the most prevalent but also the most effective of these, as it completely neutralizes the charge of Lipid A from -1.5 to 0; the addition of PEtN only results in a minor shift to -1.0.<sup>4</sup>



**Table 3-1:** Bacterial Resistance Mechanisms to CAMPs Involving Covalent Modifications to Cell Surface Molecules (Modified from Ref. 1)

CAMP resistance phenotype	Gene(s)	Resistance to	Bacteria*
Addition of L-lysine or L-alanine to phosphatidylglycerol (L-PG; A-PG) in cell membrane	<i>mprF</i>	Arenicin-1, CAP18, gallidermin, HBD-3, HNP1-3, LL-37 lugworm beta-sheet peptide, lysozyme, magainin II, melittin, nisin, NK-2, polymyxin B, protamine, protegrin 3 and 5, tachyplesin 1, vancomycin	<i>Staphylococcus aureus</i>
	<i>lysC</i>		<i>Bacillus anthracis</i>
	<i>lysX</i>		<i>Listeria monocytogenes</i>
	<i>PA0920</i>		<i>Mycobacterium tuberculosis</i> <i>Pseudomonas aeruginosa</i>
D-alanylation of lipoteichoic acid (LTA) and teichoic acid in bacterial cell wall (WTA)	<i>dlt operon</i>	Cecropin B, colistin, gallidermin, HNP1-3, indolicidin, CRAMP, magainin II, nisin, polymyxin B, protegrin 1, 3 and 5, tachyplesin 1 and 3	<i>Staphylococcus aureus</i>
	<i>dltA</i>		<i>Listeria monocytogenes</i> Group B <i>Streptococcus</i> Group A <i>Streptococcus</i> <i>Streptococcus pneumoniae</i> <i>Enterococcus faecalis</i>
Synthesis and extension of lipooligosaccharide (LOS)	<i>lpxA</i> <i>waaF</i> , <i>lgtF</i> , <i>galT</i> , <i>cstII</i>	Crp4, Fowl-1, HD-5, LL-37, polymyxin B	<i>Neisseria meningitidis</i> <i>Campylobacter jejuni</i>
Addition of pEtN to lipid A	<i>lpxE<sub>HP</sub></i> <i>cj0256</i> <i>pmrC</i> <i>lptA</i>	LL-37, protegrin 1, polymyxin B	<i>Helicobacter pylori</i> <i>Campylobacter jejuni</i> <i>Salmonella enterica</i> <i>Neisseria gonorrhoeae</i> <i>Neisseria meningitidis</i>
Addition of aminoarabinose to lipid A	<i>pmr genes</i>	C18G, HBD-2, polymyxin B, protegrin 1, synthetic protegrin analogs	<i>Salmonella enterica</i> <i>Proteus mirabilis</i> <i>Pseudomonas aeruginosa</i> <i>Klebsiella pneumoniae</i>
Acylation of lipid A	<i>pagP</i>	C18G, colistin, CP28, HBD-2, LL-37, magainin II, CRAMP, protegrin 1, PGLa, polymyxin B and E	<i>Salmonella</i> spp.
	<i>rcp</i>		<i>Legionella pneumophila</i>
	<i>htrB</i>		<i>Haemophilus influenzae</i>
	<i>msbB</i>		<i>Vibrio cholerae</i>
	<i>lpxM</i>		<i>Klebsiella pneumoniae</i>
Phosphorylcholine in LPS	<i>licD</i>	LL-37	<i>Haemophilus influenzae</i>
Synthesis of polysaccharide capsule	<i>cps</i>	HBD-1 and 3, HNP-1 and 2, lactoferrin, polymyxin B, protamine, CRAMP, CRAMP-18, HNP-1 and 2, LL-37, protegrin 1, polymyxin B, $\beta$ -defensin-1, 2 and 3	<i>Klebsiella pneumoniae</i>
	<i>siaD</i>		<i>Neisseria meningitidis</i>
	<i>sia operon</i>		<i>Staphylococcus epidermidis</i>
	<i>ica genes</i> <i>cap</i>		

Gram-positive bacteria take a similar approach by modifying negatively charged phospholipids in the membrane. Most often, this involves the acylation of phosphatidylglycerol (PG) with either lysine or alanine (Figure 3-2).<sup>5</sup> Such mechanisms have also been implicated in daptomycin resistance, as PG is the membrane target of the lipopeptide.<sup>6</sup>

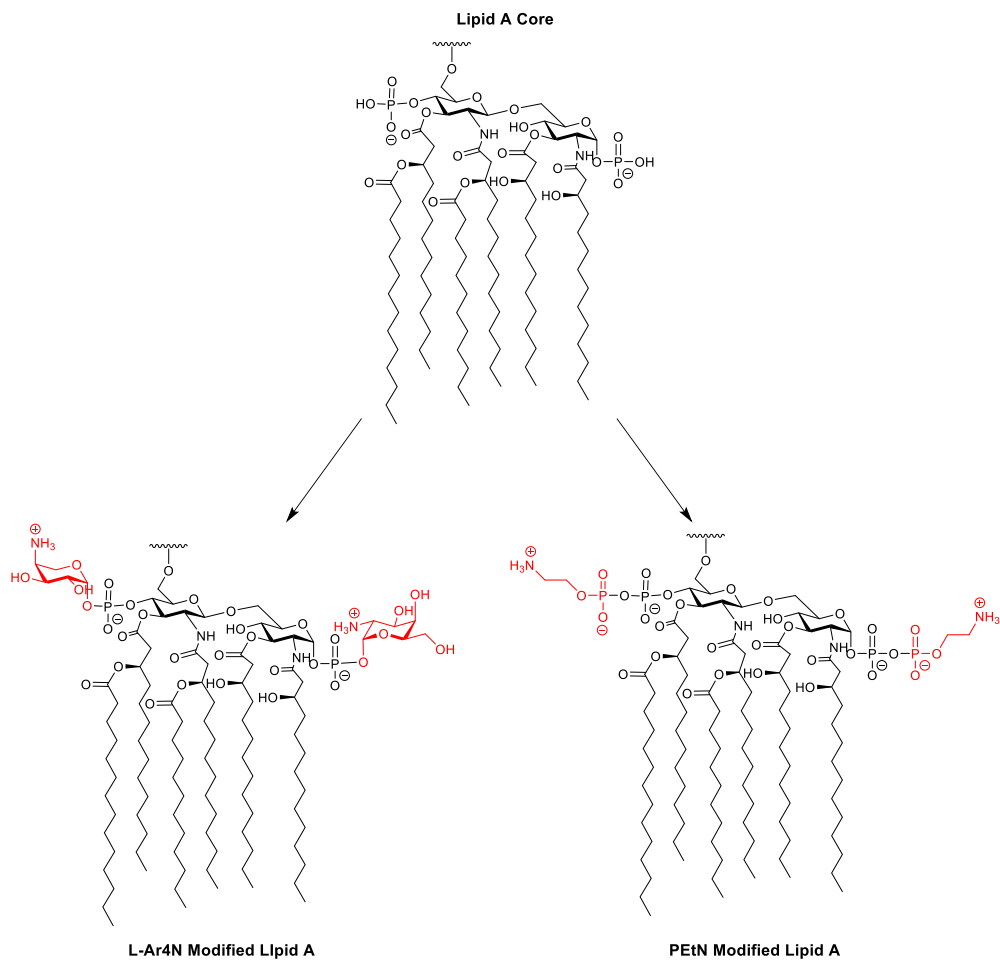


**Figure 3-1:** Lipid A and its modified structures that can elicit CAMP resistance. The two modifications (shown in red) can be made to either the 4'-phosphate, 1-phosphate or both.

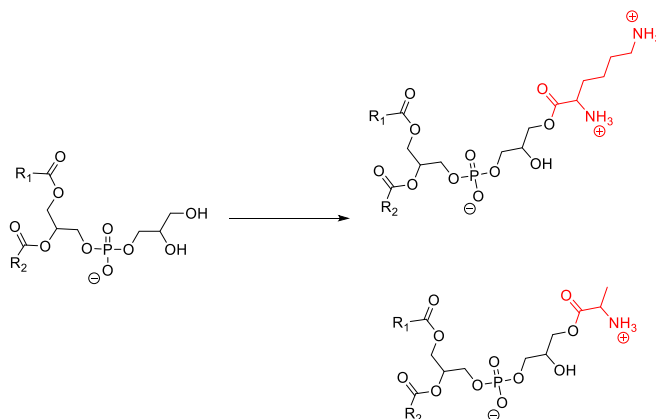
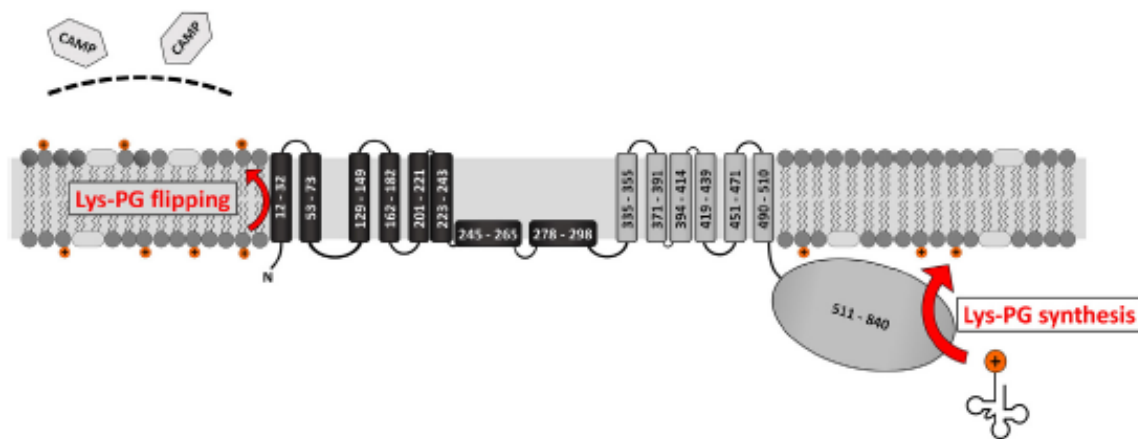


**Figure 3-2:** Phosphatidylglycerol and its modified structures that can elicit CAMP resistance. The two modifications (shown in red) involve the acylation of a glycerol alcohol with either lysine or alanine.

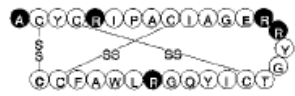
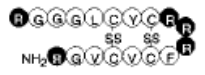


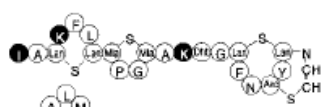
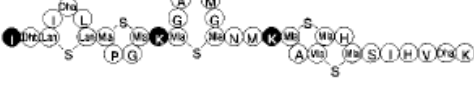




### 3.1.2 Multiple Peptide Resistance Factor (MprF)-Mediated Resistance and the Significance of Lys-PG

CAMP-resistance in *S. aureus* has been, in part, attributed to the modification of PG in the plasma membrane to include an L-lysine residue (Figure 3-2). This new phospholipid is known as lysyl-phosphatidylglycerol (Lys-PG) and has a +1 charge, in contrast to the -1 charge of PG. Multiple peptide resistance factor (MprF) is the transmembrane protein found to be responsible for the presentation of this modification.<sup>7</sup> First, the Lys-PG synthase domain of MprF acylates PG on the inner leaflet with free L-lysine after which the translocase domain flips it to the outer leaflet, presenting the new cationic charge to the cell's environment (Figure 3-3).<sup>8,9</sup>



**Figure 3-3:** Depiction of MprF in a bacterial membrane. In the Lys-PG synthase domain, a charged lysyl tRNA allows for the modification of PG on the inner leaflet of the membrane. The transmembrane flippase domain is responsible for moving Lys-PG from the inner leaflet to the outer leaflet, displaying the cationic charge on the surface of the cell. Taken from Ref. 9.

**Table 3-2:** MICs of Common CAMPs Towards Wild-Type and *mprF* Knockout *S. aureus*. Gramicidin S and Gramicidin D are provided as representative uncharged AMPs, which are not affected by the presence of Lys-PG. Taken from Ref. 7.

		Minimal inhibitory concentration (μM) against <i>S. aureus</i> Sa113		
		Wild-type (pRB473)	<i>mprF</i> :: <i>erm</i> (pRB473)	<i>mprF</i> :: <i>erm</i> (pRB <i>mprF</i> )
<b>Defensin HNP-1*</b> (human neutrophils)		>60	4.4	>60
<b>Protegrin 3</b> (porcine leukocytes)		13	1.1	8.8
<b>Protegrin 5</b> (porcine leukocytes)		9.5	1.1	5.3
<b>Tachyplesin 1</b> (horseshoe crab)		12 30 <sup>‡</sup>	0.4 0.9 <sup>‡</sup>	ND ND <sup>‡</sup>
<b>Gallidermin</b> ( <i>S. gallinarum</i> )		2.1	0.3	2.3
<b>Nisin</b> ( <i>L. lactis</i> )		14	0.5	14
<b>Magainin II<sup>§</sup></b> (clawed frog skin)		18	4.4	17
<b>Melittin</b> (honeybee venom)		8.5	2.1	6.0
<b>Gramicidin S</b> ( <i>B. brevis</i> )		3.9	3.1	2.3
<b>Gramicidin D</b> ( <i>B. brevis</i> )		0.5	0.3	0.6

Although the existence of aminoacylated-PGs had been known for decades,<sup>10</sup> the *mprF* gene in *S. aureus* had not been reported until the work by Peschel and co-workers published in 2001.<sup>7</sup> Through their efforts with transposon mutagenesis, this group identified MprF as the protein responsible for the production of Lys-PG and also observed that activity of several different CAMPs could be restored through *mprF* gene knockout (Table 3-2). Additionally, they found that CAMPs bound less efficiently to *S. aureus* expressing Lys-PG. Since then, proteins related to MprF have been identified in 31 gram-positive

genera.<sup>11</sup> This data, along with the aforementioned Lys-PG expression observed in daptomycin resistant bacteria, has supported MprF and Lys-PG as clinically relevant targets.

### *3.1.3 Use of Reversible Covalent Interactions for Drug Target Affinity*

As much of drug development has been steered towards target based discovery, a myriad of strategies to achieve potent and selective binding has been utilized. In nature, highly selective binding associations are achieved via combinations of non-covalent interactions. This allows for reversibility of these interactions, such that different activities can be turned on or off as necessary to the cell. However, in some drug therapies, it may be more beneficial to permanently modify the desired target. For example, a drug which can covalently bind a bacteria-specific target can make a potent antibiotic, as is the case with penicillin.<sup>12</sup> Unfortunately, this strategy comes with a higher propensity towards toxic off-target effects via irreversible modification of off-target proteins.

The use of reversible covalent interactions offers a promising intermediate between non-covalent and covalent target binding: they offer the potency and molecular specificity of their irreversible counterparts, but have a lower risk of off-target toxicity, much like non-covalent interactions.<sup>13</sup> Further target specificity can also be gained through non-covalent modifications with the surrounding protein landscape. Currently, there are a few potential or already

approved drugs that take advantage of reversible covalent interactions with targets displaying cysteines or diols (Figure 3-4).<sup>12</sup>

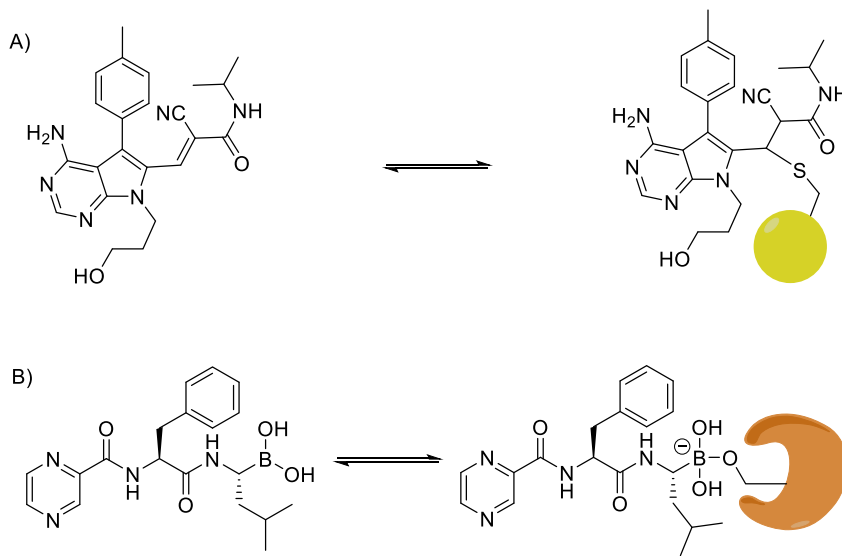


**Figure 3-4:** Examples of small molecule drugs that bind using reversible covalent interactions. A) Structure of an  $\alpha$ -cyanoacrylamide based inhibitor of RSK2 kinase; the cyano-substituted acrylamide was added to the structure of a known kinase-binding scaffold, increasing its potency and selectivity. B) Structure of bortezomib, a FDA-approved for multiple myeloma; it is active via boronate formation with an activated threonine in the 26S proteasome, mimicking the transition state of this residue in the proteasome. Structures and information from Ref. 13.

Recently, our group and others have reported the use of 2-formylphenyl boronic acid (2-FPBA)<sup>14</sup> and 2-acetylphenyl boronic acid (2-APBA)<sup>15-17</sup> for specific targeting of biological amines. In normal aqueous conditions, Schiff base formation is not thermodynamically favorable, due to its required elimination of water. However, with the addition of the boronic acid ortho to the carbonyl, a stabilizing dative bond can be formed between the nitrogen and boron, decreasing the energetic penalty of eliminating water (Figure 3-5). Specifically, our group has demonstrated potent and selective binding *in vitro* to gram-

positive bacteria over mammalian and gram-negative cells.<sup>17</sup> Additionally, by incorporating the unnatural amino acid AB1 into a cationic peptide (Hlys-AB1), we were able to selectively label *S. aureus* over Jurkat cells and maintained potent binding, even in the presence of serum proteins (Figure 3-6). This stable labeling demonstrated the ability for this molecule to resist off-target binding, as serum proteins contain a high number of lysines.

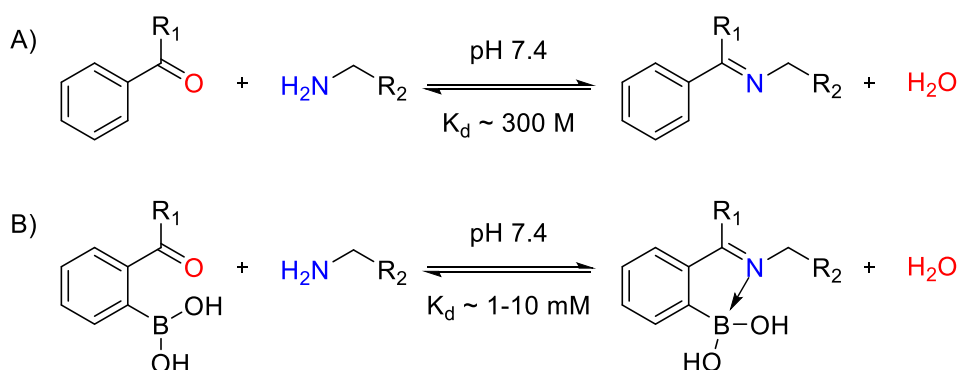


**Figure 3-5:** Depiction of A) Schiff base and B) iminoboronate formation at physiological conditions. The stabilizing effects of the addition of a boronic acid ortho to the ketone can be observed in the drastic decrease in  $K_d$  for 2-APBA compared to acetophenone.

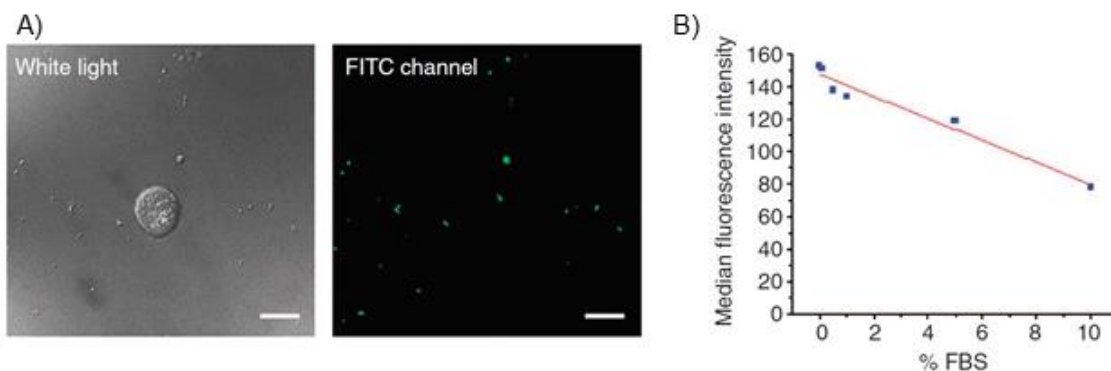


**Figure 3-6:** Study of Hlys-AB1 with Jurkat and *S. aureus* cells. A) Confocal microscopic images of a co-culture of Jurkat and *S. aureus* cells. As can be seen in the FITC channel, fluorophore labeled Hlys-AB1 shows preferential staining of the *S. aureus* over Jurkat cells. B) The graph displays the concentration dependent FBS inhibition of *S. aureus* staining as analyzed by flow cytometry. FBS can be included up to 10% with only 50% inhibition of staining. Modified from Ref. 17.

To explain this selectivity, we considered the lipid membrane composition of the gram-positive bacteria tested compared to Jurkat cells. Mammalian cells predominantly contain sphingomyelin (SM) and phosphatidylcholine (PC), which both present quaternary amines unable to form Schiff bases. On the other hand, *S. aureus* has been observed to present Lys-PG, as mentioned earlier in this section. Using model membrane systems, we were able to demonstrate selective binding for Lys-PG and phosphatidylethanolamine (commonly found in *B. subtilis*) containing liposomes compared to those containing PC and PG. As such, we concluded our peptides can obtain selectivity for *S. aureus* over Jurkat cells as a result of their varied lipid compositions.

#### *3.1.4 Designing Peptides Incorporating 2-APBA for Potent Antibacterial Activity Towards Lys-PG Presenting S. aureus*

With the success we saw for selective labeling of *S. aureus*, we envisioned taking this strategy a step further. As stated above, a prevalent mechanism for *S. aureus* to gain resistance against cationic antimicrobials is to express Lys-PG on the outer leaflet of their plasma membrane, thus weakening the electrostatic interactions used by the antimicrobial peptide to target these cells. In our own data provided in the previous chapter, we observed the effects of this change in membrane electrostatics, as our mutants saw a greater loss in potency towards *S. aureus* compared to *B. subtilis* with increasing charge (see Table 2-4). Given this trend, we hypothesized that the addition of a Lys-PG specific moiety, namely



APBA containing unnatural amino acid AB3, would allow us to regain potency of CAMPs, and could possibly increase the selectivity for these bacteria over mammalian cells.

We chose to continue working with gramicidin peptides, as we already had extensive experience studying and characterizing them. Gramicidin A (gA) naturally exists as part of a mixture of similar peptides (gB and gC) named gramicidin D (gD).<sup>18</sup> gA is generally considered to be the most responsible for the activity of gD, as it makes up 80% of the total mixture. The other two peptides, gB and gC, replace the tryptophan at residue 11 with a phenylalanine and a tyrosine, respectively. Based on these naturally tolerated differences, we were confident that a mutation with similar structure would also be accepted without significant perturbation to the peptide.

Instead of using gA3K as a scaffold for peptides including the 2-APBA moiety, we chose to use the triple arginine mutant, gA3R, due to our observation that potent iminoboronate formation can occur between intramolecular 2-APBAs and lysines, resulting in peptide cyclization.<sup>19</sup> Next, we decided to mutate the final tryptophan (residue 15) to AB3. Though this is not the position changed in gB and gC, the choice of residue 15 was ideal for two reasons. First, this position is closest to the lipid head groups when the peptide is properly folded into the membrane,<sup>20</sup> making it the least likely to disrupt the  $\beta$ -helical structure when conjugated through iminoboronates. Additionally, we predicted this position

would best tolerate the increase in hydrophilicity from tryptophan to AB3, since it resides closest to the membrane-water interface. The proposed sequence for this series of gA3R peptides can be seen in Figure 3-7.

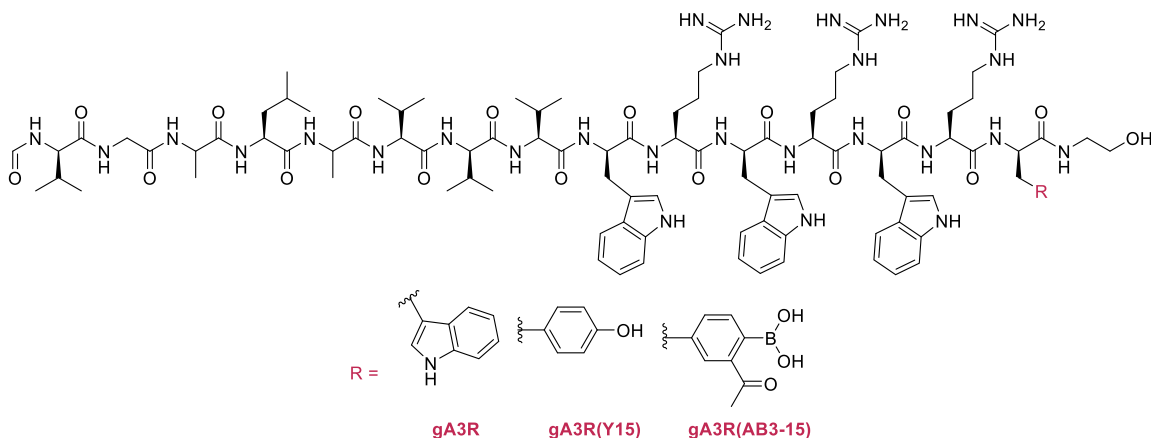


**Figure 3-7:** Structures of gA3R Mutants

To test our hypothesis, we compared antimicrobial activity of gA3R(AB3-15) to that of gA3R and found that addition of the 2-APBA warhead actually decreased our potency. We speculated that this was due to membrane binding preventing proper folding or mobility of the peptide once attached to the cell. We went on to consider using a co-treatment of gA3R and a Lys-PG targeting peptide. Working with Kelly A. McCarthy towards this goal, we found that the potency of gA3R could be increased when applied in the presence of a cyclic peptide with potent Lys-PG binding.

Overall, we believe that these results will lead to new strategies for targeting bacteria with CAMP resistance. We are currently working towards

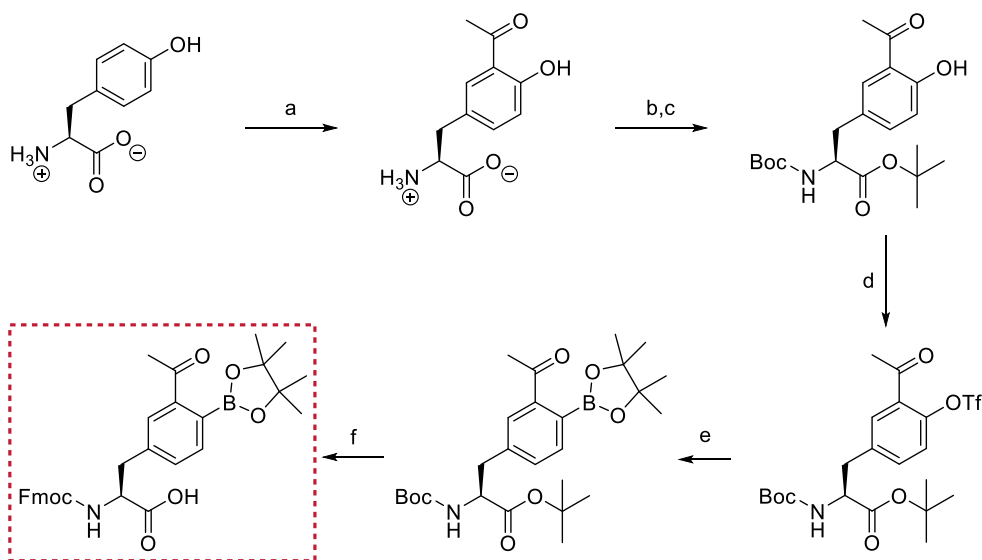
exploring this further and improving our knowledge on Lys-PG in gram-positive bacteria.

### 3.2 Use of gA3R(AB3-15) for Treatment of Lys-PG Presenting Bacteria

#### 3.2.1 Synthesis of Fmoc-AB3(pin)-OH

The unnatural amino acid AB3, synthesized as previously reported by our group (Scheme 3-1),<sup>19</sup> is a more rigid structure compared to AB1,<sup>17</sup> giving it a lower entropic penalty for binding. Along with this more favorable characteristic, AB3 is closely related to the structure of phenylalanine. This makes its structure more similar to mutations observed in gB or gC, suggesting it would be accommodated better in the gramicidin structure.

**Scheme 3-1:** Synthetic Route to Fmoc-AB3(pin)-OH



a)  $\text{AlCl}_3$ ,  $\text{CH}_3\text{COCl}$ , Nitrobenzene,  $100^\circ\text{C}$ ; b)  $(\text{Boc})_2\text{O}$ , THF/ $\text{H}_2\text{O}$ ,  $\text{Na}_2\text{CO}_3$ ; c) t-butyl 2,2,2-trichloroacetimidate, EtOAc,  $60^\circ\text{C}$ ; d)  $(\text{CF}_3\text{SO}_2)_2\text{O}$ , DCM,  $\text{Et}_3\text{N}$ ; e) 8 mol%  $\text{Pd}(\text{dppf})\text{Cl}_2/\text{dppf}$ , KOAc,  $\text{B}_2\text{pin}_2$ , dioxane,  $87^\circ\text{C}$ ; f) i) 60% TFA in DCM; ii) neat TFA; iii) Fmoc-OSu, DCM

Following the reported synthesis, we started with L-tyrosine and performed a Friedel-Crafts acylation with acetyl chloride to install the acetyl group ortho to the alcohol. As the alcohol is an ortho/para directing group and the para position is already occupied by the  $\alpha$ -carbon, only one product was obtained. The acylated product is obtained by precipitation from concentrated HCl and used without purification for Boc-protection of the main chain amine and tert-butyl protection of the carboxylic acid. After silica gel column chromatography, the yield over these three steps was about 40%.

To prepare the material as a substrate for Miyaura borylation, the next step was triflate protection of the phenyl alcohol. Following purification, this step has near quantitative yield. The crucial and most sensitive step of this synthesis was the Miyaura borylation. Done in an inert atmosphere, this cross-coupling reaction installs the pinacol-protected boronic acid. The temperature was found to be very important to limiting the degree of protodeboronation that occurred, and thus was strictly maintained at 85-87°C. After purification, this step generally yielded 50-60% pure product. Finally, deprotection of both the Boc and tButyl groups followed by Fmoc protection of the amine prepared the amino acid for SPPS.

### 3.2.2 Synthesis of gA3R(AB3-15)

To achieve this peptide sequence, we were required to first couple Fmoc-AB3(pin)-OH to Wang resin. Being a benzyl alcohol functionalized resin,

attaching the first residue requires esterification mediated by *N,N'*-diisopropylcarbodiimide (DIC) and a catalytic amount of 4-dimethylaminopyridine (DMAP). After this coupling, the loading efficiency can be measured by cleaving Fmoc from a small fraction of the resin and measuring the absorbance of dibenzofulvene in the resulting solution.<sup>21</sup> In this case, about 70% loading was achieved. Repeating the procedure, with half the equivalents of AB3 and DIC, provided the resin with >90% loading, which was taken on to be used in peptide synthesis, following the same synthetic route as previous gA peptides.

After resin cleavage and side-chain deprotection, the desired peptide mass was not obtained. By examining the different steps of our resin treatment after peptide synthesis, we concluded that the ethanolamine treatment used to install the C-terminal modification was incompatible with our unnatural AB3. Specifically, it appeared that ethanolamine treatment could lead to either displacement of the pinacol with ethanolamine, which was not reversible by acidic RP-HPLC purification, or complete loss of the boronic acid. At this point, we investigated alternatives for installing the C-terminal ethanolamine group.

To avoid exposing our unnatural amino acid to ethanolamine, we looked into ways to install the modification at the beginning of the peptide synthesis. This would require the use of a resin to which an alcohol could be conjugated. Considering several different options, we chose to work with a

trichloroacetimidate-functionalized Wang resin.<sup>22</sup> The necessary materials could be readily prepared from the Wang resin we used previously and simply required the synthesis of Fmoc-protected ethanolamine as a substrate. After successful conjugation of Fmoc-ethanolamine, SPPS can proceed normally (Figure 3-8).

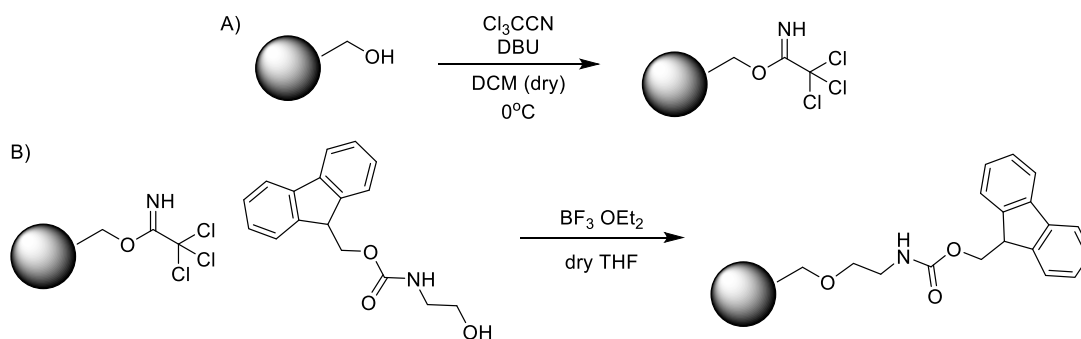


**Figure 3-8:** Preparation of Resin for gA3R(AB3-15) Synthesis. A) Conversion of the Wang resin alcohol to a trichloroacetimidate (TCA); B) Coupling of Fmoc-ethanolamine to TCA resin.

To convert the benzyl alcohol to the trichloroacetimidate, Wang resin was swelled in dry DCM then stirred with trichloroacetonitrile in the presence of 1,8-diazabicyclo[5.4.0]undec-7-ene (DBU).<sup>22</sup> It was found that the degree of conversion was dependent on both the resin being thoroughly dried prior to swelling and the temperature of the reaction. As such, the resin was dried under vacuum and kept under argon for the duration and the reaction, which was maintained at 0°C. The conversion of the alcohol to the trichloroacetimidate was monitored by FT-IR (see Figure 3-9). Specifically, the disappearance of the peak at 3566 nm corresponding to the O-H stretch of the benzyl alcohol and the appearance of a new peak at 3338 nm corresponding to the N-H stretch of the

acetimidate were monitored. It was found that one hour of reaction was sufficient for full conversion.

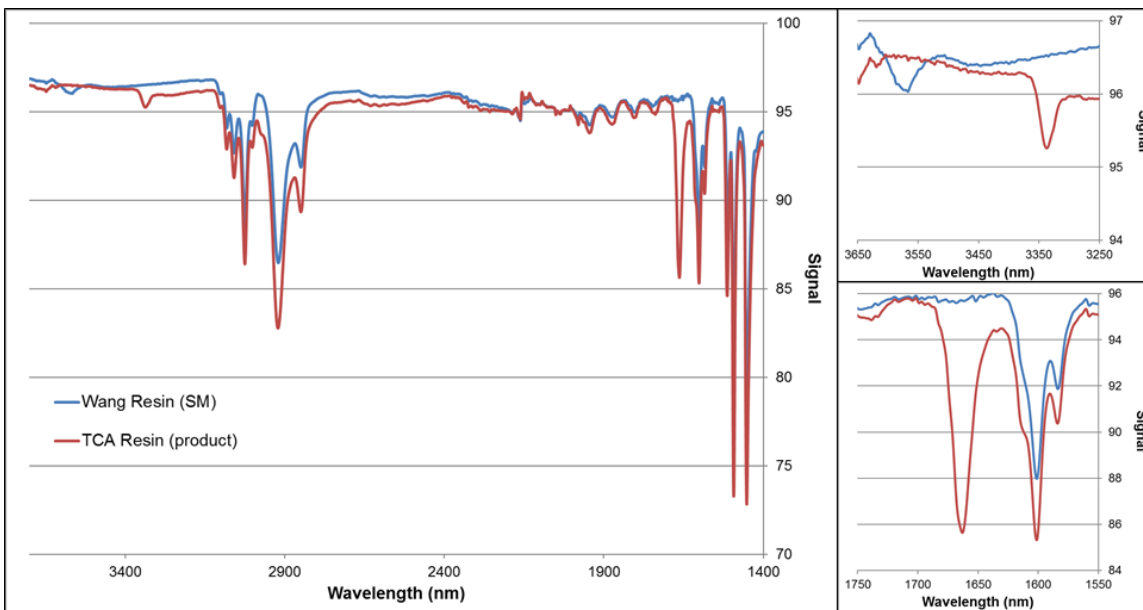


**Figure 3-9:** Solid state FT-IR spectra for the conversion of Wang resin to TCA resin. A) Spectrum from 1400-3600 nm; B) Segment from 3250 to 3650 nm, displaying the peak shifting from the benzyl alcohol O-H stretch (3566 nm) to the acetimidate N-H stretch (3338 nm); C) Segment from 1550 to 1750 nm, showing the formation of a peak at 1662 nm.

The subsequent reaction to couple the Fmoc-ethanolamine was also found to be very dependent on dryness of the solvent. As such, dry THF was removed from a still immediately prior to the reaction and the resin was washed twice with this solvent before adding the other reagents. The conversion to this ether bond was also be monitored by FT-IR, specifically looking for the disappearance of the peaks related to the trichloroacetimidate at 1662 and 3338 nm and the appearance of the ether stretch at 1724 nm (Figure 3-10). Additionally, a capping step using methanol was included after it was observed that complete conversion was difficult to achieve; this would prevent any undesirable side reactions by

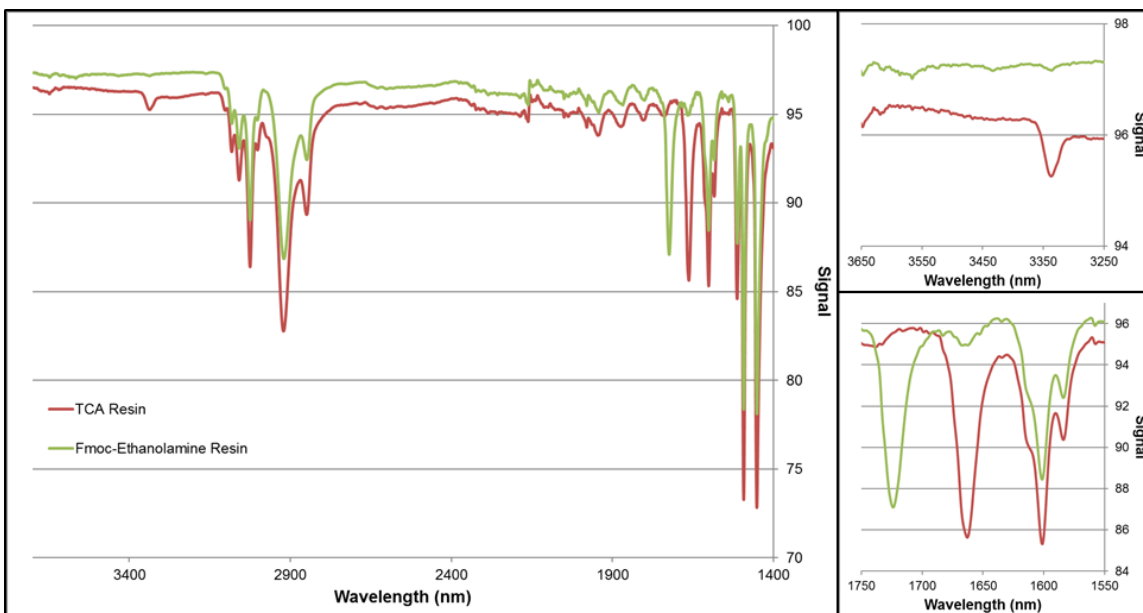


**Figure 3-10:** Solid state FT-IR for the coupling of 2-(Fmoc-amino)ethanol to TCA resin. A) Spectrum from 1400-3600 nm; B) Segment from 3250 to 3650 nm, displaying the disappearance of the acetimidate N-H stretch (3338 nm); C) Segment from 1550 to 1750 nm, showing the disappearance of the TCA peak at 1662 nm and the formation of the ether stretch at 1724 nm.

quenching remaining reactive trichloroacetimidate groups prior to peptide synthesis. Along with the IR analysis, loading of the resin can be determined using the same Fmoc-loading test as the Wang resin or also by measuring the amount of Fmoc-ethanolamine that can be recovered from resin cleavage. Both of these methods provided comparable loadings in the range of 90-95%.

With the resin prepared, gA3R(AB3-15) was synthesized as before. Unfortunately, similar issues as observed with the original Wang resin were encountered, most likely due to poor coupling to the ethanolamine, such that free ethanolamine was released during peptide cleavage. This was supported via NMR data which confirmed the presence of ethanolamine after TFA cleavage



following a single residue coupling. At this point, we chose to synthesize the peptide without this C-terminal modification (Figure 3-11) and compare it to the corresponding gA3R peptide. To best mimic the natural structure, we used the Rink amide resin, leaving a C-terminal amide instead of the carboxylic acid that would result from using the Wang resin. This yielded a relatively clean peptide that was straightforward to purify.

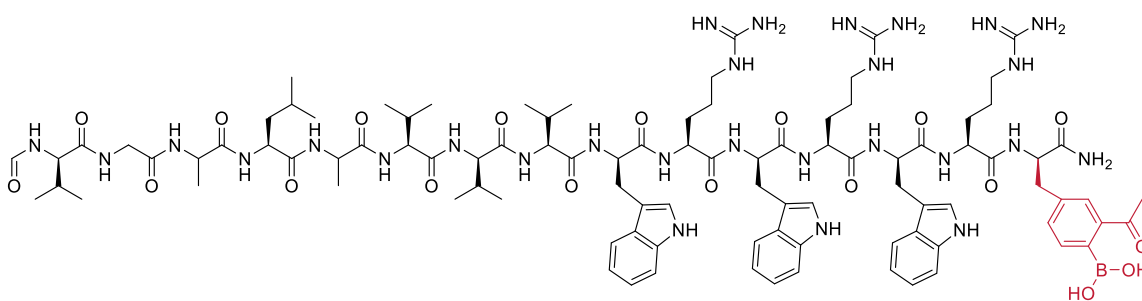


**Figure 3-11:** Structure of final gA3R(AB3-15)-NH<sub>2</sub> peptide from Rink Amide resin.

### 3.2.3 Characterizing the Antimicrobial Activity of gA3R(AB3-15)-NH<sub>2</sub>

Initially, we analyzed a control with Trp15 mutated to Tyr, mimicking gB. As gA is considered to be the most active peptide in the gD mixture, little work has been reported investigating the antimicrobial activity of gB or gC. To compare gA3R with gA3R(Y-15), we determined the MIC of each peptide with *S. aureus* (Figure 3-12). From this, we observed that there was about a 3-fold decrease in activity at a final peptide concentration of 10  $\mu$ M. These results also show a slight decrease in activity when the ethanolamine group is removed. We

characterized gA3R(AB3-15) in the same way, but unfortunately the results were a bit noisy and difficult to interpret (Figure 3-13).

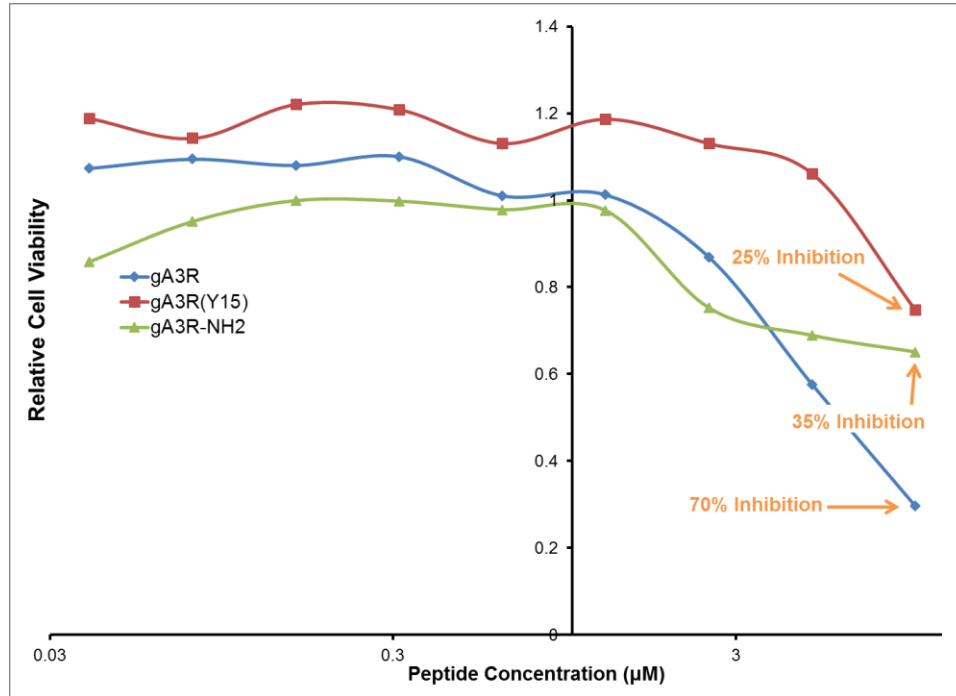


**Figure 3-12:** MIC Assay of gA3R mutants with *S. aureus*.

Given the difficulty in drawing conclusions from the MIC results, we chose to instead use our cell killing assay to get a more quantitative comparison of the effects of adding AB3 to the gA sequence. However, from these results (Figure 3-14), it is clear that the addition of AB3 proved to be detrimental to the activity of gA3R. Compared to gA3R-NH<sub>2</sub> (without ethanolamine), a four-fold loss in activity is observed.

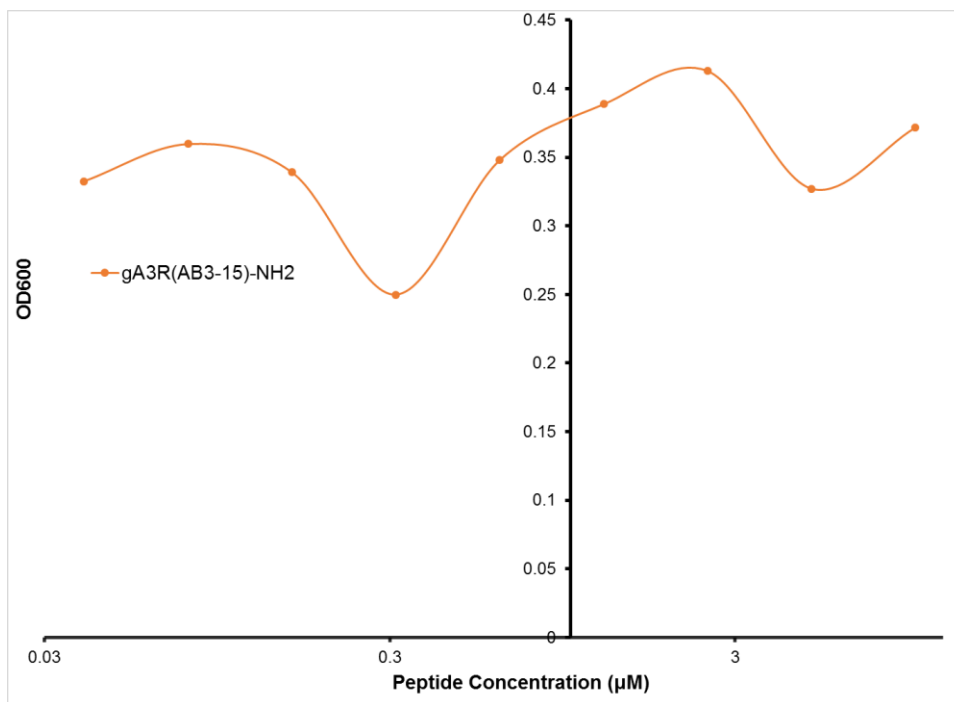


**Figure 3-13:** MIC Assay of gA3R(AB3-15)-NH<sub>2</sub> with *S. aureus*.

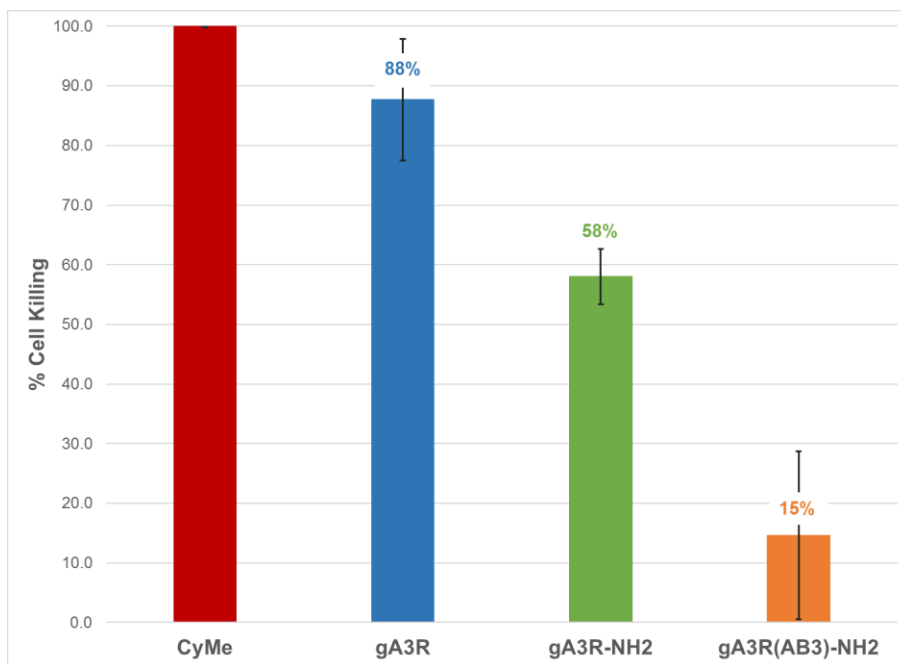


**Figure 3-14:** Cell killing assay of gA3R mutants with *S. aureus*. Percent cell killing is reported above each peptide.

We considered two possibilities that may have led to these results. First, it could be that the reversible covalent binding of AB3 to Lys-PG on the cell surface

hinders the peptide's ability to insert and properly fold into the membrane. If the peptide is folding properly, it could also be that this interaction between AB3 and Lys-PG either slows or completely prevents its mobility in the membrane, limiting pore-forming dimerization. With gA3R(AB3-15) performing worse in the MIC assay than gA3R(Y15), we were confident that this loss in activity was not solely due to decreased membrane association caused by the mutation from tryptophan. We began to think of other ways to prove our hypothesis that targeting and neutralizing Lys-PG would improve the activity of cationic gA peptides.

### **3.3 Resensitizing *S. aureus* to gA3R Using a Lys-PG Binding Peptide**

Given that including AB3 in a CAMP did not enhance its antimicrobial potency, we looked towards treating cells with two separate peptides: a peptide displaying a Lys-PG-specific binding motif and a cationic antimicrobial peptide. To achieve this, a collaboration was initiated with Kelly A. McCarthy.

In her work, Kelly sought to create 2-APBA presenting peptides with selectivity for Lys-PG (found in *S. aureus*) over the other prevalent amine presenting lipid phosphatidylethanolamine (PE; a major lipid found in *B. subtilis*). Towards this goal, Kelly investigated the effects of multivalency and peptide cyclization on binding potency. Using flow cytometry, she found the

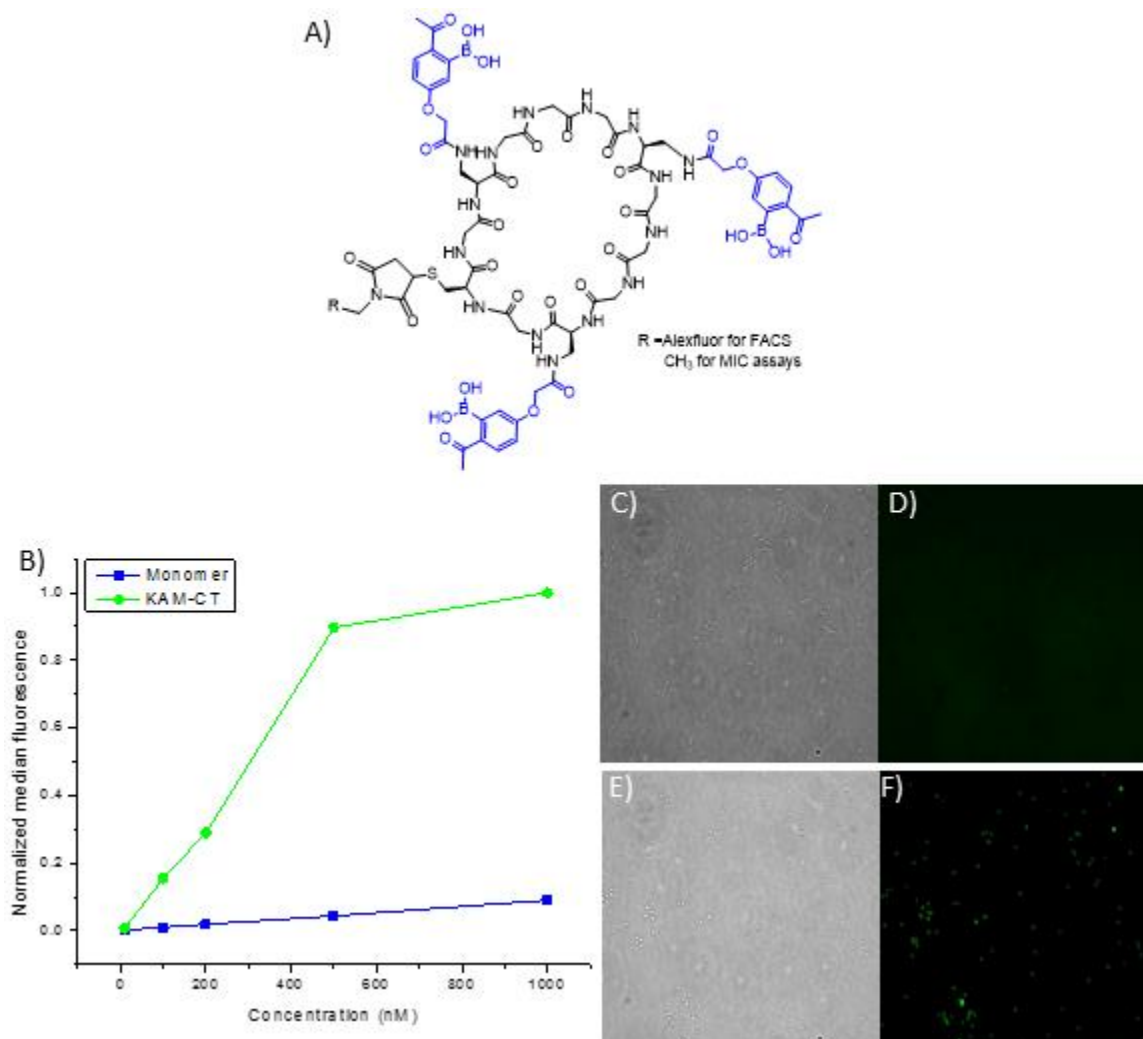


**Figure 3-15:** Structure and characterization of KAM-CT. A) Structure of KAM-CT, with 2-APBA structures shown in red. B) Flow cytometry data of different 2-APBA presenting peptides with *S. aureus*. This showed that the cyclic trimer was the most potent binder, saturating fluorescence at around 1  $\mu$ M. C) White light microscopy image of *B. subtilis*. D) Fluorescence microscopy image of *B. subtilis*. E) White light microscopy image of *S. aureus*. F) Fluorescence microscopy image of *S. aureus*. All microscopy experiments were done using 500 nM KAM-CT. Data collected and analyzed by Kelly A. McCarthy.

cyclic trimer peptide (referred to as KAM-CT, structure shown in Figure 3-15 A) to have the most potent binding to *S. aureus* cells (Figure 3-15 B), saturating at about 1.0  $\mu$ M. Additionally, through fluorescence microscopy, she observed that KAM-CT was not binding to *B. subtilis* cells at relevant concentrations (Figure 3-

15 C-F), demonstrating selectivity for *S. aureus*. Given these results, we chose to use KAM-CT for our antimicrobial studies.

We first looked at the antimicrobial activity of KAM-CT alone. At concentrations up to its cell binding saturation point, we saw no activity in the MIC assay (Figure 3-16). Moreover, no significant reduction in cell counts were observed in the cell killing assay at a concentration of 1  $\mu\text{M}$  (data not shown). This confirms that the cell binding alone of this peptide is not enough to elicit changes in bacterial viability.

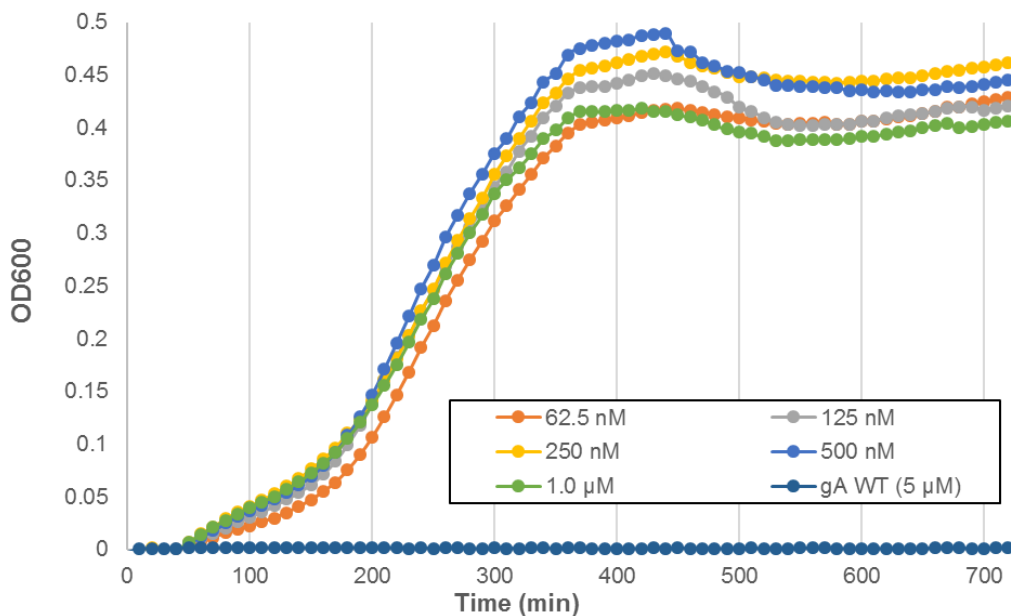


**Figure 3-16:** MIC experiment with various concentrations of KAM-CT against *S. aureus*. gA WT is included as a positive control. This data shows no significant inhibition up to 1.0  $\mu\text{M}$  peptide.

Next, we studied KAM-CT as part of a combination treatment with gA3R. For this, we used the same MIC conditions, but added the cyclic trimer at a final concentration of 1  $\mu\text{M}$  to each sample. We observed a two-fold decrease of the

MIC of gA3R for the cyclic trimer treated samples compared to untreated controls (Figure 3-17). Based off the original reports by Peschel and co-workers,<sup>7</sup> this small increase is not unexpected, as fully knocking out the *mprF* gene decreased the MIC with *S. aureus* of linear AMPs similar to gA3R by only about four- to five-fold. Considering KAM-CT is unlikely to be sequestering every Lys-PG, a two-fold difference is still considered to be relatively significant. As such, our experiments demonstrate an important proof-of-concept for this strategy towards resensitizing Lys-PG presenting bacteria to cationic antibiotics.

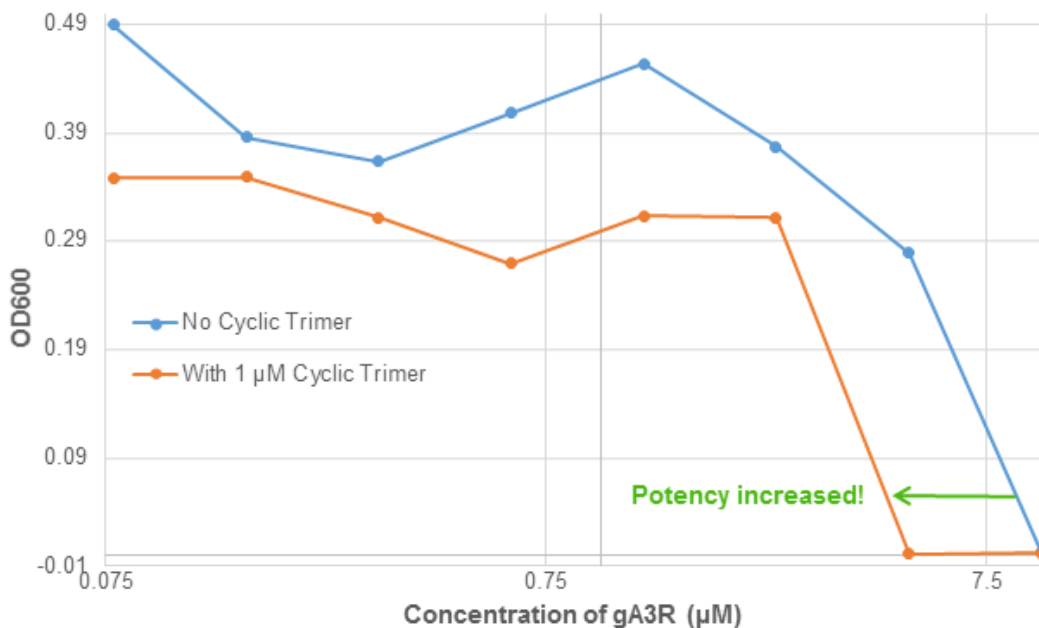


**Figure 3-17:** MIC data of gA3R with and without KAM-CT against *S. aureus*. This data suggests that the co-treatment with KAM-CT can increase the potency of gA3R by two-fold.

### 3.4 Conclusions and Future Work

Through this work, we have learned that the targeting of Lys-PG is a promising strategy for combating bacterial resistance to cationic antimicrobials.

Our initial work with gA3R(AB3-15)-NH<sub>2</sub> demonstrated that incorporating the Lys-PG targeting moiety directly into a membrane active AMP was not effective for gA. We believe this is most likely due to the tight binding interaction between AB3 and Lys-PG limiting peptide mobility. This could be preventing the peptide's proper folding into the membrane as the active  $\beta$ -helical structure or slowing its dimerization through the membrane. However, we cannot make a general conclusion on whether this would work or not for other less structured AMPs. Fortunately, by separating the potent Lys-PG binding and antimicrobial activities into two different peptides, we demonstrated that co-treatment of these molecules can increase the potency of the antimicrobial agent alone.

Work is currently being continued to explore this strategy and its applicability beyond gA3R. This includes the study of other potent Lys-PG binding peptides. Additionally, alternative strategies to target and reverse the resistance caused by Lys-PG are being investigated.

### ***3.5 Experimental Procedures***

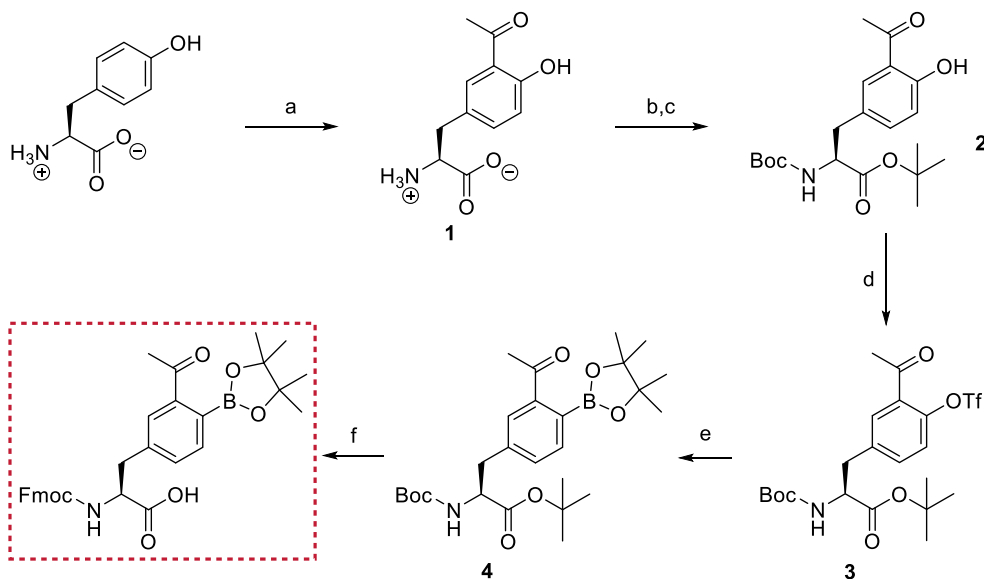
#### *3.5.1 General Methods*

Fmoc-Trp-Wang resin and all Fmoc-protected amino acids were purchased from either Advanced Chemtech (Louisville, KY) or Chem Impex Int. Inc. (Wood Dale, IL). Unprotected valine and other chemicals were obtained from Sigma-Aldrich or Fisher Scientific unless otherwise indicated. Peptide synthesis was carried out on a Tribute peptide synthesizer (Protein Technologies, Tucson, AZ). <sup>1</sup>H NMR



data were collected on a VNMRS 500 MHz or 600MHz NMR spectrometer, as indicated. Mass spectrometry data were generated by using an Agilent 6230 LC TOF mass spectrometer. The peptide concentration of all gA3R samples used in this study was determined by measuring their absorbance at 280 nm ( $\epsilon = 22,760 \text{ M}^{-1}\text{cm}^{-1}$  total of four tryptophan residues) on a Nanodrop 2000c UV/Vis spectrometer by cuvette. KAM-CT concentrations were determined by mass, as they did not include a chromophore with known extinction coefficient. Gram-positive *Staphylococcus aureus* (ATCC 6538) were purchased as lyophilized cell pellets from Microbiologics (Cloud, MN). FT-IR data was recorded on Nicolet iS10 FT-IR spectrometer (ThermoFisher Scientific, Waltham, MA).

### 3.5.2 Synthesis of Fmoc-AB3(pin)-OH<sup>19</sup>



a)  $\text{AlCl}_3$ ,  $\text{CH}_3\text{COCl}$ , Nitrobenzene,  $100^\circ\text{C}$ ; b)  $(\text{Boc})_2\text{O}$ , THF/ $\text{H}_2\text{O}$ ,  $\text{Na}_2\text{CO}_3$ ; c) t-butyl 2,2,2-trichloroacetimidate, EtOAc,  $60^\circ\text{C}$ ; d)  $(\text{CF}_3\text{SO}_2)_2\text{O}$ , DCM,  $\text{Et}_3\text{N}$ ; e) 8 mol% Pd(dppf) $\text{Cl}_2/\text{dppf}$ , KOAc, B<sub>2</sub>pin<sub>2</sub>, dioxane,  $87^\circ\text{C}$ ; f) i) 60% TFA in DCM; ii) neat TFA; iii) Fmoc-OSu, DCM

### **Synthesis of (S)-2-(3-acetyl-4-hydroxyphenyl)-1-carboxyethanaminium chloride (1)**

Anhydrous aluminum chloride (14.7 g, 111 mmol) was added slowly to a solution of L-tyrosine (5 g, 28 mmol) in dry nitrobenzene (100 mL) at RT. This slightly exothermic reaction was stirred at RT for 15 minutes. Then, acetyl chloride (2.59 g, 33 mmol) was added dropwise, during which a color change was observed from red to yellow. The reaction mixture was heated at 100 °C with stirring for six hours and turned to a dark green thick solid after cooling to room temperature. The solid was dissolved in 1N HCl and the nitrobenzene layer was removed. The aqueous layer was washed with ethyl acetate (3 × 150mL), then concentrated until precipitation was observed. It was allowed to continue to precipitate at 4 °C overnight. The desired product (1) precipitated as a light tan solid and was collected via vacuum filtration.

### **Synthesis of (S)-tert-butyl 3-(3-acetyl-4-hydroxyphenyl)-2-((tert-butoxycarbonyl)amino)propanoate (2)**

**1** (used as is from previous reaction) was dissolved in 120 mL water, neutralized with NaOH pellets, and brought to pH 9 with sodium bicarbonate. While stirring in an ice bath, 80 mL of THF was added to the reaction mixture. To this, Boc-anhydride (7.2 g, 33.1 mmol) was added. The reaction mixture was warmed to room temperature and stirred for 3 hours. Before extraction, THF was removed by rotary evaporation. Then 250 mL ethyl acetate was added before the mixture

was acidified to pH ~2-3 with 1N HCl. The product was extracted with ethyl acetate (3 x 150 mL), then the combined organic layers were washed with brine (200 mL) and dried over Na<sub>2</sub>SO<sub>4</sub>. Solvent was removed by rotary evaporation and the product was dried further under high vacuum. The resulting solid was dissolved in dry ethyl acetate (120 mL), to which tert-butyl 2,2,2-trichloroacetimidate (6.8 g, 31.1 mmol) was added. The reaction mixture was refluxed for 6 hours, at which point half equivalent more of tert-butyl 2,2,2-trichloroacetimidate (2.3 g, 10.4 mmol) was added and the reaction mixture was refluxed overnight. After solvent removal, the residue was purified through silica gel using 10% ethyl acetate in hexane to give the desired product **3** as a white solid (3.53 g, 33.7% over three steps). <sup>1</sup>H NMR (CDCl<sub>3</sub>) δ: 12.15 (s, 1H), 7.51 (s, 1H), 7.29-7.27 (d, J=7.4 Hz, 1H), 6.91-6.89 (d, J=7.6 Hz, 1H), 5.04-5.02 (d, J=8.2 Hz, 1H), 4.45-4.41 (q, J=4.6 Hz, 1H), 3.08-2.98 (m, 2H), 2.61 (s, 3H), 1.42 (s, 18H); <sup>13</sup>C NMR (CDCl<sub>3</sub>) δ: 204.31, 170.77, 161.34, 154.99, 137.81, 131.33, 126.80, 119.38, 118.28, 82.27, 79.83, 77.82, 54.69, 28.95, 26.59. MS-ESI<sup>+</sup>: *m/z* calculated for C<sub>20</sub>H<sub>29</sub>NO<sub>6</sub> [M+Na]<sup>+</sup> = 402.1893, found 402.1963.

**Synthesis of (S)-tert-butyl 3-(3-acetyl-4-(((trifluoromethyl)sulfonyl)oxy)phenyl)-2-((tert-butoxycarbonyl)amino)propanoate (3)**

**2** (1.49 g, 3.93 mmol) was dissolved in anhydrous dichloromethane (8.0 mL) and triethylamine (1.59 g, 15.7 mmol) was added while stirring under an argon

environment. The reaction mixture was cooled to  $-78^{\circ}\text{C}$  using a dry ice/acetone bath and trifluoromethane sulfonic anhydride (1.67 g, 5.89 mmol) was added slowly over the course of five minutes. The reaction mixture was allowed to stir at room temperature for 30-60 min. Afterwards, the reaction was quenched with saturated sodium bicarbonate (50 mL) and the mixture was allowed to stir for 5 min. The product was extracted with dichloromethane (3 x 50 mL). The combined organic layers were washed with brine (50 mL) and dried over  $\text{Na}_2\text{SO}_4$ . After removing the solvent, the crude product was purified on silica gel with 15% ethyl acetate in hexane to yield **3** as a yellow gummy product (1.58 g, 79%).  $^1\text{H}$  NMR ( $\text{CDCl}_3$ )  $\delta$ : 7.62 (s, 1H), 7.44-7.41 (d,  $J=8.2$  Hz, 1H), 7.26-7.25 (d,  $J=7.2$  Hz, 1H), 5.12-5.10 (d,  $J=8.3$  Hz, 1H), 4.50-4.46 (q,  $J=5.4$  Hz, 1H), 3.20-3.07 (m, 2H), 2.62 (s, 3H), 1.42 (s, 9H), 1.40 (s, 9H);  $^{13}\text{C}$  NMR ( $\text{CDCl}_3$ )  $\delta$ : 196.38, 170.22, 150.94, 145.60, 137.74, 134.81, 131.78, 122.15, 119.84, 117.29, 82.83, 80.08, 54.84, 37.93, 28.49, 27.98, 27.81; MS-ESI<sup>+</sup>:  $m/z$  calculated for  $\text{C}_{12}\text{H}_{12}\text{F}_3\text{NO}_6\text{S}$  [M-(Boc+tBu)+H] = 356.0416, found 356.0391.

#### Synthesis of Boc-AB3(pin)-OtBu (**4**)

**3** (1.58 g, 3.09 mmol),  $\text{B}_2\text{pin}_2$  (2.37 g, 9.32 mmol),  $\text{Pd}(\text{dppf})\text{Cl}_2$  (177 mg, 0.242 mmol, 8 mol%) 1,1'-Bis(diphenylphosphino)ferrocene(dppf) (244 mg, 0.244 mmol) and potassium acetate (915 mg, 9.32 mmol) were dissolved in anhydrous dioxane (20 mL). The reaction mixture was bubbled with argon for 20 minutes and it was allowed to stir at  $85\text{-}88^{\circ}\text{C}$  for 1 hour. Water (80 mL) was then added to

quench the reaction and the product was extracted with ethyl acetate (3 x 80 mL). The combined organic layers were washed with brine (100 mL) and dried over Na<sub>2</sub>SO<sub>4</sub>. The solvent was removed under vacuum and the crude product was purified on silica gel using 17.5% ethyl acetate in hexane to yield **4** (762.5 mg, 50.4%). <sup>1</sup>H NMR (CDCl<sub>3</sub>) δ: 7.58 (s, 1H), 7.43-7.42 (d, *J*=7.6 Hz, 1H), 7.33-7.31 (d, *J*=7.3 Hz, 1H), 4.90-4.89 (d, *J*=8.1 Hz, 1H), 4.48-4.44 (q, *J*=5.3 Hz, 1H), 3.19-3.08 (m, 2H), 2.57 (s, 3H), 1.41 (s, 30H); <sup>13</sup>C NMR (CDCl<sub>3</sub>) δ: 199.81, 170.53, 155.00, 140.92, 137.30, 133.57, 132.27, 129.58, 83.68, 82.30, 79.79, 54.39, 37.87, 28.30, 28.00, 24.85; <sup>11</sup>B NMR (CDCl<sub>3</sub>) δ: 31.10; MS-ESI<sup>+</sup>: *m/z* calculated for C<sub>26</sub>H<sub>40</sub>BNO<sub>7</sub> [M+H]<sup>+</sup> = 490.2976, found 490.2996.

### Synthesis of Fmoc-AB3(pin)-OH

**4** (1.96 g, 4.0 mmol) was dissolved in 10 mL anhydrous DCM and stirred in an ice bath as 15 mL TFA was added. This was allowed to come to room temperature and stirred for 2.5 hours. The solvent was reduced to a minimal volume by rotary evaporation. The sticky residue was dissolved in neat TFA (15 mL) and stirred for an additional one hour. The solvent was removed by rotary evaporation and dried further through the addition and subsequent rotary evaporation of DCM and methanol. To remove any residual TFA, it was azeotroped with toluene until dry. Before moving on to the next reaction, the mixture was dried under high vacuum for 45 min. The residue was then dissolved in anhydrous DCM (10 mL) and stirred as NMM (2.20 mL, 20.0 mmol) was added. To this, Fmoc-Osu (1.08 g,

3.20 mmol) was added and the mixture was allowed to stir under argon overnight. The next day, additional Fmoc-Osu (0.20 mmol, 68 mg) was added every 30 min until all the starting material appeared to be consumed by TLC. To this, 2N HCl (75 mL) was added and the product was then extracted with ethyl acetate (3x75 mL). The combined organic layers were washed with brine (100 mL) then dried over Na<sub>2</sub>SO<sub>4</sub>. The resulting solid was purified by silica gel chromatography using 50% ethyl acetate, 1% acetic acid in hexane to yield Fmoc-AB3(pin)-OH (1.41 g, 63.4%). <sup>1</sup>H NMR (600 MHz, CDCl<sub>3</sub>) δ 7.77-7.73 (d, J = 7.6 Hz, 2H), 7.59 (s, 1H), 7.56-7.52 (d, J = 7.6 Hz, 2H), 7.44-7.41 (d, J = 7.4 Hz, 1H), 7.41-7.37 (t, J = 7.5 Hz, 3H), 7.32-7.26 (dddd, J = 8.7, 7.5, 2.9, 1.3 Hz, 3H), 5.36-5.32 (d, J = 8.2 Hz, 1H), 4.72-4.68 (q, J = 6.8 Hz, 1H), 4.40-4.36 (d, J = 7.1 Hz, 2H), 4.21-4.15 (t, J = 7.1 Hz, 1H), 3.26-3.13 (ddd, J = 42.4, 14.1, 5.7 Hz, 2H), 2.50 (s, 3H), 1.44 (s, 12H). <sup>13</sup>C NMR (CDCl<sub>3</sub>) δ 200.33, 173.65, 155.79, 143.68, 141.27, 136.77, 133.47, 132.41, 129.40, 127.75, 127.10, 125.04, 119.97, 83.92, 67.20, 54.23, 47.05, 37.50, 31.57, 24.82, 22.64, 14.11; MS-ESI<sup>+</sup>: *m/z* calculated for C<sub>32</sub>H<sub>35</sub>BNO<sub>7</sub> [M+H]<sup>+</sup> = 556.2507, found 556.2606.

### 3.5.3 Conjugation of AB3 to Wang Resin

Wang resin (0.100 mmol, loading=0.600 mmol/g, 167 mg) was swelled in the minimal amount of DMF for 1 hour. At the same time, Fmoc-AB3(pin)-OH (1.00 mmol, 555.43 mg) was dissolved in the minimal amount of dry DCM with a few drops of DMF added to aid solubility. This was put in an ice bath and diisopropylcarbodiimide (0.500 mmol, 63.1 mg, 78.3 μL) was added. This was

stirred for 20 min, then the solvent was removed by rotary evaporation. The resulting solid was resuspended in the minimal amount of DMF then added to the resin. This was stirred for 1 hour, then washed 6xDMF, 6xDCM and dried. Loading of the resin was determined using the standard Fmoc cleavage test.<sup>21</sup> This gave a loading of 0.332 mmol/g. The procedure was repeated using 5 eq Fmoc-AB3(pin)-OH and 2.5 eq DIC, instead of 10 and 5, respectively. This resulted in a loading of 0.550 mmol/g.

#### 3.5.4 Synthesis of 2-(Fmoc-amino)ethanol<sup>23</sup>

Ethanolamine (364.1 mg, 5.96 mmol) was dissolved in acetone/saturated aqueous sodium bicarbonate (2:1, 60 mL) and stirred as Fmoc-Osu (2.02 g, 5.99 mmol) was added. This was allowed to stir at room temperature overnight. To the mixture, water (40 mL) and ethyl acetate (50 mL) were added. The mixture was then acidified to pH ~3 using 1 N HCl. The aqueous layer was removed and the organic layer was washed with 1 N HCl (3 x 40 mL), saturated aqueous sodium bicarbonate (1 x 40 mL) and brine (1 x 40 mL) then dried over Na<sub>2</sub>SO<sub>4</sub>. The solvent was removed by rotary evaporation providing a white solid in quantitative yield. Proton NMR showed less than 8% free ethanolamine. <sup>1</sup>H NMR (600 MHz, CDCl<sub>3</sub>) δ 7.78 - 7.74 (d, J = 7.5 Hz, 2H), 7.61 - 7.56 (d, J = 7.4 Hz, 2H), 7.43 - 7.37 (t, J = 7.4 Hz, 2H), 7.34 - 7.28 (t, 2H), 5.29 - 5.13 (s, 1H), 4.45 - 4.40 (d, J = 6.8 Hz, 2H), 4.24 - 4.18 (t, J = 6.9 Hz, 1H), 3.73 - 3.67 (q, J = 5.1 Hz, 2H), 3.37 - 3.31 (q, J = 5.4 Hz, 2H), 2.27 - 2.21 (d, J = 5.3 Hz, 1H).

### 3.5.5 Preparation of 2-(Fmoc-amino)ethanol Resin<sup>22</sup>

Wang resin (0.500 mmol, 557.2 mg) was suspended in anhydrous DCM (5 mL). To this, trichloroacetonitrile (1 mL) was added. This was put into an ice bath and stirred for 5 min before the addition of DBU (100  $\mu$ L). This was continued to stir in the ice bath for 1 hour. The resin was then washed (2 x DMF, 5 mL, 5 min; 2 x DCM, 5 mL, 5 min). Full conversion of the benzyl alcohol was confirmed by the disappearance of an IR stretch at 3566 nm. Without drying, the TCA resin was reswelled in anhydrous DCM (5 mL) for 15 min. The resin was then washed with dry THF (2 x 5 mL). To this, 2-(Fmoc-amino)ethanol (425.0 mg, 1.5 mmol) was added, dissolved in dry THF (5 mL). This was stirred under nitrogen for 5 min before  $\text{BF}_3 \cdot \text{OEt}_2$  (35  $\mu$ L, 0.28 mmol) was added. The suspension was stirred for 1 hour, 45 min. To cap any unreacted trichloroacetimidate, methanol (1.0 mL) was added and the mixture was stirred for an additional 5 min. The resin was collected by filtration and washed several times with THF (5 mL), methanol (5 mL) and then DCM (5 mL). The resin was fully dried under vacuum before checking conversion by FT-IR. Conversion was monitored by the disappearance of the TCA stretches at 3338 nm and 1662 nm and the formation of the stretch at 1724 nm, corresponding to the ether bond formed between the resin and the alcohol from 2-(Fmoc-amino)ethanol. Loading efficiency was checked via two different methods. Using a standard Fmoc-cleavage procedure<sup>21</sup> performed in triplicate, the loading was found to be 0.497 mmol/g. Additionally, 2-(Fmoc-



amino)ethanol was cleaved from the resin (61 mg) using 10% TFA in DCM for 1 hour. The resin was washed with DCM and methanol, then all filtrates were combined and the solvent was removed by rotary evaporation. The resulting mixture was suspended in water (20 mL) and extracted using ethyl acetate (3 x 15 mL). Combined organic layers were washed with brine (20 mL) then dried over Na<sub>2</sub>SO<sub>4</sub> before the solvent was removed by rotary evaporation. This yielded 9.3 mg 2-(Fmoc-amino)ethanol, confirmed by <sup>1</sup>H NMR, providing a loading of 0.537 mmol/g.

### 3.5.7 Synthesis of gA3R Peptides

Synthesis was performed as previously reported by our group<sup>24</sup>. Ethanolamine derivatized peptides were synthesized on Fmoc-Trp-Wang resin (100 mg, 0.500 mmol/g, 0.05 mmol) or Fmoc-Tyr(tBu)-Wang resin (loading) using standard Fmoc/tBu chemistry. The peptides were cleaved off the resin by treating the resin with ethanolamine (40% v/v in DMF, 55°C, 5 hours). Then the resin was filtered through a medium fritted plastic funnel and rinsed three times with DCM and methanol. Prior to precipitation, the mixture was reduced to a minimal volume. To precipitate the peptide, six to seven times in volume DI water was then added. The peptide was collected by centrifugation (14,000 rpm, 1.5 hr) and the pellet was dried by lyophilization to obtain the side-chain protected peptide. The side chain protecting groups were removed by treating the pellet with Reagent K at room temperature for two hours. Once the reaction is finished, cold

diethyl ether was added to precipitate the crude peptide which was again centrifuged (14,000 rpm, 1.5 hours) and lyophilized. For peptides using 2-(Fmoc-amino)ethanol resin, peptide synthesis was carried out the same way. The crude peptide was cleaved using Reagent K, as the ethanolamine treatment was unnecessary. For peptides on Rink amide resin, peptide synthesis was carried out as stated above and the crude peptide was cleaved using Reagent K to yield the C-terminal amidated peptide. The crude material was purified by RP-HPLC (Waters Prep LC, Jupiter 10  $\mu$ m C4 300A Column). The identity and purity of each peptide was confirmed by LC/MS (Agilent 2630 LC TOF, Phenomenex, Jupiter 5  $\mu$ m C4 300R column). All peptides were confirmed to have purity of 95% or higher.

#### 3.5.8 Minimum Inhibitory Concentration Measurements<sup>25</sup>

Minimal inhibitory concentrations (MICs) were measured against gram-positive *Staphylococcus aureus* (ATCC 6538) in LB media. Specifically, a single colony selected from an LB agar plate was grown overnight in broth at 37°C with agitation and diluted 100 times into fresh broth the next morning. OD600 was monitored until a value between 0.5 and 0.6 was reached. The cells were diluted by a factor previously determined to achieve a concentration of  $\sim 5 \times 10^5$  colony forming units per mL (cfu/mL). In a sterile 96-well plate, the cell suspension (200  $\mu$ L) was added to each well. To each well, serial diluted (2-fold) peptides in DMSO (2  $\mu$ L) were added in triplicates. For experiments studying co-treatment

of peptides, KAM-CT was added at a final concentration of 1.0  $\mu\text{M}$  immediately before the AMP. Using a microtiter plate reader (SpectraMax M5, Molecular Devices, Sunnyvale, CA), the OD600 was monitored overnight while incubating at 37°C, with readings taken every 10 minutes after the plate was shaken for 15 seconds. Using the time point where OD600 of the blank (untreated) sample began to reach stationary phase, MICs were determined to be the lowest concentration for which cell growth was not observed.

### 3.5.9 Cell Killing Assays with *S. aureus*

A single colony of *S. aureus* was selected from an LB agar plate and grown overnight in LB broth, incubating at 37°C with agitation. In the morning, this was a small aliquot was taken and diluted 100 times in fresh broth. The OD600 was monitored until it reached  $\sim 0.6$ . This culture was centrifuged (4000 rpm, 5 min) and washed with 10 mM tris acetate buffer (pH 7.4) two times. The final cell solution was diluted to  $\sim 5 \times 10^5$  cfu/mL in fresh buffer. In a sterile 96-well plate, the cell suspension (200  $\mu\text{L}$ ) was added to each well and 2  $\mu\text{L}$  of 125 $\mu\text{M}$  peptide in DMSO were added in triplicate. The plate was incubated for 10 min at 37°C. Aliquots of each sample (10  $\mu\text{L}$ ) were diluted into fresh buffer (990  $\mu\text{L}$ ) and mixed before an aliquot (100  $\mu\text{L}$ ) was spread on LB agar plates. The plates were allowed to incubate at 37°C overnight. Individual colonies were counted on each plate and triplicates were averaged for each peptide. To calculate a percent viability, the average number of colonies for each peptide was divided by the

average number of colonies for blank samples and multiplying by 100. Percent killing was then considered to be the percent viability subtracted from 100.

### 3.6 References

- (1) Anaya-López, J. L.; López-Meza, J. E.; Ochoa-Zarzosa, A. *Crit. Rev. Microbiol.* **2012**, 39 (March), 1–16.
- (2) Li, X.-Z.; Nikaido, H. *Drugs* **2004**, 64 (2), 159–204.
- (3) Steinbuch, K. B.; Fridman, M. *Med. Chem. Commun.* **2016**, 7 (1), 86–102.
- (4) Nikaido, H. *Microbiol. Mol. Biol. Rev.* **2003**, 67 (4), 593–656.
- (5) Ernst, C. M.; Peschel, A. *Mol. Microbiol.* **2011**, 80 (2), 290–299.
- (6) Jones, T.; Yeaman, M. R.; Sakoulas, G.; Yang, S.-J.; Proctor, R. A.; Sahl, H.-G.; Schrenzel, J.; Xiong, Y. Q.; Bayer, A. S. *Antimicrob. Agents Chemother.* **2008**, 52 (1), 269–278.
- (7) Peschel, A.; Jack, R. W.; Otto, M.; Collins, L. V.; Staubitz, P.; Nicholson, G.; Kalbacher, H.; Nieuwenhuizen, W. F.; Jung, G.; Tarkowski, A.; van Kessel, K. P. M.; van Strijp, J. A. G. *J. Exp. Med.* **2001**, 193 (9).
- (8) Ernst, C. M.; Staubitz, P.; Mishra, N. N.; Yang, S.-J.; Hornig, G.; Kalbacher, H.; Bayer, A. S.; Kraus, D.; Peschel, A. *PLoS Pathog.* **2009**, 5 (11), e1000660.
- (9) Slavetinsky, C.; Kuhn, S.; Peschel, A. *Biochim. Biophys. Acta - Mol. Cell Biol. Lipids* **2016**.

- (10) Macfarlane, M. G. *Nature* **1962**, 196 (4850), 136–138.
- (11) Roy, H. *IUBMB Life* **2009**, 61 (10), 940–953.
- (12) Singh, J.; Petter, R. C.; Baillie, T. A.; Whitty, A. *Nat. Rev. Drug Discov.* **2011**, 10 (4), 307–317.
- (13) Bandyopadhyay, A.; Gao, J. *Curr. Opin. Chem. Biol.* **2016**, 34, 110–116.
- (14) Gutiérrez-Moreno, N. J.; Medrano, F.; Yatsimirsky, A. K.; Sreevidyac, T. V.; Sarojini, B. K.; Nicholls, A.; Ringnalda, M.; W. A. Goddard, I.; Honig, B. *Org. Biomol. Chem.* **2012**, 10 (34), 6960.
- (15) Cal, P. M. S. D.; Vicente, J. B.; Pires, E.; Coelho, A. V.; Veiros, L. F.; Cordeiro, C.; Gois, P. M. P. *J. Am. Chem. Soc.* **2012**, 134 (24), 10299–10305.
- (16) Cal, P. M. S. D.; Frade, R. F. M.; Cordeiro, C.; Gois, P. M. P. *Chem. - A Eur. J.* **2015**, 21 (22), 8182–8187.
- (17) Bandyopadhyay, A.; McCarthy, K. A.; Kelly, M. A.; Gao, J. *Nat. Commun.* **2015**, 6, 6561.
- (18) DUBOS, R. J.; HOTCHKISS, R. D. *Trans. Stud. Coll. Physicians Philadelphia* **1942**, 10 (1), 11–19.
- (19) Bandyopadhyay, A.; Gao, J. *J. Am. Chem. Soc.* **2016**, 138 (7), 2098–2101.
- (20) Ketchum, R. R.; Lee, K.-C.; Huo, S.; Cross, T. A. *J. Biomol. NMR* **1996**, 8 (1).
- (21) Gude, M.; Ryf, J.; White, P. D. *Lett. Pept. Sci.* **2002**, 9 (4–5), 203–206.

- (22) Yan, L. Z.; Mayer, J. P. *J. Org. Chem.* **2003**, *68* (3), 1161–1162.
- (23) Maynard, S. J.; Almeida, A. M.; Yoshimi, Y.; Gellman, S. H. *J. Am. Chem. Soc.* **2014**, *136* (47), 16683–16688.
- (24) Wang, F.; Qin, L.; Pace, C. J.; Wong, P.; Malonis, R.; Gao, J. *ChemBioChem* **2012**, *13* (1), 51–55.
- (25) Wiegand, I.; Hilpert, K.; Hancock, R. E. W. *Nat. Protoc.* **2008**, *3* (2), 163–175.

## **Chapter 4**

### **Design and Screen of a Cyclic Peptide Library Containing a 2-APBA Warhead for the Discovery of Novel Binders to Lipid II Stem Peptide\***

*\*The work of this chapter has been jointly performed with Kaicheng Li.*

## ***4.1 Introduction***

### *4.1.1 Use of Libraries for Novel Peptide Discovery*

The use of library based ligand discovery has many benefits over rational design strategies. First, it allows for investigating multiple related structures at the same time, yielding an extensive structure-activity study in a single screen. Library screening also allows for a less biased selection of compounds to study. Additionally, pharmaceutical companies typically use library screens as a fast and efficient method for looking at a catalog of unrelated compounds. However, this approach is not without its downfalls. Due to the arbitrary nature of screening, libraries can yield varying amounts of false positives, making hit validation a very crucial step. Furthermore, designing screening schemes which can incorporate a graded output, such that hits can be compared for potency within the experiment before validation, is nontrivial.

In the case of peptides, library approaches have taken several leaps forward in the past decade or so. Peptide libraries can be split into two separate families: biological or chemical synthetic approaches (Figure 4-1).<sup>1</sup> For biology-based library platforms, including phage and bacteria display, genetic materials are used to generate and sequence libraries. In these techniques, the host organism's machinery is used to produce the library of interest, and then the library compounds are displayed on the surface of the organism. Drawbacks to these



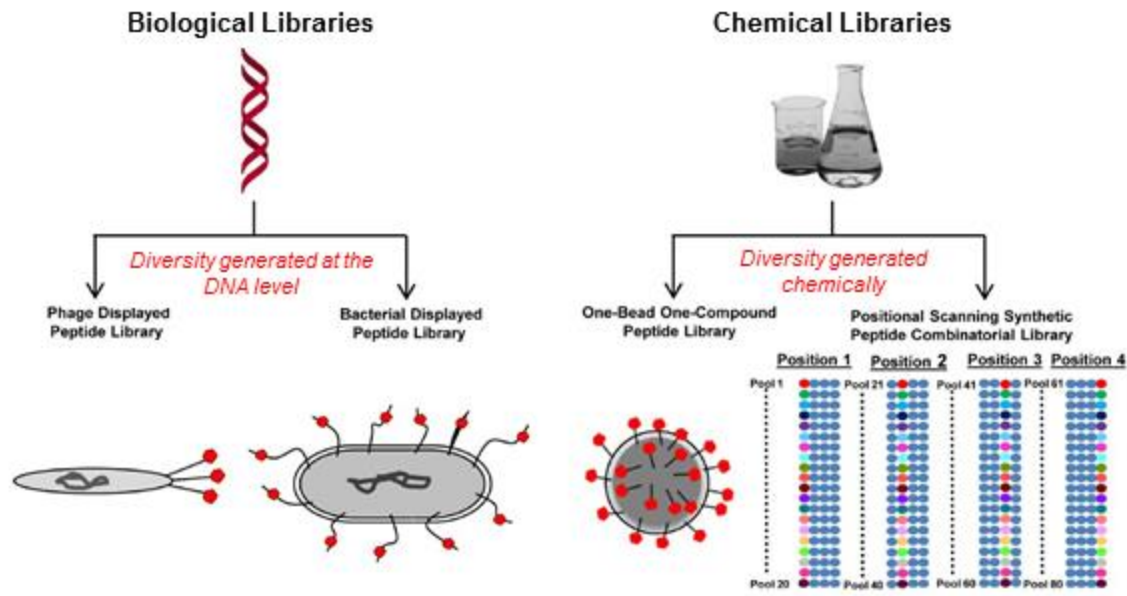


**Figure 4-1:** Depiction of two major classes of peptide library scaffolds. Biological libraries display peptides of interest on the exterior of a given organism, using a designed DNA plasmid for generation of the library such that hits can be sequenced using Sanger sequencing. Chemical libraries involve strategies of splitting resin at designed steps in peptide synthesis and typically use mass-spectrometry techniques for sequencing. Modified from ref. 1.

techniques include being limited to canonical amino acids,<sup>2</sup> although modification strategies for incorporating unnatural functionalities are becoming much more prevalent (Figure 4-2).<sup>3-7</sup> Additional limitations include the dependence on the organism's tolerance of the library compound for its successful expression.

The fully synthetic approach can be viewed as more challenging to generate than biological libraries, but it allows for much more exotic structures and unnatural sequences.<sup>2</sup> A major limitation for the structures of synthetic peptide libraries is their compatibility with mass spectrometry, which is used for sequencing. In the past, this has limited the incorporation of cyclic structures or

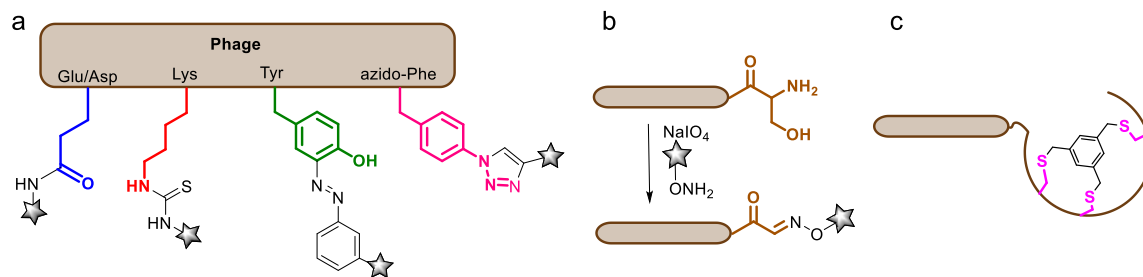


**Figure 4-2:** Literature reported examples of modifications that can be made on phage display libraries. a) side-chain specific modifications for the covalent attachment of unnatural structures, including the incorporation of azido-Phe using Amber codon suppression; b) N-terminal serine specific modification using various oxime  $\alpha$ -nucleophiles; c) bicyclization through the chemical crosslinking of three cysteines. Figure used with permission from Kelly A. McCarthy.

unnatural linkages difficult to sequencing with typical mass-spectrometry techniques.<sup>8</sup> However, this limitation is commonly circumvented with the use of one-bead-two compound (OBTC) libraries,<sup>9</sup> such that two peptides are produced for each desired library member. For screening of a OBTC library, one peptide is used as the screening compound and is assumed to be the active entity, while the other moiety, which is compatible with the sequencing technique chosen, simply affords a way to identify each library hit (Figure 4-3).<sup>1</sup>

As the usage of library screening has grown, techniques that are hybrids between biological and synthetic approaches have emerged, such as DNA-encoded libraries.<sup>10-12</sup> Taking a similar approach as one-bead-two-compound libraries, DNA-encoded libraries have the desired library compound attached to a DNA fragment, which can act as the coding sequence (Figure 4-4). To achieve this, a short DNA sequence (four to eight base pairs) is assigned to each variable library

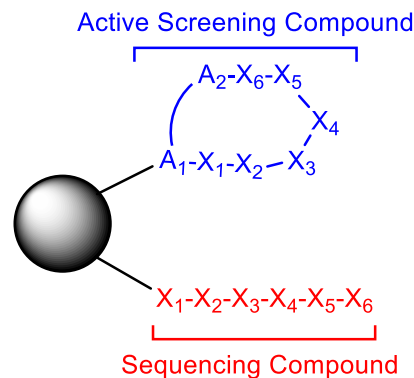


**Figure 4-3:** Cartoon of a one-bead-two-compound library. In this example, the amino acids kept constant for cyclization (A<sub>1</sub> and A<sub>2</sub>) are eliminated in the sequencing compound to present a linear structure compatible with either Edmund degradation or MS/MS analysis.

component and ligated to the corresponding resin after splitting. As such, a unique DNA sequence can be obtained for each library member. This has allowed for the use of high throughput DNA sequencing to identify library hits without the limitations on library design.<sup>13</sup> Most often, this approach has been reported for small molecule libraries, but has the unfortunate drawback of being relatively expensive, as many short oligomers are required to ensure that each code is unique. Also, distinct overhangs are typically included for each split step as a way to prevent incorrect ligation of truncated chains in subsequent steps. As such, the number of oligomers required quickly increases with an increasing number of variable positions.

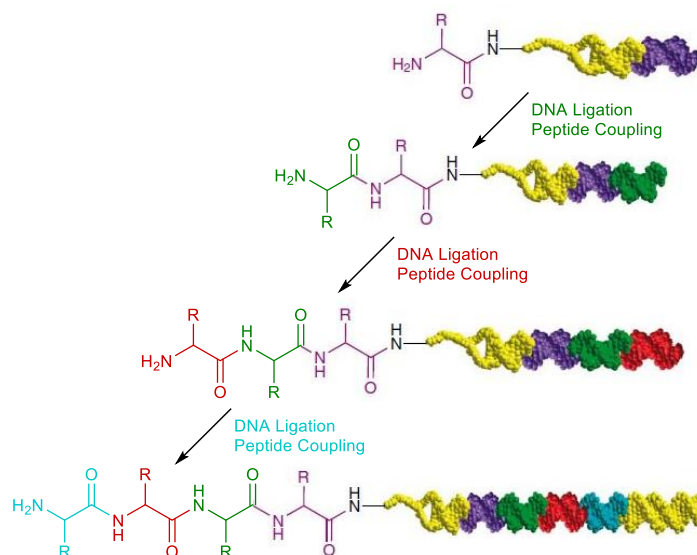


**Figure 4-4:** Depiction of DNA-encoded library. With each step, a DNA ligation and chemical reaction, in this case a peptide coupling, is performed. Color scheme shows corresponding amino acid and DNA segments. Yellow represents the universal beginning and ending primers, used for PCR and sequencing. Figure modified from Ref. 11.

The power in DNA-encoded libraries comes from the breadth of information that can be gathered during a single screen and its allowance for unnatural structures. As is the case with biological library approaches, sequencing from genetic information can be much less convoluted than mass spectrometry based approaches, allowing for quicker analysis of a larger pool of hits. This information can generate a structure-activity relationship, and clarify which hits are most likely to give the desired response to the target based on the identification of common features.<sup>11</sup>

#### 4.1.2 Peptidoglycan and Vancomycin

Gram-positive bacteria consist of a plasma lipid membrane surrounded by a thick cell wall. The cell wall, specifically referred to as the peptidoglycan, is a

structured polymer of sugars and amino acids with a lipid anchor attaching it to the plasma membrane. Its main purpose is to provide structural strength to the cell, especially as a way to counteract osmotic pressure.<sup>14,15</sup> Strands of peptidoglycan in gram-positive bacteria are crosslinked through short peptides, creating a lattice structure from which the cell wall gets its strength. A depiction of the exterior of a gram-positive cell can be seen in Figure 4-5.

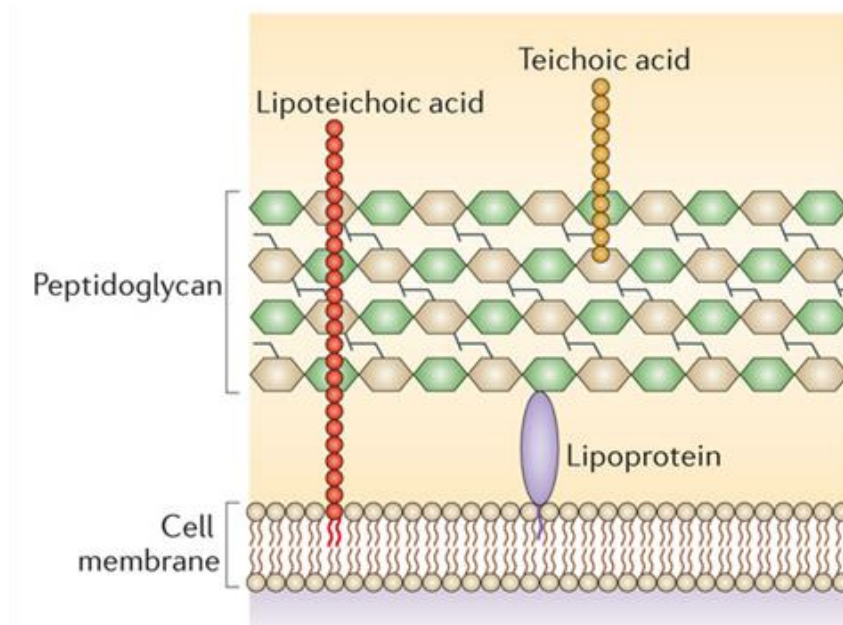


**Figure 4-5:** Cartoon depiction of the exterior of a gram-positive cell. Sugars in the peptidoglycan are represented as hexagons, with *N*-acetylmuramic acid (NAM) shown in yellow and *N*-acetylglucosamine (NAG) in green. Peptide crosslinks between NAM sugars and shown as grey lines. Modified from Ref. 14.

As the outermost cellular component, the peptidoglycan is a readily available target for antibacterial drugs. By eliminating the necessity of ligands to pass through the plasma membrane, this target avoids the complications of membrane permeability in designing drugs. Additionally, peptidoglycan's vital role in cellular viability makes it ideal for bactericidal targeting. Hallmark drugs,

such as penicillin,<sup>16</sup> and even our own immune system have mechanisms that act by targeting different bacterial cell wall components to weaken the peptidoglycan.<sup>17</sup>

Vancomycin is a glycopeptide antibiotic produced by the soil bacterium *Streptomyces orientalis*.<sup>18</sup> When originally isolated and studied, it was found especially promising as it was active against penicillin-resistant *S. aureus* and originally elicited very little propensity towards resistance. Vancomycin binds to the terminal D-Ala-D-Ala sequence of the crosslinking pentapeptide in gram-positive peptidoglycan via a network of five hydrogen bonds (Figure 4-6A).<sup>19</sup> This binding event prevents crosslinking, thus destroying the cell wall's integrity and resulting in cell death due to lack of osmotic pressure regulation. However, resistance to vancomycin has increased since its clinical introduction, causing the drug to be limited to gram-positive infections that are unresponsive to other antibiotics.

Resistance to vancomycin occurs through a fairly small target modification that is triggered by an elegant gene cascade.<sup>20</sup> The modification involves the substitution of the final D-Ala with a D-Lac, which transforms the final amide bond into an ester bond. The disruption of this single hydrogen bond was found to be significant enough to abolish vancomycin binding (Figure 4-6B). Although this modification was originally observed in *Enterococci* species,<sup>21</sup> the eminent threat of horizontal gene transfer to *S. aureus* resulted in reassignment of vancomycin to use

only in highly resistant infections. Nonetheless, vancomycin resistance was ultimately observed in *S. aureus* in the late 1990s.<sup>22</sup>

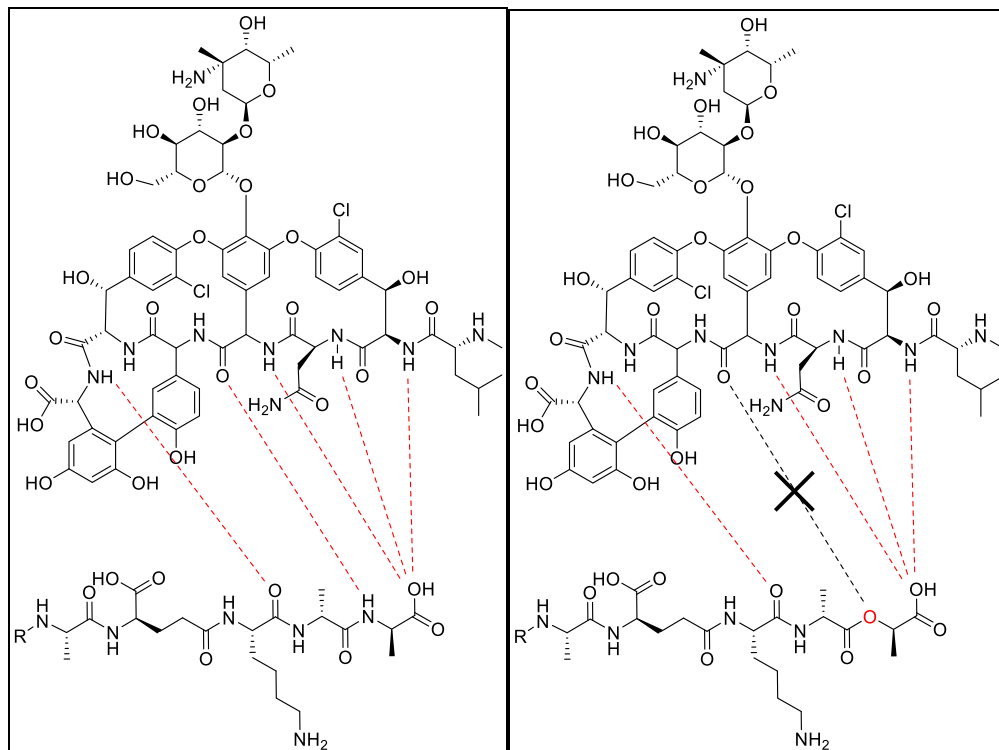


**Figure 4-6:** Structure of vancomycin binding to the lipid II stem peptide. Shown with A) wild-type and B) vancomycin-resistant strains *S. aureus*. Hydrogen bonds are shown in red. The mutation to D-Lac is shown in the resistant strain with the disrupted hydrogen bond.

#### 4.1.3 Design and Evolution of Library Scaffold

As mentioned in the introduction (Chapter 1), bacterial resistance has been observed within the first few years of clinical use of an antibiotic. Vancomycin, however, can be considered one of the exceptions to this; resistance was not observed until about 30 years after the drug had been deployed. Such a privileged structure is ideal to mimic for the development of new antibiotics.

Immediately preceding the terminal D-Ala-D-Ala fragment of the lipid II stem peptide in *S. aureus* is a lysine. This was of special interest to us, as our group has been successful in targeting biologically relevant amines with our 2-APBA derivatives. We hypothesized that a cyclic or multicyclic peptide could be designed to mimic the potent binding of vancomycin and including a 2-APBA moiety would be advantageous in targeting this lysine (Figure 4-7). With the unique reactivity and critical function of this lysine, we envisioned its targeting would decrease the risk of resistance development compared to vancomycin. Furthermore, we expected that the elimination of a hydrogen bond observed in vancomycin-resistant strains of bacteria would be less detrimental for our designed peptides, as the additional iminoboronate interaction is stronger than the lost contact. With vancomycin being an especially difficult scaffold to manipulate for rational design, we chose to explore the use of library screening to discover 2-APBA presenting peptides with potent lipid II stem peptide binding.

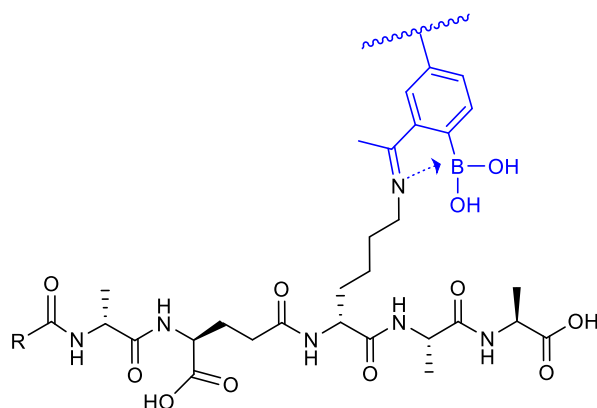


**Figure 4-7:** Depiction of iminoboronate formation between the lysine of the lipid II stem peptide and AB3 in a designed peptide.



Seeking not only to include an unnatural amino acid, but also a cyclic peptide structure, we proposed the use of a DNA-encoded library platform. This would allow us to perform sequencing using a separate entity from the peptides being screened. Unfortunately, this platform proved to be relatively expensive, even just during the original optimization of synthetic conditions. As a result, we moved forward using a one-bead-two-compound library synthesized through a core-and-shell strategy.

#### *4.1.4 Design of a Stringent Screening Process*

The rapid reversibility of iminoboronates makes these structures non-ideal for traditional screening methods. Furthermore, our target of interest is a short peptide. Unlike a protein target, this peptide will not contain a well-defined binding pocket. This makes washing during screening more likely to remove potent binders, as the location of binding is more solvent exposed. Without washing, we would likely have a much higher percentage of false positives, decreasing our chances of success. However, the structure of the iminoboronate can be covalently captured via reduction of the imine bond, as we have observed for intramolecular cyclization of peptides.<sup>23</sup> Creating a covalent linkage between our target and library hits would allow us to perform stringent washes to remove any false positives due to non-specific interactions (Figure 4-8), thus increasing our confidence in obtaining successful hits.

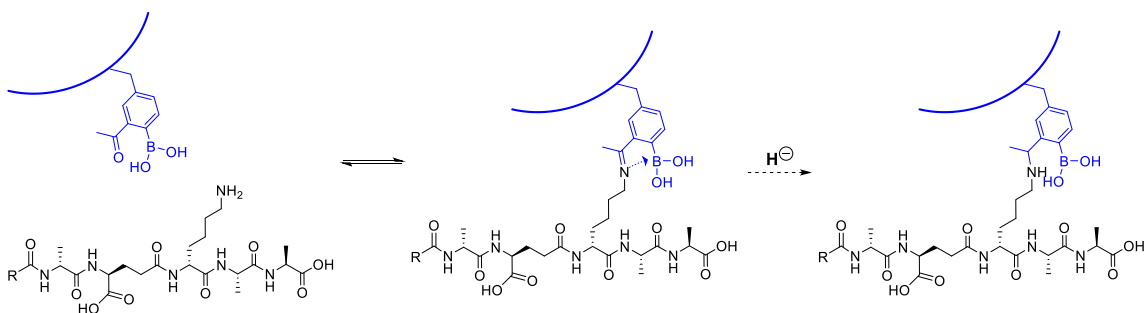


**Figure 4-8:** Proposed strategy for the covalent capture of hits via iminoboronate reduction. After the reversible conjugation of AB3 with the lysine side chain in the lipid II stem peptide, addition of a hydride donor will reduce the imine, producing a covalent bond between the target peptide and the hit peptide on resin.

To increase our screening stringency even further, we chose to use a two-step screening approach. The first step, involving an avidity pulldown, would allow us to screen a large scale library with a rapid output. The second step, using fluorescence microscopy for hit isolation, would provide a much more careful selection of positive hits.

While we were successful in optimizing the synthesis and accurate sequencing of our library, gathering about 20 hits and synthesizing nine for validation, we found no potent binders during validation. We attempted multiple strategies to confirm the success of our screen to no avail.

In light of these results, we decided to validate our library and covalent capture screening approach by screening against transferrin. We were successful in sequencing 20 of hits from this screen using fluorescence microscopy following  $\text{NaBH}_4$  reduction. Of these, three have been synthesized and studied for binding to transferrin using fluorescence anisotropy. From this validation, we observed

selective binding for transferrin over human serum albumin, with the best hit tested so far having a  $K_d$  of 25-30  $\mu\text{M}$ . Collectively, we conclude our hit selection for the screen with lipid II stem peptide was flawed but that our library has the potential to produce potent and selective binders in a model protein system.

## ***4.2 Exploration of a DNA-Encoded Peptide Library***

### *4.2.1 Preparation of Tentagel Resin*

To synthesize our library, we chose to use a 90  $\mu\text{m}$  Tentagel  $\text{NH}_2$  resin. Tentagel resins include a poly(ethylene glycol) (PEG) shell surrounding the polystyrene base found in normal SPPS resins. PEG based resins are very commonly used when synthesizing peptide libraries for on-bead screening due to the fact that they can readily swell in both organic and aqueous solvents. This allows for the resin to be taken from synthetic conditions in DMF and put into aqueous buffers for screening.

To prepare the resin for library synthesis, we first coupled Fmoc-glycine and measured the efficiency by the Fmoc-loading procedure. It has been reported that coupling the first amino acid to the Tentagel resin, despite having a terminal free amine, can be relatively more difficult than subsequent residues.<sup>24</sup> As such, we used 5 eq Fmoc-glycine with 5 eq each of HATU and HOBT to the resin for a coupling time of two hours. This procedure was repeated if less than 90% coupling was measured, such that the peptide capacity per bead could be maximized. After this, any remaining amines were acetyl-capped to prevent any heterogeneity in

the peptide chains on the same beads. Next, to provide a sufficient spacer from the resin, we coupled a second Fmoc-glycine using standard HBTU-chemistry.

We chose to use a photolabile linker (PLL)<sup>25</sup> to attach our desired peptide to the resin. As the peptides were going to be screened while still on the resin, we needed a resin cleavage strategy that would allow us to deprotect the side chain protecting groups with TFA. Using a PLL, the library hits could be cleaved individually by exposing the resin to UV light at a wavelength of 365 nm (Figure 4-9). To incorporate this into our library resin, we coupled the commercially available Fmoc-Photolabile Linker after the double glycine linker, providing the final resin prepared for library synthesis. After this coupling, the resin was protected from light to prevent premature cleavage.

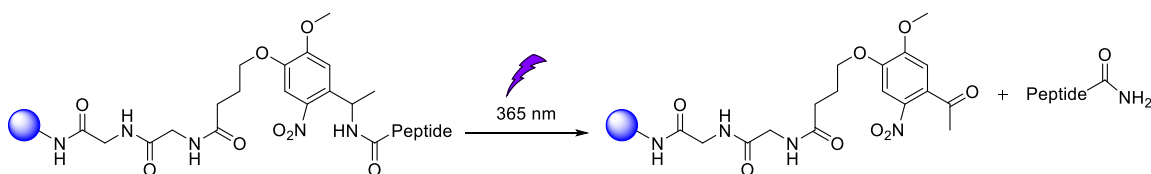


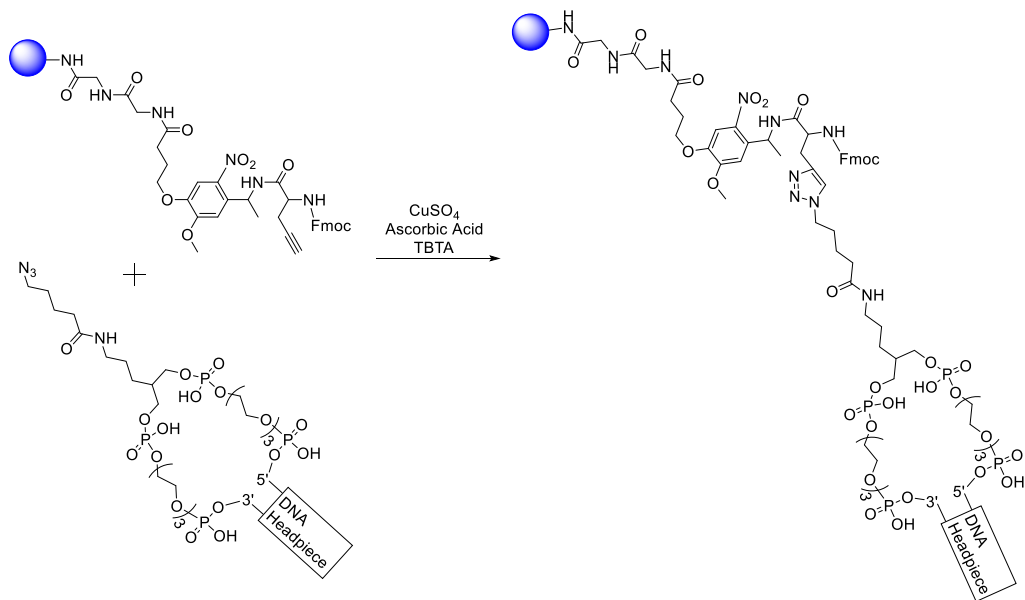
**Figure 4-9:** Structure of the photolabile linker used for the library and resulting products after UV cleavage.

#### 4.2.2 Optimization of DNA Tag Synthesis and Sequencing

Synthesis of a DNA-encoded library involves alternating steps of peptide synthesis and DNA ligation. As we are much more familiar with peptide synthesis and strategies to optimize it in a library setting, we chose to first optimize the necessary steps toward creating the DNA tag following a published procedure.<sup>26</sup> A test set of DNA oligomers corresponding to each residue was purchased, along

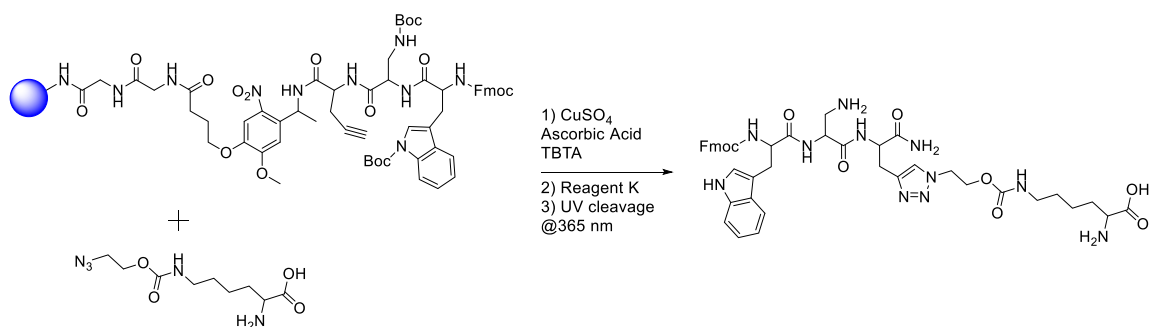
with the necessary headpiece to covalently attach the DNA to the peptide and primers for PCR amplification.

**Scheme 4-1:** CuAAC Reaction for the Covalent Attachment of DNA to Tentagel Resin



We chose to covalently attach the DNA to the Tentagel resin using Cu(I)-catalyzed alkyne-azide cycloaddition (CuAAC). This required the inclusion of propargylglycine between the PLL and our library peptide sequence, as the DNA headpiece included an azide handle (Scheme 4-1). Without an effective way to monitor the DNA headpiece attachment, we first used azido-lysine to confirm the effectiveness of our conditions (Scheme 4-2). For this, a test peptide was synthesized to include diaminopropionic acid (Dap) and Trp such that the reaction could be analyzed by LC/MS. We were happy to see that our desired product was the only new mass observed in the LC/MS after the CuAAC reaction (Figure 4-10). These conditions were then used for attachment of the DNA headpiece.

#### Scheme 4-2: Test CuAAC Reaction for Conjugation to Tentagel Resin



As mentioned above, no effective readout was found to analyze the yield of the CuAAC reaction between the peptide on resin and the DNA headpiece. This required us to move on with subsequent DNA ligation steps and analyze our final product by polymerase chain reaction (PCR) and denaturing polyacrylamide gel electrophoresis (PAGE). We ligated a universal starting sequence followed by six variable sequences (one for each diversity element in the peptide sequence) and ending with a universal ending sequence using T4 ligase. Maintaining an identical sequence at the beginning and the end of the DNA tag would allow for a single primer to be used for sequencing and provide an alignment sequence for tag identification after sequencing (Figure 4-11).

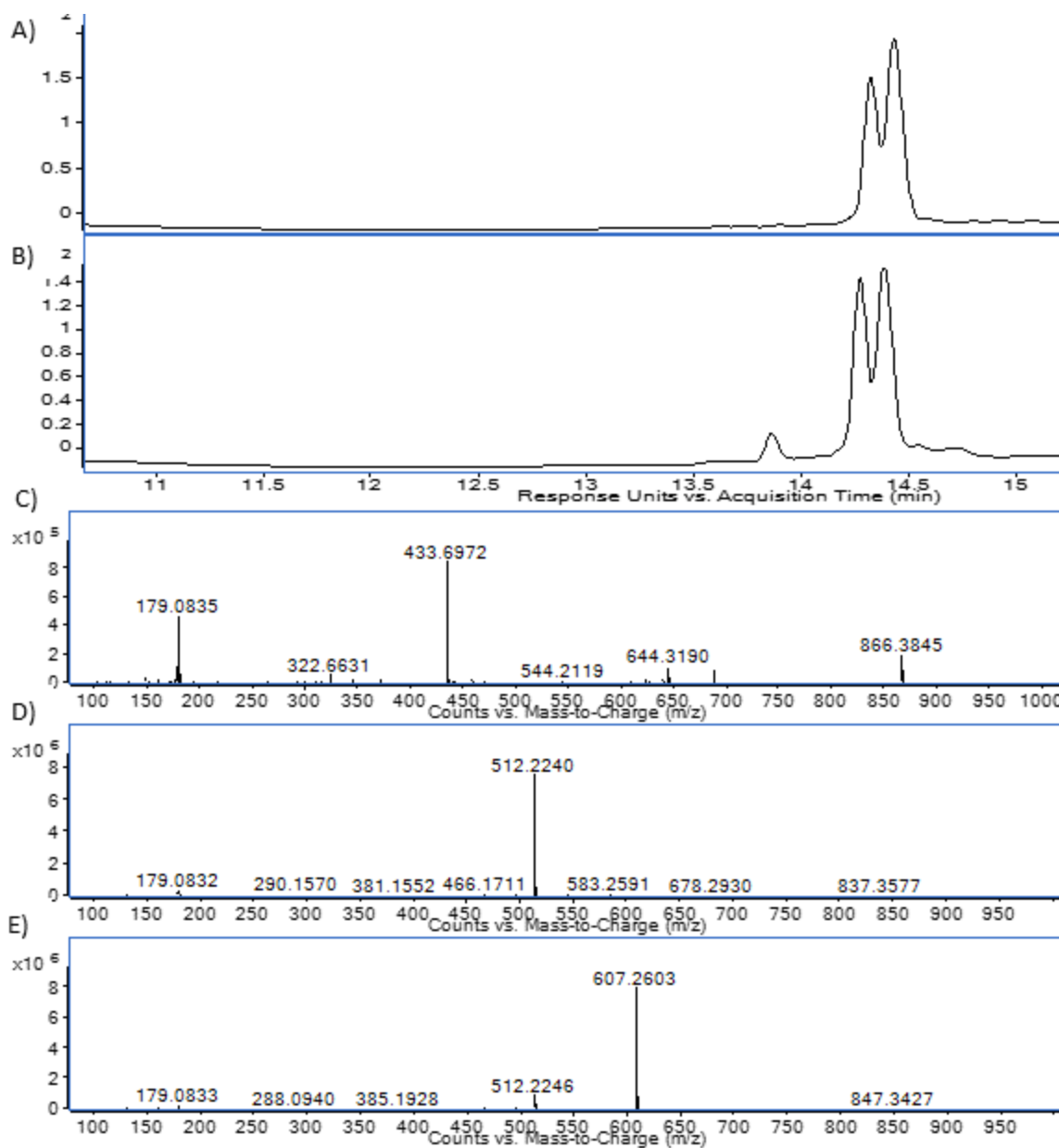


**Figure 4-10:** LC/MS Data for CuAAC Test Reaction with Azido-lysine. UV traces at 280 nm of A) peptide starting material and B) reaction mixture after CuAAC treatment. C) Extracted mass for peak at 13.8 min ( $[433.6972]^{2+}$ ,  $[866.3845]^{1+}$ ) correspond to the product. D) Extracted mass for peak at 14.3 min ( $[512.2240]^{1+}$ ) corresponds to peptide starting material missing Pra. E) Extracted mass for peak at 14.4 min ( $[607.2603]^{1+}$ ) corresponds to the starting material including Pra.

5'-TGACTCCCGCCGCCAGTCCTGCTCGCTTCGCTACATGGAAGAGAGGTCA  
AGTTTCAGGTTACGGAGCACTAAACCTCAATTCACAAAGAGCGCAATCCCATG  
CCTGTTTGCCGCCAGTTGTTGTGCCAC-3'

**Figure 4-11:** Sequence of DNA used for testing of library ligation conditions. Black = headpiece sequence; Red = universal sequences used for alignment; Blue = encoding sequence; Orange = position specific overhangs.

Conveniently, PCR can be performed on the DNA oligomers while still on resin. After optimization of the PCR and PAGE conditions, we found that sufficient amounts of DNA were ligated on resin to allow for detection of oligomers with the desired length by ethidium bromide staining (Figure 4-12A). The DNA samples were excised from the gel, run through a second round of PCR with extension primer and analyzed by PAGE before preparing samples for sequencing (Figure 4-12B). All samples sent to Eton Bioscience for Sanger sequencing provided the expected coding sequence.

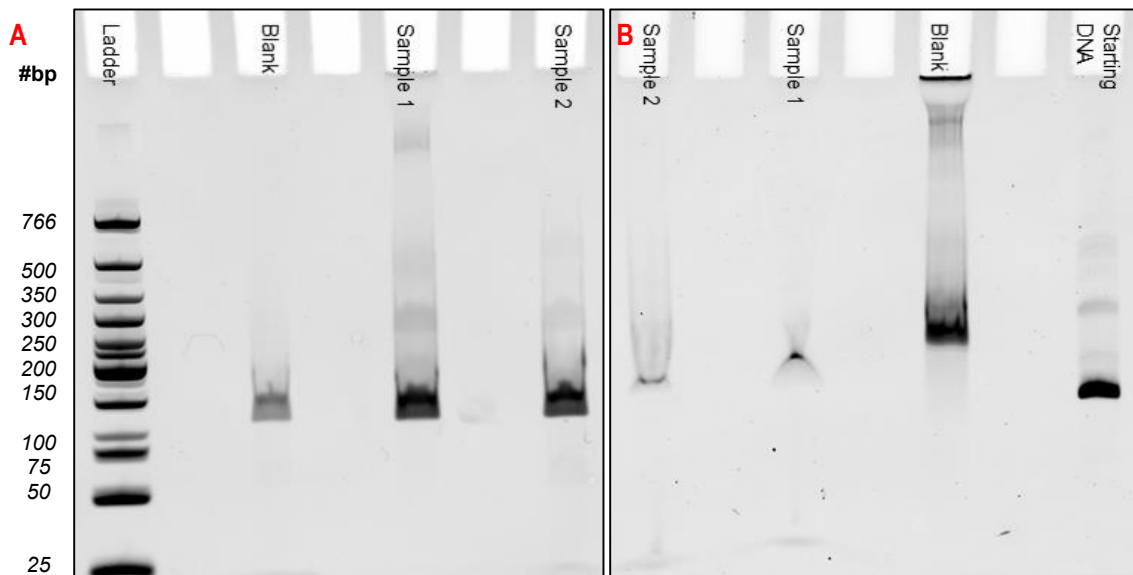


**Figure 4-12:** Denaturing PAGE of PCR reactions for single beads. A) Resin as template and B) with excised DNA from gel A as template. The product from gel B is expected to be longer original template (starting DNA) as an extra primer is included to provide extra length.



#### 4.2.3 Simultaneous Peptide Synthesis and DNA Ligation Conditions

Having confirmed our DNA ligation and sequencing conditions were successful, we moved on to optimize the simultaneous synthesis of library peptides and DNA tags. It has been reported,<sup>27</sup> and is not surprising, that different chemical reaction conditions can result in scission of DNA backbones or modification of DNA bases. Considering this, we needed to confirm that the conditions of our proposed library synthesis would not have such a detrimental effect on the DNA tag that it could no longer yield enough DNA for confident sequencing after hit selection.

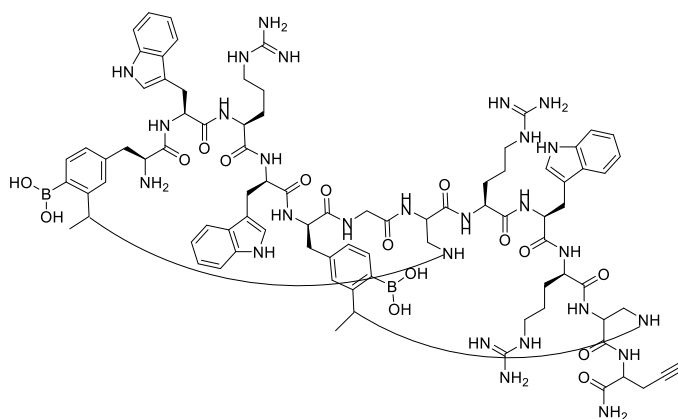


**Figure 4-13:** Structure of bicyclic peptide used to test conditions for simultaneous DNA ligation and peptide synthesis.

Using a model peptide sequence (Figure 4-13), we performed a mock library synthesis. After the full process, the resin was checked for quality of both the DNA and the peptide. Fortunately, despite the harsh conditions of peptide synthesis and side chain deprotection, enough DNA remained intact providing

the correct sequence (Figure 4-14). However, we were not as successful with the peptide synthesis, observing what appeared to be deletion products (Figure 4-15).

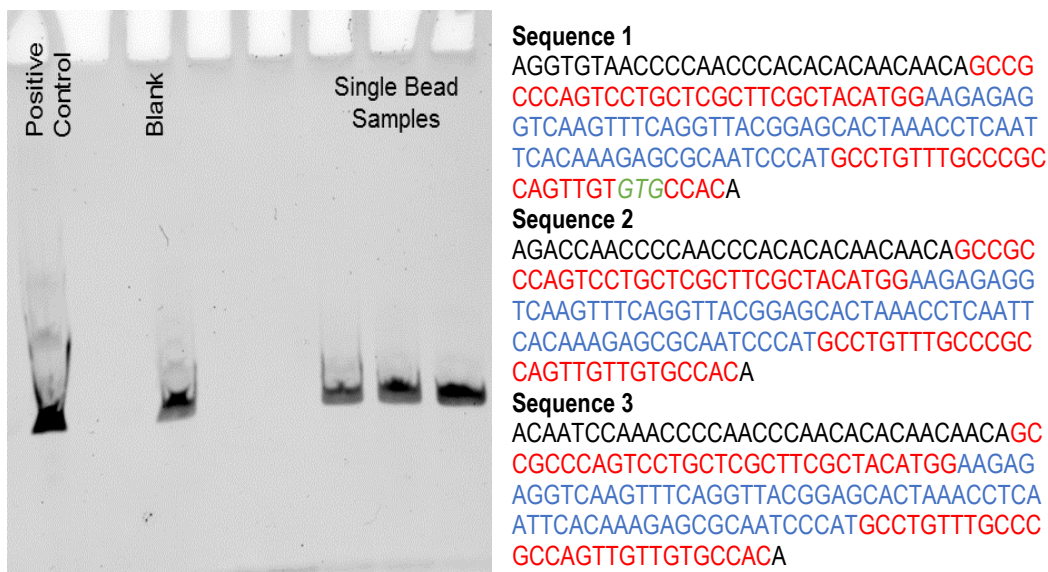


**Figure 4-14:** Results of library test ligation. A) Denaturing PAGE gel for single bead samples after reactions to mimic the DNA encoded library synthesis and B) sequences provided by Eton Bioscience, Inc. In the gel, the positive control included was a single bead sample from previous test of ligation. In the sequencing data, black = DNA base pairs outside of the alignment sequence, red = universal alignment sequences, blue = coding sequence and green = base pairs with the incorrect sequence.

We thoughtfully considered what may have been going wrong with the peptide synthesis. Changing the peptide sequence and running controls which did not include DNA ligation did not improve our peptide product. Previously, we had experienced issues with using Reagent K with AB3 containing peptides. However, using an optimized cleavage cocktail also did not improve the final peptide quality. By comparing to other peptide sequences that had been successfully synthesized, we determined that the route of the problem was the combination of AB3 and propargylglycine. This was confirmed by performing an alkyne capping reaction using azidoacetic acid prior to side chain deprotection

(Figure 4-16). We concluded that this issue could be remedied by performing a capping step of the alkyne after attachment of the DNA headpiece. Strangely, we the second major product was the peptide containing the unreacted alkyne. It was unclear why this did not interfere with the side-chain deprotection in the same way it did under the original conditions. However, at this time we determined the cost of the platform was not sustainable and therefore did not explore this further.

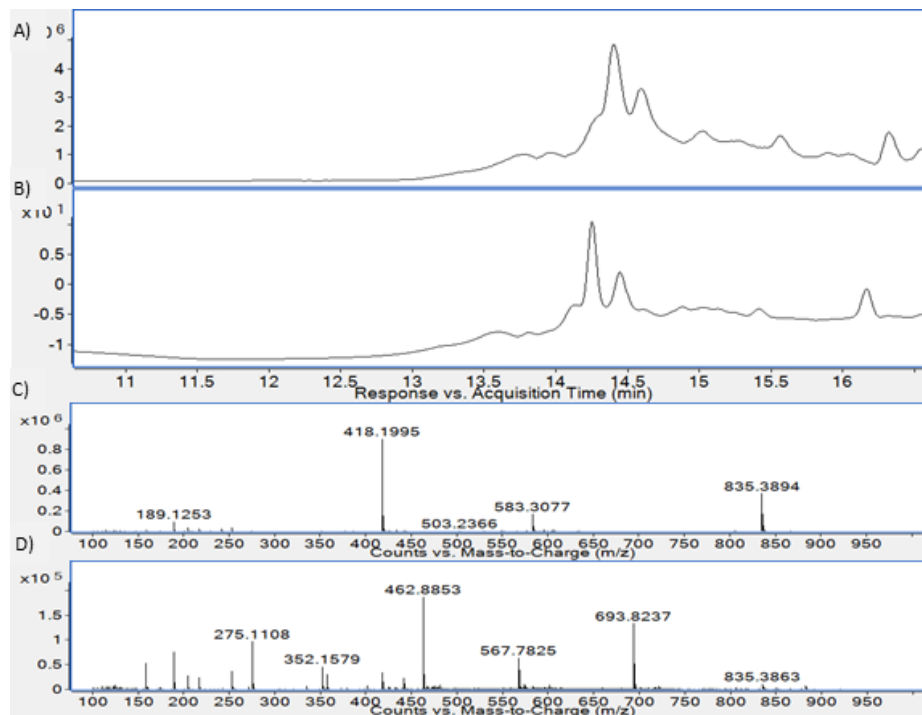


**Figure 4-15:** LC/MS analysis of peptide from test DNA encoded library synthesis. A) TIC trace and B) UV trace at 254 nm for sample. Extracted masses C) at 14.4 min ( $[418.1994]^{3+}$ ,  $[835.3894]^{2+}$ ) and D) 14.5 min ( $[462.8853]^{3+}$ ,  $[693.8237]^{2+}$ ) did not correspond to any desired peptide sequences.

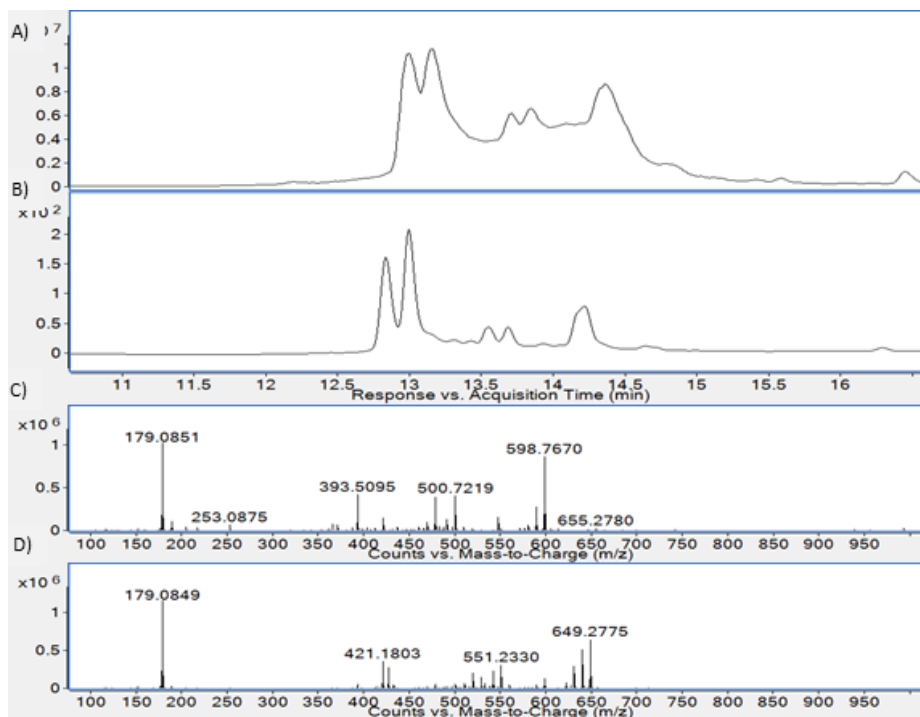


**Figure 4-16:** LC/MS analysis of peptide from test DNA encoded library synthesis after capping with azido acetic acid. Extracted masses for C) peak at 12.9 min ( $[598.7670]^{2+}$ ) corresponds to peptide with unreacted propargylglycine and D) peak at 13.1 min ( $[649.2775]^{2+}$ ) corresponds to product with the alkyne capped with azido acetic acid. This demonstrated that desired peptide masses were not observed in Figure 4-15 due to reactivity of the alkyne during side chain deprotection.

### 4.3 One-Bead Two-Compound Library of Monocyclic Peptides

#### 4.3.1 Library Structure Design

As our goal for the design of this library was to mimic the privileged scaffold and peptide targeting of vancomycin, we wanted to incorporate a cyclic structure with various amino acids displaying both hydrogen bond donors and acceptors. We chose a set of seven amino acids (Figure 4-17) that represent the different structural characteristics we were interested in, along with different hydrophobic structures to incorporate the possibility for hydrophobic interactions. We believed that this sampling of the amino acids would be sufficient

for a preliminary screen from which we could gather structure-activity relationships to influence later optimization.

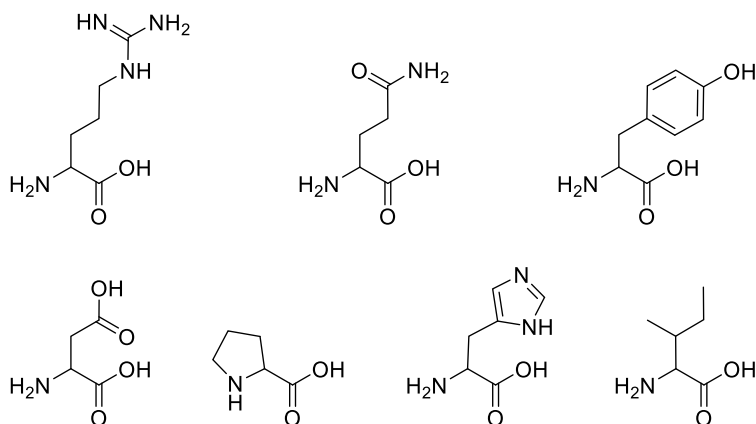


**Figure 4-17:** Structures of seven amino acids chosen for library. Arginine, Glutamine, Tyrosine, Aspartic acid, Proline, Histidine and Isoleucine.

#### 4.3.2 Utilization of a Core-and-Shell Strategy

In collaboration with Aaron J. Mauris in the Weerapana lab, we were able to pursue a mass-spectrometry based sequencing approach. We learned early on that the presence of our unnatural amino acid, AB3, prevented us from obtaining confident sequencing results from the modified SEQUEST program, as the correct sequence from a known sample was not found. This was most likely due to the fact that the boronic acid functionality can exist in different hydroxylated forms when analyzed by ESI, such that an expected mass fingerprint could not be extracted. As a result, we chose to use a core-and-shell arrangement for the incorporation of AB3 into our sequence, creating separate library peptides with and without this functional group.

Core-and-shell arrangements are a common way to construct one-bead-two-compound libraries and are dependent on certain qualities of the resin used for library synthesis. In our case, the characteristic of Tentagel resin that makes it ideal for on-resin screens, swelling in aqueous and organic solvents, can also be taken advantage of during library synthesis. By using water and an immiscible organic solvent, distinct layers within the resin can be created. Reactions can then be limited to the outer layer of the resin using reagents only soluble in the solvent in this layer (Figure 4-18).

In order to obtain a core-and-shell arrangement, the resin transferred from DMF to water by washing with increasing ratios of water to DMF at the desired step in synthesis; in our case, this was performed directly before the coupling of AB3. The resin was then fully equilibrated in water by soaking it overnight. The

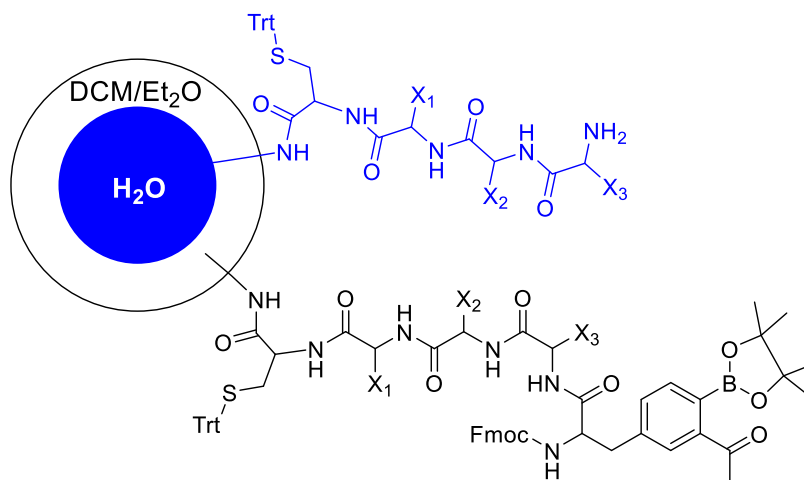


**Figure 4-18:** Structure of core/shell arrangement for our one-bead-two-compound library. The sequence in blue represents the core structure, contained within the water layer and unable to react. The sequence in black represents the shell structure, contained within the organic layer and accessible to coupling reagents for AB3.

excess solvent is removed, such that the resin remains swollen, and the desired reagents are added as a solution in a 50:50 mixture of diethyl ether and dichloromethane (DCM).<sup>28</sup> Since neither of these solvents are miscible with water, only the peptide chains on the outermost section of the resin are exposed to the peptide coupling reagents. After the AB3 coupling is complete, the resin is washed with DCM, to prevent exposure of the core peptide chains to any remaining activated AB3, then with DMF. The resin is then re-equilibrated in DMF and library synthesis is continued on.

In our hands, the use of DIC as a coupling agent for AB3 with the core-and-shell arrangement provided 70% coupling of AB3, as determined by LC/MS analysis (Figure 4-19). Completing the full peptide synthesis and submitting samples to Aaron demonstrated that the 30% peptide not containing AB3 was sufficient to provide confident sequencing results on a single bead level.

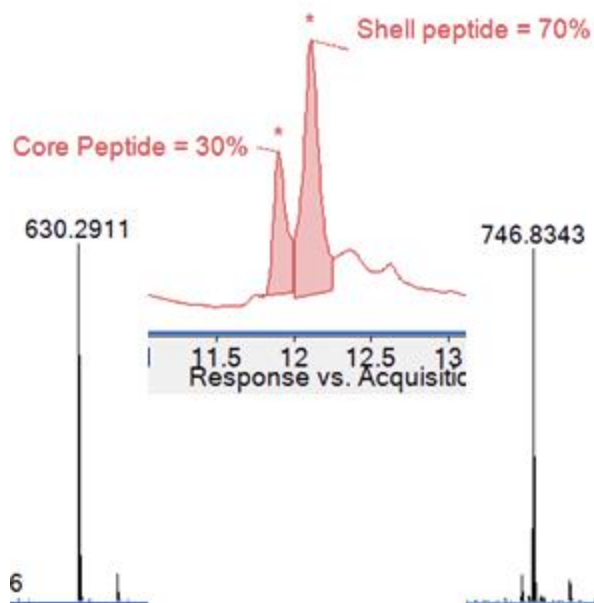


**Figure 4-19:** LC/MS analysis of a model core/shell peptide. The peptide sequence is Ac-Cys-Val-His-Val-(AB3)-Gln-Pro-Arg-Cys-Tyr-NH<sub>2</sub> with both cysteines capped using iodoacetamide. Both displayed masses are for [M+2H]<sup>2+</sup>, matching expected masses of 1260.58 and 1493.67 for the core and shell sequences, respectively. The mass difference of 233.09 matches the residue mass of AB3.

#### 4.3.3 Cysteine Disulfide Formation for Reversible Cyclization

Next, we attempted to achieve a second core-and-shell arrangement for the final residue. We pursued this step with the aim of incorporating a second AB3, allowing for a multicyclic structure to be formed through the selective reduction of iminoboronates between AB3 and lysine (i.e. sequence seen in Figure 4-13). Unfortunately, we were unsuccessful towards this goal. Creating a second core/shell arrangement yielded us with four different peptide sequences, yielding a mixture too complicated for our analysis. As a result, we settled on first exploring a monocyclic structure formed via disulfide bond between N- and C-terminal cysteines (Figure 4-20). The use of disulfide cyclization allowed for the



linearization of the sequencing compound prior to UV cleavage and mass-spec sample preparation.

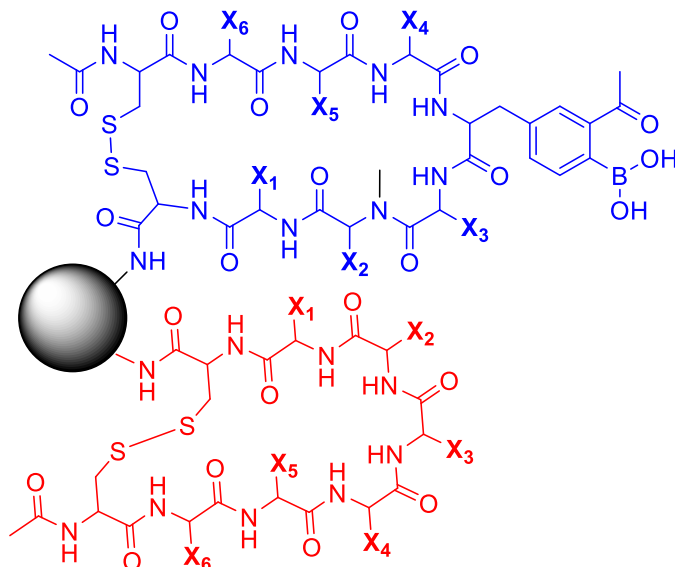


**Figure 4-20:** Structure of final library design. The sequence displayed in blue corresponds to the screening compound while the sequence in red displays the sequencing compound. X = variable side chain, from the amino acids in Figure 4-17.

Originally, we pursued both air and DMSO-mediated on-resin oxidation for cyclization. Unfortunately, neither of these methods yielded the desired result. We observed that air oxidation proceeded on the time scale of days, while DMSO-mediated oxidation created a relatively significant impurity. Looking into the literature, we found a method for on-resin peptide disulfide formation using N-chlorosuccinimide (2 equivalents) in DMF. An appealing feature to this cyclization method was that it was complete within 15 min using relatively mild reagents. Using these conditions, we found complete cyclization without the formation of significant impurities. For mass-spec analysis, subsequent reduction of the

disulfide using TCEP and iodoacetamide capping of the free thiols after the full synthesis of our test library member yielded the desired sequence.

#### *4.3.4 Total Synthesis of the Library*

In order to create the library, we utilized a split-and-pool strategy. Taking the bulk resin prepared up to the PLL, we coupled the first cysteine. After Fmoc deprotection, the resin was suspended in DMF and evenly distributed into seven RVs, one for each amino acid. The individual amino acids were dissolved in 0.4 M NMM in DMF and each was added to a RV. After a one hour coupling, the resin was combined into the original RV, washed with DMF six times then Fmoc deprotected, ready for the next split. This procedure was repeated two more times, yielding the peptide up to the AB3 residue. AB3 is coupled to the peptide in the established core/shell procedure and the split-and-pool is carried on after this.

When all of the variable residues have been added, the N-terminal cysteine is coupled to the bulk library resin. We chose to also acetyl cap the N-terminus, providing us with a possible location for fluorophore labeling during hit validation without altering the overall charge and characteristics of the peptide. The side chains are then deprotected using 10% water in TFA for four hours. Finally, peptides are cyclized using the established conditions, yielding the desired final library structure.

#### 4.3.5 Quality Control Analysis of the Library

As we could not analyze the success of the library synthesis by analyzing a bulk sample, we prepared single bead samples and submitted for MS/MS sequencing. Of 20 beads, we observed ten beads to have clean enough spectra for confident sequencing (Table 4-1).

*Table 4-1: Quality Control Analysis of Library Sequencing*

Sample	Top Hit Sequence	QC Check?	Sample	Top Hit Sequence	Pass QC?
1	YPPDYQ	√	11	No sequences	X
2	RDYDPD	√	12	No sequences	X
3	HPHIRQ	√	13	IRDHYQ	√
4	No sequences	X	14	No sequences	X
5	IDYDYR	√	15	YRHDIYH	√
6	No sequences	X	16	No sequences	X
7	PDQDHQ	√	17	HPHYPI	√
8	No sequences	X	18	No sequences	X
9	IQHHII	√	19	YYHIHD	√
10	IQHHII	√	20	No sequences	X

Top hit sequences are listed with just the six variable amino acids. For samples which did not pass QC, the SEQUEST program was either unable to find a library peptide sequences matching the mass spec data, the top two sequences were too close in spectral counts or the number of spectral counts for the top sequence was below 80.

#### 4.4 Design and Validation of a Screening Scheme for Lipid II Stem Peptide Binders

##### 4.4.1 Developing Intermolecular Imine Reduction Conditions for 2-APBA and Lysine

Our earliest work studying the association between 2-APBA functionalities and lysine demonstrated that the iminoboronate formed was rapidly reversible. Under the conditions of library screening, this would result in many of the hits being lost during washing steps as a result of a shift in the equilibrium towards

the dissociated forms after resuspension in fresh buffer. On the other hand, not performing any washing steps throughout our screen would result in the collection of false positives, as non-specific binders would not be removed. However, iminoboronate formation has a distinctive feature that could overcome both of these potential downfalls.

The quintessential feature of screening for library hits with reversible iminoboronate binding became that they could be covalently captured using hydride reduction. In a similar way as reductive amination was used in Chapter 2, reduction of iminoboronates yields amines which are no longer freely dissociable (displayed in Figure 4-8). Our group has already demonstrated the utility of this in the case of intramolecular peptide cyclization,<sup>23</sup> though it has yet to be obtained when the 2-APBA and amine are located on separate molecules.

In our previous work, reduction was achieved using sodium cyanoborohydride; as such, we used these conditions as our starting point for analyzing the possibility of intermolecular iminoboronate reduction. We chose to study a model reaction of the reduction between simple 2-APBA and lysine (Figure 4-21), analyzing the degree of reduction by <sup>1</sup>H NMR. We explored changes in the concentration of NaCNBH<sub>3</sub> and the temperature the reaction (Table 4-2). However, the only change we observed was the reduction of the acetyl group to the corresponding secondary alcohol.

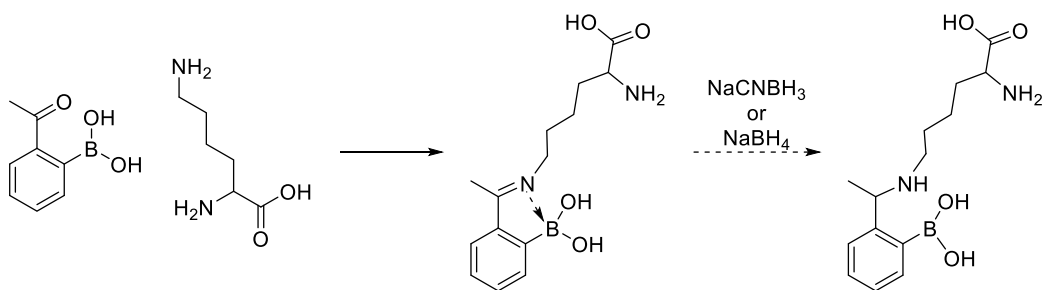


**Figure 4-21:** Test reaction used for optimizing conditions of intermolecular iminoboronate reduction.

**Table 4-2: Optimization of Iminoboronate Reduction**

Reducing Agent (Conc.)	Temperature	Imine Reduction Observed?
NaCNBH <sub>3</sub> (50 mM)	RT	No
NaCNBH <sub>3</sub> (25 mM)	RT	No
NaCNBH <sub>3</sub> (12.5 mM)	RT	No
NaCNBH <sub>3</sub> (50 mM)	0°C	No
NaBH <sub>4</sub> (50 mM)	RT	Yes

*Analysis of imine reduction between 2-APBA and lysine performed using NMR*

We hypothesized that the kinetics of NaCNBH<sub>3</sub> imine reduction were not rapid enough to capture the iminoboronate before dissociation occurred. We chose to attempt the iminoboronate capture using a stronger hydride donor, namely sodium borohydride (NaBH<sub>4</sub>). Studying the same original reaction conditions as with NaCNBH<sub>3</sub>, we were happy to see reduction of the imine was occurring with NaBH<sub>4</sub> at about 10-15% conversion (Figure 4-22). Furthermore, we observed that the acetyl groups on the unreacted AB<sub>3</sub> were also reduced, which could be beneficial to our screen, as it would prevent any secondary binding of the target from occurring after the reduction. To more clearly quantify the amount of conjugated product captured, we switched the amine used to Fmoc-lysine, providing us with a chromophore to use in LC/MS analysis (Figure 4-23). Based on the K<sub>d</sub> obtained via NMR titration, we expect about 30% conjugate to be formed

under these conditions before reduction. Considering this, we estimated that we obtained about 50% of the expected reduced product.

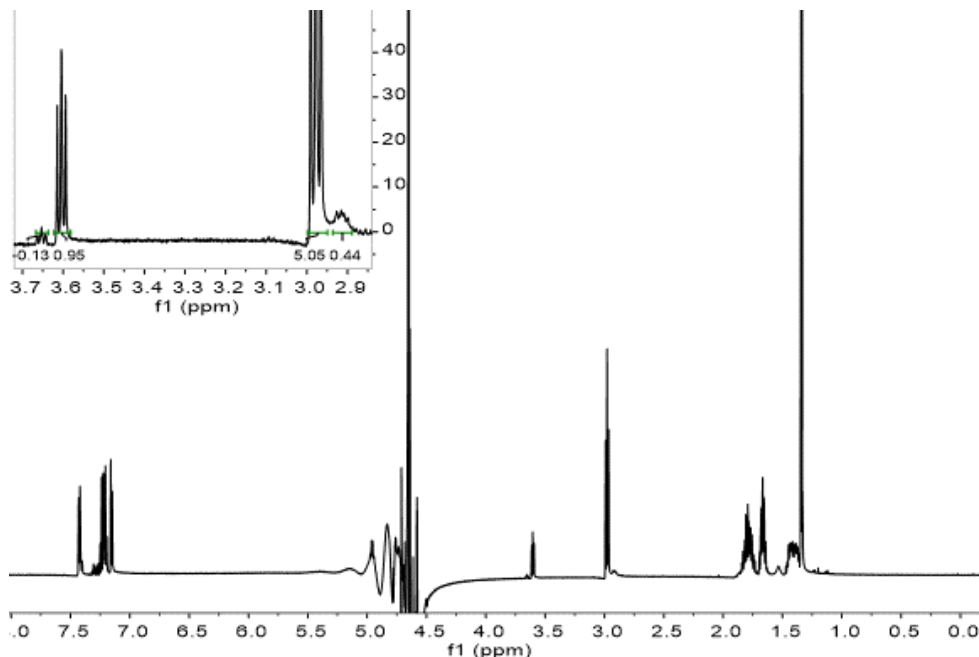


**Figure 4-22:** NMR Spectrum of 2-APBA and Lysine Reduction with  $\text{NaBH}_4$ . In the inset, the peaks between 3.55 and 3.70 ppm show the proton on the  $\alpha$ -carbon with the conjugate peak integrating to 0.13 and the unmodified lysine peak integrating to 0.95. The peaks between 2.90 and 3.00 correspond to the protons on the  $\epsilon$ -carbon and amine with the unmodified lysine peak integrating to 5.05 and the conjugate peak integrating to 0.44.

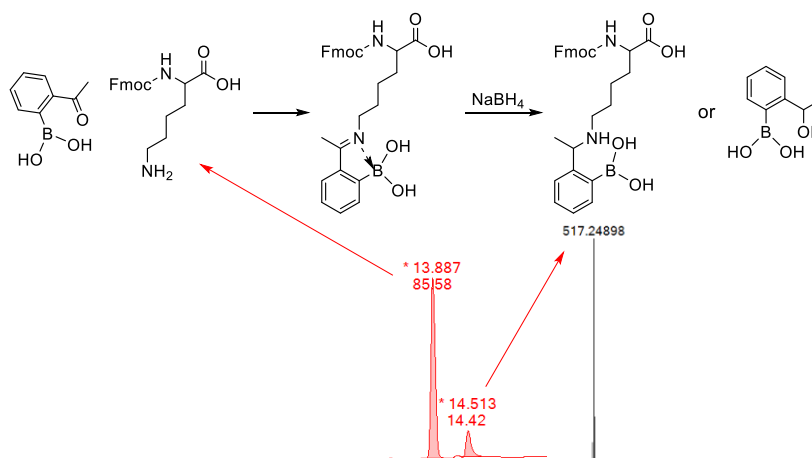


**Figure 4-23:** Test reaction between 2-APBA and Fmoc-lysine. LC/MS data shows 14.5% conversion to the iminoboronate reduction product with the other peak corresponding to unchanged starting material.

#### *4.4.2 Hit Selection via Affinity-mediated Pull-down*

A common strategy to extract binders during library screening is through an affinity tag on the target, such as with the addition of a target-specific antibody or by biotinylating the target for binding to streptavidin, for pull-down.<sup>29,30</sup> As our target was only a short peptide, we saw the best option as being to add a biotin handle at the end of the peptide, opening up a wide variety of pull-down methods. The biotin group was expected to be small enough to not interfere significantly with target binding of the library, and could be easily attached to the N-terminus through amide bond formation, as biotin contains a free carboxylic acid not involved in its interaction with streptavidin.

We were interested in the streptavidin-coated magnetic Dynabeads to perform our desired affinity pull-down. The magnetic beads are straightforward in practice and would not require us to obtain any extra equipment in order to use them. They also have an added benefit in being rapid for pull-down. However, they do suffer from high false positive rates and a somewhat lower false negative rates.<sup>31</sup> With the library screen we envisioned, both of these could be overcome. In the case of the high false positive rate, we were planning on doing a second fluorescence microscopy-based screen. This would give us an opportunity to discard false positives from the initial screen before sequencing. As for the false negatives, literature has shown that this can be remedied by including multiple copies of all the library members.<sup>31</sup> For the scale we planned to screen against, we

expected eight to nine copies of each library peptide, greatly decreasing the probability of all copies of a hit being left behind as a false negative.

We moved on to study the necessary conditions for magnetic bead pull-down as they pertained to our own screen. To do this, we synthesized the desired screening target on Tentagel beads, such that the biotin was covalently attached to the bead, similar to what we expected for our library hits in the actual screen (Figure 4-24). Conveniently, the fluorescein tag resulted in the positive control beads turning from colorless to orange. This allowed us to analyze the mixture using simple white light microscopy.

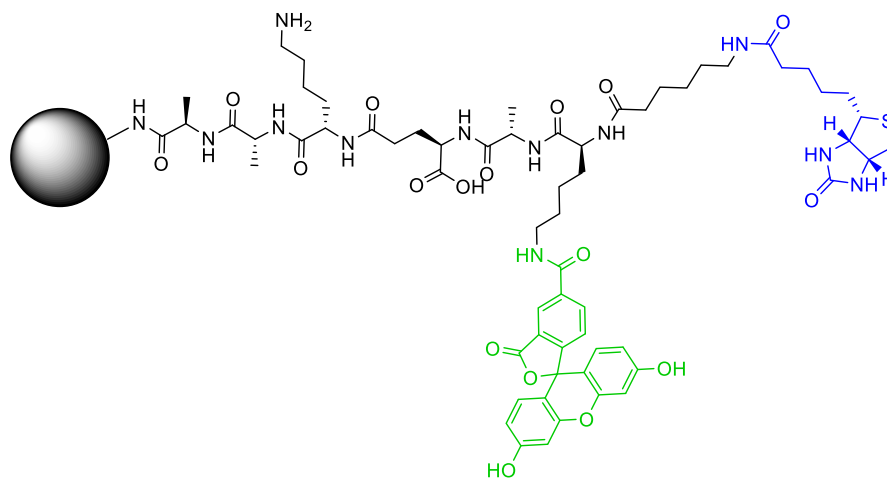


**Figure 4-24:** Structure of positive control on Tentagel resin. This sequence was used as a control for optimizing the magnetic pull-down and fluorescence microscopy screening conditions. The biotin handle is shown in blue and fluorescein is shown in green.

Taking these positive control beads, we doped them into samples of blank beads at hit rates of 1% and 0.1%. After equilibrating the beads in PBS buffer with 0.1 mg/mL BSA overnight, the streptavidin-coated magnetic beads were added and the mixture was allowed to incubate for two hours. A magnet was applied to



the sample and the supernatant with any unbound Tentagel beads was removed. The magnet was removed to release the magnetic beads with captured Tentagel resin which were then resuspended in PBS buffer with 0.1 mg/mL BSA for washing. The pull-down was repeated and the final collection was analyzed under the microscope to determine the numbers of recovered positive control vs. blank beads.

In the 1% hit rate experiment, we were able to recover 75% of the positive control beads with only 12% of the blank beads, resulting in a six-times enrichment of the positive control and a close to nine-times reduction in the blank beads. In the 0.1% hit rate experiment, we recovered 55% of the positive control beads with only 3.4% of the blank beads, resulting in a 15-times enrichment of the positive control and about a 30-times reduction in the blank beads. Additionally, we looked at the captured beads under the fluorescence microscope. By fluorescence, positive controls were easily distinguished from the blank beads (Figure 4-25). Given the success of these control experiments, we were confident the magnetic pull-down would be a viable option for our first screening step.

#### *4.4.3 Selection of Hits Using Fluorescence Microscopy*

Fluorescence-based screening is a common strategy used in library selections. Targets containing a fluorophore tag are relatively easy to obtain and

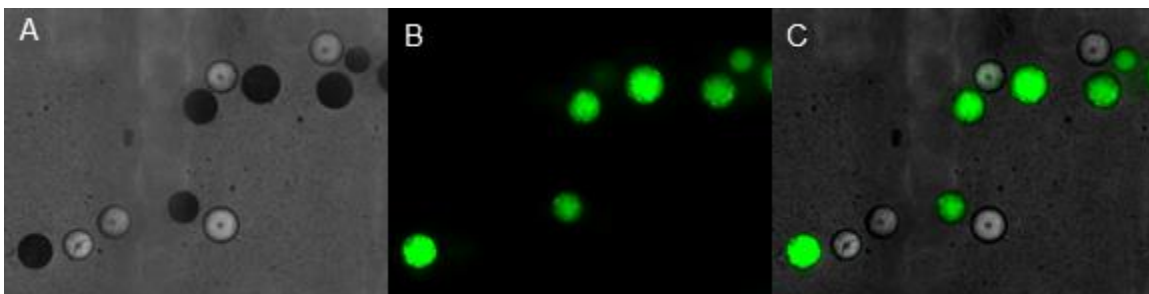


**Figure 4-25:** Microscopy images from Dynabead magnetic pull-down optimization. A) White light; B) FITC channel; C) Overlay. From the overlay, the positive control beads (colored green to show fluorescence) are easily distinguished from the blank beads. Dynabeads can be seen as small black dots in the white light and speckle the positive control beads in the FITC channel.

performing selections with fluorescence microscopy or large particle sorting tend to be fairly straightforward. In our case, we would need to use microscopy in order to separate single beads for sequencing. This made fluorescence microscopy an attractive strategy as it would combine the necessary hit separation with a second round of screening.

A degree of binding caused by non-specific interactions between the library and the target is widely known to occur during on-resin screening. Typically, this is caused by hydrophobic interactions between the resin material and the target of interest. As such, we wanted to be sure that this would not hinder the distinction between hit and non-hit beads during fluorescence analysis. We looked at three different sets of prepared Tentagel resin: the first was the blank resin, serving as our negative control; the second had carboxyfluorescein coupled to the resin, serving as our positive control with the theoretical maximum fluorescence we



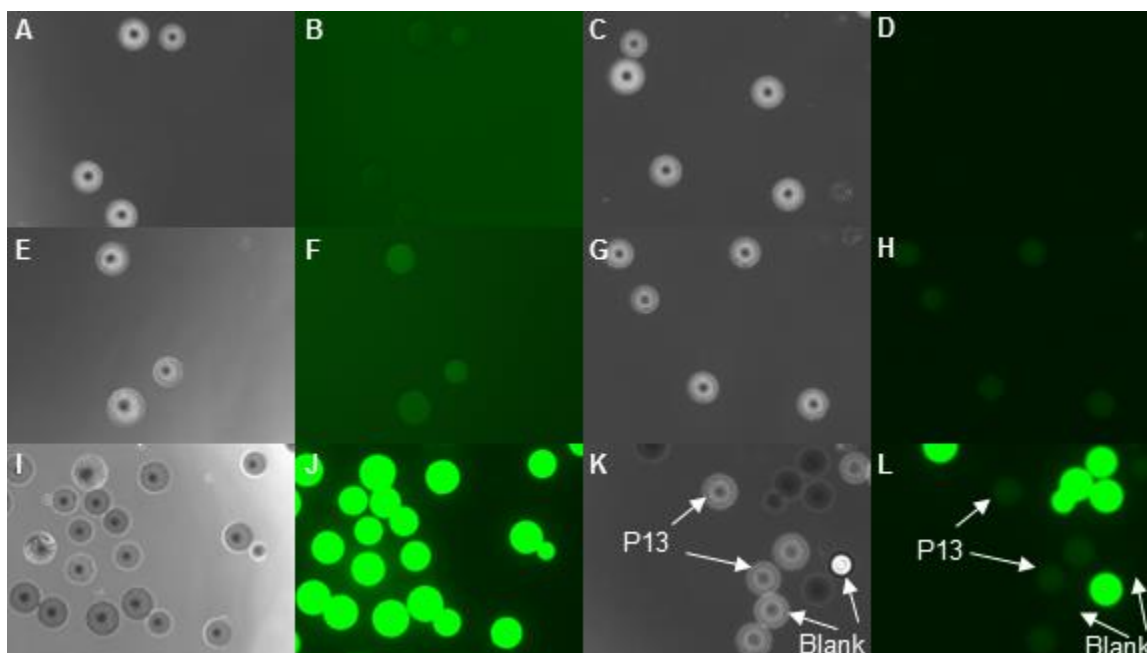


**Figure 4-27:** Fluorescence microscopy images of various sets of prepared Tentagel resin. A) White light and B) FITC channel images of blank resin with target peptide, no washes; C) White light and D) FITC channel images of blank resin with target peptide after one wash; E) White light and F) FITC channel images of P13 resin with target peptide, no washes; G) White light and H) FITC channel images of P13 resin with target peptide after one wash; I) White light and J) FITC channel images of positive control resin; K) White light and L) FITC channel images of all three resins mixed together. Positive control resin is observed to have the brightest fluorescence, but blank and P13 resins are still distinguishable when contained in the same sample.

With these images, we were confident that hits would be distinguishable from false positives after the magnetic pull-down selection. This is better displayed by a sample of mixed resin, where the blank, P13 and positive control resins were imaged in the same sample. They also demonstrate that we could expect little non-specific binding caused by the resin alone after just a single wash, decreasing the occurrence of false positives. After the iminoboronate reduction, we planned to perform multiple washes to remove any remaining target peptide and to alleviate non-specific interactions.

#### 4.4.4 Final Screening Scheme and Known Sequence Validation

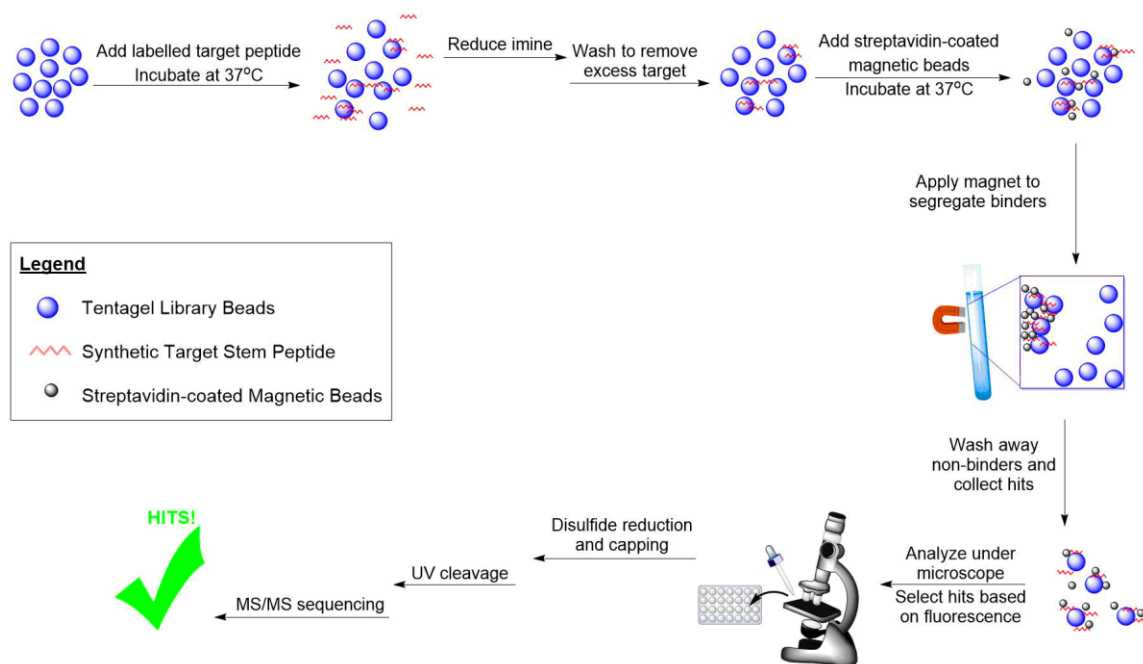


**Figure 4-28:** Depiction of final optimized screening scheme for our cyclic library against lipid II stem peptide.

With all steps in our proposed screen optimized, we designed a final screening scheme (Figure of 4-28). After side chain deprotection and cyclization of the peptide resin, it would first be equilibrated in PBS buffer (pH 7.4) overnight. The resin was then washed three times with PBS buffer (pH 7.4) containing 1.0 mg/mL BSA to serve as a blocking agent. The final solution suspended the library beads at a concentration of 17.5 mg beads/mL. To this, the target peptide was added to a final concentration of 10  $\mu$ M and the suspension was rotated while incubating at 37°C for 1 hour. The iminoboronate was reduced by adding sodium borohydride at a concentration of 50 mM and rotating the sample for 15 min. The resin was then washed PBS buffer (pH 7.4) six times and resuspended in PBS

buffer + 1.0 mg/mL BSA. To this, streptavidin magnetic beads (stock=10 mg/mL) were added to a final concentration of 0.1 mg/mL. This solution was allowed to rotate while incubating at 37°C for two hours to allow for efficient association of the biotin and streptavidin. The magnetic selection was performed and washed once. After washing, the collected hits and magnetic beads were suspended in PBS buffer (pH 7.4).

The collection of hits would then be examined under the fluorescent microscope and selected based on relative fluorescence. All the hits were segregated from the non-hits and treated with TCEP to break the disulfide cyclization then capped with iodoacetamide. Individual beads were then separated into individual microconical tubes for UV cleavage. The individual samples were provided to Aaron as a 20  $\mu$ L solution in 95% water, 5% acetonitrile and 0.1% TFA.

It was not completely clear whether any of the steps in our screen would have negative effects on our confidence in the sequencing results. As such, we prepared 1 mg of a known sequence and subjected it to a round of screening. The expected sequence was successfully obtained from the mass-spec analysis of all four single bead samples submitted. With this, we were confident that the sequences obtained from hits after screening would be accurate.

#### 4.4.5 Screening and Sequencing of the Library

We subjected 350 mg of our library, a scale which provides eight or nine repeats of each library peptide, to our screen. We collected 29 hits, treated them to disulfide reduction, cysteine capping and resin cleavage. The samples were prepared for LC/MS/MS analysis and submitted for sequencing. From analyzing this data, we established 18 hit sequences (Table of 4-3). Of these, we selected 10 to move forward to validation. Hits for validation were picked based on our confidence in sequencing, which includes observing the corresponding mass for the screening peptide with the given top hit sequence.

**Table 4-3: Hits from Library Screening of Lipid II Stem Peptide**

Sample	Sequence	Picked for Validation	Sample	Sequence	Picked for Validation
1	RHYRYQ	√	16	YRYPPR	√
2	N/A	X	17	YRIRDI	X
3	PHPRQQ	X	18	HQYYR	X
4	PRHYHH	X	19	N/A	X
5	RRRYHR	X	20	YDDDDP	X
6	N/A	X	21	IRYHYP	√
7	N/A	X	22	HYQRRY	√
8	N/A	X	23	PHRRQI	X
9	RIIHPI	√	24	IHHRQY	X
10	N/A	X	25	HIDPRR	√
11	HRHDYR	√	26	IHQYPH	√
12	RRIYRQ	X	27	N/A	X
13	RQHYPQ	√	28	PIPHRQ	X
14	YHIDQP	X	29	YIDIQP	X
15	YIDHQH	√			

## **4.5 Hit Validation**

### *4.5.1 Synthesis of Selected Hits*

Selected hits were synthesized on Rink amide resin then cleaved using 82.5% TFA, 5% phenol, 5% water, 5% thioanisole and 2.5% triisopropylsilane. The peptide was precipitated two times using cold diethyl ether and dried under vacuum to yield the crude peptide. Each peptide was purified by reverse-phase HPLC and collected samples were lyophilized. To cyclize the peptide, the lyophilized peptide was then dissolved in 10% DMSO in water at a final concentration of 1 mM. This was allowed to stir open to air and was monitored by LC/MS for conversion to the cyclic product. After full conversion was observed, the peptide was lyophilized and stored at -20°C.

### *4.5.2 Validating Hits using MIC*

Initially, we chose to perform hit validation by examining the peptides' ability to inhibit the growth of *S. aureus* using an MIC assay. As our goal from this library was to find a peptide with potent antimicrobial activity, using an MIC assay was the most direct way to measure this. We studied the first four hits that had been synthesized (Hit 1, 13, 16 and 21) at concentrations up to 10  $\mu$ M in the standard micro-dilution MIC assay. Unfortunately, none of these gave any significant inhibition within this concentration range (Figure 4-29).



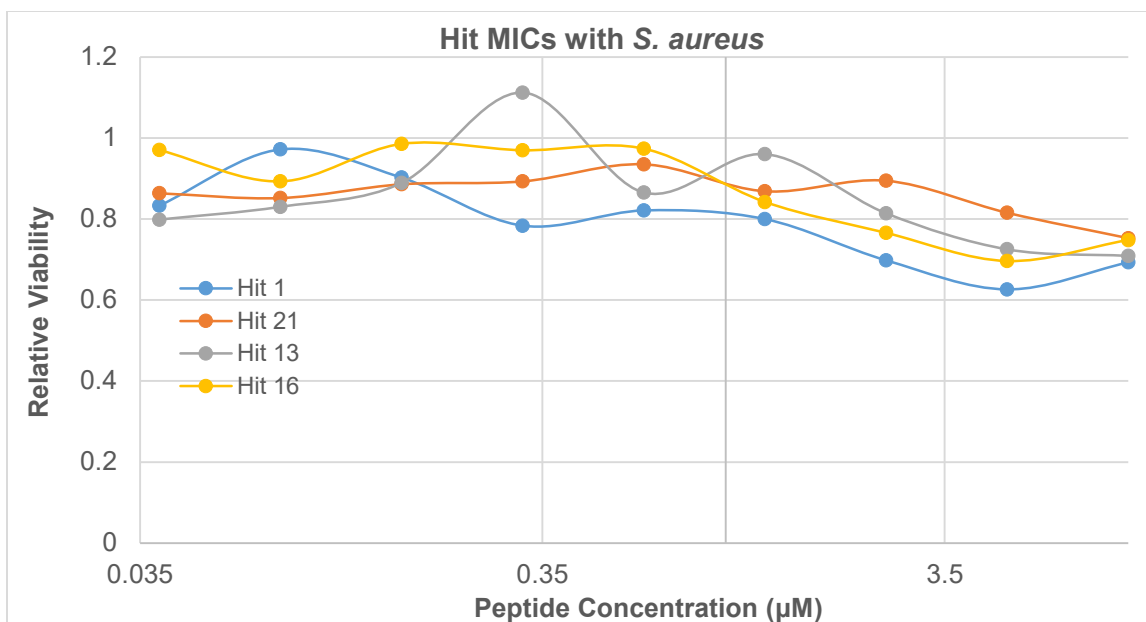


**Figure 4-29:** MIC plots for first four hits with *S. aureus*. None of the hits appear to demonstrate any growth inhibition towards the bacteria.

#### 4.5.3 Validating Hits using a UV-Vis Titration with the Target Peptide

After the lack of success in using the MIC assay, we decided to look instead at the binding potency of our hits to the target peptide, as this is what we had explicitly selected for. As fluorescence anisotropy did not appear to be the best assay to use in this case, we considered using a titration monitored by UV-vis spectroscopy. We have observed that the absorption maximum of 2-APBA shifts from 254 nm to 280 nm upon the formation of iminoboronates. As such, a titration can be used to calculate  $K_d$  of the binding between the 2-APBA moiety and an amine by plotting the change in absorbance at 280 nm with the increasing concentration of the amine (Figure 4-30) In our case, this would be the hit and target peptides, respectively.

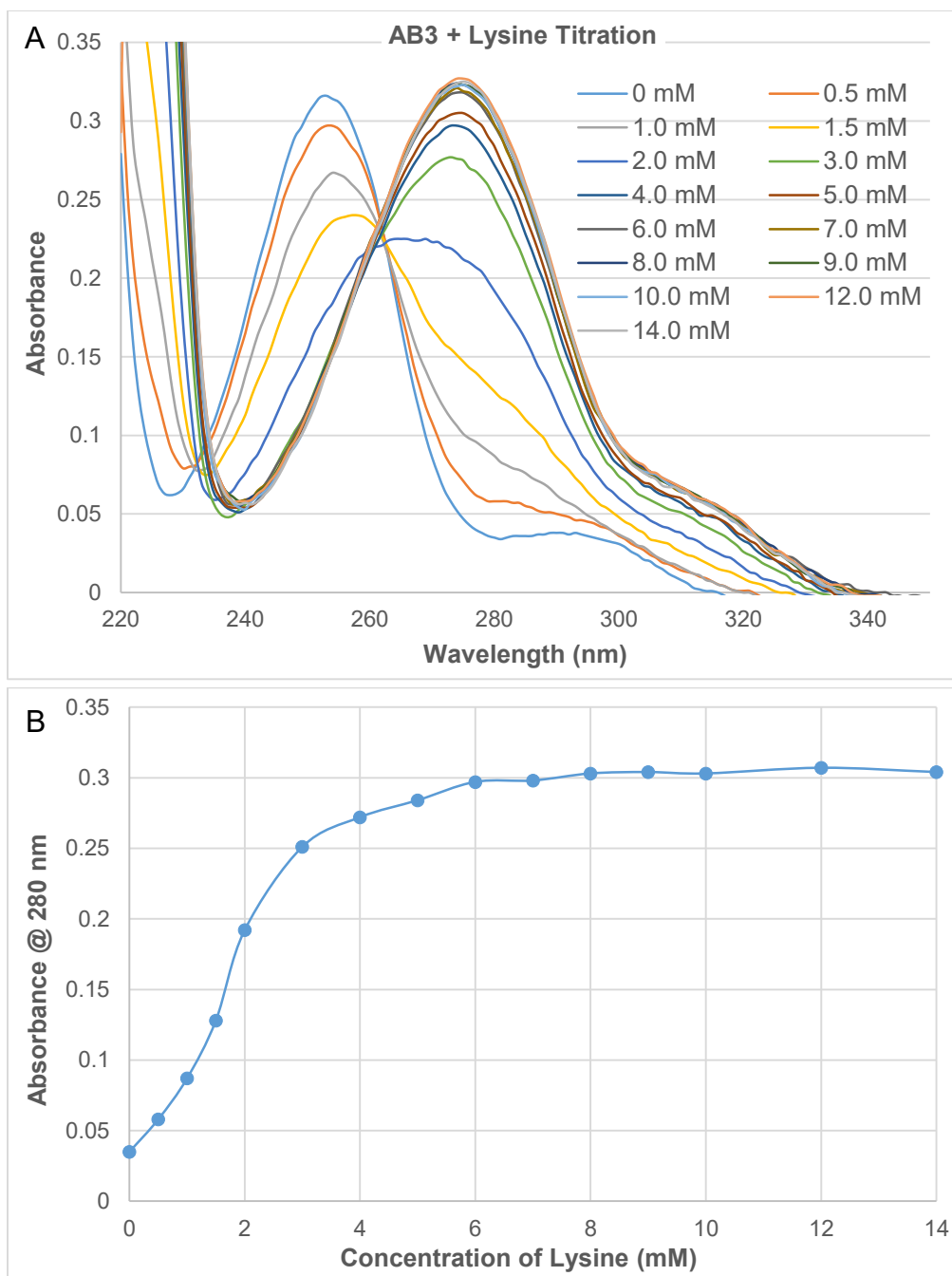


**Figure 4-30:** Titration of AB3 with lysine monitored by UV-vis absorbance. A) UV trace for changing concentration of lysine; B) Titration curve for the absorbance at 280 nm with increasing concentration of lysine.

To confirm the effectiveness of this strategy, hit peptides were first titrated with simple 2-methoxyethylamine. These titrations showed similar UV-vis profiles to that of 2-APBA with 2-methoxyethylamine with similar  $K_d$ 's (Figure 4-

31). Based on this data, we found the hit peptides sufficiently capable of iminoboronate formation with a simple amine. However, when the titrations were performed between the hit peptides and our biotin-labelled target peptide, no shift in the UV-vis spectrum appeared, even in the range of low millimolar target concentration (Figure 4-32). We found this very strange, as even if the rest of the target peptide was not contributing to binding interactions, we should observe a  $K_d$  similar to lysine alone. To confirm that the target peptide behaved as expected under these titration conditions, we titrated AB3 alone with this peptide. We saw similar results as with the hit peptides, with no significant change in the UV-vis trace (Figure 4-33A). Additionally, we estimated the  $K_d$  of 2-APBA with the target peptide to be about 14 mM by proton NMR (Figure 4-33B). As this is very close to that of 2-APBA with lysine, we expected to see a similar change in the absorbance profile during the titration of AB3 with the target, but this was not the case. We concluded that this type of titration would not be an effective way to validate our hits and considered alternative options.

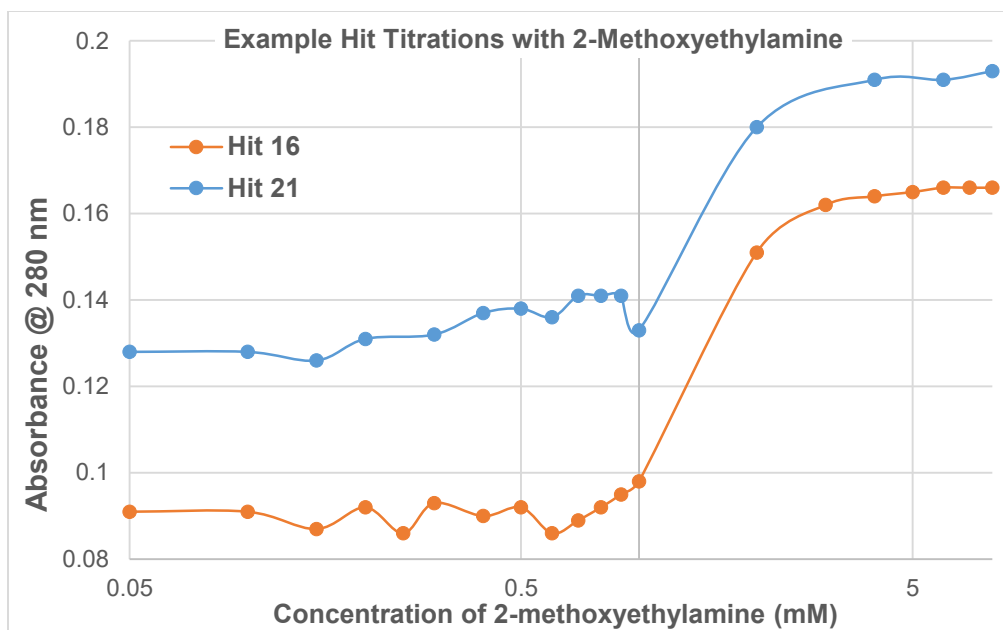


**Figure 4-31:** Example titrations of hit peptides with 2-methoxyethylamine (2-MEA). 2-MEA was used as a positive control for UV-vis titrations of the hit peptides.

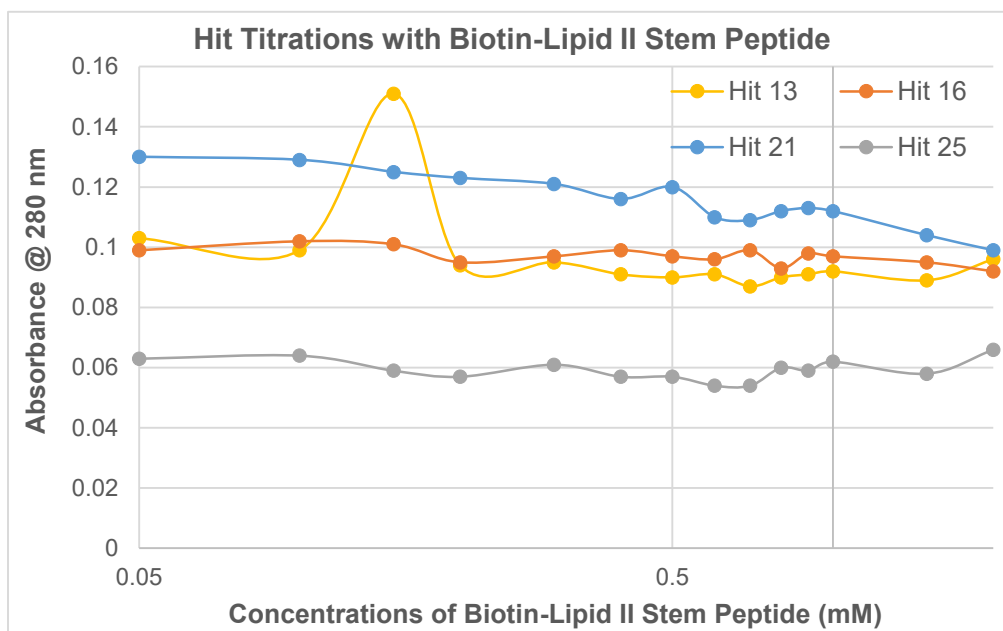


**Figure 4-32:** Titrations of hit peptides with biotin-lipid II stem peptide. Even up to 2 mM, very little change was observed. The small decrease in absorbance at 280 nm was likely an artifact of the peptides' dilutions.

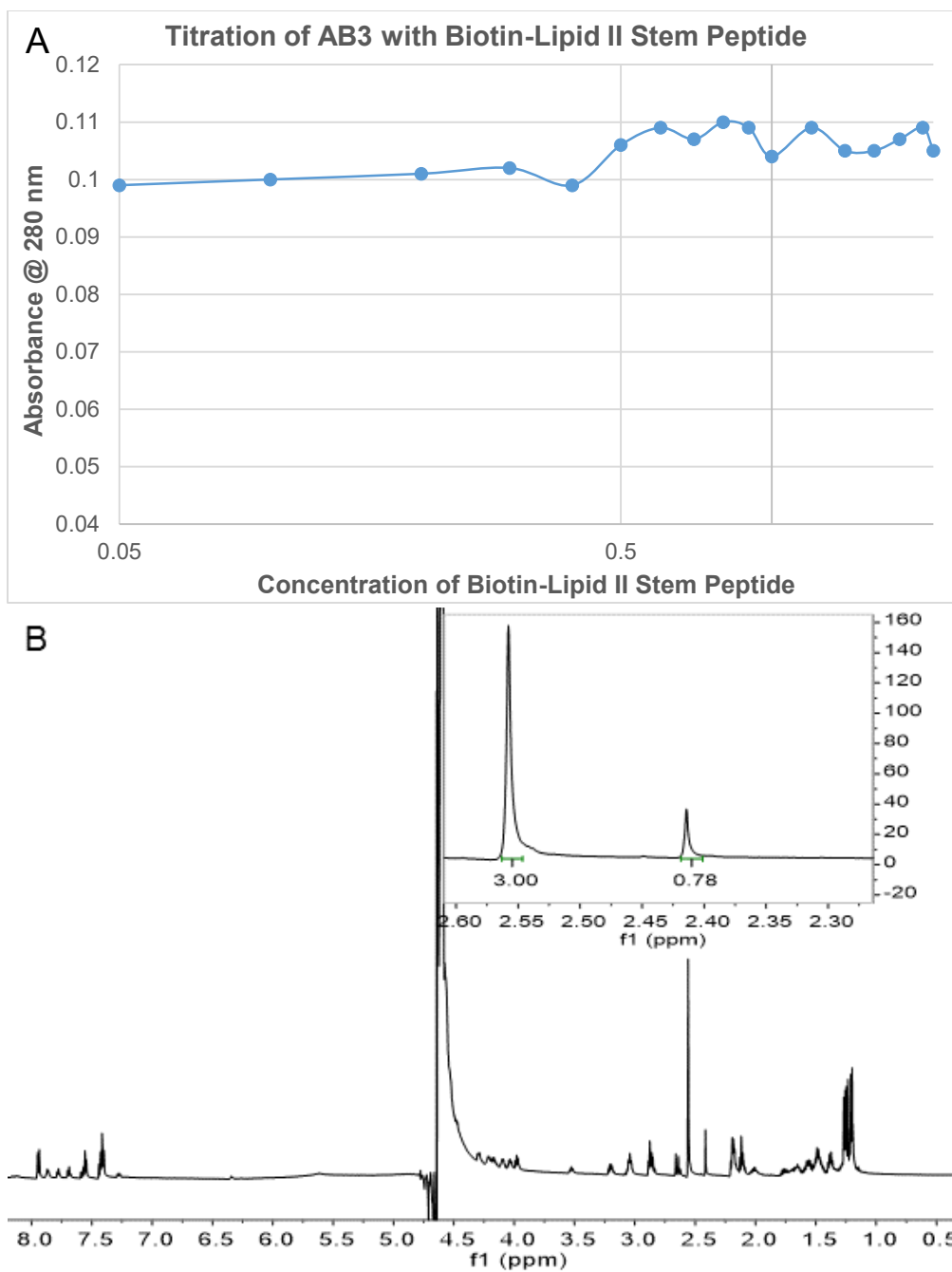


**Figure 4-33:** Titrations of AB3 with biotin-lipid II stem peptide. A) UV-vis absorbance shows no change at 280 nm, indicating no binding; B) NMR of 5 mM 2-APBA and 5 mM biotin-lipid II stem peptide in 10% D<sub>2</sub>O in PBS buffer (pH 7.4). The inset shows acetyl peaks assigned to the ketone of 2-APBA (2.56 ppm) and to the iminoboronate complex (2.42 ppm). Based on the relative integration of the acetyl peaks, the  $K_D$  is estimated to be 14 mM.

#### *4.5.4 Validating Hits using Iminoboronate Reduction*

In our last attempt to validate our hit peptides from our screen, we again sought to imitate conditions from our screen using sodium borohydride reduction. To do this, we chose to mix each hit peptide at equal concentrations with the target peptide and attempt to capture the covalent conjugate in this same way.

Each hit at 500  $\mu\text{M}$  was mixed with the target peptide at 500  $\mu\text{M}$  in PBS buffer, adjusting the pH to 7.4 as necessary. This was allowed to equilibrate at 37°C for one hour before sodium borohydride was added to a final concentration of 50 mM. The sample was analyzed by LC/MS to evaluate the degree of reduction. Unfortunately, among all the hits tested, none were observed to have any detectable conjugated product.

#### *4.5.5 Hit Validation – What May Have Gone Wrong?*

The only conclusion we were able to draw from our attempts at hit validation was that our screen was unsuccessful. Despite all the controls run before the screen to best optimize it, none of the hits collected demonstrated detectable binding. Discouraged by these results, we have speculated on several reasons that may have led our screen to not yield effective results.

One possibility for the poor hit validation considers the multivalency effect. Not an uncommon pitfall in library screening, having multiple copies of the same library molecule in close proximity can increase the apparent potency of binding.

When the hit is then dispersed in a homogenous solution, the cooperative binding potency is lost. Another possibility we have considered was that the difficulty associated with targeting a peptide prevented us from obtaining real hits, as it provides much fewer points of interactions compared to a protein. Thus, it could be that the observed hits were caused by random binding that could not be recreated in the conditions used for validation.

Additionally, it is possible our fluorescence intensity was not properly normalized. When selecting hits, it would have been better to keep the microscope settings for lamp intensity and exposure time consistent with our positive control images. Although we cannot be sure, there is the possibility that the fluorescence observed was falsely high, making selected hits appear brighter. When returning to the library resin to consider new targets, we observed a high amount of auto-fluorescence from the beads alone. This corresponded with poor quality sequencing of the resin at this time. Since we were not diligent in monitoring the change in auto-fluorescence over time, it also cannot be confirmed that this did not have a negative effect on our screen. We did learn that this auto-fluorescence is mostly limited to the FITC fluorescence channel, demonstrating that the best way to avoid this interference would be to not use a green fluorophore.

#### *4.6 Targeting Transferrin: Selective Binding to a Single Protein in a Complex Mixture*

Gaining selectivity for a single protein in a complex mixture is typically a nontrivial undertaking. Playing a very important role in pharmacokinetics and pharmacodynamics, selectivity can also be difficult to predict. However, one of the advantages of library-based ligand discovery is that it can offer avenues towards tightening selectivity. Library selections can include other relevant proteins as competitors or negative screens to remove strong binders of undesired proteins, providing a better chance at selectivity.

A relevant complex mixture of proteins can be seen in blood serum. The human plasma proteome is estimated to contain about 100,000 proteins with these spanning concentrations over 12 orders of magnitude.<sup>32</sup> The clinical relevance of these proteins is easy to see: any drug, regardless of its mode of administration, first encounters these proteins as it is transported through the blood. As such, the degree to which a drug binds to these proteins can have a high impact on its pharmacokinetics, and finding the correct balance for this is critical for a drug's clinical success. As a way to take advantage of this, much work has been done investigating serum protein binding as a method of drug delivery.

Transferrin (Tf), as one of the more abundant serum protein, has been studied for its drug carrier capabilities. Specifically, clinical trials were taken to phase III for the convection-enhanced delivery (CED) of diphtheria toxin by



linking it to Tf for the treatment of brain glioblastomas.<sup>33</sup> The complex is taken up through Tf-mediated endocytosis upon binding to the glioma cells and the toxin is cleaved after cell entry. Although it was found effective through phase I and II trials,<sup>33</sup> the clinical trial was stopped by the sponsor (Xenova Biomedix) during phase III in the anticipation that the study's endpoints would not be reached.<sup>32</sup> Nonetheless, this study demonstrated the potential for Tf-based drug delivery.

With the advantages of reversible covalent binding included in our platform, drug delivery via Tf binding could be achieved without the need for *ex vivo* formulation of the protein-drug conjugate. Additionally, having a small peptide drug, rather than a large protein, can increase the number of possible administration methods. Finally, a lower immune response can be expected from the treatment if the endogenous Tf is used instead.

Toward this end, we sought to perform screening of our library against Tf. By performing our screen in the presence of relevant concentrations of human serum albumin (HSA), the most abundant protein in the blood, we expected to find a selective binder for Tf.

#### *4.6.1 Designing a Screen for Transferrin*

To design our screen, we first investigated the availability of modified Tf protein. We found that there were many possible modifications available, including biotinylated and fluorescent proteins. Unfortunately, there did not appear to be any commercially available protein with both a biotin handle and a

fluorescent tag, causing us to reconsider our previous screening scheme. With the fluorescence microscopy screen being more sensitive and less prone to false positives, we decided on using a fluorescently labelled Tf for our screen. Specifically, we purchased rhodamine-labelled Tf; we chose to switch from fluorescein to rhodamine after observing some degree of Tentagel auto-fluorescence in the FITC channel. In contrast, library beads visualized in the rhodamine channel were nearly undetectable.

To favor Tf-selective hits, we chose to include HSA in the screening matrix. We chose only to include HSA instead of screening all serum proteins as it is the most abundant and, therefore, the most likely protein to interfere with selective binding in the blood. Using the rhodamine-Tf at a concentration of 0.08 mg/mL, we included HSA at a concentration of 1.6 mg/mL, as it is typically observed at concentrations 10-20 times higher than that of Tf in serum samples.

#### *4.6.2 Screen and Hit Selection for Transferrin Binding Cyclic Peptides*

In order to examine non-specific binding, we examined the blank Tentagel resin within the same conditions of our screen. We observed very little non-specific fluorescence on the beads, even without any washing (Figure 4-34). With this, we were confident that beads with better binding would have an increased fluorescence when looking under the fluorescence microscope.

After equilibrating 50 mg of the library resin in PBS buffer (pH 7.4) overnight, it was washed three times with PBS buffer then suspended in PBS

buffer with 1.6 mg/mL HSA (2.3 mL). To this, a 1 mg/mL stock of rhodamine-Tf (200  $\mu$ L) was added. The library was allowed to incubate with the protein at 37°C while rotating for one hour. Sodium borohydride was added to a final concentration of 50 mM and the reduction was allowed to occur for 15 min. The library was then washed four times with PBS buffer (pH 7.4), once with PBS buffer (pH 5) and one final time with PBS buffer (pH 7.4). Microscopy images of the library resin after screening can be seen in Figure 4-35.

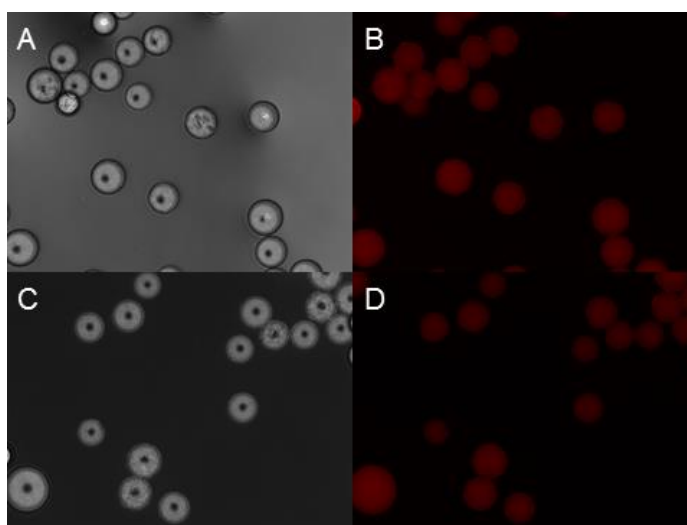


**Figure 4-34:** Microscopy images of blank Tentagel resin under the rhodamine-Tf screening conditions. A) White light and B) rhodamine channel images without any washes. C) White light and D) rhodamine channel images of resin after complete washing protocol for screen.

#### 4.6.3 Sequencing and Analysis of Hits from Screening Transferrin

A total of 21 hits were collected and provided to Aaron for sequencing. Of these, 18 yielded sequences with confident data (Table 4-4). In contrast to our sequencing data for the lipid II stem peptide screen, a few different common

patterns were observed amongst these sequences. This included a tyrosine repeat and an RYY sequence, which were observed in five and two of hits, respectively.

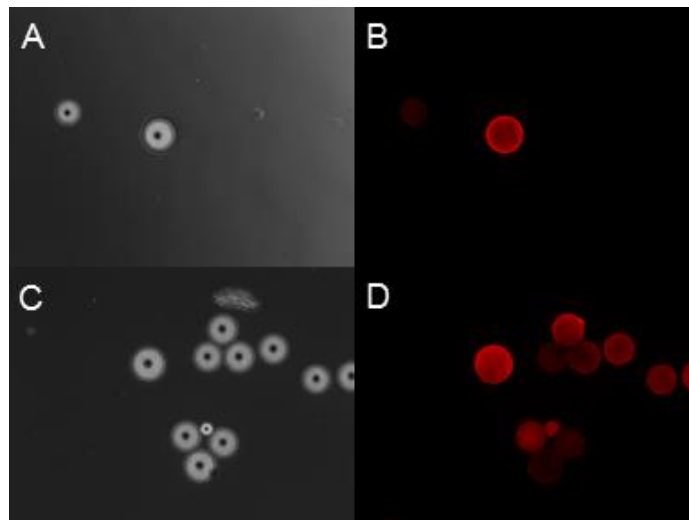


**Figure 4-35:** Microscopy images of library resin under the rhodamine-Tf screening conditions after reduction. A&C) White light; B&D) rhodamine channel images.

*Table 4-4: Hits from Library Screening of Transferrin*

Sample	Sequence	Picked for Validation	Sample	Sequence	Picked for Validation
1	RYYHRH	√	12	YRIDQP	X
2	IYYPRY	√	13	N/A	X
3	HIRRQY	X	14	RYQQRY	√
4	RHQIIH	√	15	DYYRYP	X
5	QIRHDH	√	16	PHRDYI	X
6	DHDYYI	√	17	HIYQHY	X
7	N/A	X	18	YDRHRY	√
8	YPHYRD	X	19	RDYRHY	X
9	N/A	X	20	RHRRYR	√
10	IYHQDY	√	21	RHPRQY	√
11	HDYYRH	√			

#### 4.6.4 Hit Validation for Transferrin

Initially encouraged by the YY repeats, we chose to synthesize the first two hits for validation, which were also two of the brightest beads observed during screening. As it had somewhat contrasting qualities to hits 1 and 2, we also chose hit 10 for validation. All three peptides were synthesized using standard Fmoc-based SPPS on Rink amide resin. The N-terminus was labelled on resin using carboxyfluorescein, providing a fluorophore necessary for validation using fluorescence anisotropy. The peptides were then cleaved with a modified Reagent K (80% TFA, 7.5% w/v phenol, 5% water, 5% thioanisole and 2.5% triisopropylsilane) and purified by RP-HPLC. The final purity was confirmed by LC/MS analysis to be >90%. The purified peptides were cyclized using DMSO-mediated air oxidation to provide the final peptide structure, monitoring for complete oxidation by LC/MS.

For validation using fluorescence anisotropy, we studied each peptide at a concentration of 200 nM with varying concentrations from 0-10 mg/mL of human Tf. In this experiment, carboxyfluorescein was used a negative control (Figure 4-39), to distinguish any non-specific binding as a result of the fluorophore. From this data, it would appear that Hit 1 (Figure 4-36) and 10 (Figure 4-38) bind well to Tf while Hit 2 (Figure 4-37) performed worse than fluorescein alone, indicating very little to no binding. We can make a preliminary conclusion that Hit 1 has the

best binding to Tf with an estimated  $K_d$  of 2-2.5 mg/mL (25-30  $\mu$ M). This is significant, as the serum concentration range of Tf is 2.5-3.5 mg/mL.<sup>32</sup>

The hits were also studied with human serum albumin (HSA) to demonstrate their degree of selectivity for transferrin. We were happy to see that Hit 1 (Figure 4-36) showed nearly zero binding to HSA compared to fluorescein alone. Comparatively, Hit 10 had more significant binding to HSA (Figure 4-38), although it is still very low. Hit 2 appeared to have better binding to HSA than Tf (Figure 4-37), suggesting it may have been in a false positive from our screen. Overall, we concluded that Hit 1 and 10 both had preferential binding to Tf, with Hit 1 performing slightly better. Our current and future plans include determining

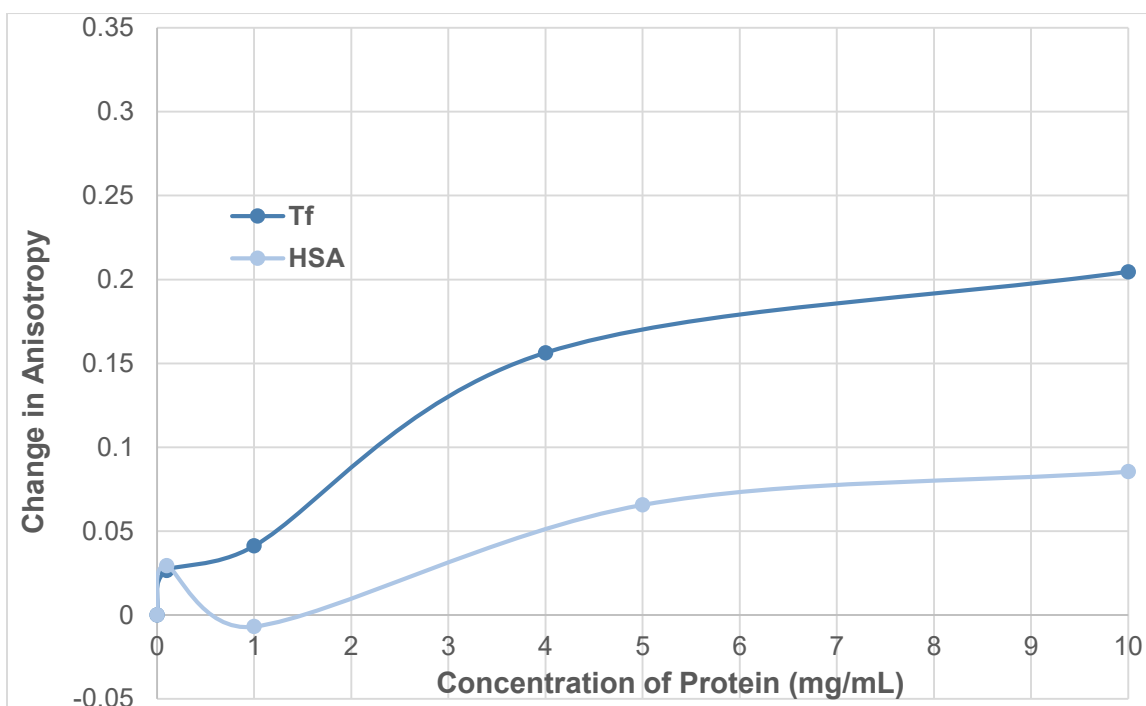


**Figure 4-36:** Hit 1 validation by fluorescence anisotropy with Tf and HSA. Hit 1 was studied at 200 nM with various concentrations of each protein. Points represent averages of triplicate samples.

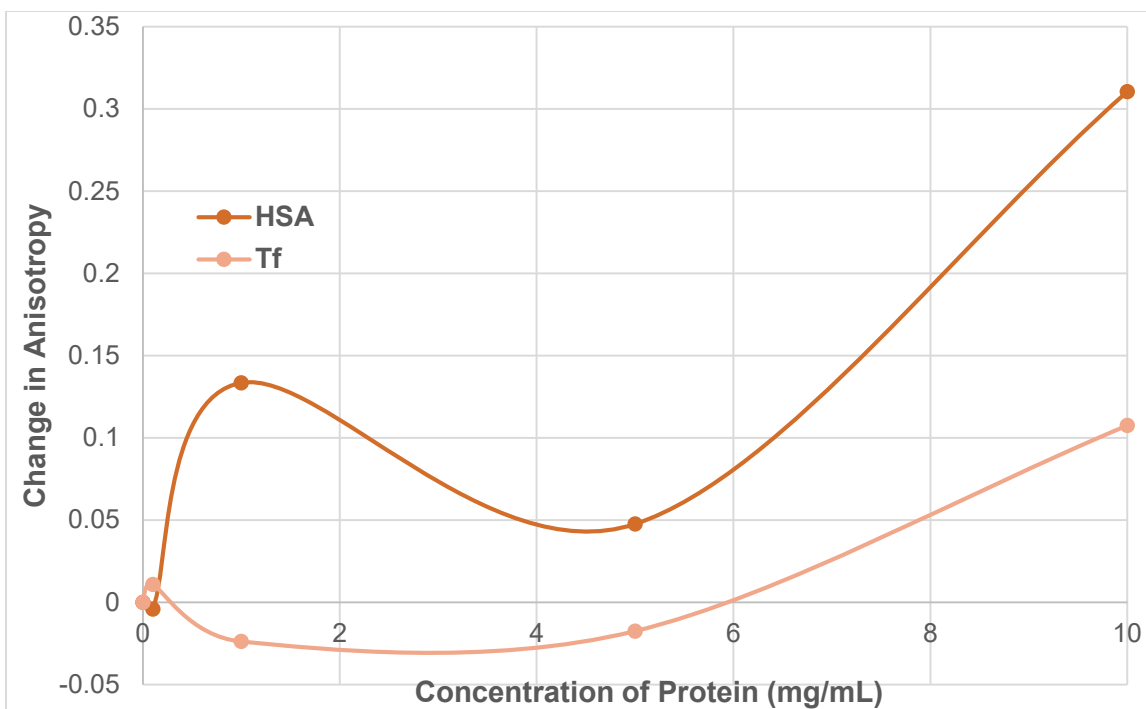


**Figure 4-37:** Hit 2 validation by fluorescence anisotropy with Tf and HSA. Hit 2 was studied at 200 nM with various concentrations of each protein. Points represent averages of triplicate samples.

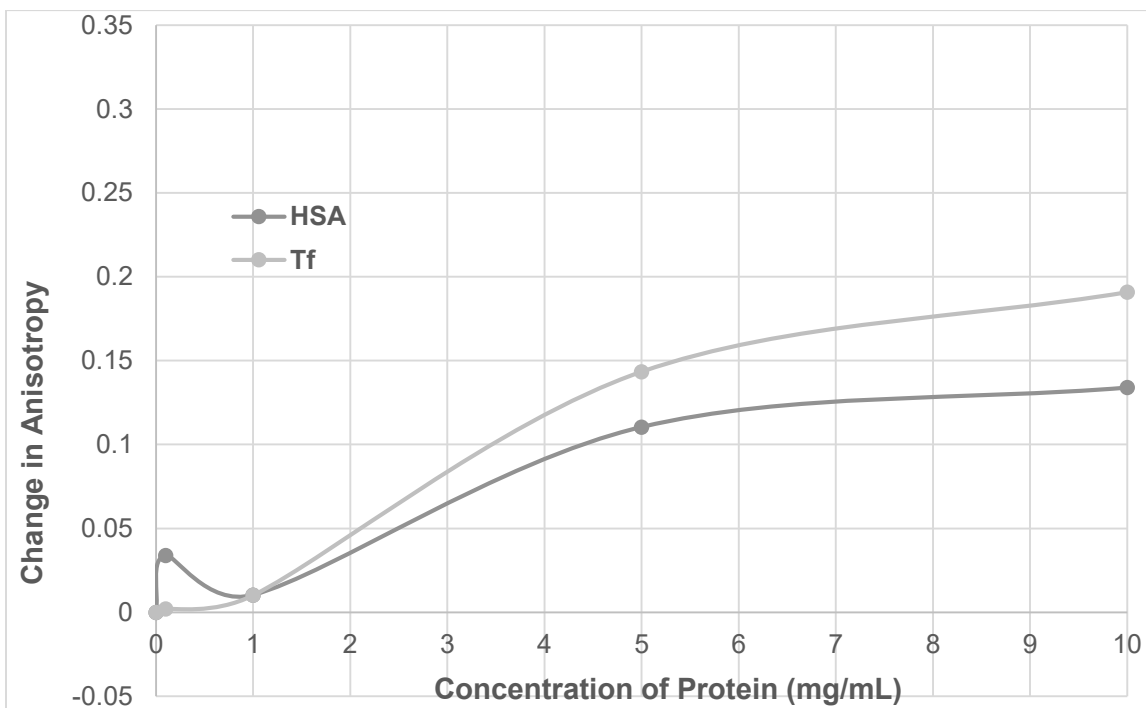


**Figure 4-38:** Hit 10 validation by fluorescence anisotropy with Tf and HSA. Hit 10 was studied at 200 nM with various concentrations of each protein. Points represent averages of triplicate samples.

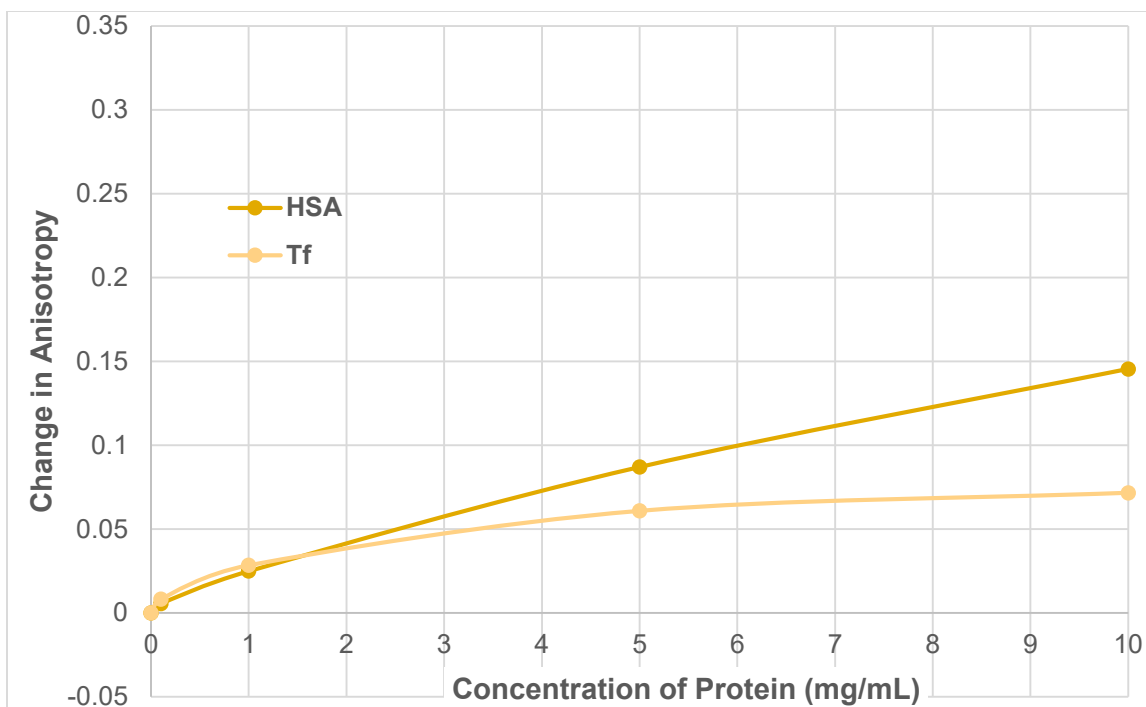


**Figure 4-39:** Fluorescein control for hit validation by fluorescence anisotropy with Tf and HSA. Fluorescein was studied at 200 nM with various concentrations of each protein. Points represent averages of triplicate samples.

dependence of this selective binding on the iminoboronate interaction and compare the binding of selected hits to that of other random sequences from the library.

#### **4.7 Conclusions and Future Work**

In this work, we have demonstrated the utility of a cyclic library containing a 2-APBA warhead for the discovery of selective protein binders. We have established a confident sequencing technique for OBTC libraries using LC/MS/MS analysis with Aaron J. Mauris in the Weerapana lab, which can easily be transferred for use with other poorly behaving unnatural amino acids. Although we were unsuccessful in identifying binders to the lipid II stem peptide,



our screen with transferrin demonstrated our ability to pullout selective binders in a physiologically relevant complex mixture.

Potent binding to Tf offers many potential applications beyond simply a proof-of-concept experiment. This includes drug delivery and antimicrobial applications. Transferrin is already well documented for its use in drug-protein fusion products for drug delivery, but this requires *ex vivo* production of the fusion before administration of the drug. With our reversible covalent binding, one could imagine a drug of interest could be conjugated to one of our peptides instead for binding to natural Tf in the patient's blood.

Several bacterial species, including *Neisseriaceae meningitides* and *N. gonorrhoeae*, contain membrane bound transferrin binding proteins (Tbp). TbpA and TbpB bind host Tf and function together to extract iron;<sup>34,35</sup> both have been found necessary to the bacteria for colonization and infection of their host. If our peptides are observed to bind in the same location as TbpA or TbpB, they could be used as an indirect treatment for these infections. Targeting the host rather than the bacterial protein could be imagined to illicit lower degrees of resistance, as the bacterium is not being directly engaged by the drug. However, for such an application, it would be critical to be demonstrate that the peptide drug is occupying the same binding location as these proteins.

For future work, we plan to further validate hits of our Tf screen. This includes synthesizing and studying more hit sequences as well as demonstrating the role of iminoboronate formation in the protein binding.

## **4.8 Experimental Procedures**

### *4.8.1 General Materials and Methods*

All Fmoc-protected amino acids and Rink amide resin were purchased from either Advanced Chemtech (Louisville, KY) or Chem Impex Int. Inc. (Wood Dale, IL). Tentagel S NH<sub>2</sub> resin was purchased from Peptides International (Louisville, KY). DNA oligomers were purchased from Integrated DNA Technologies (Coralville, IA) and sequencing was performed by Eton Bioscience, Inc. (Charlestown, MA). Other chemicals were obtained from Sigma-Aldrich or Fisher Scientific unless otherwise indicated. Peptide synthesis was carried out on a Tribute peptide synthesizer (Protein Technologies, Tucson, AZ). <sup>1</sup>H NMR data were collected on a VNMRs 500 MHz or 600MHz NMR spectrometer, as indicated. Mass spectrometry data were generated by using an Agilent 6230 LC TOF mass spectrometer. The peptide concentration of all hit peptide samples used in this study was determined by measuring their absorbance at 254 nm ( $\epsilon = 6,960 \text{ M}^{-1}\text{cm}^{-1}$  for AB3) on a Nanodrop 2000c UV/Vis spectrometer by cuvette. Gram-positive *Staphylococcus aureus* (ATCC 6538) was purchased as lyophilized cell pellet from Microbiologics (Cloud, MN).

#### 4.8.2 Preparation of Tentagel Resin for Library Synthesis (Tentagel-Gly Resin)

Tentagel resin (357 mg, 0.100 mmol) was swelled in DMF (3.0 mL) for two hours then washed with DMF (3 x 3.0 mL). Fmoc-glycine (0.500 mmol, 148.6 mg), HOBt (0.500 mmol, 67.6 mg) and HATU (0.500 mmol, 190.1 mg) was dissolved 0.4 M NMM in DMF (3.0 mL) then added to the resin. The resin was mixed for two hours then washed with DMF (6 x 3.0 mL) and DCM (3 x 3.0 mL). The resin was fully dried before determining the loading via Fmoc cleavage. When preparing the library, if the loading was below 0.220 mmol/g, the procedure was repeated. The resin was then swelled again for two hours and mixed with acetyl capping reagents (1.0 mL DMF, 500  $\mu$ L DIPEA, 600  $\mu$ L acetic anhydride) for 1 hour then washed with DMF (6 x 3.0 mL) before use in peptide synthesis.

#### 4.8.3 Preparation of Peptide for On-Resin DNA Ligation

Tentagel-gly resin (98.5 mg, 0.203 mmol/g, 0.020 mmol) was swelled in DMF (2.0 mL) for 1.5 hours on the synthesizer. To this was coupled Fmoc-Gly (0.100 mmol, 29.73 mg + 0.090 mmol HBTU, 34.13 mg - 30 min), Fmoc Photolabile linker (0.060 mmol, 31.23 mg + 0.055 mmol HBTU, 20.86 mg - 90 min), Fmoc-Propargylglycine (0.060 mmol, 20.12 mg + 0.055 mmol HBTU, 20.86 mg - 90 min), Fmoc-Dap(Boc) (0.060 mmol, 25.59 mg + 0.055 mmol HBTU, 20.86 mg - 90 min) and Fmoc-Trp(boc) (0.100 mmol, 52.66 mg + 0.090 mmol HBTU, 34.13 mg - 30 min). The resin was washed with DCM (6 x 2.0 mL) then dried. A small portion of the resin was analyzed by LC/MS. This showed two major products, including the desired

peptide and a propargylglycine deletion. As so few equivalents are used for the azide-DNA headpiece in the click reaction, the amount of full peptide observed was deemed sufficient and the peptide was not remade for test reactions. When preparing for test peptide synthesis and simultaneous DNA ligation, the peptide was remade using 0.100 mmol Fmoc-Pra and 0.100 mmol Fmoc-Dap(Boc) to increase the amount of the full length peptide.

#### *4.8.4 Click Reaction for the Attachment of DNA Headpiece<sup>26</sup>*

The prepared resin (5 mg) was soaked in click reaction buffer (CRB, 50% DMSO, 30 mM triethylammonium acetate (TEAA), 0.04% Tween 20, pH 7.5) (120  $\mu$ L) for two hours. It was then washed with CRB (2 x 120  $\mu$ L) then suspended in CRB (170  $\mu$ L). A prepared solution of Cu(II) sulfate (6.3 mM) and ascorbic acid (0.3 M) in 66% DMSO in H<sub>2</sub>O was added to the resin (17.1  $\mu$ L) along with Tris[(1-benzyl-1H-1,2,3-triazol-(4-yl)-methyl)amine (2 nmol). This was incubated for 5 min at 40°C. The resin was centrifuged for 30 sec at 1000 rcf. A stock of N<sub>3</sub>-HDNA (1 mM in DMSO, 4  $\mu$ L) was diluted in a 200 mM triethyl ammonium acetate buffer + 2mM ascorbic acid (3.7  $\mu$ L). This solution was added to the resin and immediately mixed via vortexing then incubated while stirring (4 hours, 40°C). After incubation, the resin was centrifuged again and the supernatant was removed. The resin was washed with Bis-Tris propane breaking buffer (BTPBB, 100 mM NaCl, 10 mM EDTA, 1% SDS, 1% Tween 20, 10 mM Bis-Tris, pH 7.6) (3 x 120  $\mu$ L). The resin was then incubated in BTPBB (120  $\mu$ L, overnight, RT) then washed with Bis-Tris

propane wash buffer (BTPWB, 50 mM NaCl, 0.04% Tween 20, 10 mM Bis-Tris, pH 7.6) (3 x 120  $\mu$ L), DI water (3 x 120  $\mu$ L) and DMF (3 x 120  $\mu$ L). The resin was stored in a solution of DMF at -20°C.

#### 4.8.5 DNA Ligation to Resin<sup>26</sup>

Top and bottom strands of each encoding oligomer were prepared as 120  $\mu$ M stocks in 50 mM NaCl, 1 mM Bis-Tris, pH 7.6. Prior to use in ligation to resin, the corresponding strands (50  $\mu$ L each) were mixed, heated at 60°C for 5 min then allow to cool to RT for 5 min to anneal the two strands together. To prepare the resin for DNA ligation, it was first washed with 50:50 DMF/H<sub>2</sub>O (1 x 3.75 mL) followed by BTPWB (4 x 3.75 mL). After the final wash, the resin was incubated with shaking (30 min, RT, 700 rpm) then washed with Bis-Tris propane ligation buffer (BTPLB, 50 mM NaCl, 10 mM MgCl<sub>2</sub>, 1 mM ATP, 0.02% Tween 20, 10 mM Bis-Tris, pH 7.6) (1 x 3.75 mL). The oligomer sequences can be seen in Table 4-5. For encoding step 1, the resin was washed with BTPWB (3 x 600  $\mu$ L) then rotated for 1 hour at RT. After rotation, the resin was washed with Bis-tris propane ligation buffer (BTPLB, 500 mM NaCl, 100 mM MgCl<sub>2</sub>, 10 mM ATP, 0.2% Tween 20, 100 mM Bis-tris, pH 7.6) (1 x 600  $\mu$ L) and left in a minimal amount of solvent. To resin, 720U of T4 ligase (1.8  $\mu$ L), 10xBTPLB (60  $\mu$ L), the front primer duplex ( $\approx$ 0001[ $\pm$ ]) and coding sequence 1 duplex ( $\approx$ 1101[ $\pm$ ]) were added and diluted to 600  $\mu$ L with DI water. The solution was rotated at room temperature overnight then washed with BTPWB (3 x 600  $\mu$ L), methanol (1 x 600  $\mu$ L) and DMF (2 x 600  $\mu$ L). This was

then rotated at 37°C for 2 hours. For encoding steps 2-5, resin was washed with BTPLB (1 x 600 µL). To the resin the corresponding DNA duplex solution (100 µL), T4 ligase (0.9 µL), 10XBTPLB (60 µL) and DI water (439 µL) were added and the solution was rotated for 3 hours at RT. For the final encoding step, the resin was washed with BTPLB (1 x 600 µL). To this coding sequence 6 ( $\approx 2603[\pm]$ ) (100 µL), end primer ( $\approx 0701[\pm]$ ) (100 µL), 10XBTPLB (60 µL), T4 ligase (1.8 µL) and DI water (338 µL) were added. The solution was rotated for 4 hours at RT then washed with BTPWB (3 x 600 µL), methanol (1 x 600 µL) and DMF (3 x 600 µL). The resin was stored as a solution in DMF at -20°C.

**Table 4-5: Sequences of Oligomers for DNA-Encoded Library**

<b>Identifier #</b>	<b>Sequence</b>
Headpiece	/5Phos/GAGTCA/iSp9//iAzideN//iSp9/TGACTCCC
$\approx 0001[+]$	/5Phos/GCCGCCAGTCCTGCTCGCTTCGCTAC
$\approx 0001[-]$	/5Phos/CCATGTAGCGAAGCGAGCAGGACTGGGCGGCGG
$\approx 1101[+]$	/5Phos/ATGGAAGAGAGG
$\approx 1101[-]$	/5Phos/TGACCTCTCTT
$\approx 2201[+]$	/5Phos/TCAAGTTTCAG
$\approx 2201[-]$	/5Phos/AACCTGAAACT
$\approx 1302[+]$	/5Phos/GTTACGGAGCA
$\approx 1302[-]$	/5Phos/TAGTGCTCCGT
$\approx 2402[+]$	/5Phos/CTAAACCTCAA
$\approx 2402[-]$	/5Phos/GAATTGAGGTT
$\approx 1503[+]$	/5Phos/TTCACAAAGAG
$\approx 1503[-]$	/5Phos/GCGCTCTTTGT
$\approx 2603[+]$	/5Phos/CGCAATCCCAT
$\approx 2603[-]$	/5Phos/AGGCATGGGATT
$\approx 0701[+]$	/5Phos/GCCTGTTTGCCCGCCAGTTGTTGTGCCAC
$\approx 0701[-]$	/5AmMC6/GTGGCACAACAACCTGGCGGGCAAAC
<b>Overhangs are shown in italics; [+]</b> - top strand, <b>[-]</b> - bottom strand	

#### 4.8.6 Simultaneous Peptide Synthesis and DNA Ligation

The prepared resin with clicked DNA headpiece (5.2 mg) was washed with DMF (3 x 120  $\mu$ L). The terminal Fmoc was removed with 20% piperidine in DMF (2 x 120  $\mu$ L, 5 min) then washed with DMF (6 x 120  $\mu$ L) and BTPWB (3 x 600  $\mu$ L). This was rotated in BTPWB (600  $\mu$ L) for 1 hour then washed with BTPWB (1 x 600  $\mu$ L) and BTPLB (1 x 600  $\mu$ L). The first ligation step was then performed in the same way as above. After ligation, the resin was washed with BTPWB (3 x 600  $\mu$ L), methanol (3 x 600  $\mu$ L) and DMF (3 x 600  $\mu$ L) then rotated in DMF for 2 hours at 37°C. The DMF was removed and a solution of Fmoc-Arg(Pbf) (0.0200 mmol, 12.98 mg) and HBTU (0.0195 mmol, 7.40 mg) in 0.4M NMM in DMF (120  $\mu$ L) was added. This was rotated for 30 min then washed with DMF (6 x 120  $\mu$ L). This alternating Fmoc deprotection, DNA ligation and amino acid coupling was repeated for two more steps, leading to residue 5 in the sequence. After the coupling of Fmoc-Arg(pbf), the resin was maintained in DMF for the coupling of Fmoc-Dap(boc), Fmoc-Gly and Fmoc-AB3(pin). After the Fmoc deprotection of AB3, the resin was washed with DMF (6 x 200  $\mu$ L) and BTPWB (3 x 600  $\mu$ L) then rotated in BTPWB (600  $\mu$ L) for one hour. At this point, the alternating DNA ligation and amino acid coupling procedure was continued for the last two encoding sequences and the end primer. After the final ligation, the resin was washed with BTPWB (3 x 600  $\mu$ L), methanol (3 x 600  $\mu$ L) and DMF (3 x 200  $\mu$ L) then rotated in DMF (200  $\mu$ L) overnight. The final two residues (Fmoc-Trp(boc) and Fmoc-AB3(pin)) were

coupled to the resin. After the final Fmoc deprotection, the resin was treated with Reagent K (200  $\mu$ L) for one hour. At this point, the resin was split in half. One half of the resin was treated with NaCNBH<sub>3</sub> (25 mM in 10xPBS, 120  $\mu$ L) for 5 min then washed with 1XPBS (6 x 200  $\mu$ L). Samples from both halves were analyzed by single bead PCR and PAGE to determine the success of the DNA ligation and by LC/MS after photocleavage to determine the success of peptide synthesis.

#### *4.8.7 PCR Analysis of DNA Tag*

For single bead samples, one bead was selected under the microscope into a PCR tube and suspended in water (5  $\mu$ L). To each sample 10xStandard Taq reaction buffer (2  $\mu$ L), dNTP stocks (10 mM, 0.4  $\mu$ L), Taq enzyme (0.2  $\mu$ L), primer 1 and primer 2 (10  $\mu$ M stock, 0.6  $\mu$ L for each primer) were added then diluted to 20  $\mu$ L with 10% DMSO, 1.23M betaine in water. To prepare DNA for sequencing, PCR samples were prepared with purified excised DNA (2  $\mu$ L), 10xStandard Taq reaction buffer (5  $\mu$ L), dNTP stocks (10 mM, 1.0  $\mu$ L), Taq enzyme (0.5  $\mu$ L), sequencing primer (0.5  $\mu$ L), primer 2 (1.4  $\mu$ L) and primer 3 (1.5  $\mu$ L) were mixed together then diluted to 50  $\mu$ L with 10% DMSO, 1.23M betaine in water. Primer sequences can be seen in table 4-6. Thermocycling conditions can be seen in Table 4-7. PCR reaction mixtures were purified using denaturing PAGE (8% 19:1 polyacrylamide:bis, 8 M urea in 1XTBE) The gel was stained using 0.5  $\mu$ g/mL ethidium bromide in 1XTBE. For sequencing samples, PCR reactions were run



through a PCR clean up and submitted to Eton Bioscience, Inc. at concentration of 10-20 ng/ $\mu$ L (20  $\mu$ L samples). Sequencing was done using primer M13F(-40).

**Table 4-6: Sequences of PCR Primers**

Identifier #	Sequence
Primer 1	5'-GCCGCCAGTCCTGCTCGCTTCGCTAC-3'
Primer 2	5'-GTGGCACAACAACCTGGCGGCCAAAC-3'
Primer 3	5'-GTTTCCCAAGTCACGAC-3'
Sequencing Primer	5'-CGCCAGGTTTTCCAGTCACGACCAACCACCCAAACCACAAA CCCAAACCCCAAACCCAACACACAACAACAGCCGCCAGTCCT GCTCGCTTCGCTAC-3'

**Table 4-7: Thermocycling Conditions for PCR**

Step	Temperature	Time
1	95°C	30 sec
2	95°C	20 sec
3	52°C	15 sec
4	72°C	20 sec
5	68°C	5 min
6	4°C	Hold
<b>Steps 2-5 repeated for 30 cycles</b>		

#### 4.8.8 DNA Extraction from Gel

Single bead PCR products were excised from the gel and corresponding pieces were mixed with acrylamide gel elution buffer (0.5 M ammonium acetate, 10 mM magnesium acetate tetrahydrate, 1 mM EDTA and 0.1% w/v SDS) (2xvolume of gel piece). The samples were incubated at 37°C while shaking overnight then centrifuged (14,000 rpm, 1 min, 4°C). The supernatant was removed and put into a fresh microcentrifuge tube. The gel pieces were washed with acrylamide gel elution buffer (25% volume of original solution), centrifuged and the supernatant was combined with that of the first step. The DNA was extracted from this solution

by adding an equal volume of 1:1 v/v phenol/chloroform solution, centrifuging (14,000 rpm, 1 min, 4°C) and removing the top aqueous layer. This was then washed with an equal volume of chloroform. The DNA was precipitated from the aqueous layer by adding 200 proof ethanol (2xvolume of sample) and keeping on ice for 30 min. The sample was centrifuged (14,000 rpm, 15 min, 4°C), the supernatant was removed and the pellet was dissolved in TE buffer (pH 8.0). This was precipitated a second time and dissolved in water. Concentration of samples were determined by NanoDrop and the final sample was stored at 4°C.

#### *4.8.9 UV Cleavage of Peptides from Tentagel Resin*

Resin was suspended in HPLC-grade methanol (20 µL/bead) and irradiated with UV light (365 nm) for one hour. Before LC/MS analysis, the methanol was removed by evaporation and the sample was dissolved in buffer A.

#### *4.8.10 Peptide Library Preparation*

Tentagel-gly resin (800 mg, 0.197 mmol) was swelled for 2 hours in DMF (8.0 mL) then washed with DMF (3 x 8.0 mL). To this, Fmoc-Gly (0.984 mmol, 292.55 mg + HBTU, 0.886 mmol, 335.86 mg), Fmoc-Photolabile linker (0.984 mmol, 512.20 mg + HBTU, 0.886 mmol, 335.86 mg) and Fmoc-Cys(trt) (0.984 mmol, 576.34 mg + HBTU, 0.886 mmol, 335.86) were coupled. The resin was then split into seven fractions. Amounts of each amino acid can be found in Table 4- . The amino acids were dissolved in 1.5 mL and each was added to a separate fraction of resin. After 1 hour of stirring, the resin was recombined, Fmoc deprotected then split again.

This was repeated for a total of three amino acids. After Fmoc deprotection of the third amino acid, the combined resin was washed with DMF (3 x 8.0 mL), 3:1 DMF/water (3 x 8.0 mL), 1:1 DMF/water (3 x 8.0 mL), 1:3 DMF/water (3 x 8.0 mL) and water (3 x 8.0 mL). The resin was stirred in water overnight and excess solvent was removed. To the resin, a solution of Fmoc-AB3(pin) (0.197 mmol, 109.42 mg), DIC (0.197 mmol, 31  $\mu$ L) in 1:1 DCM/Et<sub>2</sub>O (8.0 mL) was added. This was mixed for 1 hour, then washed with DCM (3 x 8.0 mL) and DMF (6 x 8.0 mL). Fmoc deprotection was performed and the split-and-pool procedure was carried on for three additional residues. After the final split, Fmoc-Cys(trt) (0.984 mmol, 576.34 mg + HBTU, 0.886 mmol, 335.86) was coupled. The resin was stored at -20°C as the fully protected peptides until needed for screening. Library resin was freshly prepared from this stock before the screen. To prepare the library for screening, a portion of resin (350 mg) was Fmoc deprotected (3 x 3.0 mL, 5 min), acetyl capped (1.0 mL DMF, 600  $\mu$ L DIPEA, 500  $\mu$ L acetic anhydride), side chain deprotected (4 x 5.0 mL 10% water in TFA, 1 hour) and cyclized (15 mM N-chlorosuccinimide in DMF, 5.0 mL for 15 min).

#### *4.8.11 Synthesis of Dual-labelled Target Peptide*

The peptide was prepared using Fmoc-based SPPS with Fmoc-D-Ala Wang resin. To install the fluorescein, Fmoc-Lys(alloc) was added to the end of the sequence. After installation of 6-(Fmoc-amino)caproic acid and biotin, the alloc deprotection was performed with on resin (0.01 mmol) using phenylsilane (120  $\mu$ L) and Pd-

tetrakis (22 mg) in DCM (680  $\mu$ L). 5(6)-Carboxyfluorescein (0.050 mmol, 18.82 mg + HBTU, 0.045 mmol, 17.07 mg) was coupled to the free lysine side chain. The peptide was cleaved from resin using Reagent K then purified by RP-HPLC and lyophilized. The peptide was stored protected from light at -20°C.

#### *4.8.12 Preparation of Quality Control Single-Bead Samples*

A fraction of the library resin (10 mg) was removed and swelled for 2 hours in DMF (1.0 mL). It was then subjected to Fmoc deprotection, acetyl cap and side chain deprotection conditions. The cysteines were capped with iodoacetamide (20 mM in PBS, pH 7.4, 500  $\mu$ L) for 1 hour. Single beads were separated into PCR tubes and cleaved in methanol (20  $\mu$ L) according to UV cleavage conditions. The methanol was evaporated and the samples were dissolved in 100  $\mu$ L Buffer A. Each sample was filtered through a 0.45  $\mu$ m PTFE syringe filter and the filter was washed with an additional 100  $\mu$ L Buffer A. This was then concentrated by speed-vac to 20  $\mu$ L total volume. Samples were submitted to Aaron J. Mauris for LC-MS/MS analysis.

#### *4.8.13 LC-MS/MS Sequencing of Single Bead Samples*

Mass Spectrometry was performed on a LTQ Orbitrap Discovery XL (Thermo Fisher) coupled to an EASY-nLC 1000 nanoLC (Thermo Fisher). Samples (10 $\mu$ L) were loaded on to a 100  $\mu$ m fused silica column with a 5  $\mu$ m tip, hand packed with 10 cm of Aqua C18 reverse-phase resin (Phenomenex), using the EASY-nLC autosampler. Samples were eluted using a gradient 0-100% buffer B in buffer A

over 180 minutes (buffer A: 95% water, 5% acetonitrile, 0.1% formic acid; buffer B: 20% water, 80% acetonitrile, 0.1% formic acid). The flowrate was set to 400 nL/min and the spray voltage was set to 3.5 kV. One full MS1 scan (400-1800 m/z) was followed by 8 data dependent scans of the  $n^{\text{th}}$  most intense ion.

Peptides were assigned to MS2s using the SEQUEST algorithm,<sup>36</sup> searching against a reverse-concatenated database of all possible library sequences. To account for the n-terminal acetyl group, a glycine residue was added to the n-terminus of all peptide sequences in the database, and a static modification was specified for glycine (-15.0109 m/z), to modify the mass of glycine to that of an acetyl group. Static modifications were also specified for cysteine residues (+57.0215 m/z, iodoacetamide alkylation), and the C-terminus (-0.98402 m/z, c-terminal amide). MS2 matches were assembled by library member matches using DTASelect 2.0.<sup>37</sup> Peptides were required to be intact (-Smn 9), single peptide matches were allowed (-p 1), and the delta mass was used for statistics (--mass).

#### *4.8.14 Sodium Borohydride Reduction of Intermolecular Iminoboronates*

For NMR analysis, 2-APBA (8 mM) and lysine (8 mM) were dissolved in 10% D<sub>2</sub>O in PBS buffer (pH 7.4). The corresponding conditions for reduction with NaCNBH<sub>3</sub> or NaBH<sub>4</sub> were performed and the <sup>1</sup>H NMR was taken at 600 MHz. For LC/MS analysis, 2-APBA and Fmoc-D-Lysine hydrochloride were dissolved in PBS buffer, pH 7.4. To this, NaBH<sub>4</sub> (final concentration = 50 mM) was added and mixed for 15 min.

#### *4.8.15 Screening of Library against Lipid II Stem Peptide*

Prepared library resin (350 mg) was equilibrated in PBS buffer, pH 7.4 (20 mL) in a Falcon tube overnight. This was washed with PBS buffer (3 x 20 mL) then suspended in 0.1 mg/mL BSA solution in PBS buffer (20 mL). To this, the dual-labelled target peptide was added and the solution was incubated at 37°C while rotating for 1 hour. NaBH<sub>4</sub> (38 mg) was added and the reaction was mixed for 15 min. The resin was then washed with PBS buffer (6 x 20 mL) and resuspended in 0.1 mg/mL BSA solution in PBS buffer (20 mL). To this, streptavidin-coated Dynabeads (200 µL) were added and the resin was incubated at 37°C while rotating for 2 hours. A rare Earth metal magnet was applied to the side of the Falcon tube and kept in place for 2 minutes to allow for all of the Dynabeads to be collected. The supernatant was then removed along with any library resin that did associate with the Dynabeads. The magnet was then removed and the Dynabeads with remaining library resin was resuspended in 0.1 mg/mL BSA solution in PBS buffer (20 mL). The magnetic pull down was repeated two more times to remove any non-specific binders and the final hits and Dynabeads were suspended in 0.1 mg/mL BSA solution in PBS buffer (10 mL). The solution was pipetted onto a glass slide (10 µL at a time) and the brightest beads were extracted and collected into a microcentrifuge tube.

#### *4.8.16 Preparation of Hit Samples for Sequencing*

The collected hits were washed 3 times with PBS buffer, pH 7.4 then subjected to TCEP reduction (50 mM in PBS buffer) and iodoacetamide capping (20 mM in PBS buffer). Beads were segregated into individual PCR tubes, suspended in HPLC-grade methanol (20  $\mu$ L) and subjected to UV cleavage. After cleaving, the methanol was removed by evaporation and the samples were dissolved in 100  $\mu$ L Buffer A. Each sample was filtered through a 0.45  $\mu$ m PTFE syringe filter and the filter was washed with an additional 100  $\mu$ L Buffer A. This was then concentrated by speed-vac to 20  $\mu$ L total volume. Samples were submitted to Aaron J. Mauris for LC-MS/MS analysis.

#### *4.8.17 Synthesis of Hit Peptides for Validation*

All hits were synthesized using Fmoc-based SPPS on Rink amide resin. The N-terminus was acetyl capped. Crude peptides were cleaved from resin using a modified Reagent K (80% TFA, 7.5% w/v phenol, 5% water, 5% thioanisole and 2.5% triisopropylsilane) then precipitated twice using cold diethyl ether. Crude peptides were purified using RP-HPLC to >90% purity. Lyophilized pure peptides were cyclized using DMSO-mediated oxidation by dissolving in 10% DMSO in water and stirring at RT until LC/MS analysis showed no remaining linear peptide. DMSO and water were removed by lyophilization and final peptides were stored at -20°C.

#### 4.8.18 Minimum Inhibitory Concentration Assay

Minimal inhibitory concentrations (MICs) were measured against gram-positive *Staphylococcus aureus* (ATCC 6538) using the broth microdilution method in LB media. Specifically, a single colony selected from a LB agar plate was grown overnight in broth at 37°C with agitation and diluted 100 times into fresh broth the next morning. OD600 was monitored until a value between 0.5 and 0.6 was reached. The cells were diluted by a factor previously determined to a concentration of  $\sim 5 \times 10^5$  colony forming units per mL (cfu/mL). In a sterile 96-well plate, the cell suspension (200  $\mu$ L) was added to each well. To each well, serial diluted (2-fold) peptides in DMSO (2  $\mu$ L) were added in triplicates. Using a microtiter plate reader (SpectraMax M5, Molecular Devices, Sunnyvale, CA), the OD600 was monitored overnight while incubating at 37°C, with readings taken every 10 minutes after the plate was shook for 15 seconds. Using the time point where OD600 of the blank (untreated) sample began to level off, MICs were determined to be the lowest concentration for which cell growth was not observed.

#### 4.8.19 UV-Vis Titration of Hit Peptides with Biotin-Lipid II Stem Peptide

Hit peptide stocks were diluted to a concentration of 50  $\mu$ M in PBS buffer, pH 7.4. 2-methoxyethylamine and biotin-lipid II target peptide, dissolved in PBS buffer, pH 7.4, were titrated into both blank and hit peptide solutions and the UV spectrum was recorded. A blank subtraction was performed for each new concentration of 2-MEA or biotin-lipid II target peptide. Plots were made stacking



the UV spectrum at each concentration of amine as well as a plot of concentration of amine vs. absorbance at 280 nm.  $K_d$ 's could be estimated as the midway point of the titration curve from the absorbance at 280.

#### *4.8.20 Sodium Borohydride Reduction of Hit Peptides and Biotin-Lipid II Stem Peptide*

Hit peptides and biotin-lipid II target peptide (dissolved in PBS buffer, pH 7.4) were mixed at 500  $\mu$ M each. The pH was checked and adjusted to 7.4 as necessary. The samples were allowed to incubate at 37°C for 1 hour before sodium borohydride was added to a concentration of 50 mM. This was allowed to react for 15 min, then samples were diluted to a peptide concentration of 100  $\mu$ M and analyzed by LC/MS.

#### *4.8.21 Screening of Library against Rhodamine-Transferrin*

Prepared library resin (50 mg) was suspended in PBS buffer, pH 7.4 (2.5 mL) and equilibrated overnight. The resin was washed with PBS buffer (3 x 2.5 mL) and suspended in a 1.6 mg/mL solution of human serum albumin in PBS buffer (2.3 mL). To this, rhodamine-labelled transferrin (1 mg/mL stock, 200  $\mu$ L) was added. The mixture was incubated at 37°C with rotation of one hour. Sodium borohydride was added to a final concentration of 50 mM and allowed to react for 15 min. The resin was then washed with PBS buffer, pH 7.4 (4 x 2.5 mL), PBS buffer, pH 5 (1 x 2.5 mL) and finally again PBS buffer, pH 7.4 (1 x 2.5 mL). The resin was analyzed using fluorescent light microscopy with a rhodamine filter. The brightest beads were segregated from others and collected. The peptides were linearized using

TCEP treatment and cysteines were capped with iodoacetamide. Single beads were separated into PCR tubes, suspended in HPLC-grade methanol (20  $\mu$ L) and subjected to UV cleavage conditions. The methanol was removed by evaporation and the samples were dissolved in 100  $\mu$ L Buffer A. Each sample was filtered through a 0.45  $\mu$ m PTFE syringe filter and the filter was washed with an additional 100  $\mu$ L Buffer A. This was then concentrated by speed-vac to 20  $\mu$ L total volume. Samples were submitted to Aaron J. Mauris for LC-MS/MS analysis.

#### *4.8.22 Synthesis of Hit Peptides for Validation*

All hits were synthesized using Fmoc-based SPPS on Rink amide resin. After full peptide synthesis, carboxyfluorescein was coupled to the N-terminus. Crude peptides were cleaved from resin using a modified Reagent K (80% TFA, 7.5% w/v phenol, 5% water, 5% thioanisole and 2.5% triisopropylsilane) then precipitated twice using cold diethyl ether. Crude peptides were purified using RP-HPLC to >90% purity. Lyophilized pure peptides were cyclized using DMSO-mediated oxidation by dissolving in 10% DMSO in water and stirring at RT until LC/MS analysis showed no remaining linear peptide. DMSO and water were removed by lyophilization and final peptides were stored at -20°C.

#### *4.8.23 Fluorescence Anisotropy for Hit Validation with Transferrin*

In a 96-well plate (Costar 3603, black plate, clear bottom), the desired protein was added at varying concentrations from 0-10 mg/mL in triplicates from a protein stock (20 mg/mL in PBS buffer, pH 7.4). To this, the hit peptide (2  $\mu$ L, 20  $\mu$ M stock

in PBS buffer, pH 7.4) was added to each well. Anisotropy was measured every 5 min over 1 hour with an excitation wavelength of 495 nm and an emission wavelength 532 nm with a 515 nm cutoff. Change in anisotropy is recorded as the average of triplicate samples for the given protein concentration with the average of triplicate samples for the peptide alone subtracted.  $K_d$ 's are estimated based on the protein concentration where 50% binding is observed.

#### 4.9 References

- (1) Gray, B. P.; Brown, K. C. *Chem. Rev.* **2014**, 114 (2), 1020–1081.
- (2) Liu, R.; Lam, K. S. *Wiley Encycl. Chem. Biol.* **2009**, 3, 575–587.
- (3) Tian, F.; Tsao, M.-L.; Schultz, P. G. *J. Am. Chem. Soc.* **2004**, 126 (49), 15962–15963.
- (4) Liu, C. C.; Mack, A. V.; Tsao, M.-L.; Mills, J. H.; Lee, H. S.; Choe, H.; Farzan, M.; Schultz, P. G.; Smider, V. V. *Proc. Natl. Acad. Sci. U. S. A.* **2008**, 105 (46), 17688–17693.
- (5) Day, J. W.; Kim, C. H.; Smider, V. V.; Schultz, P. G. *Bioorg. Med. Chem. Lett.* **2013**, 23 (9), 2598–2600.
- (6) Ng, S.; Jafari, M. R.; Matochko, W. L.; Derda, R. *ACS Chem. Biol.* **2012**, 7 (9), 1482–1487.
- (7) Heinis, C.; Rutherford, T.; Freund, S.; Winter, G. *Nat. Chem. Biol.* **2009**, 5 (7), 502–507.

- (8) Barnes, C.; Balasubramanian, S. *Curr. Opin. Chem. Biol.* **2000**, 4 (3), 346–350.
- (9) Liu, R.; Marik, J.; Lam, K. S. *J. Am. Chem. Soc.* **2002**, 124 (26), 7678–7680.
- (10) Brenner, S.; Lerner, R. A. *Proc. Natl. Acad. Sci. U. S. A.* **1992**, 89, 5381–5383.
- (11) Clark, M. A.; Acharya, R. A.; Arico-Muendel, C. C.; Belyanskaya, S. L.; Benjamin, D. R.; Carlson, N. R.; Centrella, P. a; Chiu, C. H.; Creaser, S. P.; Cuozzo, J. W.; Davie, C. P.; Ding, Y.; Franklin, G. J.; Franzen, K. D.; Gefter, M. L.; Hale, S. P.; Hansen, N. J. V; Israel, D. I.; Jiang, J.; Kavarana, M. J.; Kelley, M. S.; Kollmann, C. S.; Li, F.; Lind, K.; Mataruse, S.; Medeiros, P. F.; Messer, J. a; Myers, P.; O’Keefe, H.; Oliff, M. C.; Rise, C. E.; Satz, A. L.; Skinner, S. R.; Svendsen, J. L.; Tang, L.; van Vloten, K.; Wagner, R. W.; Yao, G.; Zhao, B.; Morgan, B. a. *Nat. Chem. Biol.* **2009**, 5 (9), 647–654.
- (12) Zambaldo, C.; Barluenga, S.; Winssinger, N. *Curr. Opin. Chem. Biol.* **2015**, 26, 8–15.
- (13) Mannocci, L.; Zhang, Y.; Scheuermann, J.; Leimbacher, M.; De Bellis, G.; Rizzi, E.; Dumelin, C.; Melkko, S.; Neri, D. *Proc. Natl. Acad. Sci. U. S. A.* **2008**, 105 (46), 17670–17675.
- (14) Brown, L.; Wolf, J. M.; Prados-Rosales, R.; Casadevall, A. *Nat. Rev. Microbiol.* **2015**, 13 (10), 620–630.
- (15) Shockman, G. D.; Barren, J. F. *Annu. Rev. Microbiol.* **1983**, 37 (1), 501–527.
- (16) Spratt, B. G. *Philos. Trans. R. Soc. Lond. B. Biol. Sci.* **1980**, 289 (1036), 273–283.

- (17) Zasloff, M. *Nature* **2002**, *415* (6870), 389–395.
- (18) McCormick, M. H.; McGuire, J. M.; Pittenger, G. E.; Pittenger, R. C.; Stark, W. M. *Antibiot. Annu.* **1956**, *3*, 606–611.
- (19) Loll, P. J.; Bevivino, A. E.; Korty, B. D.; Axelsen, P. H. *J. Am. Chem. Soc.* **1997**, *119* (7), 1516–1522.
- (20) Arthur, M.; Courvalin, P. *Antimicrob. Agents Chemother.* **1993**, *37* (8), 1563–1571.
- (21) Leclercq, R.; Derlot, E.; Duval, J.; Courvalin, P. *N. Engl. J. Med.* **1988**, *319* (3), 157–161.
- (22) Smith, T. L.; Pearson, M. L.; Wilcox, K. R.; Cruz, C.; Lancaster, M. V.; Robinson-Dunn, B.; Tenover, F. C.; Zervos, M. J.; Band, J. D.; White, E.; Jarvis, W. R. *N. Engl. J. Med.* **1999**, *340* (7), 493–501.
- (23) Bandyopadhyay, A.; Gao, J. *J. Am. Chem. Soc.* **2016**, *138* (7), 2098–2101.
- (24) Lian, W.; Upadhyaya, P.; Rhodes, C. A.; Liu, Y.; Pei, D. *J. Am. Chem. Soc.* **2013**, *135* (32), 11990–11995.
- (25) Holmes, C. P.; Jones, D. G. *J. Org. Chem.* **1995**, *60* (8), 2318–2319.
- (26) MacConnell, A. B.; McEnaney, P. J.; Cavett, V. J.; Paegel, B. M. *ACS Comb. Sci.* **2015**, *17* (9), 518–534.
- (27) Malone, M. L.; Paegel, B. M. *ACS Comb. Sci.* **2016**, *18* (4), 182–187.

- (28) Trinh, T. B.; Upadhyaya, P.; Qian, Z.; Pei, D. .
- (29) Liu, T.; Qian, Z.; Xiao, Q.; Pei, D. *ACS Comb. Sci.* **2011**, *13* (5), 537–546.
- (30) Olivos, H. J.; Bachhawat-Sikder, K.; Kodadek, T. *ChemBioChem* **2003**, *4* (11), 1242–1245.
- (31) Mendes, K.; Ndungu, J. M.; Clark, L. F.; Kodadek, T. *ACS Comb. Sci.* **2015**, *17* (9), 506–517.
- (32) Kratz, F.; Elsadek, B. J. *Control. Release* **2012**, *161* (2), 429–445.
- (33) Weaver, M.; Laske, D. W. *J. Neurooncol.* **2003**, *65* (1), 3–14.
- (34) Gray-Owen, S. D.; Schyvers, A. B. *Trends Microbiol.* **1996**, *4* (5), 185–191.
- (35) Calmettes, C.; Alcnatara, J.; Yu, R.-H.; Schryvers, A. B.; Moraes, T. F. *Nat. Struct. Mol. Biol.* **2012**, *19* (3), 358–360.
- (36) Eng, J. K.; McCormack, A. L.; Yates, J. R. *J. Am. Soc. Mass Spectrom.* **1994**, *5* (11), 976–989.
- (37) Tabb, D. L.; McDonald, W. H.; Yates, J. R. *J. Proteome Res.* **2002**, *1* (1), 21–26.

**Chapter 5**  
**Conclusions**

The overarching theme throughout this dissertation is the use of peptides as new antibiotics. With the major advancements for peptides in the past few decades, they are becoming more therapeutically realistic and can fit a niche that is not obtained by small molecules or biological therapeutics. Specifically in the work described in this thesis, we have explored the use of peptides as bacterial selective transmembrane channels and as synthetic receptors of important lipids. While some success has been achieved, it is important not to forget some possible limitations.

In the case of gramicidin A, we were unable to gather as much mechanistic characterization as we had hoped for. As such, it is unclear whether these cationic mutants are active using the same mechanism of action as the natural structure. This also made it difficult to define a more than rudimentary structure activity relationship, providing only limited insight to direct our next step.

Furthermore, it remains to be seen whether this scaffold would be able to produce a structure that is sufficiently potent and selective for clinical applications. The wild-type structure itself has low micromolar potency and those cationic mutants that were able to come back to this did so at the expense of selectivity. This could be a consequence of the non-specific membrane binding at the route of gA's mechanism of action. Looking at relevant examples of peptides in the clinic such as vancomycin, they are able to achieve mid-



nanomolar to sub-micromolar potency as they have a much more specific target for binding. Even in the case of nisin and daptomycin, which bind PE and PG head groups, respectively, potent activity is achieved with membrane-targeting mechanisms.

These thoughts and the difficulties met with rational design of gA peptides initially steered us towards the use of library synthesis and screening. We believed that, with careful crafting of experimental conditions, we could also achieve this type of potent binding. With this, we set out with the goal of discovering a potent binder of the lipid II stem peptide, which is the target for vancomycin. Due to technical challenges, our work has heretofore focused on libraries of monocyclic peptides that incorporate reversible covalent binding motifs, namely the 2-APBA moiety for iminoboronate formation. Despite the carefully designed screening scheme, the initial library has yet to yield positive hits for lipid II binding.

This failed endeavor, however, taught us many things about working with a peptide library and designing appropriate screening conditions. For example, the auto-fluorescence of aged TentaGel beads could give false positive hits while screening with green fluorescence. Using this knowledge, we were able to discover peptides with selective binding to transferrin labeled with a red-emitting fluorophore, which avoids the interference by the auto-fluorescence of the beads. The potency achieved from just our first few validated hits is already

significant in physiological conditions, as the estimated  $K_d$  is less than the natural protein concentration. Furthermore, by including human serum albumin at a physiologically relevant ratio to transferrin in our screen, we were able to select a specific peptide with nearly no observable binding to albumin.

Moving forward, there is still much left to be learned. For example, how specific is our binding within transferrin? Given that transferrin is roughly 80 kDa and contains 58 different lysines, it is unlikely that every hit binds in the same way. Yet, with the selectivity observed for hit 1, it is possible that the binding mechanism is specific for each peptide. The possibility of discovering multiple transferrin-specific peptides with distinct binding mechanisms opens many avenues for future research and applications.

It is conceivable that our cyclic peptide library with a 2-APBA motif would be best suitable for proteins with activated lysines. Lysine is commonly used in the active sites of proteins as a nucleophile. However, with the  $pK_a$  of the lysine side chain being about 10.5, only about 0.1% of the amines will be left deprotonated at physiological conditions. In all its cleverness, nature has found a way to remedy this in necessary proteins. By controlling the local environment with neighboring amino acids, several proteins have been found to contain lysines with perturbed  $pK_a$ 's, allowing for the amine to be more nucleophilic in the active site.<sup>1</sup>

Our system could be ideal for targeting proteins that contain these perturbed lysines. As the binding of our 2-APBA moiety occurs through nucleophilic attack by a free amine, we expect better potency and selectivity can be gained by targeting a more active lysine. Some potential targets including perturbed lysines in their active sites include penicillin binding protein 2 and acetoacetate decarboxylase.

### *Penicillin Binding Protein 2*

In *S. aureus*, penicillin binding protein 2a (PBP2a) is commonly linked to methicillin resistance.<sup>2</sup> This mutant protein, obtained through horizontal gene transfer, is very similar to the natural penicillin binding protein 2 (PBP2), but has a much lower affinity for  $\beta$ -lactam antibiotics.<sup>3,4</sup> With this lower affinity, PBP2a is able to evade inhibition of its transpeptidation activity. However, PBP2 and 2a and most other high molecular weight penicillin binding proteins (PBPs) have a second critical domain responsible for transglycosylation.<sup>5</sup> PBPs use this second domain to extend the glycan chain of peptidoglycan and contain conserved pairs of lysine and serine in their active site.

The proposed mechanism of PBP transglycosylation involves several proton-transfer events, initiated by the activation of a serine residue by a neighboring lysine.<sup>5</sup> This mechanism implies that the lysine must exist in its free base form to be able to abstract the proton from serine. With the example of moenomycin A (MmA), binding this domain, specifically including interactions

with the active site lysine, has been validated to have antibiotic potential.<sup>6</sup> Furthermore, binding to the transglycosylation domain has been observed to also shut down the PBP's transpeptidase activity,<sup>7</sup> suggesting this strategy would be effective against MRSA expressing PBP2a.

By screening our peptide library against PBP2a, we could directly inhibit the active site lysines, gaining specificity through interactions between the local environment of the lysine and the remaining residues in our cyclic peptide. Validated hits would be expected to have similar activity towards both *S. aureus* and MRSA.

#### *Acetoacetate Decarboxylase*

Acetoacetate decarboxylase (AADase), found in mammals as well as solventogenic bacteria, is responsible for the conversion of acetoacetate to acetone. With a mechanism proceeding through a Schiff-base intermediate, AADase is one of the earliest examples of a protein containing a lysine with a perturbed pK<sub>a</sub> in its active site.<sup>1</sup> When the pK<sub>a</sub> of Lys115 was measured directly, it was found to be equal to 5.96, which is 4.5 orders of magnitude lower than a typical lysine side chain.<sup>8,9</sup>

Given the binding mechanism of our 2-APBA structures, we expect that the stabilization provided by the nitrogen-boron dative bond would allow us to compete with the natural substrate of this enzyme. Furthermore, with its

perturbed  $pK_a$ , the potency of a library hit should be enough to avoid off-target binding with other lysines.

Finally, it is worthwhile to redo the lipid II stem peptide screening with optimized screening conditions. Admittedly, the lipid II stem peptide presents a more difficult target than large proteins such as transferrin as the development of synthetic receptors for small molecules still remains in its infancy. However, the impressive potency and selectivity of vancomycin (and other related molecules) toward its target suggest it is feasible to have synthetic receptors for small molecule targets. Of course, our current library of monocyclic peptides is still structurally primitive in comparison to the vancomycin scaffold. However, we submit that the utilization of novel binding mechanisms such as the iminoboronate formation improves our chance of success. In addition, it is highly desirable to build and screen multicyclic peptide libraries, which will undoubtedly better our chances of success to identify synthetic binder of lipid II stem peptide. Lastly, it is important to note that the screening platforms that we are developing, once established, should be applicable to discovering synthetic receptors for a variety of small molecule targets, which may have significant ramifications in various aspects of biology.

### *References*

- (1) Harris, T. K.; Turner, G. J. *IUBMB Life (International Union Biochem. Mol. Biol. Life)* **2002**, 53 (2), 85–98.

- (2) Pinho, M. G.; de Lencastre, H.; Tomasz, A. *Proc. Natl. Acad. Sci.* **2001**, 98 (19), 10886–10891.
- (3) Beck, W. D.; Berger-Bächi, B.; Kayser, F. H. *J. Bacteriol.* **1986**, 165 (2), 373–378.
- (4) Lim, D.; Strynadka, N. C. J. *Nat. Struct. Biol.* **2002**, 9 (11), 870–876.
- (5) Sauvage, E.; Kerff, F.; Terrak, M.; Ayala, J. A.; Charlier, P. *FEMS Microbiol. Rev.* **2008**, 32 (2), 234–258.
- (6) Fuse, S.; Tsukamoto, H.; Yuan, Y.; Wang, T.-S. A.; Zhang, Y.; Bolla, M.; Walker, S.; Sliz, P.; Kahne, D. *ACS Chem. Biol.* **2010**, 5 (7), 701–711.
- (7) Terrak, M.; Ghosh, T. K.; van Heijenoort, J.; Van Beeumen, J.; Lampilas, M.; Aszodi, J.; Ayala, J. A.; Ghuysen, J.-M.; Nguyen-Disteche, M. *Mol. Microbiol.* **1999**, 34 (2), 350–364.
- (8) Kokesh, F. C.; Westheimer, F. H. *J. Am. Chem. Soc.* **1971**, 93 (26), 7270–7274.
- (9) Frey, P. A.; Kokesh, F. C.; Westheimer, F. H. *J. Am. Chem. Soc.* **1971**, 93 (26), 7266–7269.